Selective Knockdown of Misfolded SOD1 as a Therapy for Amyotrophic Lateral Sclerosis

By

Ting Zhou

A thesis submitted to the Faculty of Graduate Studies of

The University of Manitoba

in partial fulfillment of the requirements of the degree of

DOCTOR OF PHILOSOPHY

College of Pharmacy

Rady Faculty of Health Sciences

University of Manitoba

Winnipeg, Manitoba

Copyright© 2019 by Ting Zhou

Abstract

Amyotrophic lateral sclerosis (ALS) is a fatal neurodegenerative disease that features progressive degeneration of motor neurons. Over the past two decades, a major breakthrough in ALS research is the discovery that mutations in the gene superoxide dismutase 1 (*SOD1)* are a cause of familial ALS (fALS). Strong evidence supports that the fFALS-linked *SOD1* variants are readily susceptible to posttranslational modifications, and subsequently become misfolded. Accumulation of the misfolded SOD1 triggers a toxic cascade leading to motor neuron degeneration. Studies also show that the wild type (WT) human SOD1, when modified post-translationally, undergoes aberrant conformational changes and acquires the same toxic properties that are observed in fALS-associated *SOD1* variants. Misfolded SOD1 is thus at the center of ALS pathogenesis and a common toxic factor to a subset of both familial and sporadic ALS. Targeting misfolded SOD1 is therefore a rational approach towards an effective treatment for ALS. Here I present a new approach to selectively knockdown misfolded SOD1 by insertion of the CT-4 epitope of Derlin-1 into the chaperone-mediated autophagy system (CMA). In this study, I report efficiency and specificity of CT-4 peptide in knocking down misfolded SOD1 *in vitro* and *in vivo*. Our results revealed that CT-4 treatment resulted in a selective degradation of misfolded SOD1 in a dose-, time- and lysosomal activity-dependent manner *in vitro*. The *in vivo* studies revealed that CT-4 treatment resulted in knockdown of misfolded

SOD1 in the tissues from the G93A transgenic mouse model of ALS. In addition, daily injection of CT-4 peptide significantly attenuated loss of motor neurons, delayed disease onset and extended lifespan of G93A transgenic mice of ALS. Furthermore, I explored the potential mechanisms underlying which CT-4 peptide delayed disease onset. My data indicated that knockdown of misfolded SOD1 could directly affect monocarboxylate transporter 1 (MCT1) protein expression in spinal cord, suggesting that CT-4 peptide treatment could result in preservation of MCT1 expression, maintenance of axon myelin and protection of neurons in ALS animal model. Therefore, the peptide may be developed into an effective treatment for ALS.

Keywords: amyotrophic lateral sclerosis (ALS), misfolded SOD1, chaperone-mediated autophagy, CT-4 peptide.

Acknowledgements

The moment when I left China and landed in Winnipeg was still like yesterday, now I am approaching to the end of my adventure in Canada. I would like to extend thanks to many people who I met during this wonderful journey.

First and foremost, I would like to express my sincere gratitude to my advisor Dr. Jiming Kong for the continuous support of my Ph.D. study and research, for his patience, guidance, motivation and immense knowledge. It would never have been possible for me to come to the University of Manitoba to further my study without his incredible support and encouragement.

And it's my great honor to have a great co-advisor, Dr. Yuewen Gong, and incredible committees, Dr. Geoffrey Tranmer and Dr. Hassan Marzban. I would like to offer my special thanks to you for your valuable suggestions and insightful comments during those years.

Besides my advisors and committee members, I also would like to express my great appreciation to Dr. Michael Namaka. I would like to thank him for his guidance on the cannabinoid project, and the experience of life he shared which greatly enlightened me on how to decide when facing the dilemma in life.

My sincere appreciation also goes to Dr. Teng Guan for his precious suggestions and help to improve my experimental techniques. In addition, I thank him for his valuable guidance of the ALS project in the completion of my research.

I am greatly thankful to other members from College of Pharmacy who offered kind assistance during my Ph.D. studies, including Dr. Lalitha Raman-Wilms, Dr. Frank J. Burczynski, Dr. Sheryl A. Zelenitsky, Dr. Ted Lakowski, Tina Khorshid Ahmad, Samaa Alrushaid, Yufei Chen, Yuhua Fang, Shujun Huang, Ryan Lillico, Jiaqi Yang.

Last but not the least, I would like to thank my parents, Hongwei Zhou and Yan Zhang, for your unconditional love, compressive support and unwavering belief in me. Without you, I wouldn't be walking so far today.

To my wife, Yang Guo, thank you so much for your company, your sacrifice and your constant support no matter what choice I made. Most of all, thank you for being my best friend in my life.

Many thanks go out to my friend Hui Xia for his support and encouragement throughout my study. I would also like to thank all the friends in Winnipeg, Yi Wang, Ruizhi Zhang, Cindy Xu, Chunyan Zhang, Sai Qiao, Yu Wu, Lin Zhang and Leo Zhang, you are my family in Winnipeg.

Dedication

To my parents, my wife and to all those dedicated researchers, who worked and are working hard for the advancement of science towards the welfare of mankind.

Table of Contents

Abstract ..... **i**

Acknowledgements ..... **iii**

Dedication ..... **v**

List of Figures ..... **x**

List of Tables ..... **xii**

Abbreviations ..... **xiii**

Chapter 1 Introduction **1**

1.1 Amyotrophic lateral sclerosis **2**

1.1.1 Epidemiology 3

1.1.2 Clinical presentations and diagnosis 4

1.1.3 Molecular mechanisms in ALS 6

1.1.3.1 Mitochondrial damage and oxidative stress 7

1.1.3.2 Endoplasmic reticulum (ER) stress 8

1.1.3.3 Glutamate excitotoxicity 10

1.1.3.4 Energy metabolism deficiencies and oligodendrocyte degeneration 12

1.1.3.5 Axonopathy 15

1.1.3.6 Neuron death 17

1.1.3.7 Microbiome 20

1.1.4 Therapeutic strategies 21
1.1.4.1 Multidisciplinary care 21
1.1.4.2 U.S. FDA approved drugs for ALS 22
1.1.4.3 Other efforts in therapeutic development for ALS 25
1.2 SOD1 and its role in ALS 28
1.2.1 SOD1 gene and protein 28
1.2.2 SOD1 protein misfolding and aggregation 28
1.2.3 The role of misfolded SOD1 in ALS 29
1.3 Protein degradation 32
1.3.1 Degradation by ubiquitin-proteasome system (UPS) 32
1.3.2 Degradation by autophagy-lysosome pathway (ALP) 34
1.4 Summary 35
Chapter 2 Selective knockdown of misfolded SOD1 with chaperone-mediated autophagy-based lysosomal degradation 38
2.1 Introduction 39
2.2 Materials and methods 44
2.2.1 Mice and tissue preparation 44
2.2.2 CT-4 peptide treatments 45
2.2.3 DNA isolation and genotyping 46
2.2.4 Transient transfection of hSOD1-WT/SOD1-G93A in CHO cells 48
2.2.5 Western blotting 49

2.2.6 SOD1 aggregation assay by differential extraction 50
2.2.7 Proximity ligation assay (PLA) 51
2.2.8 SOD1-G93A enriched neural stem cell (NSC) culture 52
2.2.9 Immunocytochemistry (ICC) 54
2.2.10 Electron microscopy (EM) 55
2.2.11 Histology analysis 58
2.2.11.1 Hematoxylin and eosin (H&E) staining 58
2.2.11.2 Nissl staining 59
2.2.12 Statistical analysis 60
2.3 Results 61
2.3.1 CT-4 potently decreases SOD1-G93A in dose- and time-dependent manners. 61
2.3.2 SOD1-G93A protein has higher aggregation propensity relative to wild-type human SOD1 (hSOD1-WT) protein 67
2.3.3 Knockdown of SOD1 by CT4 peptide proceeds through a lysosome involved protein degradation pathway. 71
2.3.4 Knockdown of misfolded SOD1 by CT-4 treatment in G93A transgenic mouse model of ALS. 77
2.3.5 Treatment of the G93A mice at the age of 60 days by IP injection q.d. significantly delays the onset of disease and extends lifespan. 90

2.3.6 The effect of CT-4 peptide on motor neurons number, monocarboxylate transporter 1 (MCT1) expression and axon and myelin integrity in CNS.....94
2.3.7 CT-4 peptide has no side effect on tissues of WT mice after a long-term IP injection. 102
2.4 Discussion.....106
2.5 Acknowledgement 114
Chapter 3 Conclusions and future perspectives 115
3.1 Conclusions 116
3.2 Limitations 117
3.3 Future directions 121
Reference.....124
Chapter 4 Appendix 140

List of Figures

Figure 1.1 Axonal-oligodendrocyte coupling. 14

Figure 2.1 Design of peptides and general hypothesis to be tested. 44

Figure 2.2 Treatment with CT-4 peptide results in knockdown of SOD1-G93A in primary neuron prepared from the G93A transgenic mice in dose- and in time-dependent manners. 64

Figure 2.3 Co-immunofluorescence staining of MAP2 and misfolded SOD1 after treatment with CT-4 peptide in primary neuron prepared from the G93A transgenic mice. 66

Figure 2.4 SOD1-G93A protein has higher aggregation propensity relative to hSOD1-WT protein. 70

Figure 2.5 Knockdown of SOD1 by CT4 peptide proceeds through a lysosome involved protein degradation pathway. 74

Figure 2.6 Proximity ligation assay (PLA) confirmed co-localization of misfolded SOD1 and LAMP2 after CT-4 treatment. 75

Figure 2.7 Denaturing sodium dodecyl sulfate-polyacrylamide gel electrophoresis (SDS-PAGE) western blotting analysis using misfolded SOD1 specific monoclonal antibody. 79

Figure 2.8 Injection with CT-4 peptide results in knockdown of misfolded SOD1 in the tissues from G93A transgenic mice at 24 hours post-treatment. 81

Figure 2.9 Injection with CT-4 peptide results in knockdown of misfolded SOD1 in the tissues from G93A transgenic mice at 48 hours post-treatment.....83
Figure 2.10 No obvious reduction of misfolded SOD1 was observed for 1-week recovery after CT-4 peptide treatment in the tissues from G93A transgenic mice. 85
Figure 2.11 No obvious reduction of misfolded SOD1 was observed for 2-week recovery after CT-4 peptide treatment in the tissues from G93A transgenic mice. 87
Figure 2.12 Comparation between 24- and 48-hour post-injection with CT-4 peptide in the G93A transgenic mouse model of ALS.....89
Figure 2.13 CT-4 peptide significantly delays the disease onset and prolongs survival in the G93A transgenic mouse model of ALS.....93
Figure 2.14 Nissl staining of the SC ventral horn of G93A transgenic animal with or without CT-4 peptide treatment. 96
Figure 2.15 Treatment of CT-4 peptide results in a marked increase in MCT1 expression in SC of G93A transgenic mice but not in brain. 99
Figure 2.16 Transmission electron micrograph of efferent nerve fibers in a transverse section 100
Figure 2.17 Hematoxylin and eosin (H&E) stained sections of WT mice.....105

List of Tables

Table 2.1 Complete StemPro NSC medium.....53

Table 2.2 Neural differentiation medium.....53

Table 2.3 Primary antibodies.....54

Table 2.4 Embedding medium for electron microscopy 56

Abbreviations

AAV	adeno-associated virus
ALS	amyotrophic lateral sclerosis
AD	Alzheimer’s disease
AIF	apoptosis-inducing factor
ALP	autophagy-lysosome pathway
ATG	autophagy-related genes
ATF6	activating transcription factor 6
Bad	tBcl-2-associated death
Bax	Bcl-2-associated X protein
BBB	blood-brain barrier
Bcl	B-cell lymphoma
BDNF	brain derived neurotrophic factor
bFGF	fibroblast growth factor
C9ORF72	chromosome-9 open reading frame
CACS	central animal care services
CHO	Chinese Hamster Ovary cells
CMA	chaperone-mediated autophagy
CNS	central nervous system
CSF	cerebrospinal fluid

CT-1	cardiotrophin-1
CTM	chaperone-mediated autophagy-targeting motif
DAPK1	death associated protein kinase 1
DBR	Derlin-1 binding region
Dubs	deubiquitinases
EAAT	excitatory amino acid transporter
EAE	experimental autoimmune encephalomyelitis
EBSS	Earle's balanced salt solution
EM	electron microscopy
ER	endoplasmic reticulum
ERAD	endoplasmic-reticulum-associated degradation
fALS	familial ALS
FUS	fused in sarcoma
GFAP	glial fibrillary acidic protein
GLTs	glutamate transporters
GLUT	glucose transporters
GRP	glucose-related protein
H_2O_2	hydrogen peroxide
hEGF	human epidermal growth factor
HSP	heat shock proteins
ICC	immunocytochemistry

IP	Intraperitoneal injection
iPSCs	human induced pluripotent stem cells
IRE1	inositol-requiring enzyme 1
LAMP2	lysosomal associated membrane protein 2
LMN	Lower motor neuron
MAPK	mitogen-activated protein kinase
MCT	monocarboxylate transporter
MeCP2	methyl CpG binding protein 2
MRI	magnetic resonance imaging
MS	multiple sclerosis
mSOD1	mutant SOD1
NFκB	nuclear factor κB
NGF	nerve growth factor
NMDA	non-N-methly-D-aspartate
NMJ	neuromuscular junction
NRP1	neuropilin 1
NSC	neuronal stem cells
NTFs	neurotrophic factors
OPC	oligodendrocyte precursor cell
PBS	phosphate-buffered saline
PD	Parkinson’s disease

PDL	poly-D-lysine
PDI	protein disulphide isomerase
PEG	polyethyleneglycol
PERK	protein kinase R-like ER kinase
PFA	paraformaldehyde
PLA	proximity ligation assay
PNS	peripheral nervous system
POIs	protein of interest
PPX	Pramipexole
PQC	protein quality control
qRT- PCR	quantitative reverse transcriptase polymerase chain reaction
ROS	reactive oxygen species
RPPX	dexpramipexole
RRMS	relapsing remitting multiple sclerosis
sALS	sporadic ALS
SC	spinal cord
Sema	semaphorin
SOD1	superoxide dismutase 1
TARDBP	TAR DNA-binding protein
TNFα	tumor necrosis factor alpha
UMN	upper motor neuron

UPR	unfolded protein response
UPS	ubiquitin-proteasome system
WM	white matter
WT	wild type

Chapter 1 Introduction

1.1 Amyotrophic lateral sclerosis

Amyotrophic lateral sclerosis (ALS) is a fatal neurodegenerative disease, involving the progressive degeneration of both upper and lower motor neurons. ALS is also known as Lou Gehrig's Disease, after the famous baseball player Lou Gehrig who was diagnosed with the devastating disease (1). ALS is considered as the most common motor neuron disease in adults that characteristically displays with onset of distal weakness in the arms or legs, which is indicative of lower motor neuron involvement. Muscular weakness limits the use of muscles for the execution of voluntary movements, thus causing muscular atrophy, eventually leading to respiratory muscle failure and death (2). As the disease progresses into the later stages, patients may experience a continued progressive decline of cognitive function. However, in the later stages of ALS, the ocular muscles that control vision are usually the last muscles to be affected (1).

The primary focus of clinical management for patients with ALS is symptomatic management of the disease using conventional pharmacological agents, as no cure is currently available. However, non-conventional approaches, including radiotherapy, muscle stretching and nutritional management have also been employed to alleviate the pain, respiratory dysfunction, psychiatric/cognitive disturbances, nutritional deficits and sleep related dysfunctions associated with ALS (3).

ALS is most commonly referred to as a motor neurons disease, due to the activation of abnormal programmed cell death signaling pathway during the

pathogenesis of the disease, leading to the death and degeneration of motor neurons (5). Although the molecular mechanisms involved in ALS pathogenesis vary, including mitochondrial damage, oxidative stress, endoplasmic reticulum stress, glutamate excitotoxicity, oligodendrocyte degeneration, and axonopathy, considerable progress has still been made in the investigation of different aspect of ALS pathophysiology. Several abnormal biological processes have been suggested to be involved in the mechanisms underlying the pathogenesis of ALS (6), thus making it a very complex multi-system and multi-syndrome disorder, for which no single cause can be identified. Therefore, a combination of genetic and neuropathological assessments, neuroimaging, and neuroprotective strategies would be necessary for a better understanding of this disease.

1.1.1 Epidemiology

The estimated global annual incidence of ALS is approximately 1 to 2.6 cases per 100,000 persons, and the prevalence is about 3 to 6 cases per 100,000 persons (7). Based on the family history of patients with ALS, this disease can be classified as sporadic ALS (sALS), which represents ~90% of all ALS cases, and familial ALS (fALS), which accounts for the remaining about 10% of cases (8). Sexual dimorphism has been suggested to be involved in ALS disease onset and progression (9); the incidence and prevalence of ALS is greater in males than in females (10, 11). Considerable progress has been made in the investigation of genetic aspect of ALS pathophysiology. Mutations in several genes have been

demonstrated to be involved in fALS, including chromosome-9 open reading frame 72 (*C9ORF72*) (12), *SOD1* (13), TAR DNA-binding protein (*TARDBP*) (14), fused in sarcoma (*FUS*) (15). Mutations in these four genes account for up to 70% of all familial ALS cases. With the development of genome sequencing techniques, the number of genes implicated in ALS pathogenesis is increasing, thus suggesting the complexity of the disease, and explaining the elusiveness of a cure. Besides the large number of genetic mutations, environmental and lifestyle factors are also considered to play a role in ALS, including smoking, excessive physical activity such as in athletics and veterans, exposure to environmental toxins, such as pesticide and β-methylamino-L-alanine; however, further studies are required to elucidate the implication of environmental factors in ALS development (16, 17).

1.1.2 Clinical presentations and diagnosis

ALS patients have a median survival of 3-5 years after diagnosis. Pathologically ALS is characterized by progressive degeneration of upper motor neurons (UMN) and lower motor neurons (LMN), which leads to the voluntary muscle weakness, and eventually to death usually due to respiratory failure (18).

The symptoms of UMN dysfunction can be frequently observed, including spasticity, hyperreflexia, wasted limbs, and the Babinski sign. Patients with UMN-dominant ALS normally show significant younger disease onset than that

in classic ALS patients, as well as different sex ratio, spreading pattern and clinical phenotype (19).

The symptoms of LMN dysfunction include fasciculation, muscle cramps, and muscle atrophy. Although LMN signs are predominant in majority of ALS cases, the variability and a combination of UMN and LMN signs are still a major contributor to phenotypical heterogeneous presentations of ALS cases (20, 21).

Notably, although ALS has been generally considered as a motor neuron disease, the pathological alternations are not limited to motor neurons only. Study revealed that the frequency of cognitive impairment in patients with ALS is greater than that in the patients with other neuromuscular diseases. In addition, those ALS patients with cognitive impairment had significantly shorter survival time while compared with those without (22). The assessment of LMN-dominant patients also proved that cognitive impairments, including executive dysfunction, verbal short-term memory loss, and dementia were observed in those patients (23). Thus, both of the cognitive and behavioral changes should be included in the diagnosis of ALS and are paramount for disease management.

The heterogeneous presentation and variation in disease onset and rate of progression make diagnosis of ALS challenging; therefore, there is no definitive test available up to now. Differential diagnosis and clinical investigations, including genetic testing, neuroimaging, electrophysiological studies, blood and cerebrospinal fluid (CSF) tests, magnetic resonance imaging (MRI) of the brain and spinal cord are applied to exclude other possible diseases with similar

symptoms (24, 25). El Escorial and Awaji-Shima Criteria are used as a basis for the diagnosis of ALS, which require a history of progressive weakness spreading within one or two other regions (bulbar, cervical, thoracic, or lumbar), with evidence of the involvement of both lower and upper motor neurons. The Awaji-Shima criteria simplifies the El Escorial criteria and is more suitable for clinical practice, while El Escorial criteria is normally used in research and clinical trial settings (17, 26-28).

1.1.3 Molecular mechanisms in ALS

Several abnormal biological processes have been suggested to be involved in the mechanisms underlying the pathogenesis of ALS (6). sALS and fALS are two predominant types of ALS, and appear to share some similar pathophysiological mechanisms, including mitochondrial dysfunction, excitotoxicity, protein aggregate formation, glial cell pathway disturbance, abnormal axonal transport, inflammation and neurofilament accumulation (29, 30).

Notably, the mechanisms underlying early-onset white matter (WM) pathology in multiple sclerosis (MS) are similar to those responsible for early-onset WM damage prior to motor neuron death in ALS (31-33). Therefore, elucidation of the pathological mechanisms involved in MS-induced WM damage may provide useful insight to advance the understanding of certain aspects of ALS. Furthermore, novel therapeutic approaches that target WM

pathology in the early stages of ALS, may have potential to delay the onset and progression of the disease.

1.1.3.1 Mitochondrial damage and oxidative stress

Mitochondria are the primary site of ATP production; they also have a major role in the maintenance of Ca^{2+} homeostasis, the production of free radicals and the regulation of intrinsic apoptotic pathways (34, 35). Therefore, mitochondrial dysfunction may be involved in the initial degeneration process of ALS (36).

Reactive oxygen species (ROS) are byproducts of aerobic metabolism. The cumulative production of ROS results in oxidative stress, which cause mitochondrial damage. ROS can induce mitochondrial DNA mutations, impair the mitochondrial respiratory chain, alter mitochondrial membrane permeability and ultimately leads to cell death (37). Previous studies have suggested the time- and dose-depend involvement of ROS, including superoxide ($\cdot O_2^-$), hydroxyl radical ($\cdot OH$), and hydrogen peroxide (H_2O_2), in mitochondrial damage driving motor neuron degeneration (38, 39). In both sALS and fALS, post-mortem and biopsy samples from the spinal cord and muscles show abnormalities in mitochondrial structure, number and localization with associated defects in activities of respiratory chain complexes (40). Furthermore, elevated ROS and mitochondrial dysfunction have also been observed in the extraction of spinal cord from the sALS patients (41).

Cell type-specific mitochondrial damage has been demonstrated in the pathogenesis of ALS: Mitochondrial dysfunction in astrocytes has been associated with a neurotoxic phenotype that impairs motor neuronal survival (42), with a mechanism that may involve misfolded SOD1 aggregation. Misfolded SOD1 aggregates cause mitochondrial damage due to a decrease in antioxidant activity of the enzyme, thus resulting in ROS accumulation. In addition, misfolded SOD1 may potentiate the formation of ·OH, as suggested by the increased levels of oxidation products in misfolded SOD1-transfected mice compared with controls (43). Furthermore, misfolded SOD1 protein aggregates may be responsible for impairments in axonal transport, neurotrophic factor supply, endoplasmic reticulum (ER) stress and apoptosis in glial cell responses (44, 45). m*SOD*1 is present in ~20% of patients with fALS and 3% of patients with sALS (46); however, oxidative stress and mitochondrial damage are also present in non-SOD1-linked ALS cases (47).

1.1.3.2 Endoplasmic reticulum (ER) stress

ER is an intracellular organelle that is responsible for protein quality control (PQC), as it ensures that proteins are correctly synthesized, folded, packaged and delivered in the appropriate locations. Under ER stress conditions, the unfolded protein response (UPR) signaling pathway is activated to restore cellular integrity or initiate apoptosis. Three ER stress sensors meditate the UPR, namely protein kinase R-like ER kinase (PERK), activating transcription factor 6 (ATF6) and

inositol-requiring enzyme 1 (IRE1) (48, 49). ER stress can be triggered by accumulation of unfolded or misfolded proteins in the ER lumen, and by other mechanisms, including the inhibition of ER-to-Golgi apparatus trafficking, which represents an early cellular disturbance before the induction of ER stress, Golgi fragmentation (50), misfolded SOD1 aggregation and cell apoptosis (51).

Chaperone proteins, including heat shock proteins (HSP) and members of the protein disulfide isomerase (PDI) family, ensure proteins are folded correctly. Upregulation of these proteins, which is an important part of UPR, may have a cytoprotective effect in ALS (52). Low levels of HSP in motor neurons increase their susceptibility to cell stress, thus increase their vulnerability to cell death inducers. Neuronal HSP levels depend upon the neuronal and glial production of HSP (53). Therefore, glial cells may be responsible for HSP deficits and increased ER stress, which eventually lead to motor neuron degeneration.

The ER stress sensors PERK, ATF6 and IRE1 are activated under physiological conditions, resulting in the upregulation of downstream molecules, including PDI, 78-kDa glucose-related protein (GRP78) and 94-kDa glucose-related protein (GRP94). These molecules have been associated with oligodendrocyte damage, reduced axon numbers and demyelination, which are associated with ALS progression (54, 55). Notably, an early upregulation of PDI has been reported in microglia of the spinal cord in an ALS mouse model. This study demonstrated that an early UPR in glia, caused by misfolded protein, may lead to PDI-dependent NADPH oxidase activation and contribute to

neurotoxicity in ALS (56). Motor neurons in mice with fALS were revealed to be prone to ER stress and demonstrated upregulated ER stress marker expression accompanied by axonal degeneration (57). These studies suggested that the early events in ALS may induce ER stress, which, in turn, may activate the UPR signaling pathway, ultimately resulting in motor neuron degeneration and death. Therefore, it may be hypothesized that therapeutic strategies aiming at attenuating or delaying the early events may have potential in reducing motor neuron death and disease progression in patients with ALS, thus increasing their life expectancy.

1.1.3.3 Glutamate excitotoxicity

Accumulating evidence suggests that glutamate excitotoxicity may be implicated in the mechanism of neuronal degeneration in ALS (58-60); imbalances between excitatory and inhibitory neurotransmission may contribute to the pathogenesis of the disease. Glutamate is the primary excitatory amino acid neurotransmitter in the central nervous system (CNS). Glutamate excitotoxicity has been associated with oligodendrocyte apoptosis following spinal cord injury (61). An increase in excitatory neurotransmission, as indicated by increased levels of glutamine, has been reported in the motor cortex of patients with ALS compared with health controls (60). Glutamine synthesis is catalyzed by the enzyme glutamine synthetase from glutamate and ammonia (62), and glutamine

production is used as a marker of glutamate levels to detect glutamate-induced excitotoxicity.

Astrocyte-mediated cell-specific excitotoxicity has also been implicated in the pathogenesis of ALS. Astrocytes express two glutamate transporters (GLTs), GLT-1, also known as excitatory amino acid transporter 2 (EAAT 2) and glutamate aspartate transporter, also known as EAAT 1, which participate in extracellular glutamate homeostasis and neuronal reuptake (63). EAAT loss has been observed in animal models and patients with ALS (17). Glutamate excitotoxicity, mediated by non-N-methly-D-aspartate (NMDA) receptors, has been reported to cause axonopathy, including axonal swelling, cytoskeletal disruption and neurofilament accumulation, in the distal axonal segments of spinal cord motor neurons (64). Studies suggested that glutamate excitotoxicity may be implicated in axonopathy and long-term cognitive deficits in patients with ALS. Therefore, neuroprotective agents, including vasoactive intestinal peptide, may attenuate excitotoxic damage to promote axonal regrowth, thus ameliorating the motor neurons degeneration (65, 66).

The cell-specific effects of astrocytes have been reported to participate in the activation of protein kinase C and mitogen-activated protein kinase (MAPK) pathways to confer neuroprotection. These results suggested that astrocyte activation that may differentially facilitate or prevent motor neuron degeneration. Further studies are required to elucidate the differential functions of astrocytes in the pathology of degenerative diseases, including ALS (67) and MS (68).

1.1.3.4 Energy metabolism deficiencies and oligodendrocyte degeneration

The human brain utilizes glucose and monocarboxylates, such as lactate, as primary energy source. Lactate accounts for ~33% of the total energy substrates used by the brain, representing a more important fuel source for brain metabolism than glucose. Monocarboxylate transporters (MCTs) are responsible for lactate and pyruvate transport. In the brain, three MCT isoforms have been identified, namely MCT1, MCT2 and MCT4, which are implicated in lactate flux in the CNS (69). MCT1 is expressed in astrocytes and oligodendrocytes, whereas MCT4 is expressed exclusively in astrocytes. Oligodendrocytes are critical for the production and maintenance of myelin (70), and astrocytes for the delivery of essential energy (71).

Myelin is an insulating substance, which is essential for the propagation of electrical impulse along nerve axons (72). Nerve axons are long projections that originate from the neuronal cell body and serve to transmit information in the form of electrical impulses. In addition, nerve axons transport nutrients essential for the health and physiological function of the axons and the neuronal cell bodies (73). The release of glutamate from neurons has been proved to bind and activate the oligodendroglial NMDA receptors and in turn increase oligodendroglial glucose uptake through glucose transporters (GLUT1). Then, the imported glucose would be converted into pyruvate and lactate. Lactate can be subsequently transported toward neurons through MCT1 and enter the

mitochondrial citric acid cycle to generate ATP for the neurons (Figure 1.1) (74-76).

Oligodendrocytes exhibit higher MCT1 expression, and increased lactate oxidation and lipid synthesis compared with astrocytes (32). Therefore, oligodendrocyte dysfunction may contribute to motor neuron degeneration and neuronal death in ALS. Notably, oligodendrocyte pathology becomes apparent prior to disease onset and persists during disease progression (77, 78). A previous study suggested that oligodendroglia may support axon survival and function through a myelin-independent mechanism, whereas deficiencies in energy metabolites may underlie neurodegeneration (79). In human studies and preclinical mouse ALS models, MCT1 expression was revealed to be decreased in affected brain regions, resulting in insufficient energy supply to the axons, thus leading to axon loss and motor neuron degeneration and death (32, 71, 80).

Recently, oligodendrocytes were demonstrated to contribute to motor neuron death in ALS through a SOD1-dependent mechanism (81). Oligodendrocyte degeneration has been reported to occur prior to disease onset. New oligodendrocytes are formed to compensate for the loss; however, they fail to mature, thus resulting in progressive demyelination. Furthermore, axonal demyelination has been directly associated with ALS deterioration (82). Therefore, oligodendrocyte dysfunction is considered as a major factor contributing to neuronal degeneration, with relevance to diseases including ALS (83, 84). Notably, the glial pathology in ALS, including oligodendrocyte

degeneration and impaired maturation, and its involvement in neurodegeneration, is analogous to the pathology displayed in MS (83).

These findings suggested that the molecular mechanisms involved in early-onset oligodendrocyte degeneration in ALS may also contribute to motor neuron death. Therefore, therapeutic strategies aiming at attenuating early-onset of oligodendrocyte degeneration may have potential for the effective treatment of patients with ALS.

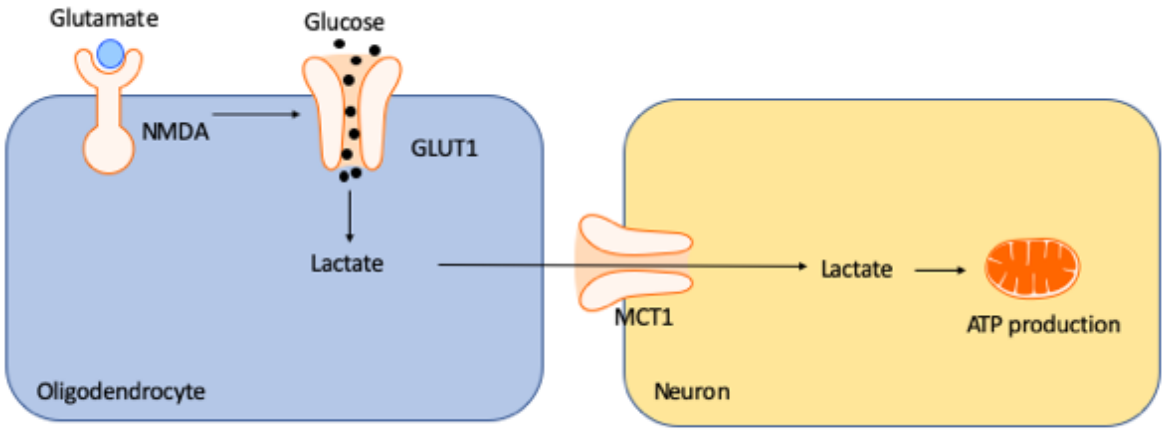


Figure 1.1 Axonal-oligodendrocyte coupling.

Glutamate from neurons activates the oligodendroglial NMDA receptors and in turn increase oligodendroglial glucose uptake through glucose transporters (GLUT1). After the conversion of glucose into lactate and pyruvate, lactate can be subsequently transported toward neurons through MCT1 and enter the mitochondrial citric acid cycle to generate ATP for the neurons.

1.1.3.5 Axonopathy

Motor neuron axonopathy has been proposed as an early initiating mechanism of ALS. Motor neuron pathology in ALS has been suggested to begin, at distal axon sites and proceeds in a retrograde manner, eventually leading to motor neuron degeneration, a hypothesis termed the 'dying back' mechanism (85). Axonopathy has also been demonstrated in animal models of ALS, including zebrafish (86), mice (87) and rats (88). In rats carrying SOD1-G93A mutation, mitochondrial accumulation of misfolded SOD1 was observed in motor neuron axons in discrete clusters located at regular intervals, instead of homogeneous axonal distribution (88). Overexpressions of misfolded SOD1 (86) and excitotoxicity (64) have been suggested to trigger axonopathy. In addition, excitotoxic axonopathy has been associated with the aberrant colocalization of phosphorylated and dephosphorylated neurofilament proteins, which subsequently induce axonal transport disruptions and swelling. In addition, axonopathy has been associated with abnormalities within the glial environment (89). Fast-fatigable motor neurons are highly susceptible to axonal degeneration, which is associated with deficiencies in proteins and lipid supply to axons (85, 90). As aforementioned, oligodendrocytes regulate axonal myelination to maintain axonal function, whereas astrocytes provide structural and trophic support for neurons. Abnormal glial-axonal interactions have been reported to be implicated in axonal swelling, neurofilament perturbations and microtubule transport defects during axon degeneration (91).

Semaphorin proteins serve as axonal growth signaling cues and are responsible for axon guidance and neurofilament organization during nervous system development (92). Class 3 semaphorins are involved in oligodendroglial migration and remyelination. Semaphorin (Sema) 3A is a repulsive guidance cue for neuronal and glial cells and induces the redistribution and depolymerization of actin filaments that results in growth cone collapse. In addition, Sema3A is expressed in MS lesions, where it impairs the recruitment and differentiation of oligodendrocyte precursor cell (OPC) and inhibits remyelination (93, 94). Conversely, Sema3F is an attractive guidance cue, which assists OPC recruitment and promotes axonal remyelination (94, 95). The roles of Sema3A have also been investigated in ALS: In an ALS mouse models, Sema3A and its receptor neuropilin 1 (NRP1) were demonstrated to induce distal axonopathy (96). Furthermore, in humans, Sema3A levels in the motor cortex were significantly upregulated in patients with ALS compared with controls. These results suggested that the increase in Sema3A may be implicated in axonal degeneration, and may be associated with the axonopathy and denervation that were observed in patients with ALS (97). Sema3A, and other class 3 semaphorins, are important regulators of axonal remyelination and of the immune responses that govern neuronal regeneration (98). Therefore, the inhibition of Sema3A may have potential as a novel therapeutic strategy for the treatment of patients with ALS. According to the ‘dying back’ hypothesis regarding motor neuron

pathology, it may be necessary to focus on motor axons and nerve terminals in order to effectively delay or prevent motor neuron degradation (99).

1.1.3.6 Neuron death

Several mechanisms, including oxidative stress, the aggregation of misfolded and mutant protein, and excitotoxicity, may disrupt homeostasis of motor neurons, ultimately causing cell death. MeCP2 (methyl CpG binding protein 2) is a nuclear protein with numerous biological functions, which serves a critical role in myelin damage in neurological conditions, including epilepsy (100) and MS (101). MeCP2E1 and MeCP2E2 are two predominant isoforms of MeCP2 that exert diverse biological effects on neuronal survival. Previous studies have revealed that MeCP2E2 promotes neuronal death and apoptosis; however, these effects may be inhibited by Forkhead box proteinG1 and Akt, which enhance neuronal survival (102, 103).

MeCP2E1 has been reported to repress brain derived neurotrophic factor (BDNF) transcription, thus resulting in the failure of myelin repair mechanism (101). BDNF serves a role in myelin repair and promotes the health of neurons, astrocytes and oligodendrocytes; therefore, BDNF deficiencies have been implicated in pathological mechanisms of ALS (104, 105). Notably, BDNF serum levels have been revealed to be significantly decreased in patients with ALS compared with in controls (106). Therefore, BDNF may have potential as a biomarker to reflect disease activity, and may serve as a basis for the development

of novel therapeutic strategies for ALS treatment (104). Neurotrophic factors (NTFs), including BDNF, have been reported to exert beneficial effects in mouse model of ALS. Treatment of SOD1-G93A transgenic mice with neurotrophic factors has been reported to inhibit neuromuscular junction degeneration, enhance axon survival, delay the onset of ALS and prolong the average lifespan of the mice (107, 108).

In ALS, apoptosis is the most common form of motor neuron death, and involves pro- and anti-apoptotic gene expression, caspase activation, the cytochrome c release and apoptosis-inducing factor (AIF) nuclear translocation (109-111). Notably, in patients with ALS, apoptotic processes are not restricted to motor neurons, but also occur in other neuronal and non-neuronal components of the CNS (112). A previous study reported increased neuronal apoptosis, accompanied by an increase in glial fibrillary acidic protein (GFAP)-positive astrocytes and increased microglia activation in the white and grey matter of several CNS regions (113). In addition, astrocytes, but not microglia, cortical neurons or myocytes, were suggested to have an integral role in the death of motor neurons in ALS (114).

At least three different molecular pathways have been reported to participate in programed cell death: the mitochondrial pathway, the death receptor pathway and the ER pathway (115). The present review explored only mitochondrial-dependent apoptosis, as it is primarily responsible for neuronal and non-neuronal cell death in ALS. The mitochondrial apoptotic pathway is activated during the

early stage of ALS, and proapoptotic signaling has been revealed to directly induces neuronal dysfunction (116). B-cell lymphoma (Bcl)-2 family members have also been reported to serve critical roles during apoptosis that lead to motor neuron death via controlling mitochondrial permeability in ALS models. The expression and distribution of Bcl-2, Bcl-extra-large, tBcl-2-associated death promoter (Bad) and Bcl-2-associated X protein (Bax) are altered in ALS mouse models, thus suggesting the presence of mitochondrial damage (112, 117). In addition, inhibition of PI3K/Akt signaling pathway can directly induce proapoptotic proteins, including Bad and Bax, and thus contribute to the degenerative and apoptotic pathways during ALS pathogenesis (118). Caspase activation and elevated cytosolic cytochrome *c* levels have also been observed in ALS cell lines, thus indicating mitochondrial-dependent apoptosis may contribute to cell death in ALS (119). However, the altered expression of Bcl-2 family proteins, the inhibition of PI3K/Akt signaling and the activation of caspase may not be the only pathways leading to motor neuron degeneration in ALS, as apoptosis is a complex process, and is known to be induced through numerous pathways (120).

AIF is a key regulator of caspase-independent apoptosis, and its increased expression has been associated with the progression of ALS. AIF has been revealed to co-translocate to motor neuronal nuclei with cyclophilin A; following binding with cyclophilin A, AIF may induced mitochondrial membrane permeabilization and cell death in a model of ALS (121). Therefore, proapoptotic

signaling may contribute to neuronal and non-neuronal degeneration that cause WM damage and motor neuron death in ALS. Therefore, inhibition of mitochondrial apoptotic pathway may have potential as another novel therapeutic approach to suppress myelin damage and/or preserve motor neuron viability and function in patients with fALS (116).

1.1.3.7 Microbiome

The microbiome-gut-brain axis is responsible for the association between the microbiome and neuroimmune and neuropsychiatric disorders (122), including MS (123, 124), autism (125) and ALS (126). The microbiome-gut-brain axis refers to the interactions between the CNS, the gastrointestinal tract and the microorganisms in the gut. Several mechanisms have been suggested to explain the influence of the gut microbiome on brain health (127): Impaired intestinal barrier function has been suggested to promote the passage of toxins from the intestinal lumen into the blood circulation and the brain. A previous study demonstrated that *Clostridium perfringens* ε-toxin may be responsible for WM damage in the CNS of mice. ε-toxin secreted into the gut was revealed to bypass the blood-brain barrier and cause mature oligodendrocyte death, demyelination and WM injury; these effects were dependent on the expression of myelin and lymphocyte protein proteolipid (128). Notably, ε-toxin has been demonstrated to exert selective toxic effects on oligodendrocytes but not astrocytes, microglia, or neurons in primary cultures (128). Furthermore, dysbiosis of the gut microbiota

has been reported in patients with MS compared with in healthy controls (129, 130), whereas gut-derived neurotoxins have been proposed as a cause of ALS (131, 132). In an ALS mouse model (SOD1-G93A), impaired gut integrity and a shift in the profile of the gut microbiome have been observed at the early stage of the disease , and have been reported there to be associated with increased disease severity (133). These findings suggested a potential role of microbiome in the progression of ALS. However, the precise alternations in the gut microbiome during ALS pathogenesis have yet to be elucidated. Numerous factors, including hygiene, antibiotics usage, microbiota composition, probiotics and diet have been proposed to influence the link between the gut microbiome and the CNS (122). Understanding the relationships between the microbiome and the neuroimmunology may aid the development of novel preventive and therapeutic interventional strategies for the treatment of CNS disorders, including ALS.

1.1.4 Therapeutic strategies

1.1.4.1 Multidisciplinary care

In the absence of a cure for ALS, current available therapeutic interventions mainly focus on symptom control by utilizing a multidisciplinary care, which has been shown to alleviate symptoms, improve quality of life and prolong survival of patients with ALS (134, 135). The multidisciplinary care in ALS includes a wide range of interventions addressing spasticity, hypersalivation, pain, muscle cramps, dysphagia, cognitive impairment, and respiratory insufficiency involving

neurologists, psychologists, nutritionists, speech therapists and physical therapists (136).

1.1.4.2 U.S. FDA approved drugs for ALS

Riluzole is the first drug approved by the US Food and Drug Administration for the treatment of patients with ALS, and it has been clinically available since 1995. However, treatment with riluzole can only marginally improve the neurological symptoms of the patients and prolong their survival by 3 - 4 months (137), whereas a previous epidemiology study reported that riluzole exerted a beneficial effect only during the first 6 months of therapy, with an apparent reversal of its beneficial effects after the 6-month time point (138). Tiglutik™ is the first thickened liquid form of riluzole, approved in 2018. This formulation was developed to help ALS patients with swallowing difficulties (https://www.tiglutik.com/).

The molecular mechanisms underlying the neuroprotective effects of riluzole in ALS have yet to be elucidated. It has been suggested that riluzole may exert its beneficial effects via preventing motor neuron excitotoxicity, through the blockade of voltage-dependent ion channels (139-141). However, riluzole has also been reported to act on astrocytes to induce neural growth factors production and improve the neuronal survival rate (141, 142). In addition, it has been demonstrated to stimulate BDNF release (143, 144). A previous study suggested the importance of BDNF during myelin repair, as increased level of BDNF were

revealed to facilitate myelin repair and offer neuroprotection in the CNS (145). Therefore, the enhancing effects of riluzole on BDNF expression may also contribute to its neuroprotective effects in patients with ALS.

Furthermore, the acute and chronic treatment of ALS mice with riluzole exerted opposite effects on the production of trophic factors in the CNS, including glial cell-derived neurotrophic factor, BDNF, cardiotrophin-1 (CT-1) and nerve growth factor (NGF) (142): Acute treatment with riluzole was revealed to induce trophic factor production in the spinal cord, sciatic nerve and brain, whereas chronic treatment exerted inhibitory effects. In their study by Dennys *et al(142)*, riluzole significantly increased CT-1 levels in the spinal cord following 15 days of continuous treatment, which returned to baseline following 30 days of treatment. In addition, riluzole increased brain BDNF levels following 6 and 15 days of treatment, which were significantly decreased following 30 days of treatment.

The levels of released BDNF appear to be a critical factor in ALS pathology, since BDNF has been reported to serve an essential roles in the development of pathologic pain (146). Increased BDNF level have been suggested to induced the development of chronic pain, whereas BDNF deficits may result in failure myelin repair mechanisms (101, 147). The findings suggested that a delicate equilibrium in the endogenous BDNF levels may be required for the maintenance of myelin repair without the induction of nociception. Therefore, therapeutic schemes that favor the acute effect with riluzole administration, and the close monitoring of

BDNF levels may have the potential to improve the therapeutic outcomes of treatment with riluzole.

After 22 years of riluzole approval, edaravone became the second FDA approved drug to effectively slow ALS progression. The exact mechanism of edaravone for treatment of ALS is yet fully understood. Evidence suggested that edaravone may act as a free radical scavenger to protect neurons, glia and vascular endothelial cells against oxidative stress (148-151). Although the clinical trial showed that edaravone could slow disease progression in a subset of patients with early ALS, there were still limitations and debates whether this drug should be provided to all patients with ALS due to the strict inclusion criteria, short clinical study duration, and no reliable pathobiological markers (152). However, the approval of edaravone encourages researcher and clinicians to translate more potential treatments into new therapies in ALS to reduced patients' suffering.

Nuedexta was approved by FDA in 2011 for the treatment of pseudobulbar affect (PBA) that associated with neurological diseases, such as ALS, stroke, Parkinson's disease (PD), Alzheimer's disease (AD) and MS. PBA is a condition characterized by inappropriate or exaggerated emotional expression (153). Nuedexta is a combination of two compounds: dextromethorphan and quinidine. Quinidine is an inhibitor of the CYP450 isoenzyme CYP2D6 to protect dextromethorphan from being broken down through O-demethylation (154). Although the underlying mechanism is unknown, this drug has been reported to

show efficacy in patients with ALS and MS (155).

1.1.4.3 Other efforts in therapeutic development for ALS

As the efficacy of riluzole is only marginal, and its administration can increase survival by only a few months, clinicians suggest that treatment with riluzole should be started at early stages of the disease in order to maximize its benefits. Novel agents with higher efficacy are currently under investigation, and various administration routes are being evaluated in order to improve the efficacy and minimize the adverse effects of the treatments (156).

Novel experimental drugs are currently being evaluated in preclinical animal models and in human clinical trials (157). Pramipexole (PPX), is a D2/D3-preferring dopamine receptor agonist, which has been demonstrated to exert beneficial effects in an EAE model of MS: PPX blocked neuroinflammatory responses, demyelination, and astroglial activation in the spinal cord and it inhibited the production of inflammatory cytokines and ROS (158). In addition, dexpramipexole (RPPX), which is the R (+) enantiomer of PPX, has also demonstrated neuroprotective effects, via acting directly on mitochondria to stabilize mitochondrial ionic conductance and reduce free radical production, thus inhibiting cell death (159-161). Early phase clinical trials in patients with ALS suggested that RPPX has a promising safety and tolerability profile, and a phase III clinal trial is currently underway to investigate its efficacy in patients with ALS (162).

Pioglitazone is a peroxisome proliferator-activated receptor- γ agonist, which has been demonstrated to exert its anti-inflammatory and neuroprotective actions. It has been suggested as a potential therapeutic agent for the treatment of MS, due to its ability to reduce TNF-α-induced myelin damage and mitochondrial dysfunction (163). In a phase I clinical trial in patients with relapsing remitting MS (RRMS), treatment with pioglitazone was reported to reduce lesion development in WM, via inhibiting demyelination and axonal degeneration (164). However, pioglitazone did not exert beneficial effects on the survival of patients with ALS, as revealed by a phase II clinical trial evaluating it as add-on therapy in combination with riluzole (165). However, riluzole was revealed to exert neurotoxic effects at the concentrations between 3 and 30 μM, which may antagonize the neuroprotective effects of several compounds being evaluated in clinical trials, including resveratrol, memantine, minocycline and lithium. Therefore, further studies are required, using a group of patients without riluzole treatment to evaluate the neuroprotective potential of novel agents in ALS (166).

Flavonoids are bioactive compounds that are derived from fruit and vegetables. Epigallocatechin-3-gallate is a flavonoid that has been demonstrated to reduce neuroinflammation, and limit demyelination and axonal damage in the EAE (experimental autoimmune encephalomyelitis) model of MS (167) and SOD1-G93A mouse model of ALS (168). The neuroprotective effects of flavonoids suggest that they may have potential as alternative therapeutic agents for the treatment of neurodegenerative diseases, including MS and ALS (169).

Stem cell transplantation has also been recognized as a potential therapeutic strategy for the treatment of patients with ALS and MS (170). A previous study demonstrated that a neural stem cell (NSC) population isolated from human induced pluripotent stem cells (iPSCs) improved the neuromuscular function and increased the life span of ALS mice, following intrathecal or intravenous administration. The results revealed that these transplanted NSCs migrated and engrafted into the CNS, where they improved the production of neurotrophic factors and reduced micro- and macrogliosis (171). Furthermore, a human study demonstrated that transplantation of autologous stem cells into patients with ALS delayed disease progression and increased survival (172). In addition, neural precursor cells transplantation has been reported to enhance remyelination in an EAE mouse MS model of extensive demyelination (173). Genetically engineered bone marrow stem cells have also been used to deliver BDNF in to EAE mice, and resulted in the significantly delayed EAE onset, which was accompanied by a reduction in demyelination and overall clinical severity (174).

ALS is a multi-syndrome disease, which is characterized by extensive genetic and phenotypic variability. Therefore, the discovery of a single agent that can be used for the treatment of all ALS patients is unlikely. Early diagnosis and early interventional therapies that target certain molecular and genetic pathways are urgently required for the treatment of patients with ALS.

1.2 SOD1 and its role in ALS

1.2.1 SOD1 gene and protein

The superoxide dismutase-1 (SOD1) is a 17 kD protein. It is a primary antioxidant enzyme of the body that is expressed ubiquitously in the cytosol, nucleus, and mitochondrial intermembrane space and functions to convert, acting as a homodimer, highly reactive superoxide to hydrogen peroxide and molecular oxygen. Hydrogen peroxide can then be broken down by catalase (175). The mature human SOD1 protein in its native form is a stable homodimer of 153-residue polypeptide in which each subunit contains one copper and one zinc ion, as well as disulfide bond formation between Cyc57 and Cyc146. Each monomer of the SOD1 protein consist of an eight-stranded, Greek-key β-barrel and two functionally important loops for metal binding and electrostatics (176). *SOD1* gene was first inherited gene identified as a primary cause of ALS in 1993, with more than 180 mutations identified accounting for 20% fALS cases, although the native SOD1 enzyme is responsible for elimination of free superoxide radical in the body and plays a major role in reduction oxidative stress as a free radical scavenger (13, 177).

1.2.2 SOD1 protein misfolding and aggregation

Protein misfolding is produced due to the imprecise folding process driven by somatic mutations, transcriptional or translational errors, breakdown of the folding and chaperone machinery, erroneous post-translational modifications or

trafficking or protein, and structural modification due to environmental changes (178). These misfolded proteins escape the “quality-control” mechanisms, and form aggregates within cells or in extracellular space (179). SOD1 aggregation is one of the best characterized hallmarks of ALS, which are found in spinal cord of both patients with ALS and transgenic mouse model (180-183). Interestingly, accumulating evidence suggests a “prion-like” property of SOD1 found in cellular and in animal models. SOD1 aggregates can accelerate or seed aggregation of the soluble protein. Misfolded SOD1 within a cell is capable to sequester and misfold wildtype SOD1 proteins, and induce subsequent aggregation. Additionally, if the aggregates are secreted and taken up by neighboring cells, these aggregates will act as a “seed” to induce a chain reaction of misfolding, aggregation and transmission (184).

Despite the findings of the aggregation pathway and the cell-to-cell transmission, our understanding of the mechanisms underlying the formation and propagation of aggregates is very limited. Therefore, one of the goals of therapeutics for ALS is to find treatments that can specifically enhance disaggregation of degrade the already-formed aggregates.

1.2.3 The role of misfolded SOD1 in ALS

Although the intramolecular disulfide bridge facilitates SOD1 stability, mutations in the *SOD1* gene can destabilize the protein and lead to misfolding and subsequent aggregations (185). The initial hypothesis for the mechanism of

which *SOD1* mutations is a cause in a subset of fALS is that the conformational changes of SOD1 contribute to the loss of metal binding and enzymatic activity, and thus lead to its toxicity to motor neurons. Studies showed that misfolded SOD1 aggregates cause mitochondrial damage due to a decreasing in the antioxidant activity of the enzyme, thus resulting in ROS accumulation. In addition, misfolded SOD1 may potentiate the formation of •OH, as suggested by the increased levels of oxidation products in misfolded SOD1-transfected mice compared with controls (43). Furthermore, misfolded SOD1 protein aggregates may be responsible for impairments in axonal transport, neurotrophic factor support, ER stress and apoptosis in glial cell responses, which are associated with the degeneration of oligodendrocytes (44, 45). Strong evidence overwhelmingly supported, however, that the neuronal toxicity of mutated SOD1 is derived from a "gain of an adverse property" rather than a loss of its anti-oxidation function (186). Indeed, many of the disease-causing mutant SOD1 enzymes retain normal levels of superoxide dismutation activity (187), and the presence of mutant SOD1 enzymes does not affect the activity and stability of normal SOD1 (188). In addition, transgenic mice expressing the mutant *SOD1* develop motor neuron degeneration in spite of normal levels of superoxide dismutation activity (186, 189). Furthermore, neither overexpression nor knockout of the normal *SOD1* gene in transgenic mice causes the disease or influences the disease progression (189, 190). The nature of gain-of-function toxicity in mutant *SOD1* variants is not fully understood. Nevertheless, increasing evidence suggests that

posttranslational modifications of SOD1 are a critical step towards gaining its toxic properties. fALS-linked *SOD1* variants are readily susceptible to post-translational modifications, and subsequently become misfolded. Failure in degradation of unfavorable SOD1 with ubiquitin and/or autophagy-proteasome system causes accumulation of protein aggregates and triggers a toxic cascade leading to motor neuron degeneration (191-194).

Additionally, wild type SOD1, when modified post-translationally, undergoes aberrant conformational changes and acquires the same toxic functions that are observed for fALS-associated *SOD1* variants (195, 196). Oxidized SOD1-G93A is readily detectable in the transgenic mice at the age of 8 weeks, which correlates well with the formation of SOD1 aggregates in spinal cord motor neurons at this stage (182). The late onset and age-dependent penetrance of the disease argues that the ALS-linked *SOD1* mutants are not initially toxic until they are post-translationally modified. Since aging is a major risk factor of ALS and oxidative stress is considered the most prominent theory of aging, post-translational oxidation of SOD1 seems a plausible common mechanism for both familial and sporadic ALS (194, 196, 197). Oxidation of SOD1 has been shown to provoke misfolding and aggregation of the SOD1 protein (198-200). Importantly, misfolded SOD1 could be derived from either mutant *SOD1* or the wild-type human SOD1 (201, 202). Therefore, misfolded SOD1 is at the center of ALS pathogenesis and a common toxic factor to a subset of both fALS and sALS.

1.3 Protein degradation

Protein function could be regulated by protein level alternation, intrinsic protein activity, and protein location change. The protein homeostasis in cell is due to the rate of protein synthesis, degradation, or both (203). Protein life span is controlled mainly by protein degradation. As such, protein degradation could either help to remove unfavorable proteins, such as toxic, misfolded, or damaged proteins, or to maintain protein homeostasis. There are several pathways for degrading proteins in cells, which will be discussed as follows:

1.3.1 Degradation by ubiquitin-proteasome system (UPS)

One of the primary pathway of protein degradation is proteasome pathway, which accounts 90 percent of the protein degradation in mammalian cells (203). Proteasomes are large 60-subunit complexes and consist of a 20S catalytic core and one or two 19S regulatory caps (204). The 19S caps are responsible for providing energy to unfold protein and translocating those unfolded polypeptides into the 20S core for degradation. The 20S catalytic core is a cylindrical, barrel-like proteasome where the protein can be rapidly degraded into peptides and further converted into amino acids (205). This process is initiated by covalently attaching a "polyubiquitin tail" to the unfavorable proteins. Three steps are involved in the ubiquitinylation: activation of E1 (ubiquitin-activating enzyme), transfer of E2 (ubiquitin-conjugating enzyme), and formation of isopeptide bond

by E3 (ubiquitin-protein ligase). Then, the 19S regulatory cap recognizes the ubiquitylated protein, followed by subsequent unfolding and degradation (205). Notably, ubiquitinylation is a reversible process. The bonds between ubiquitins and the targeted protein can be hydrolyzed by deubiquitinases (Dubs). And the released ubiquitins can be recycled for next rounds of protein degradation (206).

Manipulation of the UPS to depredate targeted proteins by therapeutic interventions can be translated into clinical treatments for cancer and other diseases. For example, the nuclear factor κB (NFκB) plays a central role in inflammation, immunity, cell growth and apoptosis. Excessive activity of NFκB is associated with inflammatory disease and cancer. Its activation is negatively regulated by UPS. Inhibition of proteasomal activity results in increased level of IκBα, which is the inhibitor of NFκB, then leads to subsequent reduced NFκB activity. Therefore, proteasome inhibitors targeted the NF κ B degradation pathway could be developed into a potential therapeutic intervention for these diseases (207).

Small molecules, as well as larger bifunctional molecules, have been studied to promote degradation of interesting target proteins (208). PROteolysis-Targeting Chimeras (PROTACs) is a novel technique aiming at diseases driven by dysregulated proteins. PROTAC is a small molecule capable to simultaneously binds E3 ligase and targeted protein, thus induce ubiquitination and degradation of targeted protein (209, 210). These emerging techniques and molecules provide the potential for the discovery of next-generation drugs.

1.3.2 Degradation by autophagy-lysosome pathway (ALP)

The major difference between UPS and ALP is that ALP recognizes and removes the vesicle-mediated large protein complex, aggregates and dysfunctional organelles, while UPS is responsible for the small and short-lived proteins (211). There are three different subtypes of autophagic pathways: macroautophagy, microautophagy, and chaperone-mediated autophagy (CMA) (212).

Macroautophagy is the best-studied type and a well-regulated process. It starts with an autophagosome or autophagic vesicle, which is a double membrane structure that envelops a portion of cytosol or an organelle. This autophagosome can grow and fuse with a lysosome to transport vesicles and its content into the lysosome for further degradation by lysosomal proteases. The amino acids, after degradation of the protein, are then delivered across the lysosomal membrane into the cytosol for new protein synthesis (203). Autophagy-related genes (ATG) have been proved to be involved in the discussed process. Numerous proteins complexes consisted of ATG gene products play a critical role in the formation of autophagosomes (213).

CMA is a high selective type of autophagy in which cytosolic protein with an exposure of specific pentapeptide KFERQ motif can be recognized by a complex of chaperones and co-chaperones, such as heat shock 70 kDa protein (HSC70). HSC70-mediated delivery of proteins enables the protein-HSC70 complex across the lysosomal membrane via LAMP-2A receptor (lysosome-associated

membrane protein type 2A). The proteins are then rapidly degraded in the lysosomal lumen. Therefore, the CMA activity is directly dependent on the level of LAMP-2A and HSC70 (211, 214, 215).

UPS and ALP have been considered as independent degradative pathways for a long time. However, a close cross-talk has been revealed between the two major pathways in protein degradation (216). In a nutshell, protein degradation plays a very critical role in the biological process in life, including cell cycle, transcription, programmed cell death or apoptosis, and removal of misfolded proteins. Protein degradation pathways could serve as therapeutic targets in human diseases.

1.4 Summary

ALS is a complex multi-system and multi-syndrome disease that affects neuronal and non-neuronal populations and is characterized by the progressive degeneration of motor neurons. Several pathological mechanisms are involved in ALS, including mitochondrial dysfunction, oxidative stress, neuronal apoptosis, ER stress, glutamate excitotoxicity, energy metabolism defects and axonopathy. Therefore, agents that are currently available for the treatment of other neurodegenerative disease aimed at these biomarkers may have potential as treatment options for patients with ALS.

The current chapter presented a comprehensive evaluation of ALS, discussing motor neuron death as the principle cause of the disease, and examining the

impact of early-onset damage, such as axonopathy and oligodendrocytes degeneration, as confirmed by neuroimaging techniques (217-220). However, the exact molecular mechanisms in ALS have yet to be elucidated. Understanding molecular mechanisms that underlie motor neuron degeneration in ALS may aid the development of improved therapeutic strategies. Current agents used for the treatments for ALS, including riluzole and edaravone, can only marginally extend the lifespan of patients with ALS. Further studies are required to elucidate the role of neuroglial pathology in the development and progression of ALS.

Additionally, this chapter offered a brief introduction of SOD1 and protein degradation pathways, which are highly related to the study of this thesis. The aim of this chapter is to explore the potential therapeutic strategies for ALS and provide a better understanding of the pharmacological mechanisms of the treatments studied in this thesis, and thus aids in developing new strategies to treat ALS and other different neurodegenerative diseases.

The hypothesis of the present Ph.D. thesis is that the CT4-directed and chaperone-mediated autophagy pathway selectively degrades misfolded SOD1 and can be developed into an effective treatment for ALS. To test this hypothesis, this study has two objectives respectively to determine: 1) the efficiency and specificity of CT4-directed and chaperone-mediated autophagy pathway in knocking down of misfolded SOD1 derived from constitutively expressed SOD1 mutants in primary cultures of neurons; and 2) the therapeutic efficacy of the CT4-directed and chaperone-medicated autophagy pathway in mouse models of

ALS when given systemically.

Chapter 2 Selective knockdown of misfolded SOD1 with chaperone-mediated autophagy-based lysosomal degradation

2.1 Introduction

Amyotrophic lateral sclerosis (ALS) is a progressive neurodegenerative disease and can be classified as sporadic ALS (sALS) which represents about 90% of all ALS cases and familial ALS (fALS) which accounts for the remaining 10%, due to genetic mutations (8). ALS is a rare but fatal disease characterized by the progressive loss of motor neurons in the brain and spinal cord. Following the death of motor neurons, the resultant muscle weakness limits the use and normal function of muscles, leading to muscular atrophy (2). Clinical trials for ALS started in the 1980s; however, the majority of experimental drugs were proved to be ineffective with the exception of riluzole and edaravone that was reported to marginally extend the lifespan of the patients (1, 4).

Over the past two decades, one major breakthrough in ALS research has involved the discovery of mutations in the gene *SOD1*, which encodes the copper-zinc (Cu/Zn) superoxide dismutase 1 and is a well-established cause of fALS (13, 221). To date, over 185 ALS-associated *SOD1* mutations have been found (222). SOD1 is a 17 kD protein that contains one copper and one zinc atom. It is ubiquitously expressed but is particularly abundant in motor neurons. The known function of this 153-amino-acid, soluble cytoplasmic and mitochondrial intermembrane space enzyme (acting as a homodimer) is to convert superoxide radicals to molecular oxygen and hydrogen peroxide (223).

Increasing evidence suggests that *SOD1* mutations are especially prone to post-translational modifications, resulting in misfolding and aggregation which

is a critical step towards gaining its toxic properties. Failure in degradation of misfolded SOD1 with ubiquitin and/or autophagy-lysosomal system causes the accumulation of insoluble SOD1 aggregates and triggers a toxic cascade, leading to motor neuron degeneration. Notably, wild-type human SOD1, when modified post-translationally, undergoes aberrant conformational changes and acquires the same toxic functions that are observed for fALS-associated *SOD1* variants. Therefore, misfolded SOD1 could be derived from either mutant SOD1 or the wild-type human SOD1 (191-194). Additionally, misfolded SOD1 protein is present in 20% of fALS cases and 3% of sALS cases (46). As such, knockdown of misfolded SOD1, a common toxic factor, would be a therapeutic strategy for both familial and sporadic ALS.

Knockdown of SOD1, achieved previously by targeting the SOD1 gene (224) or SOD1 mRNA (225, 226), has been shown to effectively slow down disease progression and prolong survival in mouse models of ALS, these strategies were not designed to target the post-translationally modified versions of SOD1 and thus may not be eventually developed into an effective treatment for ALS. In addition, manipulating gene expression at the DNA level is currently inapplicable to human beings, and RNA interference is known to have off-target effects that might affect other innocent proteins (227, 228). These ethic and technical obstacles may severely constrain the potential of these methods in drug development. At the protein level, immunization protocols aiming to reduce the burden of extracellular SOD1 mutants have been shown to alleviate disease

symptoms and prolong life spans in animal models of ALS (229). This strategy appears to be a promising disease-modifying treatment option for ALS but is challenged with hurdles such as autoimmunity-related adverse effects, and mobilization of neurotoxic insoluble SOD1 oligomers. There are currently no clinical trials on immunotherapies for ALS yet, but clinical trials on similar strategies for Alzheimer's diseases failed because of prohibitive side-effects (230).

To overcome shortcomings of DNA- and mRNA-based protein manipulations, Dr. Wang and his group have developed a simple, non-virally mediated, cell membrane-permeant, targeting peptide-based system to rapidly and reversibly knock down endogenous protein of interest (POIs) through lysosomal degradation (231). The system consists of the 11-amino acid transduction domain of HIV TAT protein capable of crossing cell membrane and the blood brain barrier, a protein binding motif that specifically bind to POIs, and finally the KEFRQ-related targeting motif destined for lysosomes. Its efficacy, specificity and broad utility have been demonstrated by targeting several natural proteins including the death associated protein kinase 1 (DAPK1, 160 kDa), the scaffolding protein PSD-95 (95 kDa) and α-synuclein (18 kDa). In rat neuronal cultures, the peptide system efficiently knocked down the targeted protein within hours in a dose- and lysosomal activity-dependent manner. Depending on the nature of the interaction between the targeting peptide and the protein target, the knockdown could be either constitutive or conditional. Importantly, this peptide

system was able to efficiently knockdown the target protein in the brains of rats when given systemically. This peptide-directed protein knockdown strategy can theoretically degrade any native cytosolic POIs.

In an attempt to extend the utility of this strategy to knockdown post-translationally modified proteins, we have found that the CT4 epitope of Derlin-1, when expressed in our chaperone-mediated autophagy system (CMA), can induce a rapid and selective degradation of misfolded SOD1. The protein Derlin-1, also known as degradation in endoplasmic reticulum protein 1, is part of a protein complex that mediates endoplasmic-reticulum-associated degradation (ERAD) (232), and is required for retrotranslocation of unfolded proteins from the endoplasmic reticulum (ER) lumen to the cytosol (233, 234). Studies show that Derlin-1 interacts with virtually all ALS-linked SOD1 mutants (235). The cytosolic carboxylterminal region of Derlin-1 (termed CT4), composed of 12 amino acids (FLYRWLPSRRGG), is minimally required and sufficient for interaction with SOD1 mutants (236). A recent study demonstrates that Derin-1 interacts with misfolded SOD1 derived from either WT or mutant forms (236). Human WT SOD1 contains a masked Derlin-1 binding region (DBR) at amino acids 6-16. When SOD1 becomes misfolded, the conformational DBR epitope of SOD1 is exposed, thus allowing binding with the CT4 motif of Derlin-1 (237).

Based on this peptide-direct protein knockdown system, we developed a conformational SOD1 sensitive knockdown peptide. As shown in Figure 2.1, the blood-brain barrier and the plasma membrane of cells; a short target protein-

binding amino acid stretch that specifically bind to the target misfolded SOD1; and the chaperone-mediated autophagy-targeting motif (CTM) that can direct the peptide-protein complex for lysosomal degradation. As mentioned above, human SOD1 proteins, when misfolded, bind to the CT4 epitope of the Derlin-1 protein. This occurs due to the exposure of a normally hidden DBR located in the N-terminus of SOD1. This interaction is specific to virtually all ALS-causing SOD1 mutants, as it caused ER stress by interfering with ERAD, resulting in motor neuron death (235, 236).

Selective clearance of misfolded SOD1 is therefore a rational approach towards developing effective treatment for ALS (238). Previous studies in our lab revealed CT4 peptide's efficacy of knocking down misfolded SOD1 induced by serum deprivation or gene mutation in cultured cell line. The data showed that CT4-directed protein knockdown method could specifically decrease the level of serum deprivation-induce misfolded SOD1 but not WT SOD1 in HEK 293T cells. Same effect was also observed in CHO cells transfected with SOD1-G93A plasmids. In this study, I determined the efficiency and specificity of the CT4-directed and CMA pathway in knocking down of misfolded SOD1 in SOD1-G93A enriched primary neurons and in human SOD1-G93A transgenic mice of ALS.

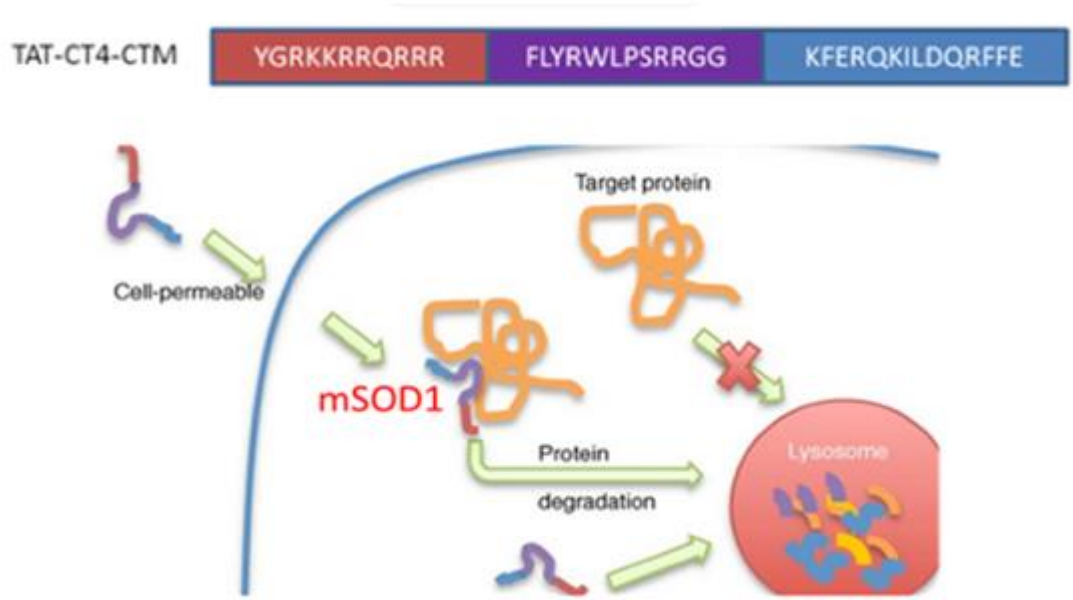


Figure 2.1 Design of peptides and general hypothesis to be tested.

A. Amino Acid sequences for various peptides.

B. The fusion peptide contains the 11 amino acids transduction domain of HIV TAT protein, capable of crossing cell membrane and the blood brain barrier, the CT4 motif that selectively bind to misfolded SOD1, and the KFERQ-like sequence destined for lysosomes.

2.2 Materials and methods

2.2.1 Mice and tissue preparation

Transgenic mice carrying human G93A mutant *SOD1* [B6.Cg-Tg(SOD1*G93A)1Gur/J; 004435] were obtained from the Jackson Laboratory (Bar Harbor, ME, USA). These mice were crossed with female mice with a C57BL/6 background for at least four generations. Colonies are maintained in the

Central Animal Care Services (CACS), University of Manitoba. And the use of the mice was performed in accordance with the Guide of Care and Use of Experimental Animals of the Canadian Council on Animal Care. Transgenic offspring were genotyped by PCR of DNA obtained from ear biopsies using a protocol provided by the Jackson Laboratory. Disease course was monitored by body weight and hindlimb extension reflex twice a week using both male and female mice. Before the onset of the disease, the animals were normal. At disease onset (18 weeks of age for the SOD1-G93A mice), the animals showed initial muscle weakness from one limb, which will spread to other limbs gradually. The disease peaked with paralysis of one or more limbs (20-22 weeks of age for G93A mice). Animal may also lose vision and bladder control. End-stage was defined as the time which the mouse could not right itself within 30 seconds when placed on its side and the body weight loss reaches 20% of the peak. The age predications were based on our previous experience with using this animal model of ALS and as well as that reported in the publications of other researchers (239). The mice were euthanized at the humane endpoint. Animals were anesthetized and transcardially perfused with 20 ml phosphate-buffered saline (PBS). Brain, spinal cord, liver and muscle tissues were collected for the following analysis.

2.2.2 CT-4 peptide treatments

To determine the effect of CT-4 peptide on SOD1-G93A protein expression, a short-term injection has been conducted. Animals (n=3-6) were randomly divided

into vehicle treated group (Control) and CT-4 peptide treated group. Beginning at 100 days of age, the G93A mice received either saline or CT-4 peptide at a dose of 10 mg/kg through intraperitoneal (IP) injection every day for continuous three days. Tissues, including spinal cord, brain, liver, and muscle from the control and treatment groups were harvest at 24 hours, 48 hours, 1 week and 2 weeks post-treatment and followed by western blot analysis.

To determine the effect of CT-4 peptide on lifespan of G93A transgenic mouse model of ALS, a long-term treatment has been conducted. Animal (n=10) were randomly divided into mCT-4 (mutant CT-4) treated group (Control) and CT-4 peptide treated group. Beginning at 60 days of age, the G93A mice were treated with either mCT-4 or CT-4 peptide at a dose of 10 mg/kg through IP injection every day until the endpoint of the experiment. Notably, mutant CT-4 is applied in the following long-term treatment studies to serve as a better control compared with saline.

2.2.3 DNA isolation and genotyping

Ear samples were lysed overnight at 55 ℃ in 300 μl of TNES buffer (1 M Tris, pH 8.5, 0.5 M EDTA, 10% SDS, 5 M NaCl, distill water) and 20 $\mu g/\mu l$ of Proteinase K (Sigma). An equal volume of phenol/chloroform (1:1) was added to the mixture, mixed gently. Then debris was separated from the samples by centrifugation for 15 minutes at 14,500 rpm, and the supernatant containing DNA was collected. DNA was precipitated using an equal volume of cold 95% ethanol

(-20℃), and the DNA was pelleted via centrifugation for 10 minutes at 14,500 rpm. The supernatant was discarded, and the pellet was washed with 70% ethanol and repeat the centrifugation to discard the ethanol. Tubes were placed in the ventilating hood to evaporate residual ethanol for 1 hour. Then the DNA was resuspended in 30 μl distilled water and stored at 4℃ until the genotype was determined using PCR.

Isolated DNA was used to determine the genotypes of progeny. Approximately 450 mice were genotyped from the breeding. 19 μl of ultra-pure water (ThermoFisher), 2.5 μl of 10× PCR buffer (200 mM Tris-HCl pH 8.4, 500 mM KCl) (ThermoFisher), 1 μl of 50 mM $MgCl_2$, 0.25 μl of 10 mM dNTPs, 0.5 μl of 10 μM forward primer (5'-CATCAGCCCTAATCCATCTGA-3'), 0.5 μl of 10 μM reverse primer (5'-CGCGACTAACAATCAAAGTGA-3'), and 0.25 μl of 5 U/μl *Taq* DNA polymerase (ThermoFisher) was added to 2 μl of sample DNA. PCR conditions for the above reactions included a three-minute initial denaturation at 95 ℃, followed by 35 cycles of a 30-second denaturation step at 95 ℃, a 30-second annealing step at 55 ℃, and a 45-second extension step at 73 ℃. And then a 10-minute final extension step at 72 ℃. PCR products mixed with gel red were separated on a 1% agarose gel. The gel was then visualized in an G:BOX imager using GeneSys imager software (Syngene, UK).

2.2.4 Transient transfection of hSOD1-WT/SOD1-G93A in CHO cells

Wild-type human SOD1 (hSOD1-WT) and SOD1-G93A constructs tagged with EGFP were constructed in the same manner as previously reported (192). hSOD1-WT gene was cloned by RT-PCR from total RNA extracted from hSOD1-WT transgenic mouse, and subcloned into pEGFP-N1 at *Sal*I site (Clontech, Palo Alto, CA, USA). The wild-type template for PCR amplification uses the following primers: 5'- GCGCGCGTCGACAAGCATGGC-3' (forward), 5'-GCGCGCGTCGACGCTTGGGGCGATCCCAAT-3' (reverse). Similarly, SOD1-G93A gene was cloned by RT-PCR from total RNA extracted from SOD1-G93A transgenic mouse, and subcloned into pEGFP-N1 at *Sal*I site. The G93A template for PCR amplification uses the following primers: 5'-CTGCTGACAAAGATGCTGTGGCCGATGTGTC-3' (forward), 5'-GACACATCGGCCACAGCATCTTTGTCAGCAG-3' (reverse). All the plasmid constructions were verified by automated sequencing.

Transfections for transient expression of hSOD1-WT/SOD1-G93A constructs were performed using FuGENE 6 transfection reagent (Promega, Madison, WI) according to the manufacturer's instructions. Briefly, Chinese hamster ovary cells (CHO) were recovered from liquid nitrogen and cultured at least one week prior to transfection to make sure that cells were growing properly. A day before transfection, CHO cells were plated in T75 flask at 1×10^5 cells/ml in the final volume of 10 ml of DEME medium complete culture medium. 24 hours later, cells were transfected with plasmids. FuGENE transfection reagent

was added to Opti-MEM medium (Invitrogen) and incubated for 5 minutes. After incubation, an appropriate amount of DNA was mixed with FuGENE/Opti-MEM to achieve the ration of reagent to DNA (3:1) and further incubated for 20 min at room temperature. After incubation, the mixture was added to the cells and incubated for 24-48 hours.

2.2.5 Western blotting

Mice tissues were collected and homogenized in 10 volumes of IP lysis buffer (Pierce, Cat# 87787, ThermoFisher) with 1% (v/v) cocktail. Homogenates were centrifuged at 21,000 × g for 30 minutes at 4 ℃ and supernatants were collected for analysis.

The total cellular samples were washed two times with ice-cold PBS, scraped with IP lysis buffer, and then transfer into a micro centrifuge tube. And the cell suspension was maintained constant agitation for 30 minutes at 4 ℃. Then the cell lysate was centrifuged at 21,000 × g for 30 minutes at 4 ℃ and supernatants were collected for analysis.

The protein concentration was determined using BCA Protein Assay Reagent (Pierce, Rockford, IL, USA). Samples were boiled for 5 min in Laemmli sample buffer containing 2.5% β-mercaptoethanol and 10 μg of sample proteins were separated by 12% TGX Stain-Free polyacrylamide gels (Cat #1610185, Bio-Rad), and transferred to PVDF membrane by Trans-Blot Turbo Transfer System (Bio-Rad). Membranes were blocked with 5% (w/v) fat-free dry milk in Tris-

buffered saline (10 mM Tris-HCl, pH 7.5, 150 mM NaCl) containing 0.05% Tween-20 for 1 hour and incubated with primary antibodies overnight at 4 ℃ (See table 2.3 for the detail of primary antibodies). Blots were washed three times in TBS buffer and then incubated with appropriate secondary antibodies for 1 hour at room temperature. The protein bands were visualized with the enhanced chemiluminescence reagent (ECL Prime, GE Healthcare, Cat# RPN2232) by an imager (ChemiDoc MP, imaging system, Bio-Rad).

2.2.6 SOD1 aggregation assay by differential extraction

The procedures were used to assess SOD1 aggregation by differential detergent extraction and centrifugation (240, 241). Cells were scraped from the culture dish in PBS and centrifuged to pellet the cells before the pellets were resuspended in 100 μl 1 × TEN (10 mM Tris, 1 mM EDTA, and 100 mM NaCl). The resuspended cell culture pellets were then mixed with an equal volume of extraction buffer A (1 × TEN, 1% Nonidet P40, and protease inhibitor cocktail 1:100 dilution) and sonicated with a probe sonicator with 50% output for 30 s (50 W at 20kHz, FB50, Fisher Scientific, Pittsburgh, PA, USA). The resulting lysate was centrifuged for 5 min at $>$ 100,000 × g in an ultracentrifuge (Optimal L-90k, Beckman Coulter, USA) to separate pellet (P1) from the supernatant (S1). The supernatant (S1) was decanted and saved for analysis. The pellet (P1) was washed with 200 μl of extraction buffer B (1 × TEN and 0.5% Nonidet P40) by sonication (50% for 30 s). The extract was then centrifuged for 5 min at $>$

100,000 × *g* in a Beckman Airfuge to separate a pellet (P2) from the supernatant. The P2 fraction was resuspended in buffer C (1 × TEN, 0.5% Nonidet P40, 0.25% SDS, and 0.5% deoxycholic acid) by sonication (50% for 30 s) and saved for analysis. Protein concentration was measured in S1 and P2 fractions by the BCA methods as described by the manufacturer (Pierce).

2.2.7 Proximity ligation assay (PLA)

Specific protein-protein interactions between LAMP2 and misfolded SOD1 were analyzed using Duolink *in situ* Red Starter Kit Mouse/Rabbit (DUO92101, Millipore Sigma Canada Co., Oakville, Ontario). CHO cells were transfected to overexpress SOD1-G93A protein tagged with GFP. These SOD1-G93A overexpressing CHO cells were seeded on poly-D-lysine (PDL) coated coverslips and were fixed by using 4% paraformaldehyde. The cells were washed with PBS and permeabilized by using 0.25% Triton X-100 in PBS for 10 mins followed by incubation with Duolink blocking solution in a preheated humidified chamber at 37 ℃ for 1 hour. Primary antibody solution containing mouse-anti-human misfolded SOD1 (B8H10) 1:1000 and rabbit-anti-human LAMP2 1:1000 was added and incubated for 1 hour in a preheated humidified chamber at 37 ℃. Then, secondary antibodies conjugated with oligonucleotides were added and incubated for 1 hour at 37 ℃, followed by incubation with ligation-ligase solution for 30 minutes at 37 ℃, which consists of two oligonucleotides and ligase. In this step, the oligonucleotides hybridize to the two PLA probes and join to a closed loop if

they are in close proximity. After ligation, the samples were incubated with amplification polymerase solution for 100 minutes at 37℃, which consists of nucleotides and fluorescently labeled oligonucleotides. Coverslips were mounted on the slide using Duolink mounting medium with DAPI. The PLA signals was visible as a distinct fluorescent spot and images were obtained using a Carl Zeiss AxioImager Z2 microscope and processed with Zen Pro imaging software (Zeiss, Germany).

2.2.8 SOD1-G93A enriched neural stem cell (NSC) culture

Time pregnant female C57BL/6 mice mated with G93A male mice were humanely euthanized by CO_2 gas followed by cervical dislocation, and embryos were removed. The day of the positive vaginal plug was considered as E0.5 of pregnancy and embryos were collected at E14.5 and placed in Earle's Balanced Salt Solution (EBSS) solution on ice. Transgenic embryos were genotyped by PCR of DNA obtained from tails. The brain was removed and then cortices were dissected out, triturated and cells passed through a 40 μM mesh. Cells were maintained in Complete StemPro NSC media containing basic fibroblast growth factor (bFGF) (20 ng/ml) and human epidermal growth factor (hEGF) (20 ng/ml) (Table 2.1), in order to maintain NSC characteristics. For NSC differentiation, the NSC were harvested by centrifugation and plated on a PDL- and laminin-coated 6-well plates in complete StemPro NSC medium (Table 2.1). Then the medium would be changed to neural differentiation medium (Table 2.2) after 2

days incubation. The cells were fed every third day by aspirating half of the medium from each well and replacing it with fresh neural differentiation medium.

Table 2.1 Complete StemPro NSC medium

Component	Final conc.	Source	Cat#
KnockOut DMEM/F-12	1×	Gibco	12660-012
GlutaMAX-I Supplement	2 mM	Gibco	35050-061
bFGF (100 μg/ml)	20 ng/ml	Gibco	PHG0024
EGF (100 μg/ml)	20 ng/ml	Gibco	PHG0314
StemPro Neural Supplement	2%	Gibco	A10508-01
Penicillin-Streptomycin-Neomycin (PSN) antibiotic mixture (100×)	1×	ThermoFisher	15640055

Table 2.2 Neural differentiation medium

Component	Final conc.	Source	Cat#
Neurobasal Medium	1×	Gibco	A35829-01
GlutaMAX-I Supplement	2 mM	Gibco	35050-061
B-27 Supplement (50×), serum free	2%	Gibco	17504-044
Penicillin-Streptomycin-Neomycin (PSN) antibiotic mixture (100×)	1×	ThermoFisher	15640055

2.2.9 Immunocytochemistry (ICC)

Cells were grown on coverslips coated with PDL. Cells were fixed in 4% paraformaldehyde in PBS pH 7.4 for 15 minutes at room temperature and then were washed three times with PBS. Samples were incubated for 10 minutes in PBS containing 0.25% Triton X-100 (PBST) for improving the penetration of the antibody. After three times wash with PBS, coverslips were incubated in 1% BSA in PBST for 30 minutes to block unspecific binding of the antibodies. After blocking, samples were incubated with primary antibodies in 1% BSA overnight at 4℃ as indicated in Table 2.3. Following three additional washes, secondary antibodies were applied and incubated for 1 hour at room temperature in the dark. After being washed three final times, cells were incubated with Hoechst 33342 (Calbiochem) to counter-stain for nuclei, and then coverslips were mounted with a drop of fluorescence mounting medium (Dako North America, Inc. Carpinteria, CA 93013, USA). These slides can be stored in the dark at -20℃ or +4℃. Fluorescence pictures were taken on a Carl Zeiss AxioImager Z2 microscope and processed with Zen Pro imaging software (Zeiss, Germany).

Table 2.3 Primary antibodies

Antibody	Host Species	Application (Dilution)	Source	Cat#
SOD1 (8B10)	Mouse	WB (1:1000)	ThermoFisher	MA1-105
SOD1	Rabbit	WB (1:1000)	Abcam	AB52950

Misfolded SOD1 (A5C3)	Mouse	WB (1:1000)	MediMabs	MM-0070-3-P
Misfolded SOD1 (B8H10)	Mouse	IF (1:100)	MediMabs	MM-0070-P
MAP2	Rabbit	IF (1:100)	ThermoFisher	PA5-17646
GFP	Mouse	IF (1:100)	Abcam	AB1218
MCT1	Mouse	WB (1:1000)	Abcam	AB90582
LAMP2	Rabbit	WB (1:1000) IF (1:500)	ThermoFisher	PA1-655

2.2.10 Electron microscopy (EM)

Mice were anesthetized by isoflurane inhalation. After anesthesia, animals were intracardially perfused with 0.1 M PBS containing 50 units/ml heparin sodium and then with fixation solution containing 2% paraformaldehyde, 2% glutaraldehyde and 0.1 M PBS (pH=7.4). The L4 (lumbar) efferent nerve fibers were then collected and further fixed in 0.1 M Sorensen's buffer (a double strength Sorensen's buffer, is prepared by mixing 5.24 g $NaH_2PO_4 \cdot H_2O$ and 23.0 g Na_2HPO_4 with 1000 ml ddH_2O, pH=7.4) containing 3% glutaraldehyde at room temperature for 3 hours. The fixed samples were washed by immersion in 0.1 M Sorensen's buffer containing 5% sucrose at 4 ℃ overnight. The next day, the samples were further washed in 0.1 M Sorensen's buffer containing 5% sucrose two times for 40 minutes each at room temperature on an orbital shaker. After the final washing, samples were stored in 0.1 M Sorensen's buffer containing 5% sucrose at 4 ℃ until post-fixation with osmium tetroxide was applied.

The samples were then transferred onto a clean glass slide. Several 1×1×1 mm tissue-blocks were made using an ethanol-treated oil-free single edge blade. The tissue blocks were then post fixed for 1-2 hours in 1% osmium tetroxide prepared in 0.1 M Sorensen's buffer at room temperature followed by washes in 0.1 M Sorensen's buffer three times for ten minutes each. After the tissues had been fixed and washed, the complete dehydration process was performed. Tissues were treated in a graded series of alcohol: 30% 10 minutes, 50% 10 minutes, 70% 10 minutes, 90% 2×10 minutes, and 100% 3×10 minutes. A treatment of methanol for 20 minutes was applied to further remove the water from the tissues, and then the tissue-blocks were incubated twice in propylene oxide for 10 minutes each to replace the residual alcohol, followed by two steps of the infiltration process for 1 hour each at room temperature as follows: an incubation in a mixture containing one part propylene oxide and two parts embedding medium and an incubation in a mixture containing two parts propylene oxide and one part embedding medium (Table 2.4). Finally, the tissue blocks were transferred into the embedding capsules (Cat#. 70000-B, Electron Microscopy Sciences) containing 700 μl pure embedding medium at room temperature for 24 hours followed by the polymerization process in an oven at 60 ℃ for 48 hours.

Table 2.4 Embedding medium for electron microscopy

Reagent	Volume (for approx. 5 blocks)
Poly/Bed 812	2.5 ml
Araldite 502	2.5 ml
DDSA	6 ml
DMP-30	225 μl

All materials were provided in the Araldite 502/PolyBed 812 Kit purchased from Polysciences, Inc. The embedding medium recipe was provided with the kit. The compositions were fully mixed by a magnet stirrer for 1 hour, then the mixture was incubated for another 1 hour to remove bubbles.

The polymerized EM blocks were collected from the embedding capsules by a capsule press (Cat#. 69920-00, Electron Microscopy Sciences). The EM blocks were trimmed so that sections would only be cut from a small of the block face. After the trimming procedure, the cutting face of the block had a length of less than 2 mm to each edge. Thick, 1 μm sections were cut manually using a diamond knife. Sections were collected and stained with 1% toluidine blue. Under a light microscope, the desired area was identified. Therefore, the cutting face of EM blocks was trimmed even smaller. Then ultrathin sections were cut using a microtome. The ultrathin sections were cut floating on the water surface of the knife reservoir. The thickness was determined by the interference color of the sections; sections with silver color indicating a thickness of 50-70 nm were selected and collected onto copper grids. The grids were air-dried on filter paper

and were stored in the grid case until the staining was performed. Several drops of 5% uranyl acetate were pipetted on a wax-coated Petri dish, and the grid containing ultrathin sections were put onto the solution drops upside down for 30 minutes followed by three washes in water. After absorbing the residual water from the grids with filter paper, the grids were incubated with 0.2% lead citrate for 10 minutes followed by three washes in water. Finally, the ultrathin sections were air-dried for 30 minutes and stored in the grid case until photography was performed using a Philips 201 electron microscope.

2.2.11 Histology analysis

2.2.11.1 Hematoxylin and eosin (H&E) staining

Wild type (WT) mice were euthanized after receiving a long-term IP injection of CT-4 peptide at a dose of 10 mg/kg from 60 days to 173 days of age. The mice were anesthetized and transcardially perfused with 0.9% NaCl. Mouse tissues (brain, heart, spinal cord, kidney, liver, muscle, lung, and spleen) were fixed overnight in 10% buffered formalin at room temperature and then stored in 70% ethanol until processing. Fixed tissues were processed for paraffin embedding. Tissues were dehydrated using 70% ethanol for 1 hour, 95% ethanol for 3 hours, 100% ethanol for 6 hours, and xylene for 2.5 hours. The tissues were then equilibrated in two melted paraffin baths, each for 6 hours. Tissues were then embedded in paraffin blocks. Blocks were incubated at 4℃ for approximately 4

hours prior to removing block molds. Tissue sections (5 μm thickness) were then cut and adhered to glass slides.

H&E staining was conducted according to routine protocols (242). Briefly, paraffin embedded tissue sections were subjected deparaffinized by incubating two times with xylene (3 minutes each time). Following deparaffinization, slides were rehydrated to water using decreasing concentrations of ethanol: absolute alcohol, 95% alcohol and distilled water (10 dips in each). Slides were then stained with hematoxylin solution for 5 min followed 5 dips in 1% acid ethanol (1% HCl in 70% ethanol) and then rinsed in distilled water. Then the sections were stained with eosin solution for 3 min and followed by dehydration with 95% alcohol followed by three changes in absolute alcohol (10 dips in each). Two changes in xylene for clearing were performed before mounting the slides. The mounted slides were then visualized using light microscopy and images were taken using a Carl Zeiss M2 microscope and processed with Zen Pro imaging software (Zeiss, Germany).

2.2.11.2 Nissl staining

G93A transgenic mice were euthanized after receiving a long-term IP injection of either CT-4 or mCT-4 peptide at a dose of 10 mg/kg from 60 days to 149 days of age. The mice were anesthetized and transcardially perfused with 0.9% NaCl, followed by 4% paraformaldehyde (PFA) (dissolved in 0.01M PBS, pH = 7.4). The L4 spinal cord segments were collected and fixed in 4% PFA (w/v) for 24h

at 4℃. Samples were dehydrated in a 30% sucrose solution for a further 24h. The sucrose solution was then changed every 24h for twice more. Lastly, samples were embedded in OCT cryocompound (Sakura CN: 1437355) and stored at -80℃ until sectioned.

Then, 12 μm-thick sections were cut and adhered to glass slides. Sections were stained with cresyl violet for Nissl staining, in according with the manufacturer's instructions (NovaUltra Nissl Stain Kit, Cat# IW-3007, IHCWORLD, USA). Images are captured using a Carl Zeiss M2 microscope and processed with Zen Pro imaging software (Zeiss, Germany). Nissl-positive cells were automatically counted in 3 randomly selected slides per sample in the ventral horn of the spinal cord and were quantified using Image J software.

2.2.12 Statistical analysis

Data are presented as the mean $\pm$ SD. For statistical comparison between two groups, Student's t-test was used. Multiple comparisons were performed by one-way ANOVA followed by Bonferroni's multiple comparisons test. Differences were considered to be statistically significant when $P < 0.05$.

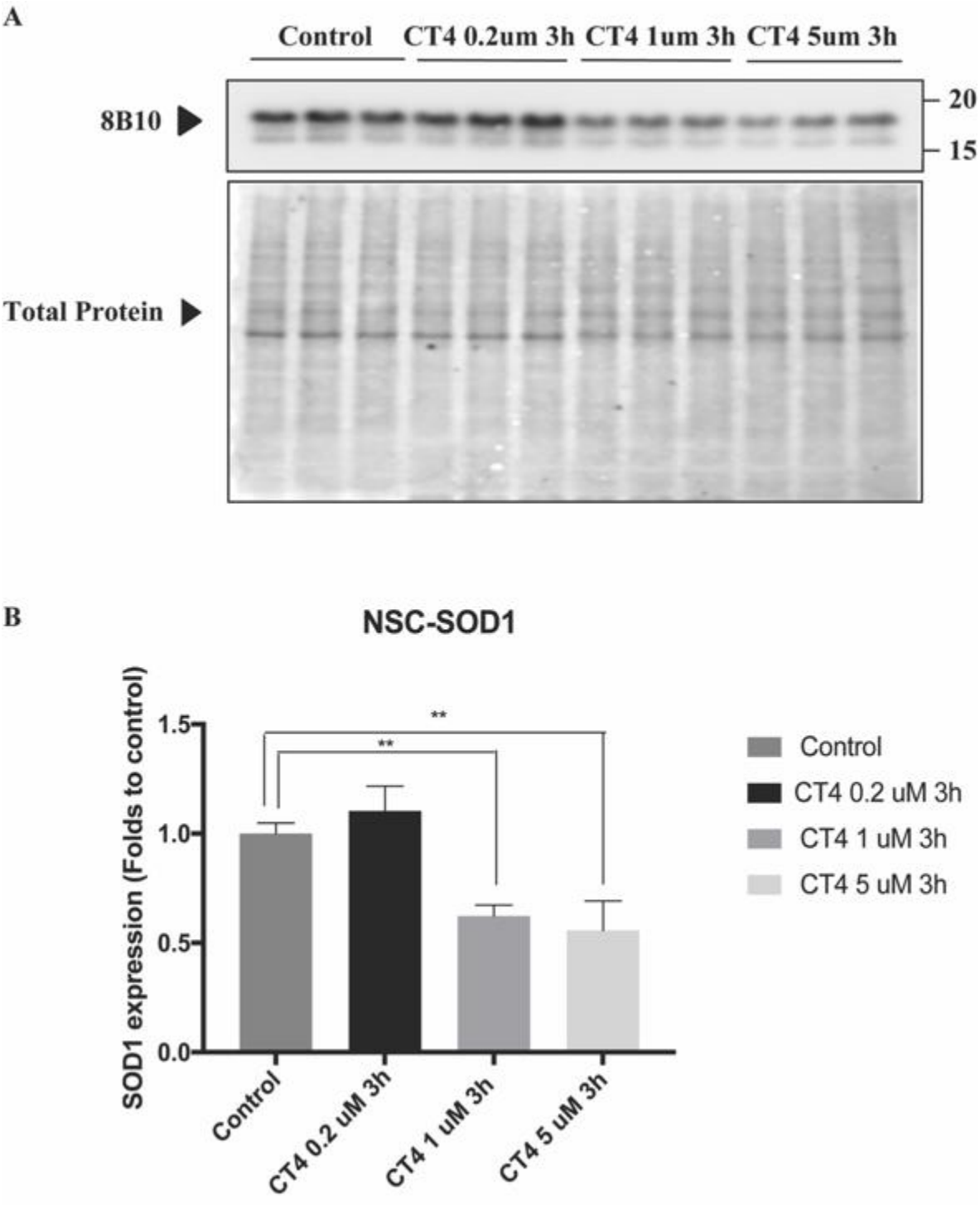
2.3 Results

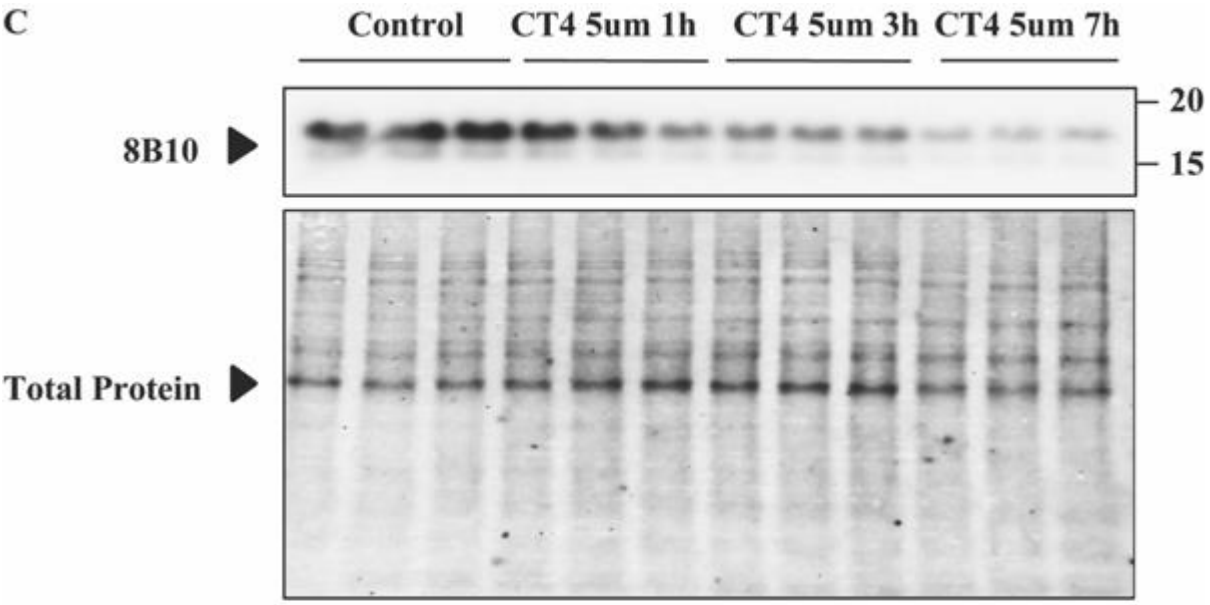
2.3.1 CT-4 potently decreases SOD1-G93A in dose- and time-dependent manners.

Neuron-enriched cultures were differentiated from G93A transgenic mice embryonic neuron stem cells (NSC). A dose-dependent study in those SOD1-G93A overexpressing neurons revealed an extensive decrease in SOD1 expression 3h after exposure to 1 μM CT-4 peptide as well as a similar decrease at concentrations of 5 μM (**P < 0.01). However, no significant differences were noted in SOD1 protein expression at 3h of 0.2 μM CT-4 exposure relative to that of control (Figure 2.2A and B). Time-course analysis of primary neurons exposed to 5 μM CT-4 demonstrated a significant reduction in SOD1 level as early as 1h (*P < 0.05). Furthermore, the significant reduction in SOD1 protein expression sustained after 4h and 7h of 5 μM CT-4 exposure (**P < 0.01; ***P < 0.001 respectively) (Figure 2.2C and D).

Consistent with these finding, co-immunofluorescence staining of MAP2 and misfolded SOD1 antibody (B8H10) revealed that the G93A mutants were reduced throughout neurons in the presence of the CT-4 peptide. Cells were treated with CT4-peptide for 2 hours at a concentration of 5 μM and then were analyzed at different recovery time points (0h, 2h, 5h and 22h). Of the cells that acquired MAP2-positive immunoreactivity, the control group had significantly higher misfolded SOD1 (B8H10) fluorescence intensity when compared to the 0h, 2h, 5h post treatment groups (Figure 2.3A – 2.3H), while the misfolded SOD1

fluorescence intensity of 22h post treatment group recovered (Figure 2.3I and 2.3J).




C
Control
CT4 5um 1h
CT4 5um 3h
CT4 5um 7h
8B10
20
15
Total Protein

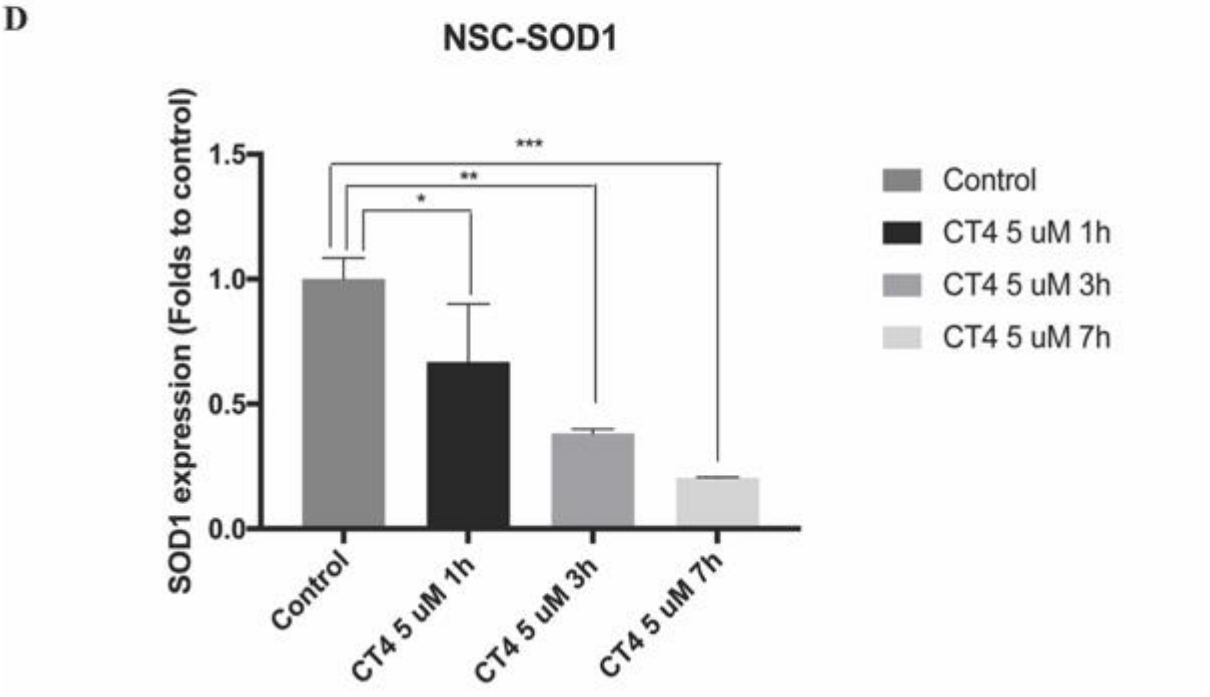

D
NSC-SOD1
SOD1 expression (Folds to control)
1.5
1.0
0.5
0.0
***
**
*
Control
CT4 5 uM 1h
CT4 5 uM 3h
CT4 5 uM 7h
Control
CT4 5 uM 1h
CT4 5 uM 3h
CT4 5 uM 7h

Figure 2.2 Treatment with CT-4 peptide results in knockdown of SOD1-G93A in primary neuron prepared from the G93A transgenic mice in dose- and in time-dependent manners.

(A) SOD1-G93A overexpressing neurons differentiated from G93A transgenic mice embryonic neuron stem cells (NSC) were treated with 0.2, 1, 5 μM CT-4 peptide for 3 hours. (B) Quantitative data of SOD1 expression. (C) SOD1-G93A over-expressing neurons differentiated from G93A transgenic mice embryonic NSC were treated with 5 μM CT-4 peptide for 1, 3, 7 hours. (D) Quantitative data of SOD1 expression. In (A) and (C), after treatment with CT-4 peptide, total cell extracts were prepared and subjected to western blot analysis using antibodies against total SOD1 (8B10). Equal volumes of lysates with a total of 10 μg protein was applied to 12% TGX Stain-Free polyacrylamide gels. Total protein generated by stain-free visualization were used to ensure equivalent loading. One-way ANOVA followed by Bonferroni's Multiple Comparison Post-Test were performed to establish significant differences with control group: *P < 0.05; **P < 0.01; ***P < 0.001. Bars represent mean $\pm$ SD, n=3 per group.

Control
(A)
(B)
20 μm
2h treatment & 0h recovery
(C)
(D)
20 μm
2h treatment & 2h recovery
(E)
(F)
20 μm
2h treatment & 5h recovery
(G)
(H)
20 μm
2h treatment & 22h recovery
(I)
(J)
20 μm

Figure 2.3 Co-immunofluorescence staining of MAP2 and misfolded SOD1 after treatment with CT-4 peptide in primary neuron prepared from the G93A transgenic mice.

SOD1-G93A overexpressing neurons differentiated from G93A transgenic mice embryonic NSC were treated with CT-4 peptide for 2 hours at a concentration of 5 μM and then were analyzed at different time points. Panels (B) (D) (F) (H) and (J) show representative microscopies images of SOD1-G93A overexpression neurons with MAP2 (Green) and misfolded SOD1 (B8H10) (Red) double immunofluorescent staining in control, 2h treatment & 0h recovery, 2h treatment & 2h recovery, 2h treatment & 5h recovery, and 2h treatment & 22h recovery, respectively. For a better display of misfolded SOD1 staining, panels (A) (C) (E) (G) and (I) show the misfolded SOD1 labeling only. Scale bar represents 20 μm.

2.3.2 SOD1-G93A protein has higher aggregation propensity relative to wild-type human SOD1 (hSOD1-WT) protein

In order to determine the aggregation propensity of SOD1-G93A protein, CHO cells were transiently transfected with the indicated wild-type human SOD1 (hSOD1-WT) and SOD1-G93A constructs. After indicated hours following transfection, cells were harvested and detergent-soluble (S1) and detergent-insoluble (P2) fractions were obtained and subjected to western blot assay using antibodies against human SOD1 (abcam) and total SOD1 (8B10) as described in the Materials and Methods section (Table 2.3). In the experiment performed by using antibody against human SOD1 (abcam), expression of hSOD1 in both hSOD1-WT and SOD1-G93A transfected group can be detected at 24- and 48-hour post-transfection in the S1 fraction (Figure 2.4A). However, in the P2 fraction, expression of hSOD1 can only be detected at 48 hours post-transfection in the cells transfected with SOD1-G93A variant (Figure 2.4B). To verify this result, I performed another experiment using antibody against total SOD1 (which can recognize human SOD1 and rodent SOD1). As expected, in the S1 fraction, expression of hSOD1 can be detected only in hSOD1-WT and SOD1-G93A transfected group at each time point, while hamster SOD1 expression can be detected in all groups (Figure 2.4C). Note that, in the P2 fraction, expression of hSOD1 can only be detected at 48- and 72-hour post-transfection in the cells transfected with hSOD1-G93A variant. In addition, two lighter SOD1-positive bands were observed in the insoluble fraction (P2) at a position corresponding to

the SOD1 dimer, indicating dimerization of the misfolded SOD1-G93A protein (Figure 2.4D). These data suggested that SOD1-G93A protein showed greater aggregation propensity while compared with hSOD1-WT protein. In addition, it took at least 48 hours for the formation of the detergent-insoluble SOD1 protein in our transient transfected CHO cells.

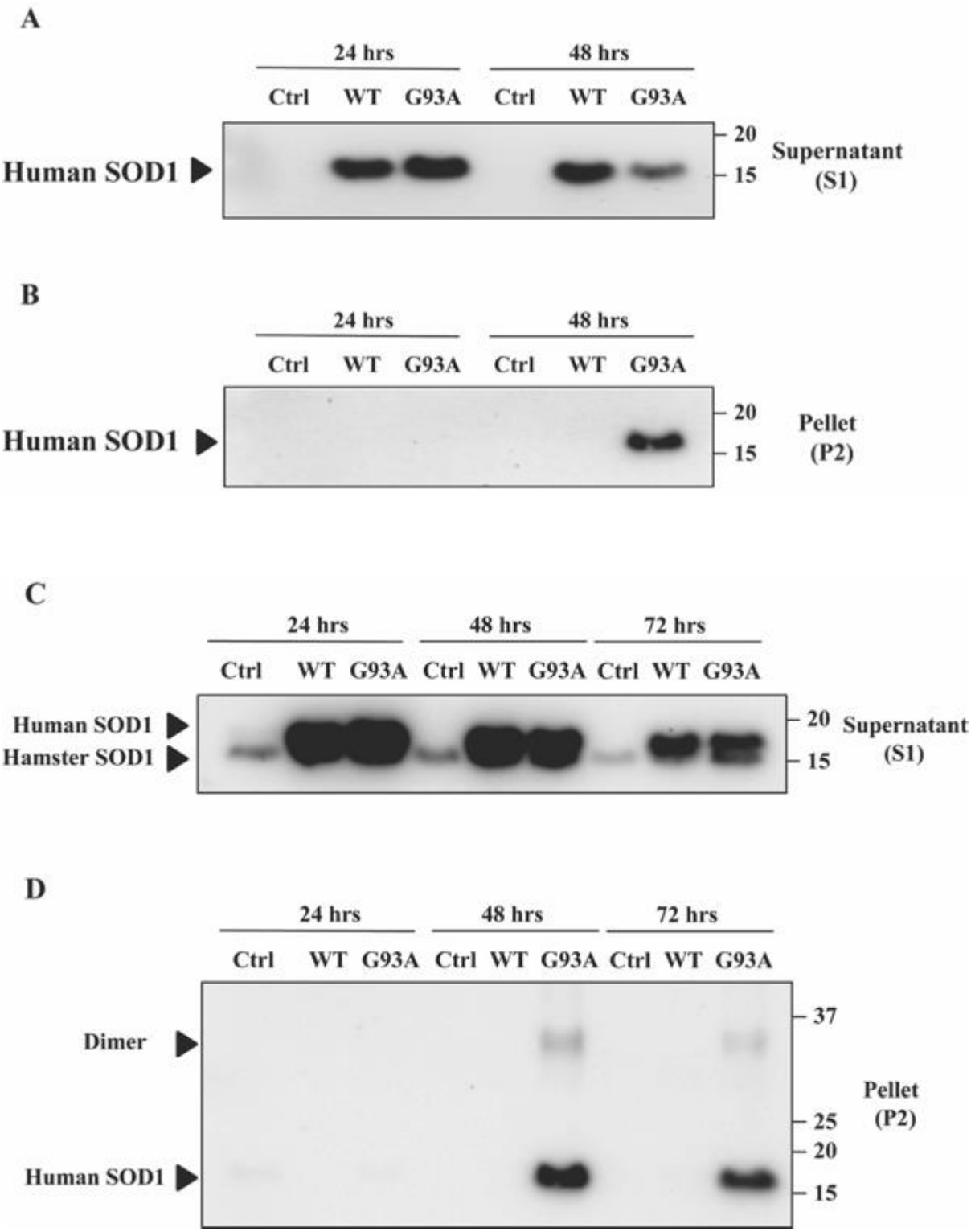

A
24 hrs
48 hrs
Ctrl
WT
G93A
Ctrl
WT
G93A
Human SOD1
20
15
Supernatant
(S1)
B
24 hrs
48 hrs
Ctrl
WT
G93A
Ctrl
WT
G93A
Human SOD1
20
15
Pellet
(P2)
C
24 hrs
48 hrs
72 hrs
Ctrl
WT
G93A
Ctrl
WT
G93A
Ctrl
WT
G93A
Human SOD1
Hamster SOD1
20
15
Supernatant
(S1)
D
24 hrs
48 hrs
72 hrs
Ctrl
WT
G93A
Ctrl
WT
G93A
Ctrl
WT
G93A
Dimer
Human SOD1
37
25
20
15
Pellet
(P2)

Figure 2.4 SOD1-G93A protein has higher aggregation propensity relative to hSOD1-WT protein.

Immunoblot of detergent-insoluble (P2) and soluble (S1) fractions of CHO cells transfected with constructs of hSOD1-WT and SOD1-G93A for indicated hours. (A and B) Blots were probed with an antibody that recognizes human SOD1 proteins. (C and D) Blots were probed with an antibody (8B10) that recognizes both rodent and human SOD1 proteins.

2.3.3 Knockdown of SOD1 by CT4 peptide proceeds through a lysosome involved protein degradation pathway.

To determine whether the knockdown of SOD1 by CT4 peptide occurs through a lysosome involved protein degradation pathway, neuron-enriched cultures differentiated from G93A transgenic mice embryonic NSC were exposed to 5 μM CT4 peptide for 3h in the presence or absence of 10 μM ammonium chloride (NH_4Cl). NH_4Cl, the weak base, is a lysosomotropic inhibitor with the inhibitory effect on the lysosomal pathway involved protein degradation (243). Treatment with CT4 peptide alone resulted in the downregulation the expression of total SOD1, and the decline of level of SOD1 in both soluble and insoluble fractions while compared with the control group (Figure 2.5) (**P < 0.01). As expected, pretreatment of cells with NH_4Cl did block the downregulation of total SOD1, soluble and insoluble SOD1 level mediated by CT4 peptide. No significate difference was noted in the SOD1 protein expression between the control group and the combined treatment with NH4Cl and CT4 peptide group.

To investigate the effect of autophagy induced by starvation on CT4 peptide treatment, I also deprived cells of nutrients by incubating them in Earle's Balanced Salt Solution (EBSS) to activated lysosome function/induce lysosomal degradation (244, 245). Nutrient deprivation of the neuronal cultures led to a significant decreased SOD1 level in all the total, soluble and insoluble fractions at an enhanced rate (Figure 2.5) (**P < 0.01; ***P < 0.001 respectively).

Duolink proximity ligation assay (PLA) will produce a positive signal when two different proteins are located within 40 nm of proximity - a distance with a potentially direct molecular interaction (246, 247). To further identify physical closeness of misfolded SOD1 and lysosome, PLA assay was performed to detect *in situ* protein co-localization using anti-GFP and anti-LAMP2 antibodies in the SOD1-G93A tagged with GFP overexpressing CHO cells treated with CT-4 peptide. CHO cells were transiently transfected with the indicated hSOD1-WT and SOD1-G93A constructs tagged with EGFP, and then these cells were treated with 20 μM CT-4 peptide for 3 hours. Our results showed an increase of PLA positive signals in CT-4 peptide treatment group, which are visible fluorescent red dots in cell body, confirming CT-4 induced co-localization and interaction of both misfolded SOD1 and LAMP2 proteins. The LAMP2 protein is a member of membrane glycoproteins, which plays a very critical role in CMA (248) (Figure 2.6). Taking together, these results suggested that our CT-4 peptide could increase misfolded SOD1 and LAMP2 binding. As such, treatment with CT-4 peptide decreases the level of misfolded SOD1 in a lysosome-dependent manner.

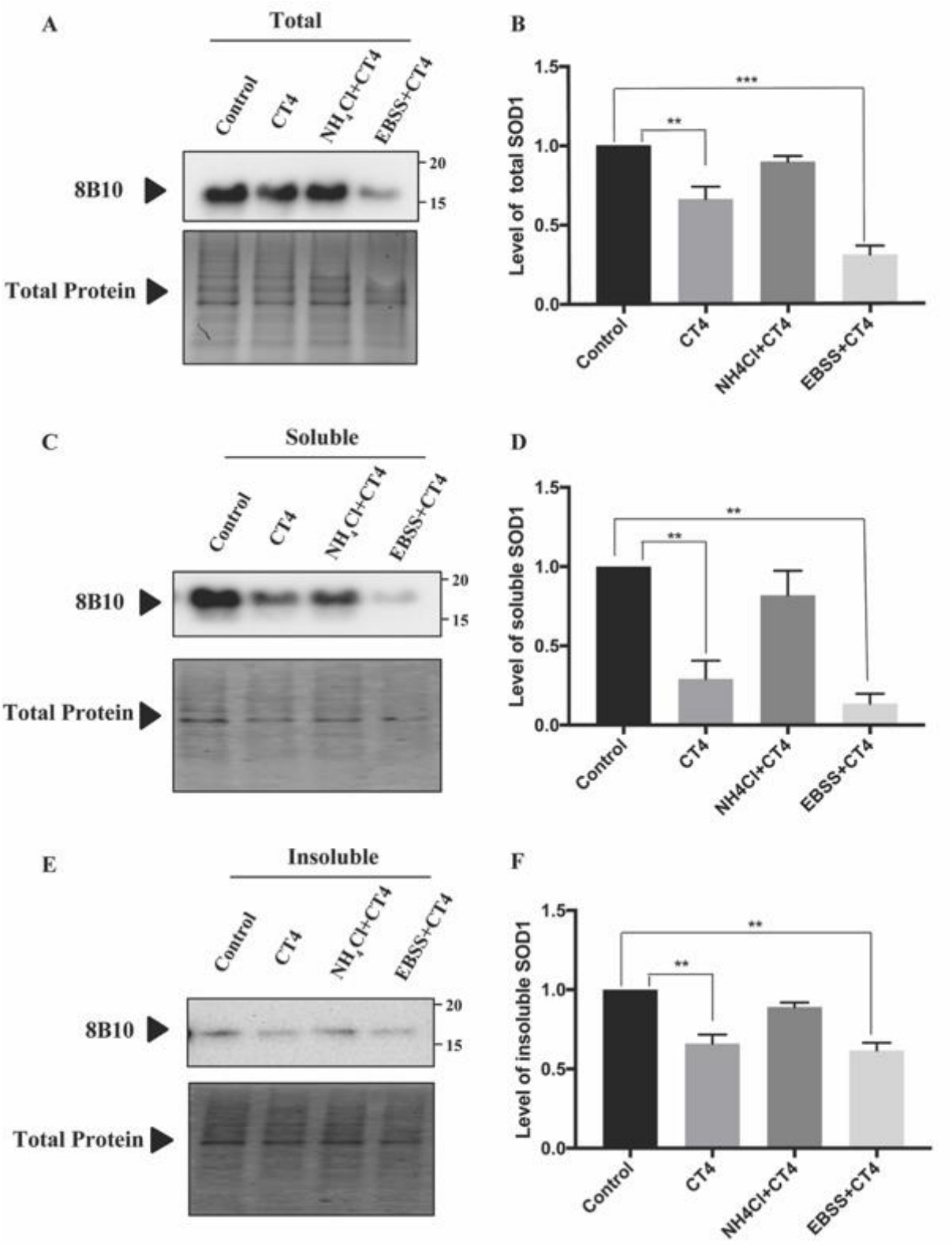

A
Total
Control
CT4
NH4Cl+CT4
EBSS+CT4
8B10
20
15
Total Protein
B
Level of total SOD1
1.5
1.0
0.5
0.0
**
***
Control
CT4
NH4Cl+CT4
EBSS+CT4
C
Soluble
Control
CT4
NH4Cl+CT4
EBSS+CT4
8B10
20
15
Total Protein
D
Level of soluble SOD1
1.5
1.0
0.5
0.0
**
**
Control
CT4
NH4Cl+CT4
EBSS+CT4
E
Insoluble
Control
CT4
NH4Cl+CT4
EBSS+CT4
8B10
20
15
Total Protein
F
Level of insoluble SOD1
1.5
1.0
0.5
0.0
**
**
Control
CT4
NH4Cl+CT4
EBSS+CT4

Figure 2.5 Knockdown of SOD1 by CT4 peptide proceeds through a lysosome involved protein degradation pathway.

Neuron-enriched cultures differentiated from G93A transgenic mice embryonic NSC were pretreated with or without 10 μM NH_4Cl or EBSS for 1hour, followed by treatment with 5 μM CT4 peptide for 3 hours. After treatment, total cellular extracts (A), detergent-soluble (C) and -insoluble (E) fractions from cells were prepared and subjected to western blot assay using antibody against SOD1 (8B10) as described in the Materials and Methods section. (B), (D) and (F) Quantitative data of SOD1 expression. Equal volumes of lysates with a total of 10 μg protein was applied to 12% TGX Stain-Free polyacrylamide gels. Total protein generated by stain-free visualization were used to ensure equivalent loading. One-way ANOVA followed by Bonferroni's Multiple Comparison Post-Test were performed to establish significant differences with control group: **P < 0.01; ***P < 0.001. Bars represent mean $\pm$ SD, n=3 per group.

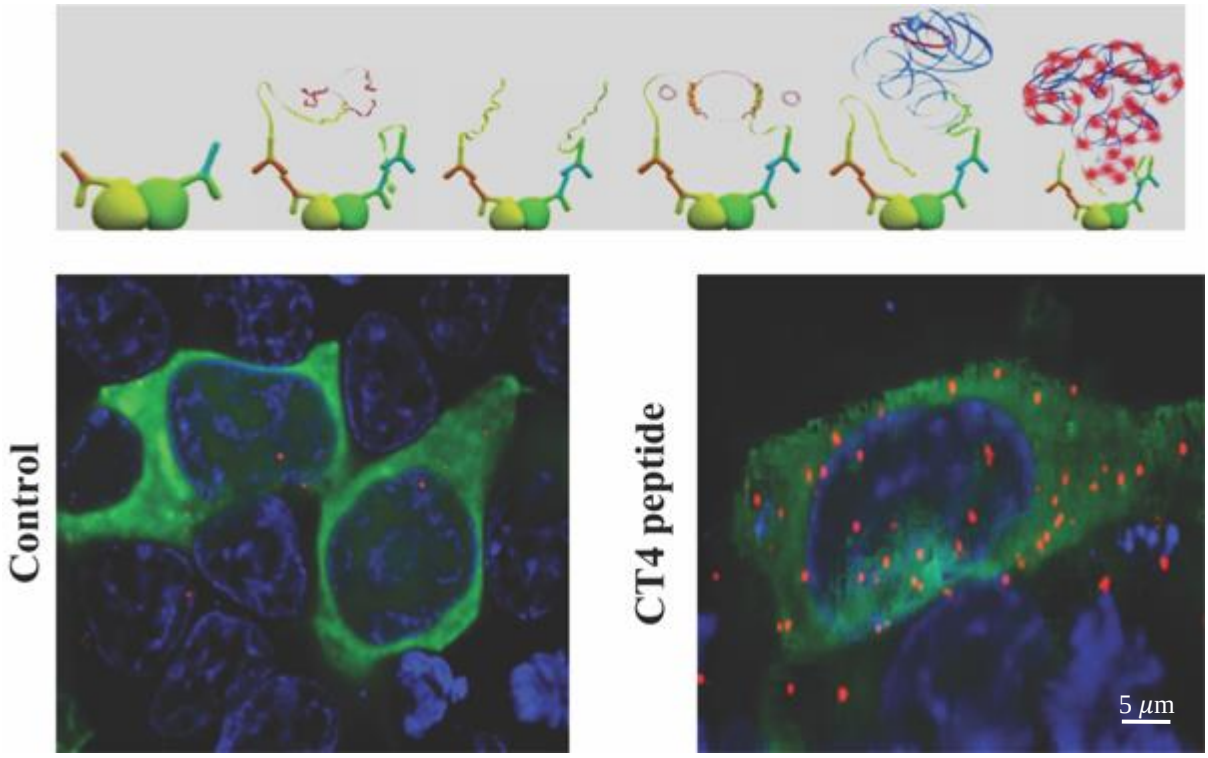


Figure 2.6 Proximity ligation assay (PLA) confirmed co-localization of misfolded SOD1 and LAMP2 after CT-4 treatment.

(A) Schematic representation of PLA reaction. The two modules (yellow and green) represent epitopes on two different proteins that are interacting. Secondary antibodies coupled with oligonucleotides (PLA probes) bind to the primary antibodies which recognizes these proteins of interest in the cell. When the PLA probes are in close proximity, connector oligos join the PLA probes and become ligated. The resulting closed, circular DNA template becomes amplified by DNA polymerase. Complementary detection oligos coupled to fluorochromes hybridize to repeating sequences in the amplicons. PLA signals are detected by fluorescent microscopy as discrete spots.

(B) SOD1-G93A tagged with GFP overexpressing CHO cells were cultured and treated with 20 μM CT-4 for 3 hours followed by PLA using anti-GFP and anti-LAMP2 primary antibodies. Red spots indicated interactions between GFP and LAMP2. Scale bar represents 5 μm.

2.3.4 Knockdown of misfolded SOD1 by CT-4 treatment in G93A transgenic mouse model of ALS.

In order to demonstrate A5C3 monoclonal antibody is more specific to ALS-associated misfolded SOD1 protein – SOD1-G93A compared to hSOD1-WT, denaturing SDS-PAGE followed by immunodetection was conducted by loading different amount protein extracts of neuron enriched culture prepared from the human WT and G93A transgenic mice embryonic NSC. Result revealed that the A5C3 antibody reacted specifically against the SOD1-G93A when the loading mount was below 10 μg, while there is no particular selectivity between hSOD1-WT and SOD1-G93A when the loading amount was above 10 μg (Figure 2.7). As such, I loaded 10 μg of each sample to obtain a preferential affinity for A5C3 antibody.

The 100-day old G93A mice received intraperitoneal (IP) injection of either saline or CT-4 peptide at a dose of 10 mg/kg body weight once every day (*q.d.*) for three days. Tissues, including spinal cord, brain, liver and muscle, were harvest at 24 hours, 48 hours, 1 week and 2 weeks post-treatment and followed by western blot analysis using antibody against misfolded SOD1 (A5C3).

Following the injection of CT-4 peptide, our results of misfolded SOD1 protein expression in spinal cord (SC), brain, liver and muscle of G93A transgenic mice revealed a significant reduction at 24 hours post-treatment when compared with control group (Figure 2.8). In addition, the marked knockdown effect on misfolded SOD1 protein by CT-4 peptide treatment was still noted in

SC, brain and liver 48 hours after injection, albeit not in muscle tissue (Figure 2.9).

In order to obtain a crude estimate of the duration of the knockdown effect by CT-4 peptide, I proceeded to detect the misfolded SOD1 protein level in G93A transgenic mice at 1- and 2-week post-injection. However, no statistic reduction of misfolded SOD1 protein level was observed for 1 week or 2 weeks recovery after CT-4 peptide treatment in our G93A transgenic mice SC, brain, liver or muscle (Figure 2.10 and 2.11).

To further validate to what extent the difference could be between 24- and 48-hour post-treatment in G93A transgenic mice, I compared the misfolded SOD1 protein expression in SC and brain for 24- and 48-hour recovery after treatment. In the SC, there was a significant reduction in the misfolded SOD1 protein expression in the 24 hours post-treatment group as compared to the control group. This significant decrease in misfolded SOD1 protein expression was maintained in the 48 hours post-treatment group relative to control. However, markedly reduction in misfolded SOD1 protein expression were noted in 24 hours post-treatment group relative to 48 hours post-treatment group (Figure 2.12 A and B). With respect to the brain tissues, our results revealed statistically significant knockdown effect in misfolded SOD1 protein expression in both 24- and 48-hour post-treatment groups relative to control. No significant differences were noted in misfolded SOD1 level in both 24- and 48-hour post-treatment groups (Figure 2.12 C and D).

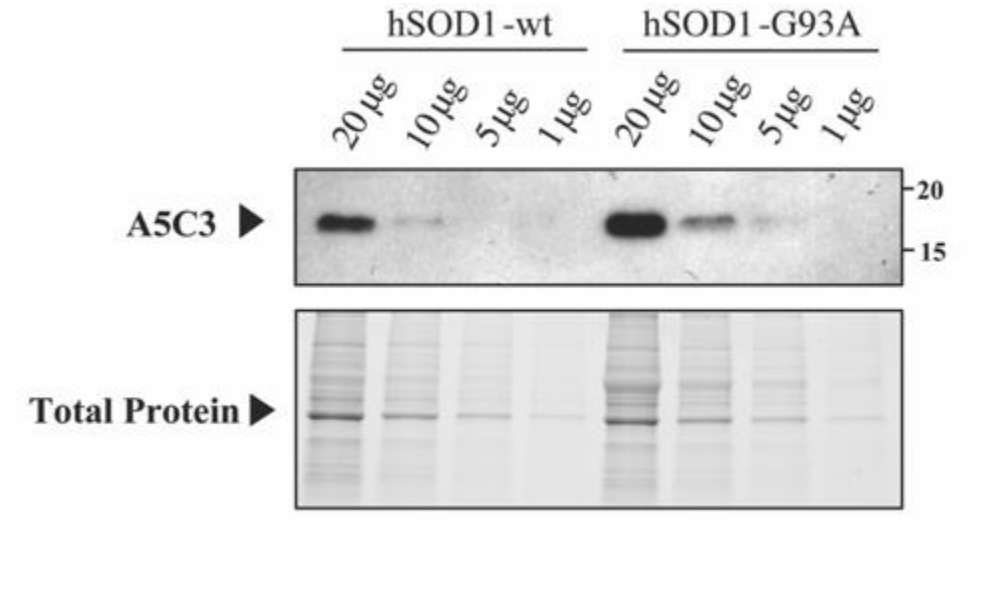


Figure 2.7 Denaturing sodium dodecyl sulfate-polyacrylamide gel electrophoresis (SDS-PAGE) western blotting analysis using misfolded SOD1 specific monoclonal antibody.

Denaturing SDS-PAGE followed by immunodetection using A5C3 monoclonal antibodies showing different affinity against hSOD1-WT and SOD1-G93A.

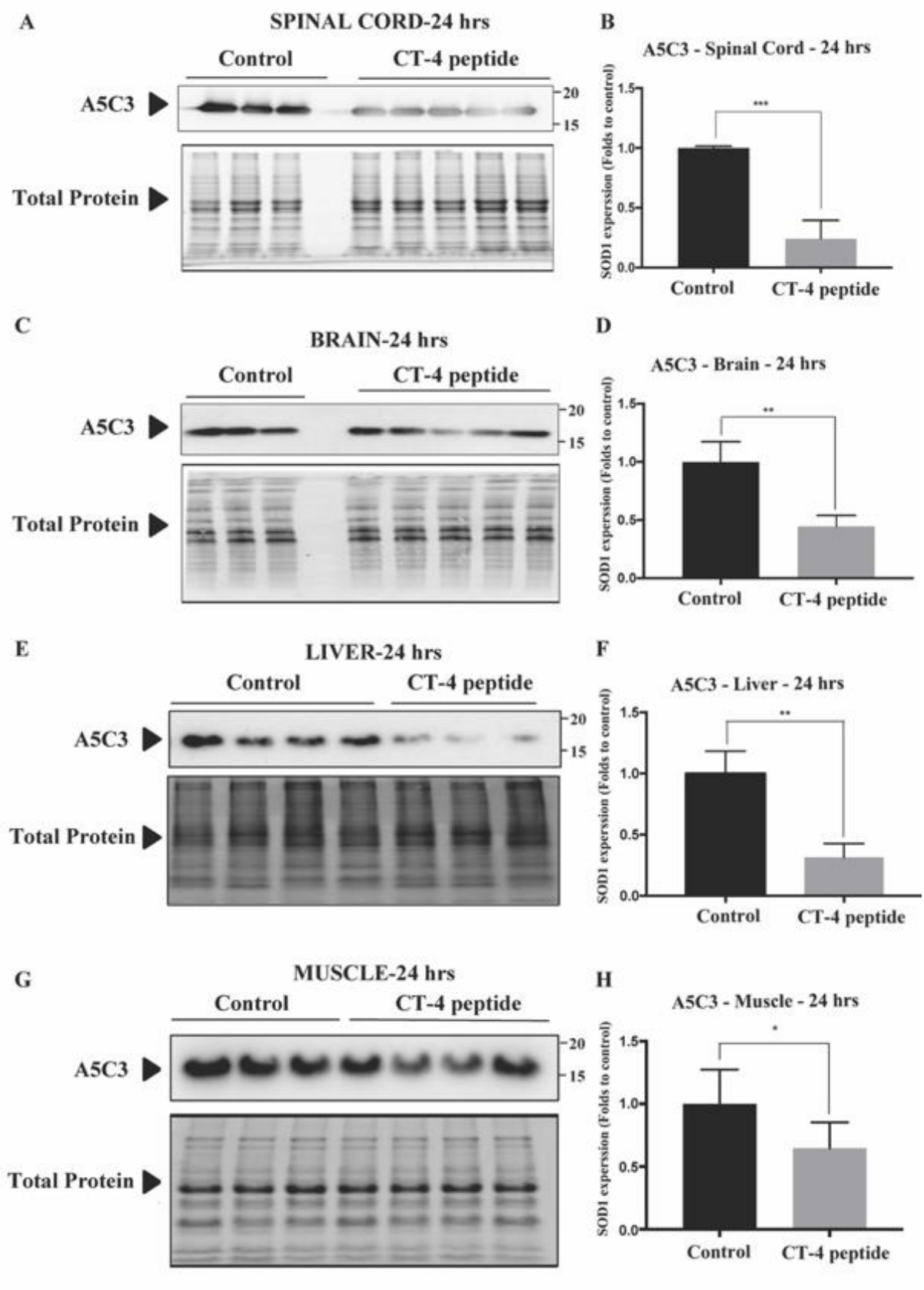

A
SPINAL CORD-24 hrs
Control
CT-4 peptide
A5C3
Total Protein
20
15
B
A5C3 - Spinal Cord - 24 hrs
SOD1 expression (Folds to control)
1.5
1.0
0.5
0.0
***
Control
CT-4 peptide
C
BRAIN-24 hrs
Control
CT-4 peptide
A5C3
Total Protein
20
15
D
A5C3 - Brain - 24 hrs
SOD1 expression (Folds to control)
1.5
1.0
0.5
0.0
**
Control
CT-4 peptide
E
LIVER-24 hrs
Control
CT-4 peptide
A5C3
Total Protein
20
15
F
A5C3 - Liver - 24 hrs
SOD1 expression (Folds to control)
1.5
1.0
0.5
0.0
**
Control
CT-4 peptide
G
MUSCLE-24 hrs
Control
CT-4 peptide
A5C3
Total Protein
20
15
H
A5C3 - Muscle - 24 hrs
SOD1 expression (Folds to control)
1.5
1.0
0.5
0.0
*
Control
CT-4 peptide

Figure 2.8 Injection with CT-4 peptide results in knockdown of misfolded SOD1 in the tissues from G93A transgenic mice at 24 hours post-treatment.

The G93A mice received intraperitoneal (IP) injection of either saline or CT-4 peptide at a dose of 10 mg/kg body weight once every day (*q.d.*) for three days at the age of 100 days. Tissues, including spinal cord (A), brain (C), liver (E), and muscle (G) from the control and treatment groups were harvest at 24 hours post-treatment and followed by western blot analysis using antibody against misfolded SOD1 (A5C3). (B, D, F, and H) Quantitative data of misfolded SOD1 expression in different tissues. Equal volumes of lysates with a total of 10 μg protein was applied to 12% TGX Stain-Free polyacrylamide gels. Total protein generated by stain-free visualization were used to ensure equivalent loading. Student's t-test was performed to establish significant differences with control group: *P < 0.05; **P < 0.01; ***P < 0.001. Bars represent mean ± SD, n≥3 per group.

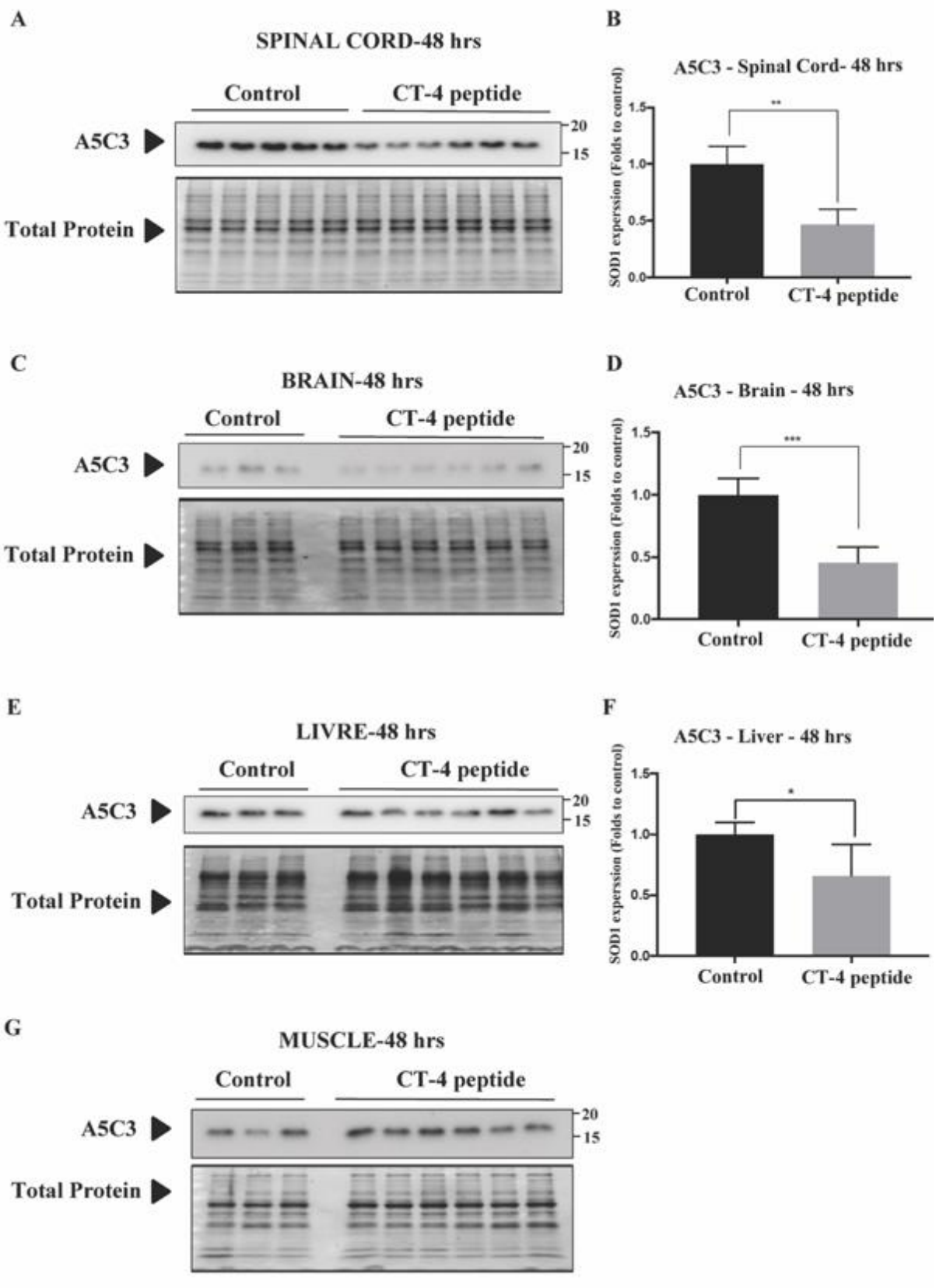

A
SPINAL CORD-48 hrs
Control
CT-4 peptide
A5C3
Total Protein
20
15
B
A5C3 - Spinal Cord- 48 hrs
SOD1 expression (Folds to control)
1.5
1.0
0.5
0.0
**
Control
CT-4 peptide
C
BRAIN-48 hrs
Control
CT-4 peptide
A5C3
Total Protein
20
15
D
A5C3 - Brain - 48 hrs
SOD1 expression (Folds to control)
1.5
1.0
0.5
0.0
***
Control
CT-4 peptide
E
LIVRE-48 hrs
Control
CT-4 peptide
A5C3
Total Protein
20
15
F
A5C3 - Liver - 48 hrs
SOD1 expression (Folds to control)
1.5
1.0
0.5
0.0
*
Control
CT-4 peptide
G
MUSCLE-48 hrs
Control
CT-4 peptide
A5C3
Total Protein
20
15

Figure 2.9 Injection with CT-4 peptide results in knockdown of misfolded SOD1 in the tissues from G93A transgenic mice at 48 hours post-treatment.

The G93A mice received IP injection of either saline or CT-4 peptide at a dose of 10 mg/kg body weight *q.d.* for three days at the age of 100 days. Tissues, including spinal cord (A), brain (C), liver (E), and muscle (G) from the control and treatment groups were harvest at 48 hours post-treatment and followed by western blot analysis using antibody against misfolded SOD1 (A5C3). (B, D, and F) Quantitative data of misfolded SOD1 expression in different tissues. Equal volumes of lysates with a total of 10 μg protein was applied to 12% TGX Stain-Free polyacrylamide gels. Total protein generated by stain-free visualization were used to ensure equivalent loading. Student's t-test was performed to establish significant differences with control group: *P < 0.05; **P < 0.01; ***P < 0.001. Bars represent mean ± SD, n≥3 in control group, n=6 in treated group.

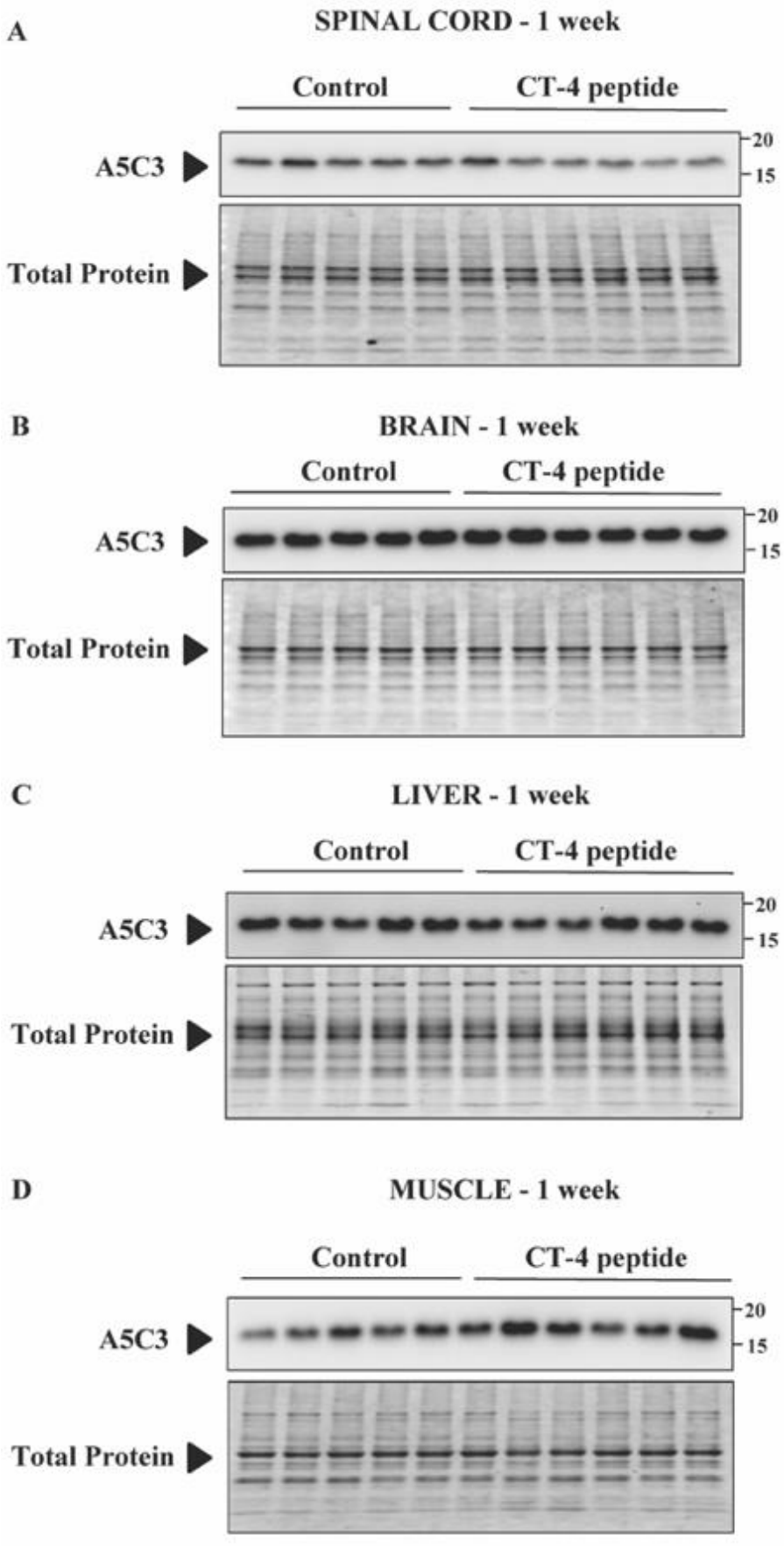

A
SPINAL CORD - 1 week
Control
CT-4 peptide
A5C3
Total Protein
20
15
B
BRAIN - 1 week
Control
CT-4 peptide
A5C3
Total Protein
20
15
C
LIVER - 1 week
Control
CT-4 peptide
A5C3
Total Protein
20
15
D
MUSCLE - 1 week
Control
CT-4 peptide
A5C3
Total Protein
20
15

Figure 2.10 No obvious reduction of misfolded SOD1 was observed for 1-week recovery after CT-4 peptide treatment in the tissues from G93A transgenic mice.

The G93A mice received IP injection of either saline or CT-4 peptide at a dose of 10 mg/kg body weight *q.d.* for three days at the age of 100 days. Tissues, including spinal cord (A), brain (B), liver (C), and muscle (D) from the control and treatment groups were harvest at 1-week post-treatment and followed by western blot analysis using antibody against misfolded SOD1 (A5C3). Equal volumes of lysates with a total of 10 μg protein was applied to 12% TGX Stain-Free polyacrylamide gels. Total protein generated by stain-free visualization were used to ensure equivalent loading, n=5 in control group, n=6 in treated group.

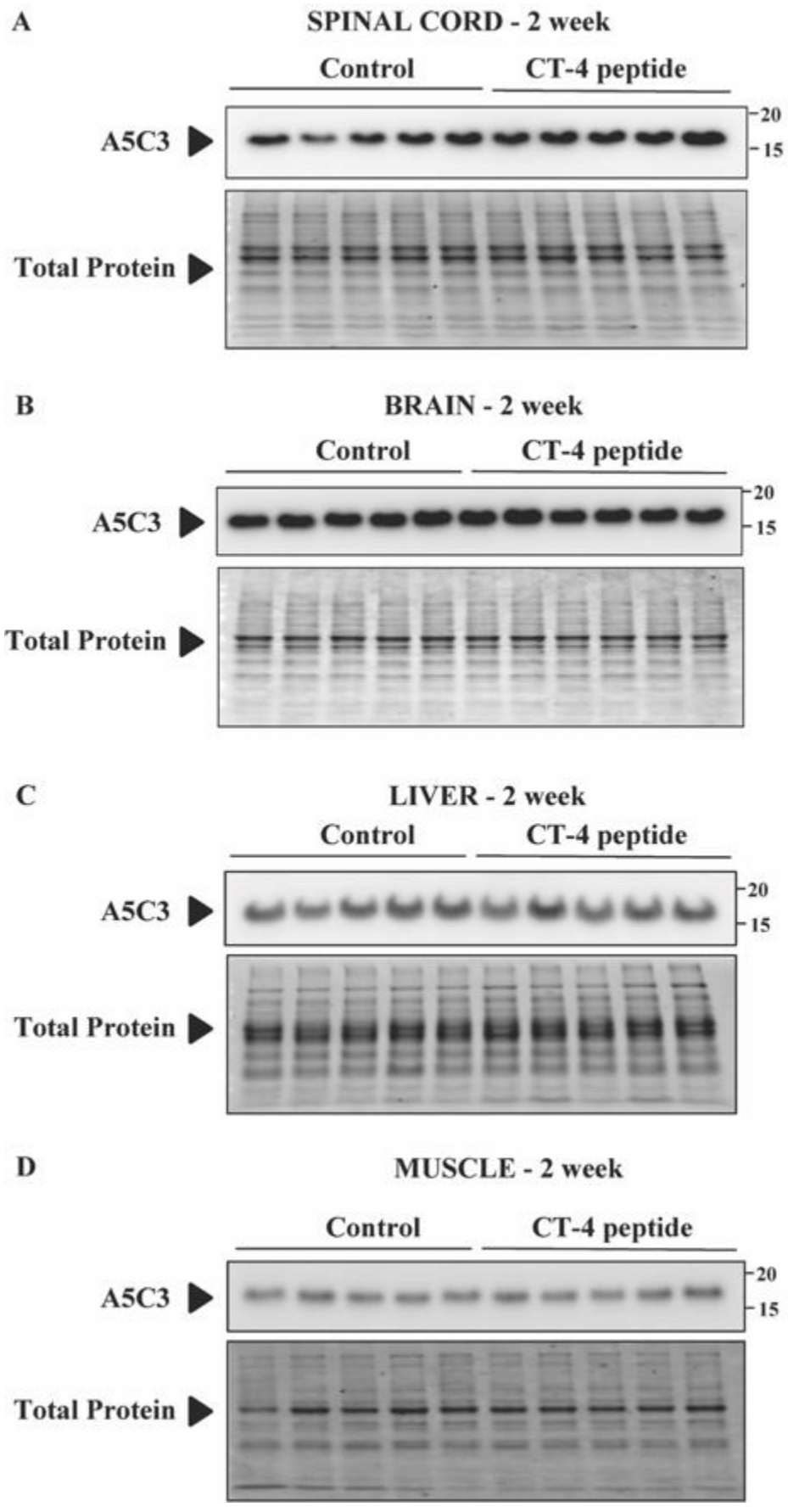

A
SPINAL CORD - 2 week
Control
CT-4 peptide
A5C3
20
15
Total Protein
B
BRAIN - 2 week
Control
CT-4 peptide
A5C3
20
15
Total Protein
C
LIVER - 2 week
Control
CT-4 peptide
A5C3
20
15
Total Protein
D
MUSCLE - 2 week
Control
CT-4 peptide
A5C3
20
15
Total Protein

Figure 2.11 No obvious reduction of misfolded SOD1 was observed for 2-week recovery after CT-4 peptide treatment in the tissues from G93A transgenic mice.

The G93A mice received IP injection of either saline or CT-4 peptide at a dose of 10 mg/kg body weight *q.d.* for three days at the age of 100 days. Tissues, including spinal cord (A), brain (B), liver (C), and muscle (D) from the control and treatment groups were harvest at 2-weeks post-treatment and followed by western blot analysis using antibody against misfolded SOD1 (A5C3). Equal volumes of lysates with a total of 10 μg protein was applied to 12% TGX Stain-Free polyacrylamide gels. Total protein generated by stain-free visualization were used to ensure equivalent loading, n=5 in control group, n≥5 in treated group.

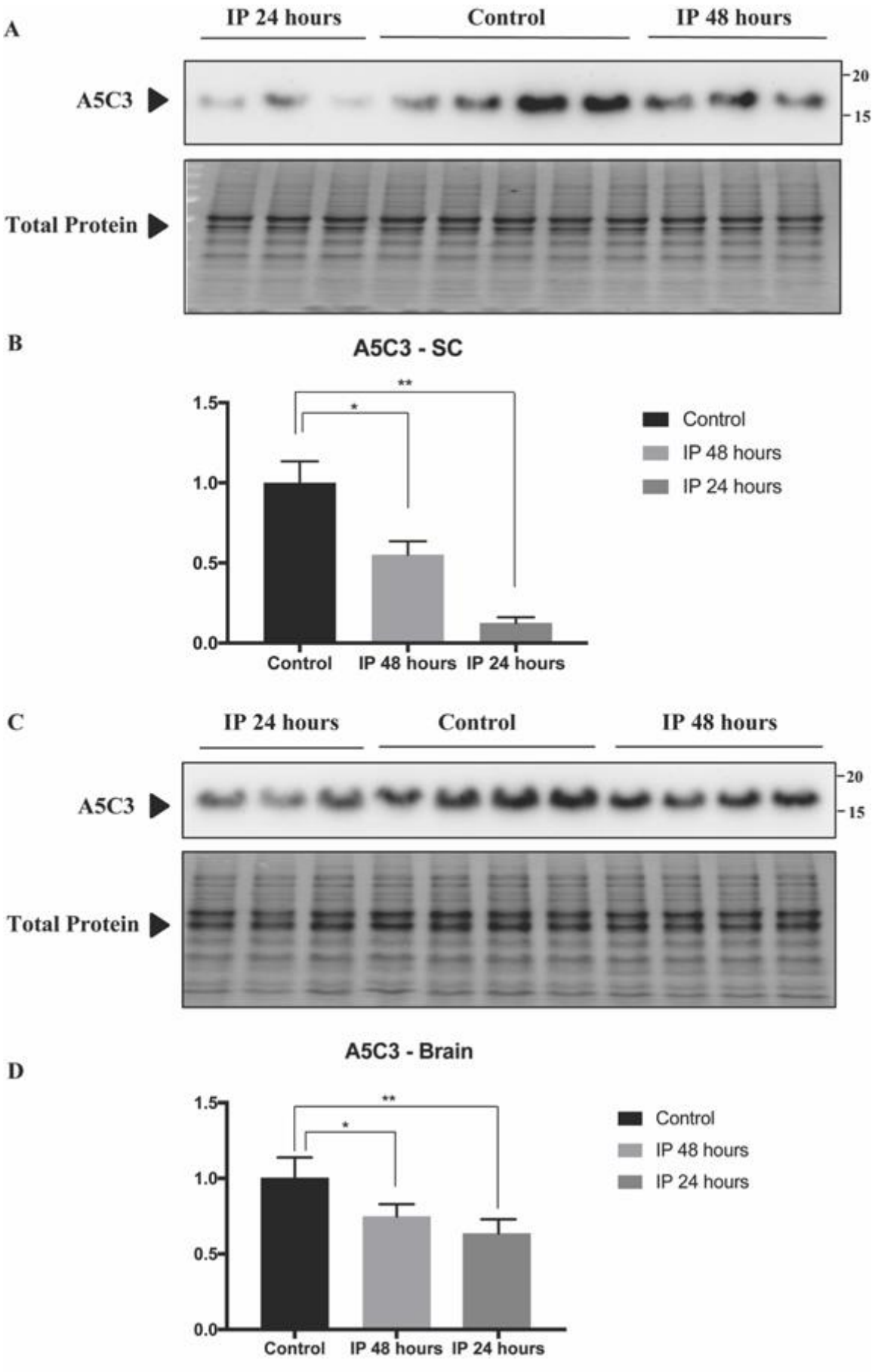

A
IP 24 hours
Control
IP 48 hours
A5C3
20
15
Total Protein
B
A5C3 - SC
**
*
1.5
1.0
0.5
0.0
Control
IP 48 hours
IP 24 hours
Control
IP 48 hours
IP 24 hours
C
IP 24 hours
Control
IP 48 hours
A5C3
20
15
Total Protein
D
A5C3 - Brain
**
*
1.5
1.0
0.5
0.0
Control
IP 48 hours
IP 24 hours
Control
IP 48 hours
IP 24 hours

Figure 2.12 Comparation between 24- and 48-hour post-injection with CT-4 peptide in the G93A transgenic mouse model of ALS.

The G93A mice received IP injection of CT-4 peptide at a dose of 10 mg/kg body weight *q.d.* for three days at the age of 100 days. Tissues, including spinal cord (A) and brain (C) from the control and treatment groups were harvest at 24- and 48-hour post-treatment and followed by western blot analysis using antibody against misfolded SOD1 (A5C3). (B and D) Quantitative data of misfolded SOD1 expression in different tissues. Equal volumes of lysates with a total of 10 μg protein was applied to 12% TGX Stain-Free polyacrylamide gels. Total protein generated by stain-free visualization were used to ensure equivalent loading. One-way ANOVA followed by Bonferroni's Multiple Comparison Post-Test were performed to establish significant differences with control group: *P < 0.05; **P < 0.01; ***P < 0.001. Bars represent mean ± SD, n=4 in control group, n=3 in IP 24 hours group, n≥3 in IP 48 hours group.

2.3.5 Treatment of the G93A mice at the age of 60 days by IP injection q.d. significantly delays the onset of disease and extends lifespan.

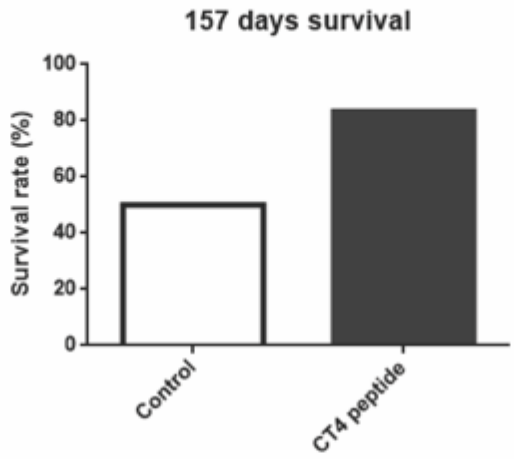
To explore whether CT-4 could alter the onset of the disease and the lifespan in the G93A transgenic mouse model of ALS, animals were treated with either 10mg/kg mCT-4 (mutant CT-4) or CT-4 peptide by IP injection *q.d.* beginning at 60 days of age, when was at the pre-symptomatic stage, until the endpoint of this study. Before the disease onset, the animals were normal. The initial muscle weakness from one limb was considered as the parameters of the disease onset as described in the Methods and Materials. As such, muscle weakness and body weight were used to monitor disease progression and survival.

Figure 2.13A showed that the survival rate in 157 days of the CT-4 peptide treatment group is ~80%, while that of the control group is ~50%. In addition, our results revealed that the disease onset was significantly delayed by 20 days (n=8; **P < 0.01) in the CT-4 peptide treatment group compared to mCT-4 treated controls. The median time of disease onset was 134 days in controls and 154 days in the CT-4 peptide group (Figure 2.13B).

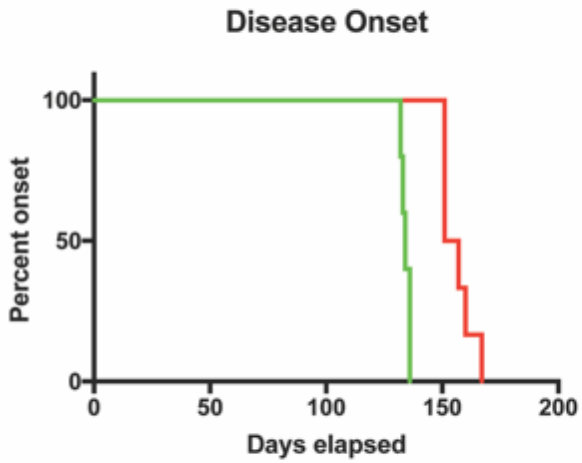
Next, I examined the effect of CT-4 peptide treatment on the survival duration of SOD1-G93A transgenic mice. The result showed that the curve of the lifespan shifted to the right in the treatment group while compared with controls. The long-term IP injection with CT-4 peptide significantly extended the lifespan by 22.5 days (n=8; ***P < 0.001). As shown in Figure 2.13C, the median time of

lifespan was 149 days in mCT-4 treated controls and 171.5 days in CT-4 peptide treatment group.

A



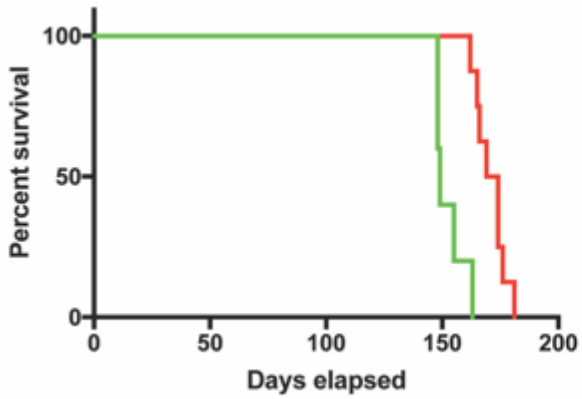
B



Control
CT4 Treated (IP injection)

Median Onset	
Control	134
Treated	154
P value summary	**

C



Control
CT4 Treated (IP injection)

Median Survival	
Control	149
Treated	171.5
P value summary	***

Figure 2.13 CT-4 peptide significantly delays the disease onset and prolongs survival in the G93A transgenic mouse model of ALS.

Beginning at 60 days of age, either mCT-4 or CT-4 peptide (10 mg/kg) was administered to G93A mice through IP injection *q.d.* until humane endpoint (20% body weight loss). (A) CT-4 peptide increased the survival rates of 157 days in G93A mice. (B) CT-4 peptide treatment delayed the onset of disease; the percentage of the animal numbers reached the disease onset was plotted against the age of the animals. (C) CT-4 peptide treatment prolonged the survival of G93A mice; the percentage of survival was plotted against the age of the animals. Student's t-test was performed to establish significant differences with control group: **P < 0.01; ***P < 0.001, n=6 per group.

2.3.6 The effect of CT-4 peptide on motor neurons number, monocarboxylate transporter 1 (MCT1) expression and axon and myelin integrity in CNS.

The effect of CT-4 peptide on the number of motor neurons in the ventral horn of spinal cord was investigated by Nissl staining. The animals were treated with either 10mg/kg mCT-4 (mutant CT-4) or CT-4 peptide by IP injection *q.d.* beginning at 60 days of age. As shown in Figure 2.14, CT-4 peptide treated animals exhibited significantly more Nissl-stained cells numbers, when compared with mCT-4 peptide treated group at 149 days pf age.

To explore the mechanism by which CT-4 delays the onset of disease in our SOD1-G93A transgenic mice, I examined the effect of CT-4 peptide on expression of MCT1 expression and integrity of axon and myelin in CNS. The 100-day old G93A mice received IP injection of 10 mg/kg body weight CT-4 peptide *q.d* for three days. SC and brain were harvest at 24 hours post-treatment and followed by western blot analysis using antibody against MCT1. Following the injection of CT-4 peptide, results revealed a significant elevation in MCT1 expression in the G93A transgenic mice SC at 24 hours post-treatment when compared with control group (Figure 2.15A and B). However, no obvious increase of MCT1 level was observed for 24 hours recovery after CT-4 peptide treatment in the brain of G93A transgenic mice relative to control (Figure 2.15C and D).

To determine the severity of axon and myelin damage in G93A transgenic mouse of ALS and the protection effect of CT-4 peptide on axon and myelin in

these animals, I assessed the integrity of axon and myelin from L4 (Lumbar) efferent nerve fibers from a WT mouse without any treatment and G93A mice of ALS treated with either mCT-4 or CT-4 peptide by IP injection *q.d.* beginning at 60 days of age. As shown in Figure 2.16, in mCT-4 treated G93A transgenic mice group, vacuoles and myelin debris were apparent, and the axon appeared distorted, when compared to the WT group, in which the myelin and mitochondria are healthy and in well-defined structure. Notably, no obvious abnormal structures were observed in the CT-4 treated group compared to mCT-4 treated group except noncompacted myelin, suggesting that CT-4 treatment could protect axon from demyelination and mitochondrial dysfunction to some extent, however, CT-4 peptide could not fully block the myelin breakdown (Figure 2.16).

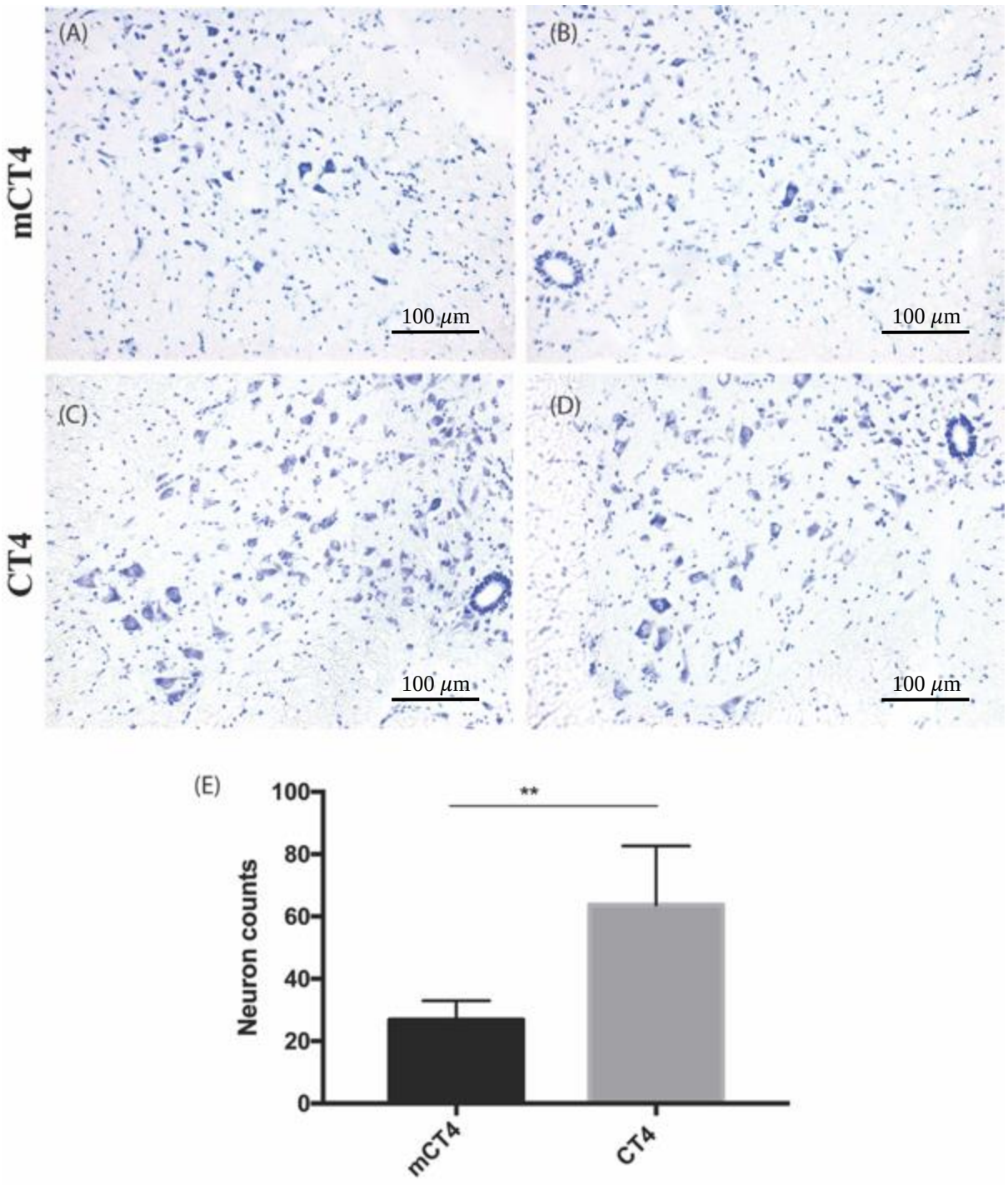


Figure 2.14 Nissl staining of the SC ventral horn of G93A transgenic animal with or without CT-4 peptide treatment.

(A and B) Nissl staining results in the ventral horn of the L4 (lumbar) SC from a 149-day-old G93A mouse of ALS treated with mCT-4 peptide by IP injection *q.d.* beginning at 60 days of age. (C and D) Nissl staining results in the ventral horn of the L4 SC from a 149-day-old G93A mouse of ALS treated with CT-4 peptide by IP injection *q.d.* beginning at 60 days of age. (E) Quantification analysis of the number of Nissl-stained cells. Scale bars represent 100 μm. Student's t-test was performed to establish significant differences with control group: **P < 0.01. Bars represent mean $\pm$ SD, n=3 per group.

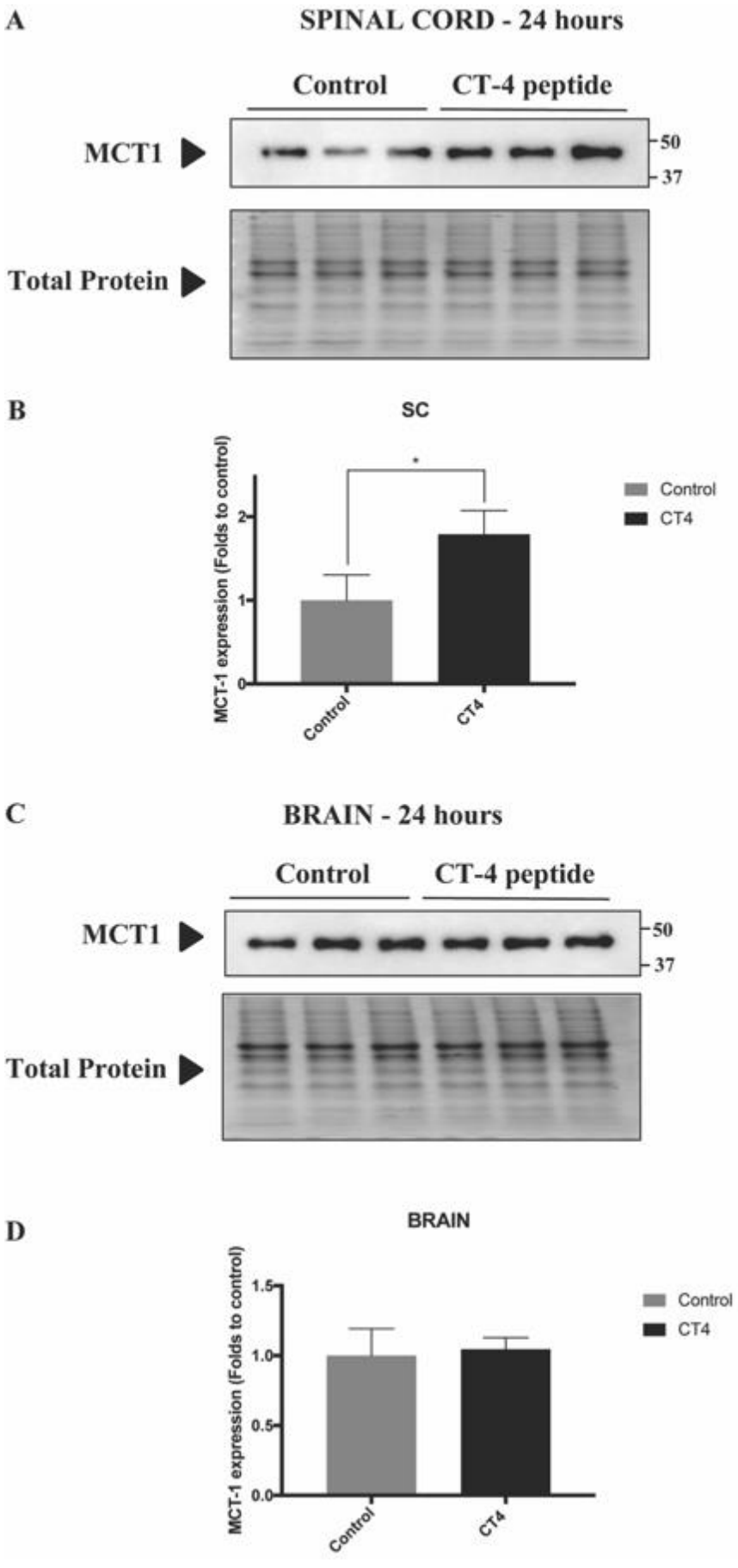

A
SPINAL CORD - 24 hours
Control
CT-4 peptide
MCT1
50
37
Total Protein
B
SC
MCT-1 expression (Folds to control)
*
Control
CT4
C
BRAIN - 24 hours
Control
CT-4 peptide
MCT1
50
37
Total Protein
D
BRAIN
MCT-1 expression (Folds to control)
Control
CT4

Figure 2.15 Treatment of CT-4 peptide results in a marked increase in MCT1 expression in SC of G93A transgenic mice but not in brain.

The G93A mice received IP injection of 10 mg/kg body weight CT-4 peptide *q.d.* for three days at the age of 100 days. SC (A) and brain (C) from the control and treatment groups were harvest at 24-hour post-treatment and followed by western blot analysis using antibody against MCT1. (B and D) Quantitative data of MCT1 expression in SC and brain. Equal volumes of lysates with a total of 10 μg protein was applied to 12% TGX Stain-Free polyacrylamide gels. Total protein generated by stain-free visualization were used to ensure equivalent loading. Student's t-test was performed to establish significant differences with control group: *P < 0.05. Bars represent mean $\pm$ SD, n=3 per group.

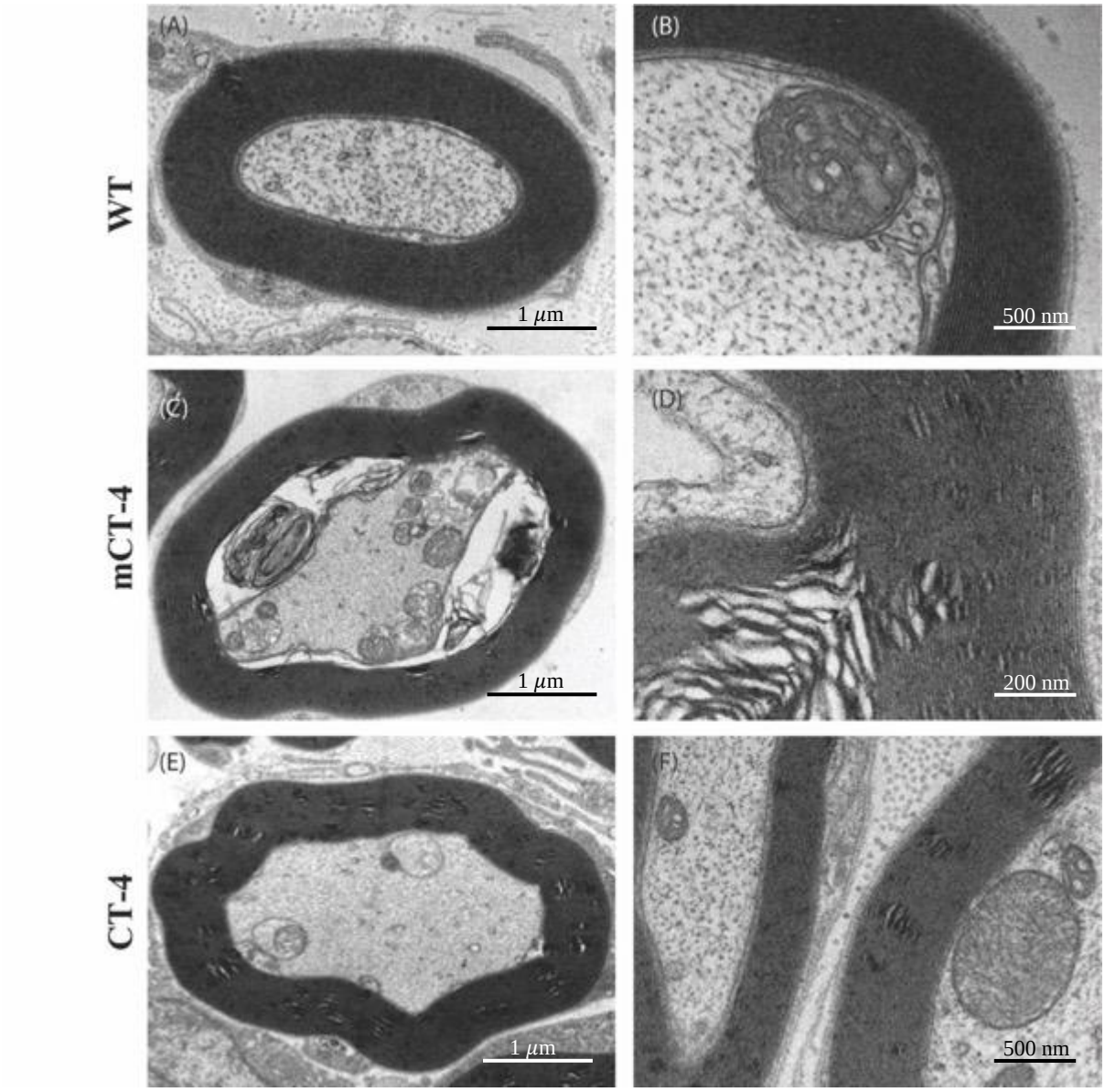


Figure 2.16 Transmission electron micrograph of efferent nerve fibers in a transverse section

(A) Healthy L4 (lumbar) efferent nerve fibers from a 157-day-old WT mouse. (B) High magnification EM demonstrates ultrastructural details of myelinated axons and mitochondria. (C) L4 efferent nerve fibers from a 158-day-old G93A mouse of ALS treated with mCT-4 by IP injection *q.d.* beginning at 60 days of age. (D) High magnification EM demonstrates abnormality of ultrastructural details of

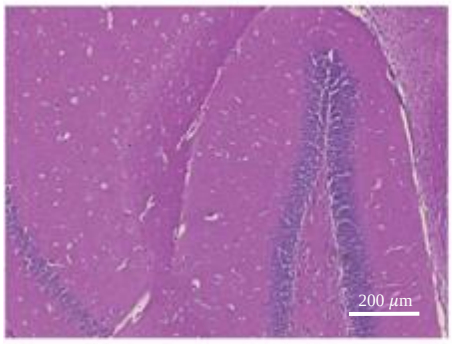
myelinated axons. (E) L4 efferent nerve fibers from a 157-day-old G93A mouse of ALS treated with CT-4 by IP injection *q.d.* beginning at 60 days of age. (F) High magnification EM demonstrates ultrastructural details of myelinated axons and mitochondria. Scale bars in (A), (C), and (E) represent 1 μm. Scale bars in (B) and (F) represent 500 *nm*. Scale bars in (D) represent 200 *nm*.

2.3.7 CT-4 peptide has no side effect on tissues of WT mice after a long-term IP injection.

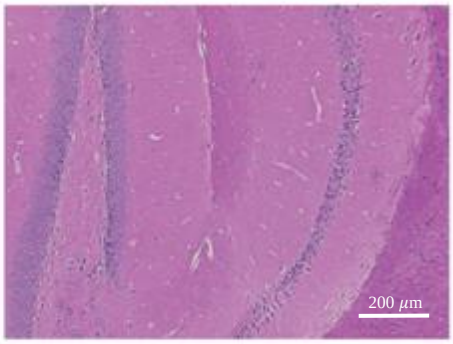
To explore the side effect of CT-peptide on organs of animals, WT mice were euthanized after receiving IP injection of CT-4 peptide at a dose of 10 mg/kg every day from 60 days to 173 days of age. H&E stains of tissues, including brain, heart, SC, kidney, liver, muscle, lung, and spleen, are shown in Figure 2.17. The H&E stained sections from these long-term treated animals showed normal histological structures.

WT	Mice #	Age	Sex
Treatment Long-term injection	A319	173	Female
	A322	173	Female

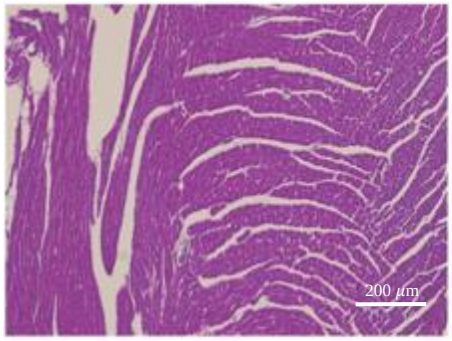
A319 Brain



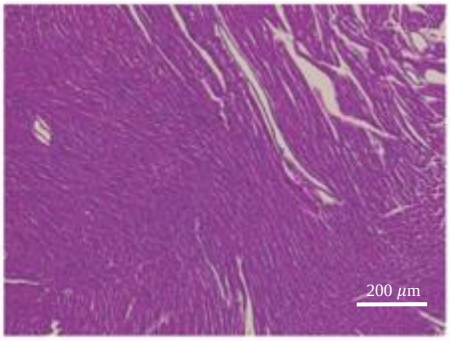
A322 Brain



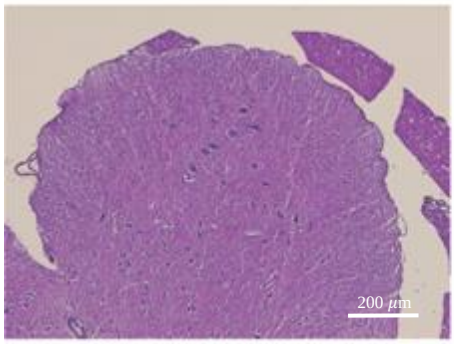
A319 Heart



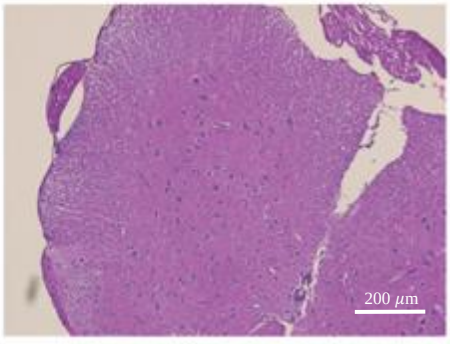
A322 Heart



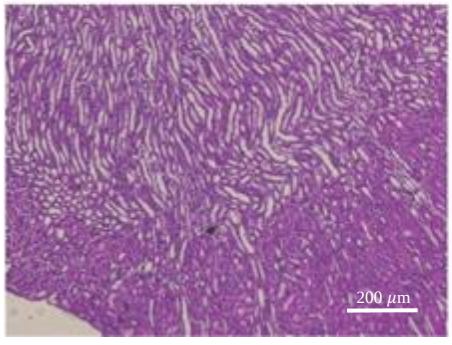
A319 Spinal Cord



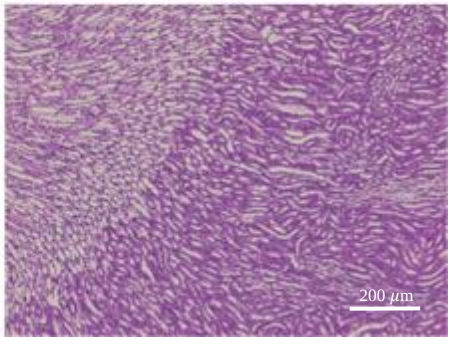
A322 Spinal Cord



A319 Kidney

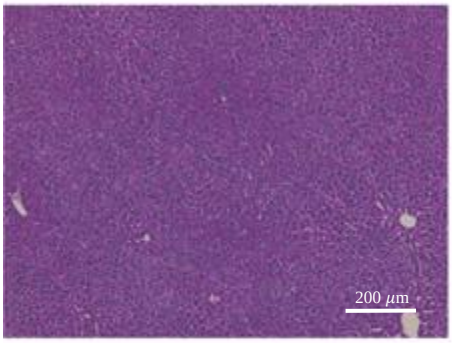


A322 Kidney

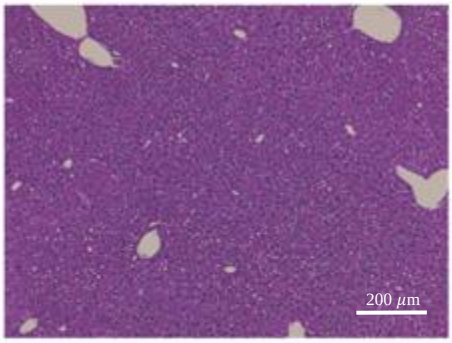


WT	Mice #	Age	Sex
Treatment Long-term injection	A319	173	Female
	A322	173	Female

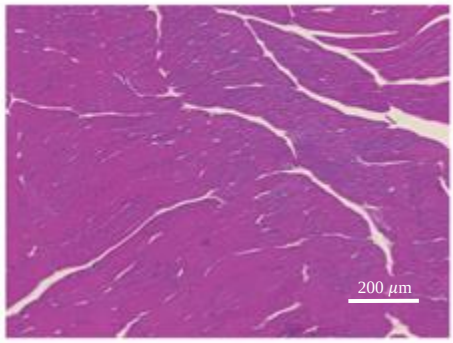
A319 Liver



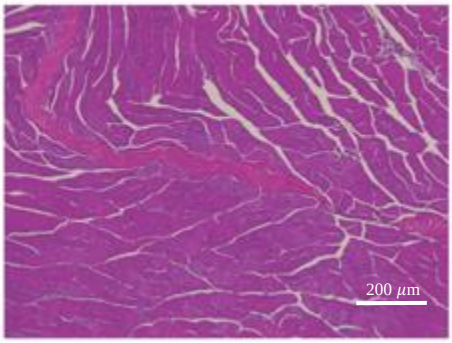
A322 Liver



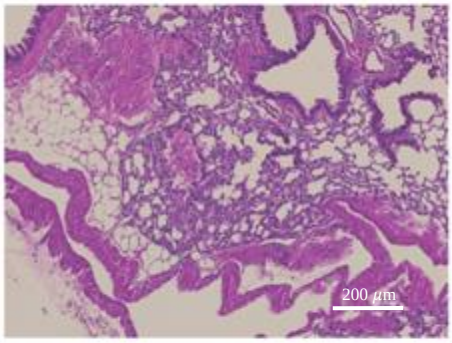
A319 Muscle



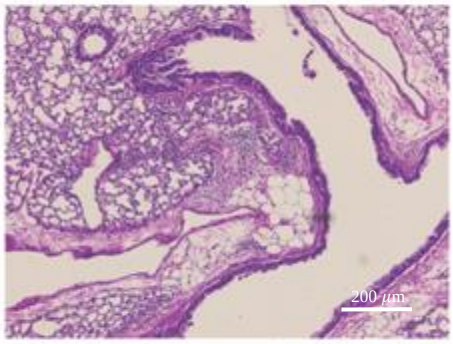
A322 Muscle



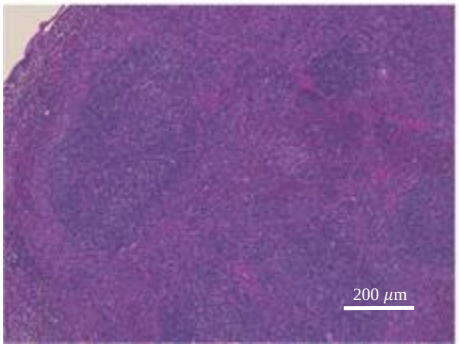
A319 Lung



A322 Lung



A319 Spleen



A322 Spleen

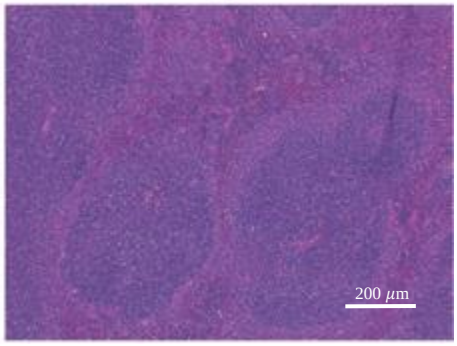


Figure 2.17 Hematoxylin and eosin (H&E) stained sections of WT mice.

Beginning at 60 days of age, WT mice received IP injection of CT-4 peptide at a dose of 10 mg/kg every day until 173 days of age. After the long-term injection, animals were euthanized and tissues, including brain, heart, SC, kidney, liver, muscle, lung, and spleen, were collected for analysis. Scale bar represents 200 μm.

2.4 Discussion

The results of this study indicated that treatment with the CT-4 resulted in a selective degradation of misfolded SOD1 in a dose-, time- and lysosomal activity dependent manner, as expected. Intraperitoneal injection of CT4 peptide at a three-day continuous dose (10mg/kg) in the G93A mouse model of ALS resulted in significant reduction of misfolded SOD1 in 24 hours and 48 hours post-treatment in the brain and spinal cord. Levels of the misfolded SOD1 could recover in one week after a three-day continuous administration. Daily injection of CT-4 peptide beginning at 60 days of age till the endpoint significantly preserved the number of motor neurons in the ventral horn of the spinal cord, and further delayed disease onset and extended lifespan of the G93A mice. Additionally, this long-term treatment can preserve MCT1 expression, protect axon from demyelination and mitochondrial dysfunction to some extent.

Since 1993, extensive evidence is accumulating that mutant/misfolded SOD1 expression plays a critical role in the pathogenesis of both fALS and sALS due to a “gain-of-function” toxicity (46, 186). Failure in degradation of misfolded SOD1 with ubiquitin and/or autophagy-lysosomal system causes the accumulation of insoluble SOD1 aggregates and triggers a toxic cascade, leading to motor neuron degeneration in ALS. Therefore, the development of treatment that could diminish misfolded SOD1 protein level has been the focus of intense interest.

In this study, I first demonstrated that our CT4-directed and chaperone-mediated autophagy approach could markedly decrease the level of SOD1-G93A in time- and dose- dependent manners in the neuron enriched culture prepared from the G93A transgenic mice embryonic NSC (Figure 2.2). In addition, our immunohistochemistry experiment results revealed that the knockdown effect of CT-4 peptide on misfolded SOD1 protein expression *in vitro* sustained even after 22 hours of the treatment (Figure 2.3).

Studies indicated that modifications to SOD1 protein, such as mutations and posttranslational modifications, cause protein misfolding and subsequent aggregation (249). In addition, the accumulation of detergent-insoluble protein aggregates is a common feature of ALS and act as transmissible agents between cells suggesting a "prion-like" property in ALS (184). As such, both of the detergent-soluble and -insoluble proteins may be potentially toxic and are considered as one of the mechanisms by which mutant/misfolded SOD1 cause ALS (241). By using aggregation assay, I then demonstrated that mutant SOD1 was prone to form the detergent-insoluble aggregates within 48 hours after transfection with SOD1-G93A plasmid. Furthermore, our data revealed that CT-4 peptide could reduce both soluble and insoluble SOD1 levels. In addition, the knockdown is more efficient for soluble SOD1 protein (Figure 2.5).

One of the major features of CT-4 is that the degradation of misfolded SO1 is regulated by the autophagy-lysosome pathway. It has been shown that NH_4Cl could inhibit lysosome activity, while nutrient deprivation with EBSS incubation

would induce the activation of lysosome function (245). In our study, pre-treatment with NH_4Cl indeed succeeded in blocking the downregulation of misfolded SOD1 mediated by CT-4 peptide. Meanwhile, it should be noted that the clearance of misfolded SOD1 protein by the treatment with CT-4 peptide could be accelerated after lysosomal activation by nutrient deprivation with EBSS incubation (Figure 2.5). In addition, results of PLA assay indicated that CT-4 peptide induced co-localization and interaction between SOD1-G93A and lysosome (Figure 2.6). Generally, these data confirmed that CT-4 peptide downregulated misfolded SOD1 protein through a lysosome involved protein degradation pathway.

In order to further validate the significant effectiveness of our CT-4 peptide in knocking down of misfolded SOD1 *in vivo*, I next examined the misfolded SOD1 protein expression in different tissues obtained from control- and CT-4-treated animals by using antibody (A5C3) against misfolded SOD1. Our results showed that interventional treatment with CT-4 peptide induced a significant decrease in misfolded SOD1 protein levels in SC, brain, liver and muscle. Notably, with respect to the CNS tissues, including SC and brain, the duration of the knockdown effect by CT-4 peptide would last at least 48 hours post treatment. Meanwhile, the knockdown effect was still observed in liver, which is one of the PNS (peripheral nervous system) tissues (Figure 2.8 and 2.9). However, our findings suggested these effects didn't sustain to one week or two weeks (Figure 2.10 and 2.11). Additionally, these data above successfully demonstrated the

ability of CT-4 peptide to cross the blood-brain-barrier (BBB) and showed the effectiveness of CT-4 peptide on CNS tissues (SC and brain) (250). In a nutshell, CT-4 peptide, as a simple, non-virally mediated, cell membrane-permeant, targeting peptide-based system, possesses the advantages of higher safety, efficacy, and selectivity to knockdown the level of misfolded SOD1 *in vitro* and *in vivo*.

As discussed above, CT-4 peptide failed to sustainably decrease *in vivo* misfolded SOD1 protein level more than one-week post-treatment. One of the reasonable explanations shall be that CT4 only targets misfolded SOD1 protein. It does not stop the misfolding process of SOD1. Another plausible explanation for our findings is that CT-4 peptide may easily degraded under *in vivo* conditions. For example, research suggested that peptides stability in different biological media varies, and the half-life of peptides ranged from ~4 to > 10,000 mins (251). Overall, peptide therapeutics have their intrinsic limitations and weakness, including poor chemical and physical stability, and a short circulating plasma half-life (252). As such, further analysis is warranted to determine the stability and half-life of CT-4 peptide in various bio-samples, including spinal cord, brain, liver, muscle and serum and different administration routes, to provide a prediction of the pharmacokinetics behavior for explanation of *in vivo* efficacies and for pharmaceutical development.

Furthermore, our daily injection of CT-4 peptide beginning at 60 days of age till the endpoint significantly delayed onset of disease and extended survival in

the G93A mouse model of ALS. In long-term study of CT-4 peptide treatment, I started the treatment at an earlier age which is 60 days old, while compared with a previous study which started the treatment at the age of 3 months (the stage of pre-onset) (253). The reason for early treatment is based on scientific findings indicating a possibility that mutant/misfolded SOD1 has a pathogenic effect early in life so that intervention should be started at the early stage of disease in order to maximize its benefits and therapeutic impacts on the disease (253).

Regarding the administration frequency of the CT-4 peptide in the long-term study, the intraperitoneal injection was conducted daily to ensure a constant peptide concentration according to the short-term treatment study which showed that the optimal effective duration of the peptide on the misfolded SOD1 level was 24 hours (Figure 2.12). Our long-term study revealed that the onset of disease has been delayed and the lifespan has been extended after CT-4 treatment compared with controls, indicating CT-4 peptide can be potentially developed into a treatment for ALS. Despite the amelioration of disease is limited, to the best of our knowledge, this is the first report that describes a selective and effective approach to knockdown of misfolded SOD1 with chaperone-mediated autophagy-based lysosomal degradation.

A critical question then arose regarding the mechanism by which CT-4 peptide treatment delayed disease onset by downregulating misfolded SOD1 expression. In this study, I investigated neuronal survival directly via Nissl staining to confirm the protective effect of CT-4 peptide on motor neurons.

Results showed the number of Nissl-stained cells was sustained in the ventral horn of the spinal cord in the CT-4 peptide treated group, indicating CT-4 peptide has a neuroprotective effect on the motor neurons of G93A transgenic mouse of ALS model (Figure 2.14).

Recent studies suggested that motor neuron degeneration in a mutant *SOD1*-mediated ALS model is non-cell-autonomous motor neuronal death, which means glial cells contributes to the death of motor neurons and disease progression (45, 254). Although the functional significance of glia has yet to be fully elucidated, extensive evidence showed that oligodendrocytes play a critical role in the pathogenesis of ALS by using mouse models of the disease (77, 80-82). Oligodendrocytes were demonstrated to contribute to motor neuron death through a SOD1-dependent mechanism, whereas oligodendrocytes degeneration has been reported to occur prior to disease onset of ALS and persists during disease progression (81). Moreover, oligodendrocytes dysfunction in both SOD1-G93A transgenic mice and patients with ALS would lead to motor neuron axons demyelination and axon degeneration (77, 82). New oligodendrocytes are formed to compensate for the loss; however, they fail to mature, thus resulting in progressive de-myelination. Furthermore, axonal de-myelination has been directly associated with ALS deterioration (82). According to the “dying back hypothesis”, one of the earliest neuronal alteration in ALS is neuromuscular junction (NMJ) disintegration, which is followed by axon degeneration that progresses to spinal motor neuron death (85, 96). In the CNS, glial cells, such as

oligodendrocytes and astrocytes, are critical for the maintenance of axonal integrity (78). Specifically, oligodendrocytes maintain structural integrity and functionality of myelin, while lipid-rich myelin ensures the speed and reliability of electrical transmission (255). Loss of glial support causes progressive axon degeneration and possibly local inflammation, both of which are likely to contribute to a variety of neuronal diseases, such as ALS, in the central and peripheral nervous systems (91). Interestingly, a study showed that oligodendroglia supply energy metabolites to axons through the monocarboxylic transporter MCT1, and the downregulation of MCT1 within oligodendroglia, or death of oligodendroglia and replacement with immature oligodendroglia will lead to axonopathy and neuron loss (80). As such, it is recognized that oligodendrocyte abnormalities are considered as a primary contributing factor involved in downstream neuronal degeneration rendering relevance to ALS (83, 84). In addition, MCT1 expression was revealed to be decreased in affected brain and spinal cords regions of ALS patients as well as mutant *SOD1* transgenic mice, resulting in insufficient energy supply to the axons, thus leading to abnormality of myelination, axon loss and motor neuron death, suggesting a critical role of MCT1 in ALS pathogenesis (32, 71, 80).

The results of our study revealed that CT-4 peptide treatment could help to increase MCT1 expression in SC of SOD1-G93A mice, albeit not in the brain (Figure 2.15), suggesting a pathway that removal of misfolded SOD1 in ALS mouse model using CT-4 peptide results in preservation of MCT1 expression,

and subsequent maintenance of axon myelin and neuron protection. This finding is in accordance with the “dying back” theory (256). As I suggested that axonopathy, such as demyelination, mitochondrial dysfunction and abnormal axon, has been proposed as an early initiating mechanism of ALS. Our electron microscopy findings confirmed that the disturbance of myelin and mitochondria in ALS animals while compared with WT animals (Figure 2.16). Furthermore, our study demonstrated that CT-4 peptide could protect axons from the abnormality shown in the mCT-4 treated G93A mice group to some extent, albeit not fully prevent the axonopathy. This finding could be explained by the CT-4 induced upregulation of MCT-1 level in SC, as glial environment and the interaction between glial and axon play a critical role in the structural and trophic support for neurons (256). The partial preservation of MCT1 expression can be considered to result in myelin and axon protection, and eventually leading to disease onset delay and lifespan prolong.

Taking together, the findings of this study showed that the CT-4 peptide could selectively reduce the level of misfolded SOD1 *in vitro* and *in vivo*. Furthermore, CT-4 peptide could effectively improve neuronal survival and attenuate loss of motor neurons. As such, CT-4 treatment is capable to delay disease onset and prolong survival in SOD1-G93A mouse model, suggesting selective clearance of misfolded SOD1 by CT-4 is therefore a rational approach towards developing effective treatment for ALS. However, the knockdown efficiency is dependent on lysosome activity and the stability of CT-4 peptide. One of the issues of this study

is that the continuous IP injection of CT-4 peptide could result in the decline of autophagy or the saturation of lysosome, leading to recovery of misfolded SOD1 expression. Another limitation of this approach is the stability and the pharmacokinetics of CT-4 peptide is unclear. The last limitation shall be that CT4 targets only misfolded SOD1, not the misfolding process of SOD1. These issues of our treatment might help to explain our *in vivo* knockdown study, which demonstrated that CT-4 peptide failed to sustainably decrease *in vivo* misfolded SOD1 protein level no more than one-week post-treatment. Further experiments will investigate the pharmacokinetics of CT-4 peptide to obtain reliable parameters and determine the elimination rates and half-life of CT-4 peptide for subsequent application. In addition, combination of CT-4 peptide and pharmacological enhancement of CMA, including ketone bodies (257) , 6-aminonicotinamide, and geldanamycin (258), or gene therapy, such as recombinant adeno-associated virus (AAV)-CT-4 treatment, could be developed as more effective approaches for treating ALS in case of saturation of lysosomal activity or peptide degradation.

2.5 Acknowledgement

The authors would like to acknowledge the support from the ALS Society of Canada (ALS Canada), the College of Pharmacy and Medicine at the University of Manitoba.

Chapter 3 Conclusions and future perspectives

3.1 Conclusions

In this study, I have attempted to determine the efficiency and specificity of the CT4-directed and chaperone-mediated autophagy pathway in knocking down of misfolded SOD1 *in vitro* and *in vivo*. Additionally, I tried to provide a better understanding of the pharmacological mechanisms of the potential treatment for ALS. Our results revealed that CT-4 peptide treatment resulted in knockdown of misfolded SOD1 derived from constitutively expressed SOD1 mutants in primary cultures of neurons and plasmid transfected cells. And then I determined the therapeutic efficacy of the CT-4 peptide on degradation of misfolded SOD1 in G93A mouse model of ALS. Our finding showed that misfolded SOD1 level has been significantly knocked down by CT-4 administration. In addition, CT-4 peptide successfully attenuated loss of motor neuron, delayed disease onset and prolonged the lifespan of transgenic animals of ALS when given systemically. Furthermore, our data suggested that CT-4 peptide treatment also played a critical role in the preservation of MCT1 expression and maintenance of axon structure which may be the plausible mechanism by which CT-4 delayed disease onset.

Misfolded SOD1 is at the center of ALS pathogenesis. Targeting misfolded SOD1 is therefore a rational approach towards an effective treatment for ALS. The peptide-directed chaperone-mediated protein degradation posits us on a

unique position to break new ground in selectively tackling the misfolded form of SOD1 and develop a treatment for ALS.

In summary, early intervention may slow the progression of ALS in the early stages of the disease, thus delay motor neuron death and increase life expectancy of patients with ALS. This whole thesis provides a better understanding of the pharmacological mechanisms of the potential treatments for ALS, and thus aids in developing new strategies to treat other different neurodegenerative diseases.

3.2 Limitations

The project provides a proof of concept that the CT-4 treatment is capable of delaying disease onset and prolonging survival in SOD1-G93A mouse model, suggesting selective clearance of misfolded SOD1 by CT-4 is a rational approach towards developing effective treatment for ALS. In addition, our study suggested that the most effective duration of CT-4 peptide knockdown effect was 3 to 5 hours post treatment *in vitro*, and 24 hours post treatment *in vivo*. Furthermore, the long-term intraperitoneal injection of CT-4 peptide delayed the disease onset and prolonged the lifespan of the mouse model of ALS for about 20 days. However, the misfolded SOD1 expression could recover within 22 hours in the cell model and the knockdown effect didn't last for one week in the mouse tissues.

Importantly, the 20-day-extension is undesirable as I expected, however, is comparable or even better when compared with previous studies: The female SOD1-G93A mice were treated with Guanabenz beginning at 40 days of age, a small molecule originally developed as an anti-hyptensive drug. The mean time of the onset was found to be extended only from 104.5 $\pm$ 2.3 days to 116.0 $\pm$ 2.4 days, while the mean survival time was from 132.2 $\pm$ 4.0 days to 150.7 $\pm$ 4.7 days (259). Cannabinoids, the bioactive ingredients of marijuana, might have been shown some mild therapeutic benefit in ALS, however, could also induce side effects, including mind-altering and partially addictive. Treatment with Δ_9-tetrahydrocannabinol, beginning at 60 days of age, extended mean survival of G93A transgenic mouse from 125.9 $\pm$ 1.6 days to 131.8 $\pm$ 2.4 days (260), while cannabinol could only delays symptom onset in SOD1-G93A transgenic mice by 17 days without affecting survival rate (261). Other compounds have also been tested for their effect on the disease onset and lifespan of G93A transgenic mice of ALS. High dose of minocycline treatment with anti-inflammatory effect showed a delay of mortality with 21 days (262). Administration with arimoclomol, a coinducer of hear shock proteins increased the animal lifespan from 125 $\pm$ 1.8 to 153 $\pm$ 2.6 days (263). Thalidomide and lenalidomide have also been proved to show similar effect on this transgenic mouse model of ALS (264).

While the knockdown efficiency is dependent on lysosome activity and the stability of CT-4 peptide, possible explanations and limitations are needed to be considered in order to maximize its therapeutic efficacy and benefits as follows:

One of the limitations of this study is that the stability and the pharmacokinetics of CT-4 peptide is unclear. Thanks to the advances in synthetic peptide technologies, peptide therapeutics nowadays play a major role in the pharmaceutical market, which is different from small molecules and proteins due to its high target specificity, high biological activity, low toxicity, low cost and ease of design and synthesis. However, the unfavorable intrinsic weakness, including poor chemical and physical stability, and a short circulating plasma half-life, limit their therapeutic efficacy and clinical translation (252, 265). Researchers are endeavoring to improve peptide-based drugs half-life, stability under physiological conditions by using various techniques, such as combination with ghrelin C-terminus (a stable peptide secreted from the stomach) (265), chemical modification with polyethylene glycol (PEG) (266), integration of D-amino acids or α-aminoxy amino acids to N-/C-terminus, and cyclization (267). According to the properties of peptide therapeutics, one of the plausible reasons that the administration of CT-4 peptide is not fully effective might be explained by its rapid clearance rate in vivo. In that case, modifications of CT-4 peptide can

result in increased resistance to proteolytic degradation, longer plasma half-life, low immunogenicity, and better distribution to target tissues. High stability and long half-life of CT-4 peptide will lead to low frequency of administration, which helps to improve and encourage patient compliance to the treatment. Additionally, gene therapy, such as recombinant adeno-associated virus (AAV)-CT-4 treatment, can also be developed to endogenously and continuously express CT-4 in vivo to avoid the instability and short half-life of peptide therapeutics.

Another issue of this approach is that the continuous IP injection of CT-4 peptide could result in the decline of autophagy or the saturation of autophagy-lysosomal pathway, leading to recovery of misfolded SOD1 expression. Researchers have developed and proved various of effective pharmacological enhancements of chaperone-mediated autophagy (CMA), including ketone bodies (257) , 6-aminonicotinamide, geldanamycin (258), and a new CMA enhancer QX77 (268). The combination of these CMA enhancers and our CT-4 peptide could be another potential solution to optimize the effectiveness of misfolded SOD1 knockdown by the peptide.

These issues of our experiments might help to explain the undesirable effect of our *in vivo* knockdown study, which demonstrated that CT-4 peptide failed to sustainably decrease *in vivo* misfolded SOD1 protein level no more than one-

week post-treatment. Further experiments will investigate the pharmacokinetics of CT-4 peptide to obtain reliable parameters and determine the elimination rates and half-life of CT-4 peptide for subsequent application. In addition, the use of FDA approved riluzole or edaravone as a positive control would be a strong support for this study to offer a better appreciation of the outcome of CT-4 treatment.

3.3 Future directions

As aforementioned, in order to improve the CT-4 therapeutic efficacy and to obtain a sustained effective duration of misfolded SOD1 knockdown effect, methods, including the modification of CT-4 into a more stable peptide, combination of CT-4 peptide and CMA enhancer, or gene therapy, could be developed as more effective approaches for treating ALS in case of saturation of lysosomal activity or peptide degradation.

As such, our next plan is to determine the stability and half-life of CT-4 peptide in various bio-samples by establishing the pharmacokinetics of the CT-4 peptide in plasma, the brain and spinal cord of mice administered intraperitoneally. Meanwhile, we are utilizing AAV vectors as a gene delivery vehicle to continuously express endogenous CT-4 peptide. This whole project

includes AAV production, intravenous delivery, and evaluation of the transgene expression. Recently, I successfully produced the CT4-AAV viruses with/without GFP tag. And our data showed that the CT4-AAV could induce a significant decrease in the level of SOD1-G93A in the neuron-enriched culture. In addition, the CT4-AAV could successfully cross the BBB and efficiently knockdown misfolded SOD1 protein level in SC and brain of G93A transgenic mouse model of ALS at the time of three weeks post intravenous tail injection.

We are currently working on to improve treatment outcomes and are cautiously optimistic that the peptide-direct protein degradation system might be developed into an effective treatment for both fALS and sALS, as I reviewed that misfolded SOD1 plays a central role of the center of ALS pathogenesis and a common toxic factor to a subset of both familial and sporadic ALS. Furthermore, several abnormal biological processes have been suggested to be involved in the mechanisms underlying the pathogenesis of ALS, thus making it a very complex multi-system and multi-syndrome disorder, for which no single cause can be identified. Therefore, the complexity of the disease suggests that a combination treatment targeting multiple pathways involving the pathogenesis of ALS might be a potential effective approach.

Notably, the application of CT-4 peptide can also be considered to expanded to treat aging and aging-associated neurodegenerative diseases. Previous work showed that mice expressing the mutant human *SOD1* gene exhibited signs of premature aging characterized by SOD1 oxidation, misfolding and aggregation. These insoluble aggregates are associated with aging and accelerated aging in transgenic mouse models of ALS (269, 270). Studies also revealed that the interaction of α-synuclein and SOD1 might be relevant for neurodegenerative disease (271, 272). Therefore, the CT-4 peptide treatments which are able to specific knockdown the level of misfolded SOD1 would be an option for scientists to explore the potential interventional strategies for aging process and other related neurodegenerative diseases.

Reference

1. Morris J: Amyotrophic Lateral Sclerosis (ALS) and Related Motor Neuron Diseases: An Overview. The Neurodiagnostic journal 55: 180-194, 2015.
2. Talbot K: Motor neurone disease. Postgrad Med J 78: 513-519, 2002.
3. Riva N, Agosta F, Lunetta C, Filippi M and Quattrini A: Recent advances in amyotrophic lateral sclerosis. Journal of neurology2016.
4. Mathis S, Couratier P, Julian A, Vallat JM, Corcia P and Le Masson G: Management and therapeutic perspectives in amyotrophic lateral sclerosis. Expert review of neurotherapeutics: 1-14, 2016.
5. Martin LJ, Price AC, Kaiser A, Shaikh AY and Liu Z: Mechanisms for neuronal degeneration in amyotrophic lateral sclerosis and in models of motor neuron death (Review). International journal of molecular medicine 5: 3-13, 2000.
6. Zarei S, Carr K, Reiley L, et al.: A comprehensive review of amyotrophic lateral sclerosis. Surgical neurology international 6: 171, 2015.
7. Talbott EO, Malek AM and Lacomis D: The epidemiology of amyotrophic lateral sclerosis. Handb Clin Neurol 138: 225-238, 2016.
8. Therrien M, Dion PA and Rouleau GA: ALS: Recent Developments from Genetics Studies. Current neurology and neuroscience reports 16: 59, 2016.
9. Li R, Strykowski R, Meyer M, Mulcrone P, Krakora D and Suzuki M: Male-specific differences in proliferation, neurogenesis, and sensitivity to oxidative stress in neural progenitor cells derived from a rat model of ALS. PloS one 7: e48581, 2012.
10. McCombe PA and Henderson RD: Effects of gender in amyotrophic lateral sclerosis. Gender medicine 7: 557-570, 2010.
11. Orsini M, Oliveira AB, Nascimento OJ, et al.: Amyotrophic Lateral Sclerosis: New Perpectives and Update. Neurology international 7: 5885, 2015.
12. Renton AE, Majounie E, Waite A, et al.: A hexanucleotide repeat expansion in C9ORF72 is the cause of chromosome 9p21-linked ALS-FTD. Neuron 72: 257-268, 2011.
13. Rosen DR, Siddique T, Patterson D, et al.: Mutations in Cu/Zn superoxide dismutase gene are associated with familial amyotrophic lateral sclerosis. Nature 362: 59-62, 1993.
14. Neumann M, Sampathu DM, Kwong LK, et al.: Ubiquitinated TDP-43 in frontotemporal lobar degeneration and amyotrophic lateral sclerosis. Science 314: 130-133, 2006.
15. Kwiatkowski TJ, Jr., Bosco DA, Leclerc AL, et al.: Mutations in the FUS/TLS gene on chromosome 16 cause familial amyotrophic lateral sclerosis. Science 323: 1205-1208, 2009.
16. Bozzoni V, Pansarasa O, Diamanti L, Nosari G, Cereda C and Ceroni M: Amyotrophic lateral sclerosis and environmental factors. Functional neurology 31: 7-19, 2016.
17. Hardiman O, Al-Chalabi A, Chio A, et al.: Amyotrophic lateral sclerosis. Nat Rev Dis Primers 3: 17085, 2017.

18. Salameh JS, Brown RH, Jr. and Berry JD: Amyotrophic Lateral Sclerosis: Review. Semin Neurol 35: 469-476, 2015.
19. Cudkowicz ME, McKenna-Yasek D, Sapp PE, et al.: Epidemiology of mutations in superoxide dismutase in amyotrophic lateral sclerosis. Ann Neurol 41: 210-221, 1997.
20. Tard C, Defebvre L, Moreau C, Devos D and Danel-Brunaud V: Clinical features of amyotrophic lateral sclerosis and their prognostic value. Rev Neurol (Paris) 173: 263-272, 2017.
21. Sabatelli M, Conte A and Zollino M: Clinical and genetic heterogeneity of amyotrophic lateral sclerosis. Clin Genet 83: 408-416, 2013.
22. Xu Z, Alruwaili ARS, Henderson RD and McCombe PA: Screening for cognitive and behavioural impairment in amyotrophic lateral sclerosis: Frequency of abnormality and effect on survival. J Neurol Sci 376: 16-23, 2017.
23. Consonni M, Iannaccone S, Cerami C, et al.: The cognitive and behavioural profile of amyotrophic lateral sclerosis: application of the consensus criteria. Behav Neurol 27: 143-153, 2013.
24. Grolez G, Moreau C, Danel-Brunaud V, et al.: The value of magnetic resonance imaging as a biomarker for amyotrophic lateral sclerosis: a systematic review. BMC Neurol 16: 155, 2016.
25. Gordon PH: Amyotrophic Lateral Sclerosis: An update for 2013 Clinical Features, Pathophysiology, Management and Therapeutic Trials. Aging Dis 4: 295-310, 2013.
26. van Es MA, Hardiman O, Chio A, et al.: Amyotrophic lateral sclerosis. Lancet 390: 2084-2098, 2017.
27. Brooks BR: El Escorial World Federation of Neurology criteria for the diagnosis of amyotrophic lateral sclerosis. Subcommittee on Motor Neuron Diseases/Amyotrophic Lateral Sclerosis of the World Federation of Neurology Research Group on Neuromuscular Diseases and the El Escorial "Clinical limits of amyotrophic lateral sclerosis" workshop contributors. J Neurol Sci 124 Suppl: 96-107, 1994.
28. Brooks BR, Miller RG, Swash M, Munsat TL and World Federation of Neurology Research Group on Motor Neuron D: El Escorial revisited: revised criteria for the diagnosis of amyotrophic lateral sclerosis. Amyotroph Lateral Scler Other Motor Neuron Disord 1: 293-299, 2000.
29. Sica RE, Nicola AF, Deniselle MC, et al.: Sporadic amyotrophic lateral sclerosis: new hypothesis regarding its etiology and pathogenesis suggests that astrocytes might be the primary target hosting a still unknown external agent. Arquivos de neuro-psiquiatria 69: 699-706, 2011.
30. Dib M: Amyotrophic lateral sclerosis: progress and prospects for treatment. 2003.
31. Libro R, Bramanti P and Mazzon E: The role of the Wnt canonical signaling in neurodegenerative diseases. Life sciences 158: 78-88, 2016.
32. Li J, Zhang L, Chu Y, et al.: Astrocytes in Oligodendrocyte Lineage Development and White Matter Pathology. Front Cell Neurosci 10: 119, 2016.
33. Abdelhak A, Junker A, Brettschneider J, et al.: Brain-Specific Cytoskeletal Damage Markers in Cerebrospinal Fluid: Is There a Common Pattern between Amyotrophic Lateral Sclerosis and Primary Progressive Multiple Sclerosis? International journal of molecular sciences 16: 17565-17588, 2015.
34. Osellame LD, Blacker TS and Duchen MR: Cellular and molecular mechanisms of mitochondrial function. Best practice & research. Clinical endocrinology & metabolism 26: 711-723, 2012.

35. Duchen MR: Roles of mitochondria in health and disease. Diabetes 53 Suppl 1: S96-102, 2004.
36. Santa-Cruz LD, Guerrero-Castillo S, Uribe-Carvajal S and Tapia R: Mitochondrial Dysfunction during the Early Stages of Excitotoxic Spinal Motor Neuron Degeneration in Vivo. ACS chemical neuroscience 7: 886-896, 2016.
37. Guo C, Sun L, Chen X and Zhang D: Oxidative stress, mitochondrial damage and neurodegenerative diseases. Neural regeneration research 8: 2003-2014, 2013.
38. Pardillo-Diaz R, Carrascal L, Munoz MF, Ayala A and Nunez-Abades P: Time and dose dependent effects of oxidative stress induced by cumene hydroperoxide in neuronal excitability of rat motor cortex neurons. Neurotoxicology 53: 201-214, 2016.
39. Kaal EC, Veldman H, Sodaar P, Joosten EA and Dop Bar PR: Oxidant treatment causes a dose-dependent phenotype of apoptosis in cultured motoneurons. Journal of neuroscience research 54: 778-786, 1998.
40. Lin MT and Beal MF: Mitochondrial dysfunction and oxidative stress in neurodegenerative diseases. Nature 443: 787-795, 2006.
41. Sharma A, Varghese AM, Vijaylakshmi K, et al.: Cerebrospinal Fluid from Sporadic Amyotrophic Lateral Sclerosis Patients Induces Mitochondrial and Lysosomal Dysfunction. Neurochemical research 41: 965-984, 2016.
42. Miquel E, Cassina A, Martinez-Palma L, et al.: Modulation of astrocytic mitochondrial function by dichloroacetate improves survival and motor performance in inherited amyotrophic lateral sclerosis. PloS one 7: e34776, 2012.
43. Liu D, Wen J, Liu J and Li L: The roles of free radicals in amyotrophic lateral sclerosis: reactive oxygen species and elevated oxidation of protein, DNA, and membrane phospholipids. FASEB journal : official publication of the Federation of American Societies for Experimental Biology 13: 2318-2328, 1999.
44. Turner BJ and Talbot K: Transgenics, toxicity and therapeutics in rodent models of mutant SOD1-mediated familial ALS. Progress in neurobiology 85: 94-134, 2008.
45. Boillee S, Vande Velde C and Cleveland DW: ALS: a disease of motor neurons and their nonneuronal neighbors. Neuron 52: 39-59, 2006.
46. Hayashi Y, Homma K and Ichijo H: SOD1 in neurotoxicity and its controversial roles in SOD1 mutation-negative ALS. Adv Biol Regul 60: 95-104, 2016.
47. Carri MT, Valle C, Bozzo F and Cozzolino M: Oxidative stress and mitochondrial damage: importance in non-SOD1 ALS. Frontiers in cellular neuroscience 9: 41, 2015.
48. Karademir B, Corek C and Ozer NK: Endoplasmic reticulum stress and proteasomal system in amyotrophic lateral sclerosis. Free radical biology & medicine 88: 42-50, 2015.
49. Jaronen M, Goldsteins G and Koistinaho J: ER stress and unfolded protein response in amyotrophic lateral sclerosis-a controversial role of protein disulphide isomerase. Frontiers in cellular neuroscience 8: 402, 2014.
50. Sundaramoorthy V, Sultana JM and Atkin JD: Golgi fragmentation in amyotrophic lateral sclerosis, an overview of possible triggers and consequences. Frontiers in neuroscience 9: 400, 2015.
51. Atkin JD, Farg MA, Soo KY, et al.: Mutant SOD1 inhibits ER-Golgi transport in amyotrophic lateral sclerosis. Journal of neurochemistry 129: 190-204, 2014.
52. Parakh S and Atkin JD: Protein folding alterations in amyotrophic lateral sclerosis. Brain research2016.

53. Kalmar B, Lu CH and Greensmith L: The role of heat shock proteins in Amyotrophic Lateral Sclerosis: The therapeutic potential of Arimoclomol. Pharmacology & therapeutics 141: 40-54, 2014.
54. Underwood CK, Kurniawan ND, Butler TJ, Cowin GJ and Wallace RH: Non-invasive diffusion tensor imaging detects white matter degeneration in the spinal cord of a mouse model of amyotrophic lateral sclerosis. NeuroImage 55: 455-461, 2011.
55. Naughton MC, McMahon JM and FitzGerald U: Differential activation of ER stress pathways in myelinating cerebellar tracts. Int J Dev Neurosci 47: 347-360, 2015.
56. Jaronen M, Vehvilainen P, Malm T, et al.: Protein disulfide isomerase in ALS mouse glia links protein misfolding with NADPH oxidase-catalyzed superoxide production. Human molecular genetics 22: 646-655, 2013.
57. Saxena S, Cabuy E and Caroni P: A role for motoneuron subtype-selective ER stress in disease manifestations of FALS mice. Nature neuroscience 12: 627-636, 2009.
58. King AE, Woodhouse A, Kirkcaldie MT and Vickers JC: Excitotoxicity in ALS: Overstimulation, or overreaction? Experimental neurology 275 Pt 1: 162-171, 2016.
59. Blizzard CA, Southam KA, Dawkins E, et al.: Identifying the primary site of pathogenesis in amyotrophic lateral sclerosis - vulnerability of lower motor neurons to proximal excitotoxicity. Disease models & mechanisms 8: 215-224, 2015.
60. Foerster BR, Pomper MG, Callaghan BC, et al.: An imbalance between excitatory and inhibitory neurotransmitters in amyotrophic lateral sclerosis revealed by use of 3-T proton magnetic resonance spectroscopy. JAMA neurology 70: 1009-1016, 2013.
61. Park E, Velumian AA and Fehlings MG: The role of excitotoxicity in secondary mechanisms of spinal cord injury: a review with an emphasis on the implications for white matter degeneration. Journal of neurotrauma 21: 754-774, 2004.
62. Cooper AJ: The role of glutamine synthetase and glutamate dehydrogenase in cerebral ammonia homeostasis. Neurochemical research 37: 2439-2455, 2012.
63. Matyja E, Taraszewska A, Naganska E, Rafalowska J and Gebarowska J: Astroglial alterations in amyotrophic lateral sclerosis (ALS) model of slow glutamate excitotoxicity in vitro. Folia neuropathologica / Association of Polish Neuropathologists and Medical Research Centre, Polish Academy of Sciences 44: 183-190, 2006.
64. King AE, Dickson TC, Blizzard CA, et al.: Excitotoxicity mediated by non-NMDA receptors causes distal axonopathy in long-term cultured spinal motor neurons. The European journal of neuroscience 26: 2151-2159, 2007.
65. Gressens P: VIP neuroprotection against excitotoxic lesions of the developing mouse brain. Annals of the New York Academy of Sciences 897: 109-124, 1999.
66. Passemard S, Sokolowska P, Schwendimann L and Gressens P: VIP-induced neuroprotection of the developing brain. Current pharmaceutical design 17: 1036-1039, 2011.
67. Lee J, Hyeon SJ, Im H, Ryu H, Kim Y and Ryu H: Astrocytes and Microglia as Non-cell Autonomous Players in the Pathogenesis of ALS. Experimental neurobiology 25: 233-240, 2016.
68. Ludwin SK, Rao V, Moore CS and Antel JP: Astrocytes in multiple sclerosis. Multiple sclerosis 22: 1114-

1124, 2016.
69. Takimoto M and Hamada T: Acute exercise increases brain region-specific expression of MCT1, MCT2, MCT4, GLUT1, and COX IV proteins. Journal of applied physiology 116: 1238-1250, 2014.
70. Lundgaard I, Osorio MJ, Kress BT, Sanggaard S and Nedergaard M: White matter astrocytes in health and disease. Neuroscience 276: 161-173, 2014.
71. Morrison BM, Lee Y and Rothstein JD: Oligodendroglia: metabolic supporters of axons. Trends Cell Biol 23: 644-651, 2013.
72. Purger D, Gibson EM and Monje M: Myelin plasticity in the central nervous system. Neuropharmacology 110: 563-573, 2016.
73. Debanne D, Campanac E, Bialowas A, Carlier E and Alcaraz G: Axon physiology. Physiological reviews 91: 555-602, 2011.
74. Alexandra IM, Constanze D and Klaus-Armin N: An emerging role of dysfunctional axon-oligodendrocyte coupling in neurodegenerative diseases. Dialogues Clin Neurosci 20: 283-292, 2018.
75. Simons M and Nave KA: Oligodendrocytes: Myelination and Axonal Support. Cold Spring Harb Perspect Biol 8: a020479, 2015.
76. Philips T and Rothstein JD: Oligodendroglia: metabolic supporters of neurons. J Clin Invest 127: 3271-3280, 2017.
77. Philips T, Bento-Abreu A, Nonneman A, et al.: Oligodendrocyte dysfunction in the pathogenesis of amyotrophic lateral sclerosis. Brain 136: 471-482, 2013.
78. Edgar JM and Nave KA: The role of CNS glia in preserving axon function. Current opinion in neurobiology 19: 498-504, 2009.
79. Funfschilling U, Supplie LM, Mahad D, et al.: Glycolytic oligodendrocytes maintain myelin and long-term axonal integrity. Nature 485: 517-521, 2012.
80. Lee Y, Morrison BM, Li Y, et al.: Oligodendroglia metabolically support axons and contribute to neurodegeneration. Nature 487: 443-448, 2012.
81. Ferraiuolo L, Meyer K, Sherwood TW, et al.: Oligodendrocytes contribute to motor neuron death in ALS via SOD1-dependent mechanism. Proceedings of the National Academy of Sciences of the United States of America 113: E6496-E6505, 2016.
82. Kang SH, Li Y, Fukaya M, et al.: Degeneration and impaired regeneration of gray matter oligodendrocytes in amyotrophic lateral sclerosis. Nat Neurosci 16: 571-579, 2013.
83. Nonneman A, Robberecht W and Van Den Bosch L: The role of oligodendroglial dysfunction in amyotrophic lateral sclerosis. Neurodegenerative disease management 4: 223-239, 2014.
84. Barateiro A, Brites D and Fernandes A: Oligodendrocyte Development and Myelination in Neurodevelopment: Molecular Mechanisms in Health and Disease. Current pharmaceutical design 22: 656-679, 2016.
85. Fischer LR, Culver DG, Tennant P, et al.: Amyotrophic lateral sclerosis is a distal axonopathy: evidence in mice and man. Experimental neurology 185: 232-240, 2004.
86. Lemmens R, Van Hoecke A, Hersmus N, et al.: Overexpression of mutant superoxide dismutase 1 causes a

motor axonopathy in the zebrafish. Human molecular genetics 16: 2359-2365, 2007.
87. Wong M and Martin LJ: Skeletal muscle-restricted expression of human SOD1 causes motor neuron degeneration in transgenic mice. Human molecular genetics 19: 2284-2302, 2010.
88. Sotelo-Silveira JR, Lepanto P, Elizondo V, et al.: Axonal mitochondrial clusters containing mutant SOD1 in transgenic models of ALS. Antioxidants & redox signaling 11: 1535-1545, 2009.
89. King AE, Dickson TC, Blizzard CA, et al.: Neuron-glia interactions underlie ALS-like axonal cytoskeletal pathology. Neurobiology of aging 32: 459-469, 2011.
90. Frey D, Schneider C, Xu L, Borg J, Spooren W and Caroni P: Early and selective loss of neuromuscular synapse subtypes with low sprouting competence in motoneuron diseases. The Journal of neuroscience : the official journal of the Society for Neuroscience 20: 2534-2542, 2000.
91. Nave KA and Trapp BD: Axon-glial signaling and the glial support of axon function. Annual review of neuroscience 31: 535-561, 2008.
92. Anderson JE, Do MQ, Daneshvar N, et al.: The role of semaphorin3A in myogenic regeneration and the formation of functional neuromuscular junctions on new fibres. Biological reviews of the Cambridge Philosophical Society2016.
93. Syed YA, Hand E, Mobius W, et al.: Inhibition of CNS remyelination by the presence of semaphorin 3A. The Journal of neuroscience : the official journal of the Society for Neuroscience 31: 3719-3728, 2011.
94. Spassky N, de Castro F, Le Bras B, et al.: Directional guidance of oligodendroglial migration by class 3 semaphorins and netrin-1. The Journal of neuroscience : the official journal of the Society for Neuroscience 22: 5992-6004, 2002.
95. Piaton G, Aigrot MS, Williams A, et al.: Class 3 semaphorins influence oligodendrocyte precursor recruitment and remyelination in adult central nervous system. Brain : a journal of neurology 134: 1156-1167, 2011.
96. Venkova K, Christov A, Kamaluddin Z, Kobalka P, Siddiqui S and Hensley K: Semaphorin 3A signaling through neuropilin-1 is an early trigger for distal axonopathy in the SOD1G93A mouse model of amyotrophic lateral sclerosis. Journal of neuropathology and experimental neurology 73: 702-713, 2014.
97. Korner S, Boselt S, Wichmann K, et al.: The Axon Guidance Protein Semaphorin 3A Is Increased in the Motor Cortex of Patients With Amyotrophic Lateral Sclerosis. Journal of neuropathology and experimental neurology2016.
98. Mecollari V, Nieuwenhuis B and Verhaagen J: A perspective on the role of class III semaphorin signaling in central nervous system trauma. Frontiers in cellular neuroscience 8: 328, 2014.
99. Dadon-Nachum M, Melamed E and Offen D: The "dying-back" phenomenon of motor neurons in ALS. Journal of molecular neuroscience : MN 43: 470-477, 2011.
100. Tao S, Yang X, Chen Y, et al.: Up-regulated methyl CpG binding protein-2 in intractable temporal lobe epilepsy patients and a rat model. Neurochemical research 37: 1886-1897, 2012.
101. KhorshidAhmad T, Acosta C, Cortes C, Lakowski TM, Gangadaran S and Namaka M: Transcriptional Regulation of Brain-Derived Neurotrophic Factor (BDNF) by Methyl CpG Binding Protein 2 (MeCP2): a Novel Mechanism for Re-Myelination and/or Myelin Repair Involved in the Treatment of Multiple Sclerosis (MS).

Molecular neurobiology 53: 1092-1107, 2016.
102. Dastidar SG, Bardai FH, Ma C, et al.: Isoform-specific toxicity of Mecp2 in postmitotic neurons: suppression of neurotoxicity by FoxG1. The Journal of neuroscience : the official journal of the Society for Neuroscience 32: 2846-2855, 2012.
103. Dastidar SG, Landrieu PM and D'Mello SR: FoxG1 promotes the survival of postmitotic neurons. The Journal of neuroscience : the official journal of the Society for Neuroscience 31: 402-413, 2011.
104. Schulte-Herbruggen O, Braun A, Rochlitzer S, Jockers-Scherubl MC and Hellweg R: Neurotrophic factors--a tool for therapeutic strategies in neurological, neuropsychiatric and neuroimmunological diseases? Current medicinal chemistry 14: 2318-2329, 2007.
105. Cellerino A, Carroll P, Thoenen H and Barde YA: Reduced size of retinal ganglion cell axons and hypomyelination in mice lacking brain-derived neurotrophic factor. Molecular and cellular neurosciences 9: 397-408, 1997.
106. Tremolizzo L, Pellegrini A, Conti E, et al.: BDNF Serum Levels with Respect to Multidimensional Assessment in Amyotrophic Lateral Sclerosis. Neuro-degenerative diseases 16: 192-198, 2016.
107. Gimenez y Ribotta M, Revah F, Pradier L, Loquet I, Mallet J and Privat A: Prevention of motoneuron death by adenovirus-mediated neurotrophic factors. Journal of neuroscience research 48: 281-285, 1997.
108. Dadon-Nachum M, Ben-Yaacov K, Ben-Zur T, et al.: Transplanted modified muscle progenitor cells expressing a mixture of neurotrophic factors delay disease onset and enhance survival in the SOD1 mouse model of ALS. J Mol Neurosci 55: 788-797, 2015.
109. Xu R, Wu C, Zhang X, et al.: Linking hypoxic and oxidative insults to cell death mechanisms in models of ALS. Brain research 1372: 133-144, 2011.
110. Oh YK, Shin KS and Kang SJ: AIF translocates to the nucleus in the spinal motor neurons in a mouse model of ALS. Neuroscience letters 406: 205-210, 2006.
111. Pedrini S, Sau D, Guareschi S, et al.: ALS-linked mutant SOD1 damages mitochondria by promoting conformational changes in Bcl-2. Human molecular genetics 19: 2974-2986, 2010.
112. Troost D, Aten J, Morsink F and de Jong JM: Apoptosis in amyotrophic lateral sclerosis is not restricted to motor neurons. Bcl-2 expression is increased in unaffected post-central gyrus. Neuropathology and applied neurobiology 21: 498-504, 1995.
113. Petrik MS, Wilson JM, Grant SC, et al.: Magnetic resonance microscopy and immunohistochemistry of the CNS of the mutant SOD murine model of ALS reveals widespread neural deficits. Neuromolecular medicine 9: 216-229, 2007.
114. Nagai M, Re DB, Nagata T, et al.: Astrocytes expressing ALS-linked mutated SOD1 release factors selectively toxic to motor neurons. Nature neuroscience 10: 615-622, 2007.
115. Guegan C and Przedborski S: Programmed cell death in amyotrophic lateral sclerosis. The Journal of clinical investigation 111: 153-161, 2003.
116. Reyes NA, Fisher JK, Austgen K, VandenBerg S, Huang EJ and Oakes SA: Blocking the mitochondrial apoptotic pathway preserves motor neuron viability and function in a mouse model of amyotrophic lateral sclerosis. The Journal of clinical investigation 120: 3673-3679, 2010.

117. Vukosavic S, Dubois-Dauphin M, Romero N and Przedborski S: Bax and Bcl-2 interaction in a transgenic mouse model of familial amyotrophic lateral sclerosis. Journal of neurochemistry 73: 2460-2468, 1999.
118. Peviani M, Tortarolo M, Battaglia E, Piva R and Bendotti C: Specific induction of Akt3 in spinal cord motor neurons is neuroprotective in a mouse model of familial amyotrophic lateral sclerosis. Molecular neurobiology 49: 136-148, 2014.
119. Shrivastava M and Subbiah V: Elevated caspase 3 activity and cytosolic cytochrome c in NT2 cybrids containing amyotrophic lateral sclerosis subject mtDNA. The International journal of neuroscience 126: 839-849, 2016.
120. Sathasivam S and Shaw PJ: Apoptosis in amyotrophic lateral sclerosis--what is the evidence? The Lancet. Neurology 4: 500-509, 2005.
121. Tanaka H, Shimazaki H, Kimura M, et al.: Apoptosis-inducing factor and cyclophilin A cotranslocate to the motor neuronal nuclei in amyotrophic lateral sclerosis model mice. CNS neuroscience & therapeutics 17: 294-304, 2011.
122. Wang Y and Kasper LH: The role of microbiome in central nervous system disorders. Brain, behavior, and immunity 38: 1-12, 2014.
123. Glenn JD and Mowry EM: Emerging Concepts on the Gut Microbiome and Multiple Sclerosis. Journal of interferon & cytokine research : the official journal of the International Society for Interferon and Cytokine Research 36: 347-357, 2016.
124. Bhargava P and Mowry EM: Gut microbiome and multiple sclerosis. Current neurology and neuroscience reports 14: 492, 2014.
125. Luna RA, Savidge TC and Williams KC: The Brain-Gut-Microbiome Axis: What Role Does It Play in Autism Spectrum Disorder? Current developmental disorders reports 3: 75-81, 2016.
126. Fang X: Potential role of gut microbiota and tissue barriers in Parkinson's disease and amyotrophic lateral sclerosis. The International journal of neuroscience 126: 771-776, 2016.
127. Galland L: The gut microbiome and the brain. Journal of medicinal food 17: 1261-1272, 2014.
128. Linden JR, Ma Y, Zhao B, et al.: Clostridium perfringens Epsilon Toxin Causes Selective Death of Mature Oligodendrocytes and Central Nervous System Demyelination. mBio 6: e02513, 2015.
129. Newland PK, Heitkemper M and Zhou Y: The Emerging Role of the Gut Microbiome in Adult Patients With Multiple Sclerosis. The Journal of neuroscience nursing : journal of the American Association of Neuroscience Nurses 48: 358-364, 2016.
130. Chen J, Chia N, Kalari KR, et al.: Multiple sclerosis patients have a distinct gut microbiota compared to healthy controls. Scientific reports 6: 28484, 2016.
131. Kaneko K and Hachiya NS: Hypothesis: gut as source of motor neuron toxin in the development of ALS. Medical hypotheses 66: 438-439, 2006.
132. Longstreth WT, Jr., Meschke JS, Davidson SK, Smoot LM, Smoot JC and Koepsell TD: Hypothesis: a motor neuron toxin produced by a clostridial species residing in gut causes ALS. Medical hypotheses 64: 1153-1156, 2005.
133. Wu S, Yi J, Zhang YG, Zhou J and Sun J: Leaky intestine and impaired microbiome in an amyotrophic lateral

sclerosis mouse model. Physiological reports 32015.
134. Rooney J, Byrne S, Heverin M, et al.: A multidisciplinary clinic approach improves survival in ALS: a comparative study of ALS in Ireland and Northern Ireland. J Neurol Neurosurg Psychiatry 86: 496-501, 2015.
135. Van den Berg JP, Kalmijn S, Lindeman E, et al.: Multidisciplinary ALS care improves quality of life in patients with ALS. Neurology 65: 1264-1267, 2005.
136. Hardiman O, Al-Chalabi A, Chio A, et al.: Amyotrophic lateral sclerosis. Nat Rev Dis Primers 3: 17071, 2017.
137. Miller RG, Mitchell JD and Moore DH: Riluzole for amyotrophic lateral sclerosis (ALS)/motor neuron disease (MND). The Cochrane database of systematic reviews: CD001447, 2012.
138. Cetin H, Rath J, Fuzi J, et al.: Epidemiology of amyotrophic lateral sclerosis and effect of riluzole on disease course. Neuroepidemiology 44: 6-15, 2015.
139. Vucic S, Lin CS, Cheah BC, et al.: Riluzole exerts central and peripheral modulating effects in amyotrophic lateral sclerosis. Brain : a journal of neurology 136: 1361-1370, 2013.
140. Cheah BC, Vucic S, Krishnan AV and Kiernan MC: Riluzole, neuroprotection and amyotrophic lateral sclerosis. Current medicinal chemistry 17: 1942-1199, 2010.
141. Bellingham MC: A review of the neural mechanisms of action and clinical efficiency of riluzole in treating amyotrophic lateral sclerosis: what have we learned in the last decade? CNS neuroscience & therapeutics 17: 4-31, 2011.
142. Dennys CN, Armstrong J, Levy M, et al.: Chronic inhibitory effect of riluzole on trophic factor production. Exp Neurol 271: 301-307, 2015.
143. Tsai SJ: Is riluzole a potential therapy for Rett syndrome? Medical hypotheses 85: 76-78, 2015.
144. Turck P and Frizzo ME: Riluzole stimulates BDNF release from human platelets. BioMed research international 2015: 189307, 2015.
145. Zhu W, Frost EE, Begum F, et al.: The role of dorsal root ganglia activation and brain-derived neurotrophic factor in multiple sclerosis. J Cell Mol Med 16: 1856-1865, 2012.
146. Obata K and Noguchi K: BDNF in sensory neurons and chronic pain. Neuroscience research 55: 1-10, 2006.
147. Caumo W, Deitos A, Carvalho S, et al.: Motor Cortex Excitability and BDNF Levels in Chronic Musculoskeletal Pain According to Structural Pathology. Frontiers in human neuroscience 10: 357, 2016.
148. Nagase M, Yamamoto Y, Miyazaki Y and Yoshino H: Increased oxidative stress in patients with amyotrophic lateral sclerosis and the effect of edaravone administration. Redox Rep 21: 104-112, 2016.
149. Banno M, Mizuno T, Kato H, et al.: The radical scavenger edaravone prevents oxidative neurotoxicity induced by peroxynitrite and activated microglia. Neuropharmacology 48: 283-290, 2005.
150. Kraus RL, Pasieczny R, Lariosa-Willingham K, Turner MS, Jiang A and Trauger JW: Antioxidant properties of minocycline: neuroprotection in an oxidative stress assay and direct radical-scavenging activity. J Neurochem 94: 819-827, 2005.
151. Watanabe T, Morita I, Nishi H and Murota S: Preventive effect of MCI-186 on 15-HPETE induced vascular endothelial cell injury in vitro. Prostaglandins Leukot Essent Fatty Acids 33: 81-87, 1988.
152. Hardiman O and van den Berg LH: Edaravone: a new treatment for ALS on the horizon? Lancet Neurol 16:

490-491, 2017.
153. Yang LP and Deeks ED: Dextromethorphan/quinidine: a review of its use in adults with pseudobulbar affect. Drugs 75: 83-90, 2015.
154. Smith R, Pioro E, Myers K, et al.: Enhanced Bulbar Function in Amyotrophic Lateral Sclerosis: The Nuedexta Treatment Trial. Neurotherapeutics 14: 762-772, 2017.
155. Cruz MP: Nuedexta for the treatment of pseudobulbar affect: a condition of involuntary crying or laughing. P T 38: 325-328, 2013.
156. Gutierrez J, Federici T, Peterson B, Bartus R, Betourne A and Boulis NM: 321 Development of Intrathecal Riluzole: A New Route of Administration for the Treatment of Amyotrophic Lateral Sclerosis Patients. Neurosurgery 63 Suppl 1: 193, 2016.
157. Browne EC and Abbott BM: Recent progress towards an effective treatment of amyotrophic lateral sclerosis using the SOD1 mouse model in a preclinical setting. European journal of medicinal chemistry2016.
158. Lieberknecht V, Junqueira SC, Cunha MP, et al.: Pramipexole, a Dopamine D2/D3 Receptor-Preferring Agonist, Prevents Experimental Autoimmune Encephalomyelitis Development in Mice. Molecular neurobiology2016.
159. Ferrari-Toninelli G, Maccarinelli G, Uberti D, Buerger E and Memo M: Mitochondria-targeted antioxidant effects of S(-) and R(+) pramipexole. BMC pharmacology 10: 2, 2010.
160. Abramova NA, Cassarino DS, Khan SM, Painter TW and Bennett JP, Jr.: Inhibition by R(+) or S(-) pramipexole of caspase activation and cell death induced by methylpyridinium ion or beta amyloid peptide in SH-SY5Y neuroblastoma. Journal of neuroscience research 67: 494-500, 2002.
161. Alavian KN, Dworetzky SI, Bonanni L, et al.: Effects of dexpramipexole on brain mitochondrial conductances and cellular bioenergetic efficiency. Brain research 1446: 1-11, 2012.
162. Corcia P and Gordon PH: Amyotrophic lateral sclerosis and the clinical potential of dexpramipexole. Therapeutics and clinical risk management 8: 359-366, 2012.
163. De Nuccio C, Bernardo A, Cruciani C, De Simone R, Visentin S and Minghetti L: Peroxisome proliferator activated receptor-gamma agonists protect oligodendrocyte progenitors against tumor necrosis factor-alpha-induced damage: Effects on mitochondrial functions and differentiation. Experimental neurology 271: 506-514, 2015.
164. Shukla DK, Kaiser CC, Stebbins GT and Feinstein DL: Effects of pioglitazone on diffusion tensor imaging indices in multiple sclerosis patients. Neuroscience letters 472: 153-156, 2010.
165. Dupuis L, Dengler R, Heneka MT, et al.: A randomized, double blind, placebo-controlled trial of pioglitazone in combination with riluzole in amyotrophic lateral sclerosis. PloS one 7: e37885, 2012.
166. Yanez M, Matias-Guiu J, Arranz-Tagarro JA, et al.: The neuroprotection exerted by memantine, minocycline and lithium, against neurotoxicity of CSF from patients with amyotrophic lateral sclerosis, is antagonized by riluzole. Neuro-degenerative diseases 13: 171-179, 2014.
167. Herges K, Millward JM, Hentschel N, Infante-Duarte C, Aktas O and Zipp F: Neuroprotective effect of combination therapy of glatiramer acetate and epigallocatechin-3-gallate in neuroinflammation. PloS one 6: e25456, 2011.

168. Koh SH, Lee SM, Kim HY, et al.: The effect of epigallocatechin gallate on suppressing disease progression of ALS model mice. Neuroscience letters 395: 103-107, 2006.
169. Solanki I, Parihar P, Mansuri ML and Parihar MS: Flavonoid-based therapies in the early management of neurodegenerative diseases. Advances in nutrition 6: 64-72, 2015.
170. Feng Z and Gao F: Stem cell challenges in the treatment of neurodegenerative disease. CNS neuroscience & therapeutics 18: 142-148, 2012.
171. Nizzardo M, Simone C, Rizzo F, et al.: Minimally invasive transplantation of iPSC-derived ALDHhiSSCloVLA4+ neural stem cells effectively improves the phenotype of an amyotrophic lateral sclerosis model. Human molecular genetics 23: 342-354, 2014.
172. Martinez HR, Gonzalez-Garza MT, Moreno-Cuevas JE, Caro E, Gutierrez-Jimenez E and Segura JJ: Stem-cell transplantation into the frontal motor cortex in amyotrophic lateral sclerosis patients. Cytotherapy 11: 26-34, 2009.
173. Einstein O, Friedman-Levi Y, Grigoriadis N and Ben-Hur T: Transplanted neural precursors enhance host brain-derived myelin regeneration. The Journal of neuroscience : the official journal of the Society for Neuroscience 29: 15694-15702, 2009.
174. Makar TK, Bever CT, Singh IS, et al.: Brain-derived neurotrophic factor gene delivery in an animal model of multiple sclerosis using bone marrow stem cells as a vehicle. Journal of neuroimmunology 210: 40-51, 2009.
175. Ayers JI and Cashman NR: Prion-like mechanisms in amyotrophic lateral sclerosis. Handb Clin Neurol 153: 337-354, 2018.
176. Sheng Y, Chattopadhyay M, Whitelegge J and Valentine JS: SOD1 aggregation and ALS: role of metallation states and disulfide status. Curr Top Med Chem 12: 2560-2572, 2012.
177. Chen S, Sayana P, Zhang X and Le W: Genetics of amyotrophic lateral sclerosis: an update. Mol Neurodegener 8: 28, 2013.
178. Kumar V, Sami N, Kashav T, Islam A, Ahmad F and Hassan MI: Protein aggregation and neurodegenerative diseases: From theory to therapy. European journal of medicinal chemistry 124: 1105-1120, 2016.
179. Dobson CM: Protein folding and misfolding. Nature 426: 884-890, 2003.
180. Brundin P, Melki R and Kopito R: Prion-like transmission of protein aggregates in neurodegenerative diseases. Nat Rev Mol Cell Biol 11: 301-307, 2010.
181. Watanabe M, Dykes-Hoberg M, Culotta VC, Price DL, Wong PC and Rothstein JD: Histological evidence of protein aggregation in mutant SOD1 transgenic mice and in amyotrophic lateral sclerosis neural tissues. Neurobiol Dis 8: 933-941, 2001.
182. Bruijn LI, Houseweart MK, Kato S, et al.: Aggregation and motor neuron toxicity of an ALS-linked SOD1 mutant independent from wild-type SOD1. Science 281: 1851-1854, 1998.
183. Johnston JA, Dalton MJ, Gurney ME and Kopito RR: Formation of high molecular weight complexes of mutant Cu, Zn-superoxide dismutase in a mouse model for familial amyotrophic lateral sclerosis. Proc Natl Acad Sci U S A 97: 12571-12576, 2000.
184. Bunton-Stasyshyn RK, Saccon RA, Fratta P and Fisher EM: SOD1 Function and Its Implications for Amyotrophic Lateral Sclerosis Pathology: New and Renascent Themes. Neuroscientist 21: 519-529, 2015.

185. Sibilla C and Bertolotti A: Prion Properties of SOD1 in Amyotrophic Lateral Sclerosis and Potential Therapy. Cold Spring Harb Perspect Biol 92017.
186. Wong PC, Pardo CA, Borchelt DR, et al.: An adverse property of a familial ALS-linked SOD1 mutation causes motor neuron disease characterized by vacuolar degeneration of mitochondria. Neuron 14: 1105-1116, 1995.
187. Borchelt DR, Lee MK, Slunt HS, et al.: Superoxide dismutase 1 with mutations linked to familial amyotrophic lateral sclerosis possesses significant activity. Proc Natl Acad Sci U S A 91: 8292-8296, 1994.
188. Borchelt DR, Guarnieri M, Wong PC, et al.: Superoxide dismutase 1 subunits with mutations linked to familial amyotrophic lateral sclerosis do not affect wild-type subunit function. J Biol Chem 270: 3234-3238, 1995.
189. Gurney ME, Pu H, Chiu AY, et al.: Motor neuron degeneration in mice that express a human Cu,Zn superoxide dismutase mutation. Science 264: 1772-1775, 1994.
190. Reaume AG, Elliott JL, Hoffman EK, et al.: Motor neurons in Cu/Zn superoxide dismutase-deficient mice develop normally but exhibit enhanced cell death after axonal injury. Nat Genet 13: 43-47, 1996.
191. Chen X, Shang H, Qiu X, et al.: Oxidative modification of cysteine 111 promotes disulfide bond-independent aggregation of SOD1. Neurochem Res 37: 835-845, 2012.
192. Chen X, Zhang X, Li C, et al.: S-nitrosylated protein disulfide isomerase contributes to mutant SOD1 aggregates in amyotrophic lateral sclerosis. J Neurochem 124: 45-58, 2013.
193. Chen X, Guan T, Li C, et al.: SOD1 aggregation in astrocytes following ischemia/reperfusion injury: a role of NO-mediated S-nitrosylation of protein disulfide isomerase (PDI). J Neuroinflammation 9: 237, 2012.
194. Chattopadhyay M and Valentine JS: Aggregation of copper-zinc superoxide dismutase in familial and sporadic ALS. Antioxid Redox Signal 11: 1603-1614, 2009.
195. Bosco DA, Morfini G, Karabacak NM, et al.: Wild-type and mutant SOD1 share an aberrant conformation and a common pathogenic pathway in ALS. Nat Neurosci 13: 1396-1403, 2010.
196. Ezzi SA, Urushitani M and Julien JP: Wild-type superoxide dismutase acquires binding and toxic properties of ALS-linked mutant forms through oxidation. J Neurochem 102: 170-178, 2007.
197. Kabashi E, Valdmanis PN, Dion P and Rouleau GA: Oxidized/misfolded superoxide dismutase-1: the cause of all amyotrophic lateral sclerosis? Ann Neurol 62: 553-559, 2007.
198. Furukawa Y, Fu R, Deng HX, Siddique T and O'Halloran TV: Disulfide cross-linked protein represents a significant fraction of ALS-associated Cu, Zn-superoxide dismutase aggregates in spinal cords of model mice. Proc Natl Acad Sci USA 103: 7148-7153, 2006.
199. Tiwari A and Hayward LJ: Familial amyotrophic lateral sclerosis mutants of copper/zinc superoxide dismutase are susceptible to disulfide reduction. J Biol Chem 278: 5984-5992, 2003.
200. Julien J-P: Amyotrophic lateral sclerosis: Unfold the toxicity of the misfolded. Cell 104: 581-591, 2001.
201. Guareschi S, Cova E, Cereda C, et al.: An over-oxidized form of superoxide dismutase found in sporadic amyotrophic lateral sclerosis with bulbar onset shares a toxic mechanism with mutant SOD1. Proc Natl Acad Sci U S A 109: 5074-5079, 2012.
202. Furukawa Y and O'Halloran TV: Posttranslational modifications in Cu,Zn-superoxide dismutase and mutations associated with amyotrophic lateral sclerosis. Antioxid Redox Signal 8: 847-867, 2006.

203. Lodish H: Molecular Cell Biology 8th Edition. 2016.
204. Labbadia J and Morimoto RI: The biology of proteostasis in aging and disease. Annu Rev Biochem 84: 435-464, 2015.
205. Finley D: Recognition and processing of ubiquitin-protein conjugates by the proteasome. Annu Rev Biochem 78: 477-513, 2009.
206. Clague MJ, Barsukov I, Coulson JM, Liu H, Rigden DJ and Urbe S: Deubiquitylases from genes to organism. Physiol Rev 93: 1289-1315, 2013.
207. Xu H, You M, Shi H and Hou Y: Ubiquitin-mediated NFkappaB degradation pathway. Cell Mol Immunol 12: 653-655, 2015.
208. Collins I, Wang H, Caldwell JJ and Chopra R: Chemical approaches to targeted protein degradation through modulation of the ubiquitin-proteasome pathway. Biochem J 474: 1127-1147, 2017.
209. Neklesa TK, Winkler JD and Crews CM: Targeted protein degradation by PROTACs. Pharmacol Ther 174: 138-144, 2017.
210. Cromm PM and Crews CM: Targeted Protein Degradation: from Chemical Biology to Drug Discovery. Cell Chem Biol 24: 1181-1190, 2017.
211. Dikic I: Proteasomal and Autophagic Degradation Systems. Annu Rev Biochem 86: 193-224, 2017.
212. Xilouri M, Brekk OR and Stefanis L: alpha-Synuclein and protein degradation systems: a reciprocal relationship. Mol Neurobiol 47: 537-551, 2013.
213. Rabinowitz JD and White E: Autophagy and metabolism. Science 330: 1344-1348, 2010.
214. Wang DW, Peng ZJ, Ren GF and Wang GX: The different roles of selective autophagic protein degradation in mammalian cells. Oncotarget 6: 37098-37116, 2015.
215. Tekirdag K and Cuervo AM: Chaperone-mediated autophagy and endosomal microautophagy: Joint by a chaperone. J Biol Chem 293: 5414-5424, 2018.
216. Korolchuk VI, Menzies FM and Rubinsztein DC: Mechanisms of cross-talk between the ubiquitin-proteasome and autophagy-lysosome systems. FEBS Lett 584: 1393-1398, 2010.
217. Sach M, Winkler G, Glauche V, et al.: Diffusion tensor MRI of early upper motor neuron involvement in amyotrophic lateral sclerosis. Brain : a journal of neurology 127: 340-350, 2004.
218. Spinelli EG, Agosta F, Ferraro PM, et al.: Brain MR Imaging in Patients with Lower Motor Neuron-predominant Disease. Radiology2016.
219. Prudlo J, Bissbort C, Glass A, et al.: White matter pathology in ALS and lower motor neuron ALS variants: a diffusion tensor imaging study using tract-based spatial statistics. Journal of neurology 259: 1848-1859, 2012.
220. Beer A, Biberacher V, Schmidt P, et al.: Tissue damage within normal appearing white matter in early multiple sclerosis: assessment by the ratio of T1- and T2-weighted MR image intensity. Journal of neurology 263: 1495-1502, 2016.
221. Deng HX, Hentati A, Tainer JA, et al.: Amyotrophic lateral sclerosis and structural defects in Cu,Zn superoxide dismutase. Science 261: 1047-1051, 1993.
222. Li HF and Wu ZY: Genotype-phenotype correlations of amyotrophic lateral sclerosis. Transl Neurodegener 5: 3, 2016.

223. Fridovich I: Superoxide radical and superoxide dismutases. Annu Rev Biochem 64: 97-112, 1995.
224. Fischer LR, Igoudjil A, Magrane J, et al.: SOD1 targeted to the mitochondrial intermembrane space prevents motor neuropathy in the Sod1 knockout mouse. Brain 134: 196-209, 2011.
225. Ding H, Schwarz DS, Keene A, et al.: Selective silencing by RNAi of a dominant allele that causes amyotrophic lateral sclerosis. Aging Cell 2: 209-217, 2003.
226. Raoul C, Abbas-Terki T, Bensadoun JC, et al.: Lentiviral-mediated silencing of SOD1 through RNA interference retards disease onset and progression in a mouse model of ALS. Nat Med 11: 423-428, 2005.
227. Castanotto D and Rossi JJ: The promises and pitfalls of RNA-interference-based therapeutics. Nature 457: 426-433, 2009.
228. Jackson AL and Linsley PS: Recognizing and avoiding siRNA off-target effects for target identification and therapeutic application. Nature reviews. Drug discovery 9: 57-67, 2010.
229. Urushitani M, Ezzi SA and Julien JP: Therapeutic effects of immunization with mutant superoxide dismutase in mice models of amyotrophic lateral sclerosis. Proc Natl Acad Sci USA 104: 2495-2500, 2007.
230. Liu YH, Giunta B, Zhou HD, Tan J and Wang YJ: Immunotherapy for Alzheimer disease: the challenge of adverse effects. Nature reviews. Neurology 8: 465-469, 2012.
231. Fan X, Jin WY, Lu J, Wang J and Wang YT: Rapid and reversible knockdown of endogenous proteins by peptide-directed lysosomal degradation. Nat Neurosci 17: 471-480, 2014.
232. Katiyar S, Joshi S and Lennarz WJ: The retrotranslocation protein Derlin-1 binds peptide:N-glycanase to the endoplasmic reticulum. Mol Biol Cell 16: 4584-4594, 2005.
233. Ye Y, Shibata Y, Yun C, Ron D and Rapoport TA: A membrane protein complex mediates retro-translocation from the ER lumen into the cytosol. Nature 429: 841-847, 2004.
234. Lilley BN and Ploegh HL: A membrane protein required for dislocation of misfolded proteins from the ER. Nature 429: 834-840, 2004.
235. Fujisawa T, Homma K, Yamaguchi N, et al.: A novel monoclonal antibody reveals a conformational alteration shared by amyotrophic lateral sclerosis-linked SOD1 mutants. Ann Neurol 72: 739-749, 2012.
236. Nishitoh H, Kadowaki H, Nagai A, et al.: ALS-linked mutant SOD1 induces ER stress- and ASK1-dependent motor neuron death by targeting Derlin-1. Genes Dev 22: 1451-1464, 2008.
237. Homma K, Fujisawa T, Tsuburaya N, et al.: SOD1 as a molecular switch for initiating the homeostatic ER stress response under zinc deficiency. Mol Cell 52: 75-86, 2013.
238. Pokrishevsky E, Grad LI and Cashman NR: TDP-43 or FUS-induced misfolded human wild-type SOD1 can propagate intercellularly in a prion-like fashion. Sci Rep 6: 22155, 2016.
239. Cui Y, Masaki K, Yamasaki R, et al.: Extensive dysregulations of oligodendrocytic and astrocytic connexins are associated with disease progression in an amyotrophic lateral sclerosis mouse model. J Neuroinflammation 11: 42, 2014.
240. Karch CM and Borchelt DR: A limited role for disulfide cross-linking in the aggregation of mutant SOD1 linked to familial amyotrophic lateral sclerosis. J Biol Chem 283: 13528-13537, 2008.
241. Wang J, Slunt H, Gonzales V, et al.: Copper-binding-site-null SOD1 causes ALS in transgenic mice: aggregates of non-native SOD1 delineate a common feature. Hum Mol Genet 12: 2753-2764, 2003.

242. Prophet EB and Pathology AFIo: Laboratory methods in histotechnology. American Registry of Pathology1992.
243. Seglen PO, Grinde B and Solheim AE: Inhibition of the lysosomal pathway of protein degradation in isolated rat hepatocytes by ammonia, methylamine, chloroquine and leupeptin. Eur J Biochem 95: 215-225, 1979.
244. Zhou J, Tan SH, Nicolas V, et al.: Activation of lysosomal function in the course of autophagy via mTORC1 suppression and autophagosome-lysosome fusion. Cell Res 23: 508-523, 2013.
245. Leeman DS, Hebestreit K, Ruetz T, et al.: Lysosome activation clears aggregates and enhances quiescent neural stem cell activation during aging. Science 359: 1277-1283, 2018.
246. Domise M, Didier S, Marinangeli C, et al.: AMP-activated protein kinase modulates tau phosphorylation and tau pathology in vivo. Sci Rep 6: 26758, 2016.
247. Yoon BC, Jung H, Dwivedy A, O'Hare CM, Zivraj KH and Holt CE: Local translation of extranuclear lamin B promotes axon maintenance. Cell 148: 752-764, 2012.
248. Bandyopadhyay U, Kaushik S, Varticovski L and Cuervo AM: The chaperone-mediated autophagy receptor organizes in dynamic protein complexes at the lysosomal membrane. Mol Cell Biol 28: 5747-5763, 2008.
249. Furukawa Y, Fu R, Deng HX, Siddique T and O'Halloran TV: Disulfide cross-linked protein represents a significant fraction of ALS-associated Cu, Zn-superoxide dismutase aggregates in spinal cords of model mice. Proc Natl Acad Sci U S A 103: 7148-7153, 2006.
250. Banks WA: Peptides and the blood-brain barrier. Peptides 72: 16-19, 2015.
251. Powell MF, Grey H, Gaeta F, Sette A and Colon S: Peptide stability in drug development: a comparison of peptide reactivity in different biological media. J Pharm Sci 81: 731-735, 1992.
252. Fosgerau K and Hoffmann T: Peptide therapeutics: current status and future directions. Drug Discov Today 20: 122-128, 2015.
253. Wang L, Grisotti G and Roos RP: Mutant SOD1 knockdown in all cell types ameliorates disease in G85R SOD1 mice with a limited additional effect over knockdown restricted to motor neurons. J Neurochem 113: 166-174, 2010.
254. Haidet-Phillips AM, Hester ME, Miranda CJ, et al.: Astrocytes from familial and sporadic ALS patients are toxic to motor neurons. Nat Biotechnol 29: 824-828, 2011.
255. Franklin RJ and Ffrench-Constant C: Remyelination in the CNS: from biology to therapy. Nature reviews. Neuroscience 9: 839-855, 2008.
256. Zhou T, Ahmad TK, Gozda K, Truong J, Kong J and Namaka M: Implications of white matter damage in amyotrophic lateral sclerosis (Review). Mol Med Rep 16: 4379-4392, 2017.
257. Finn PF and Dice JF: Ketone bodies stimulate chaperone-mediated autophagy. J Biol Chem 280: 25864-25870, 2005.
258. Finn PF, Mesires NT, Vine M and Dice JF: Effects of small molecules on chaperone-mediated autophagy. Autophagy 1: 141-145, 2005.
259. Jiang HQ, Ren M, Jiang HZ, et al.: Guanabenz delays the onset of disease symptoms, extends lifespan, improves motor performance and attenuates motor neuron loss in the SOD1 G93A mouse model of amyotrophic lateral sclerosis. Neuroscience 277: 132-138, 2014.

260. Raman C, McAllister SD, Rizvi G, Patel SG, Moore DH and Abood ME: Amyotrophic lateral sclerosis: delayed disease progression in mice by treatment with a cannabinoid. Amyotroph Lateral Scler Other Motor Neuron Disord 5: 33-39, 2004.
261. Weydt P, Hong S, Witting A, Moller T, Stella N and Kliot M: Cannabinol delays symptom onset in SOD1 (G93A) transgenic mice without affecting survival. Amyotroph Lateral Scler Other Motor Neuron Disord 6: 182-184, 2005.
262. Van Den Bosch L, Tilkin P, Lemmens G and Robberecht W: Minocycline delays disease onset and mortality in a transgenic model of ALS. Neuroreport 13: 1067-1070, 2002.
263. Kieran D, Kalmar B, Dick JR, Riddoch-Contreras J, Burnstock G and Greensmith L: Treatment with arimoclomol, a coinducer of heat shock proteins, delays disease progression in ALS mice. Nat Med 10: 402-405, 2004.
264. Kiaei M, Petri S, Kipiani K, et al.: Thalidomide and lenalidomide extend survival in a transgenic mouse model of amyotrophic lateral sclerosis. J Neurosci 26: 2467-2473, 2006.
265. Lau JL and Dunn MK: Therapeutic peptides: Historical perspectives, current development trends, and future directions. Bioorg Med Chem 26: 2700-2707, 2018.
266. Wu LC, Chen F, Lee SL, Raw A and Yu LX: Building parity between brand and generic peptide products: Regulatory and scientific considerations for quality of synthetic peptides. Int J Pharm 518: 320-334, 2017.
267. Baig MH, Ahmad K, Saeed M, et al.: Peptide based therapeutics and their use for the treatment of neurodegenerative and other diseases. Biomed Pharmacother 103: 574-581, 2018.
268. Zhang J, He J, Johnson JL, et al.: Chaperone-Mediated Autophagy Upregulation Rescues Megalin Expression and Localization in Cystinotic Proximal Tubule Cells. Front Endocrinol (Lausanne) 10: 21, 2019.
269. Song J: Transforming Cytosolic Proteins into "Insoluble" and Membrane-toxic Forms Triggering Diseases/Aging by Genetic, Pathological or Environmental Factors. Protein Pept Lett 24: 294-306, 2017.
270. Carroll J, Page TK, Chiang SC, et al.: Expression of a pathogenic mutation of SOD1 sensitizes aprataxin-deficient cells and mice to oxidative stress and triggers hallmarks of premature ageing. Hum Mol Genet 24: 828-840, 2015.
271. Helferich AM, McLean PJ, Weishaupt JH and Danzer KM: Commentary: alpha-synuclein interacts with SOD1 and promotes its oligomerization. J Neurol Neuromedicine 1: 28-30, 2016.
272. Helferich AM, Ruf WP, Grozdanov V, et al.: alpha-synuclein interacts with SOD1 and promotes its oligomerization. Mol Neurodegener 10: 66, 2015.

Chapter 4 Appendix

Implications of white matter damage in amyotrophic lateral sclerosis (Review)

TING ZHOU[1,2], TINA KHORSHID AHMAD[1], KIANA GOZDA[1], JESSICA TRUONG[1], JIMING KONG[2] and MICHAEL NAMAKA[1-5]

[1]College of Pharmacy, Rady Faculty of Health Sciences, University of Manitoba, Winnipeg, MB R3E 0T5; [2]Department of Human Anatomy and Cell Science, College of Medicine, Rady Faculty of Health Sciences, University of Manitoba, Winnipeg, MB R3E 0J9, Canada; [3]College of Pharmacy, Third Military Medical University, Chongqing 400038, P.R. China; [4]Department of Medical Rehabilitation, College of Medicine, Rady Faculty of Health Sciences, University of Manitoba, Winnipeg, MB R3E 0T6; [5]Department of Internal Medicine, College of Medicine, Rady Faculty of Health Sciences, University of Manitoba, Winnipeg, MB R3E 1R9, Canada

Received January 28, 2017; Accepted June 9, 2017

DOI: 10.3892/mmr.2017.7186

Abstract. Amyotrophic lateral sclerosis (ALS) is a fatal neurodegenerative disease, which involves the progressive degeneration of motor neurons. ALS has long been considered a disease of the grey matter; however, pathological alterations of the white matter (WM), including axonal loss, axonal demyelination and oligodendrocyte death, have been reported in patients with ALS. The present review examined motor neuron death as the primary cause of ALS and evaluated the associated WM damage that is guided by neuronal-glial interactions. Previous studies have suggested that WM damage may occur prior to the death of motor neurons, and thus may be considered an early indicator for the diagnosis and prognosis of ALS. However, the exact molecular mechanisms underlying early-onset WM damage in ALS have yet to be elucidated. The present review explored the detailed anatomy of WM and identified several pathological mechanisms that may be implicated in WM damage in ALS. In addition, it associated the pathophysiological alterations of WM, which may contribute to motor neuron death in ALS, with similar mechanisms of WM damage that are involved in multiple sclerosis (MS). Furthermore, the early detection of WM damage in ALS, using neuroimaging techniques, may lead to earlier therapeutic intervention, using immunomodulatory treatment strategies similar to those used in relapsing-remitting MS, aimed at delaying WM damage in ALS. Early therapeutic approaches may have the potential to delay motor neuron damage and thus prolong the survival of patients with ALS. The therapeutic interventions that are currently available for ALS are only marginally effective. However, early intervention with immunomodulatory drugs may slow the progression of WM damage in the early stages of ALS, thus delaying motor neuron death and increasing the life expectancy of patients with ALS.

Correspondence to: Professor Michael Namaka, College of Pharmacy, Rady Faculty of Health Sciences, University of Manitoba, Apotex Centre, 750 McDermot Avenue, Winnipeg, MB R3E 0T5, Canada
E-mail: mike.namaka@ad.umanitoba.ca

Professor Jiming Kong, Department of Human Anatomy and Cell Science, College of Medicine, Rady Faculty of Health Sciences, University of Manitoba, 745 Bannatyne Avenue. Winnipeg, MB R3E 0J9, Canada
E-mail: jiming.kong@umanitoba.ca

Key words: amyotrophic lateral sclerosis, white matter damage, molecular mechanism, neuroimaging techniques, therapeutic intervention

Contents

1. Introduction
2. WM anatomy
3. Molecular mechanisms involved in the pathogenesis of WM damage in ALS
4. Therapeutic strategies aimed to attenuate or delay WM damage and disease progression
5. Conclusion

1. Introduction

Amyotrophic lateral sclerosis (ALS) is a fatal neurodegenerative disease, involving the progressive degeneration of upper and lower motor neurons. ALS is also known as Lou Gehrig's disease, after the baseball player Lou Gehrig who was diagnosed with the disease (1). ALS can be classified as sporadic (sALS), which represents ~90% of all ALS cases, and familial (fALS), which accounts for the remaining 10% of cases (2). Sexual dimorphism has been suggested to be involved in ALS disease onset and progression (3), and the incidence and prevalence of ALS is greater in males compared with in females (4,5). Exposure to environmental toxins, such

as pesticides, has been considered a key risk factor for ALS; however, further studies are required to elucidate the implication of environmental factors in ALS development (6). ALS is the most common motor neuron disease in adults, and its onset is characterized by distal weakness in the arms or legs, indicative of lower motor neuron involvement. Muscular weakness limits the use of muscles for the execution of voluntary and involuntary movements, thus causing muscular atrophy, eventually leading to respiratory muscle failure and death (7). As the disease progresses into the later stages, patients also experience a progressive decline of cognitive function. In the later stages of ALS, the ocular muscles controlling vision are usually the last to be affected (1).

The primary focus of clinical management for patients with ALS is the symptomatic management of the disease using conventional pharmacological agents, as no cure is currently available. However, non-conventional approaches, including radiotherapy, muscle stretching and nutritional management, have also been employed to alleviate the pain, respiratory dysfunction, psychiatric/cognitive disturbances, nutritional deficits and sleep-related dysfunctions associated with ALS (8). Clinical trials for ALS started in the 1980s; however, the majority of experimental drugs proved to be ineffective with the exception of riluzole, which was reported to marginally extend the lifespan of the patients (1,9).

ALS is most commonly referred to as a motor neuron disease, due to the activation of abnormal programmed cell death signaling pathways during the pathogenesis of the disease, leading to the death and degeneration of motor neurons (10). ALS has been primarily considered a disease of the grey matter involving motor neuron degeneration; however, pathological alterations in the white matter (WM) have been reported to be more pronounced compared with those in motor neuron structures (11). In addition, WM pathophysiological processes have been detected during the early stages of ALS, prior to the appearance of clinical symptoms (12). WM is predominantly composed of myelinated and unmyelinated neuronal axons organized into specific tracts with surrounding glial cells (13). The term 'white matter' arises from the white color of the lipids, which are the main constituents of myelin. Myelin has a water content of ~40%; the dry mass is composed of 70-85% lipid (14) and 15-30% protein (15). Among the main proteins found in myelin are proteolipid protein (~50%), myelin basic protein (~30%) and minor proteins, including myelin oligodendrocyte glycoprotein, 2',3'-cyclic-nucleotide 3'-phosphodiesterase and myelin-associated glycoprotein (<1%) (16). The WM of the central nervous system (CNS) is susceptible to anoxia, trauma and autoimmune processes (17). WM damage can be induced by primary and secondary diseases associated with ischemia, inflammation, trauma and hypoxia (13). WM damage has been reported to contribute to the motor and neurological deficits associated with cognitive impairment in neurological conditions, including ALS (18), Alzheimer's disease (19), Huntington's disease (20), progressive supra-nuclear palsy (21) and multiple sclerosis (MS) (22). The severity of WM damage increases with age, leading to decreased cognitive abilities and slower conduction velocity of electrical impulses during physiological functioning (23).

The molecular mechanisms involved in WM damage vary, and include alterations in toll-like receptor-3 expression (24), absorption of *Clostridium perfringens* ε-toxin (25) and glutamate excitotoxicity during secondary spinal cord (SC) injury (26). Neuropathological alterations of the WM, including axonal degeneration and oligodendrocyte loss (27,28), have been reported in patients with ALS. A previous study using multi-modal magnetic resonance imaging demonstrated that cortical thinning and WM degeneration were associated with cognitive and behavioral impairments in motor neuron diseases (29), whereas significant WM differences have been identified between male and female patients with ALS (30).

The exact molecular mechanisms underlying WM damage in ALS have yet to be elucidated. The presence of clinical and pathological similarities between patients with ALS and MS suggests that a similar WM pathology may be implicated in the diseases (13,31). Typical symptoms of patients with MS include disability, incontinence, limb tremor, pain, spasms, fatigue and spasticity (32). Patients with ALS also display some of the common symptoms of MS; however, typical ALS manifestations also include severe muscle weakness, fasciculation, bulbar symptoms and severe respiratory abnormalities (33).

MS is an autoimmune disease, which is characterized by the immune destruction of the myelin sheath surrounding brain and SC neurons, leading to axonal and neuronal loss. Damaged myelin disrupts the conduction of electrical signals along neural fibers, which is essential for the maintenance of normal functions. Therefore, patients with MS suffer numerous neurological disabilities that negatively impact their quality of life. At present, no cure for MS is available, due to the inability to repair damaged myelin (34). Brain derived neurotrophic factor (BDNF) is a neurotrophin, which has demonstrated beneficial effects during remyelination processes and myelin repair; however, its actions can be hampered by the overexpression of its transcriptional repressor, methyl CpG binding protein 2 (MeCP2) (34,35). Despite the significant differences between MS and ALS, the overlapping symptoms and pathological alterations suggest that the progressive degeneration of central axons may be a critical process in the diseases.

Defects in several genes involved in axonal transport may contribute to axonal loss in MS and ALS (36). Notably, pathogenic mechanisms similar to those responsible for the development of neuroinflammation, excitotoxicity and axonal dysfunction in MS have also been identified in ALS (31). A previous study indicated that first-degree relatives of patients with MS had a greater risk of developing ALS and vice versa, thus suggesting that similar genes may predispose families to MS and ALS (37). Specifically, inflammatory T-lymphocytes, including T helper (Th) 1 and Th17, and the production of inflammatory mediators, including interleukin 6, have been reported to drive the inflammatory cascade implicated in the neurological deficits present in patients with ALS and MS (38). Therefore, research has turned to other neurodegenerative diseases, including MS, in order to advance the understanding of WM damage associated with ALS and promote the development of more effective therapeutic strategies (13,39). The present review discussed the key molecules that have been implicated in the common mechanisms of WM damage in MS and ALS. In addition, current therapeutic strategies for the management of ALS were also addressed.

2. WM anatomy

The WM of the CNS contains axon bundles ensheathed by myelin, which is produced by oligodendrocytes and serves as an insulator, thus facilitating the propagation of electrical impulses along the nerve axons. There are three predominant WM tracts in the CNS, composed of projection, association and commissural tracts (40). Conversely, the CNS grey matter largely contains neuronal cell bodies, dendrites, glial cells and synapses (41). Myelin is an insulating substance, which is essential for the propagation of electrical impulses along nerve axons, and is required for the physiological functioning of the nervous system (42). The myelin sheath surrounding the nerve axons in the WM tracts serves a critical role in relaying messages from the brain to the various areas of the body; it also coordinates grey matter communication between areas of the CNS (43). Nerve axons are the predominant component of WM. They are long projections that originate from the neuronal cell body and serve to transmit information in the form of electrical impulses. In addition, nerve axons transport nutrients essential for the health and physiological function of the axons and the neuronal cell bodies (44).

In the CNS, glial cells, including oligodendrocytes and astrocytes, are critical for the maintenance of axonal integrity (45). Oligodendrocytes maintain the structural integrity and functionality of myelin, and the lipid-rich myelin sheath ensures the speed and reliability of electrical transmission (46). Astrocytes are the most prevalent type of glial cell in the CNS. WM astrocytes differ from grey matter astrocytes in morphology, development and function. WM astrocytes are mainly in charge of maintaining the neuronal-glial homeostatic equilibrium, participate in oligodendrocyte lineage differentiation, provide energy supply and nutritional support to the nervous tissue by delivering trophic factors and iron, and are involved in immune and inflammatory processes (13). Although the functional significance of WM glia has yet to be fully elucidated, previous studies have reported that oligodendrocyte and astrocyte dysfunction is implicated in the pathogenesis of neurological disorders, including MS (47), ischemic stroke (40), Huntington's (20) and Alzheimer's disease (48), schizophrenia (49), psychiatric disorders (50) and ALS (51).

Recently, ALS oligodendrocytes were demonstrated to contribute to motor neuron death, through a superoxide dismutase (SOD) 1-dependent mechanism (52), whereas oligodendrocyte degeneration has been reported to occur prior to disease onset. New oligodendrocytes are formed to compensate for the loss; however, they fail to mature, thus resulting in progressive demyelination (52). Furthermore, axonal demyelination has been directly associated with ALS deterioration (53). Therefore, oligodendrocyte dysfunction is considered as a major factor contributing to neuronal degeneration, with relevance to diseases including ALS (28,54). Notably, the glial pathology in ALS, including oligodendrocyte degeneration and impaired maturation, and its involvement in neurodegeneration, is analogous to the pathology displayed in MS (28).

3. Molecular mechanisms involved in the pathogenesis of WM damage in ALS

Biological targets of ALS pathology. Several abnormal biological processes have been suggested to be involved in the mechanisms underlying the pathogenesis of ALS (55), thus making it a very complex multi-system and multi-syndrome disorder, for which no single cause can be identified (Figs. 1 and 2). Considerable progress has been made in the investigation of the genetic aspect of ALS pathophysiology. Several genes have been demonstrated to be involved in fALS, including chromosome-9 open reading frame 72 (56), SOD1 (57), coiled-coil-helix-coiled-coil-helix domain containing 10 (58), Matrin-3 (59), tumor necrosis factor (TNF) receptor-associated factor family member-associated nuclear factor-κB activator-binding kinase 1 (60), TAR DNA-binding protein (61), fused in sarcoma (62), optineurin (63), Valosin-containing protein (64), ubiquilin 2 (65), sequestosome 1 (66) and profilin (2,67,68). Recently, mutations in the NIMA related kinase 1 gene were associated with ALS (69). With the development of genome sequencing techniques, the number of genes implicated in ALS pathogenesis is increasing, thus suggesting the complexity of the disease, and explaining the elusiveness of a cure. sALS and fALS are the predominant types of ALS, and appear to share some similar pathophysiological mechanisms, including oxidative stress, excitotoxicity, aggregate formation, inflammation and neurofilament disorganization (70,71).

Notably, the mechanisms underlying early-onset WM pathology in MS are similar to those responsible for early-onset WM damage prior to motor neuron death in ALS (13,72,73). Therefore, elucidation of the pathological mechanisms involved in MS-induced WM damage may provide useful insight to advance the understanding of certain aspects of ALS. Furthermore, novel therapeutic approaches that target WM pathology in the early stages of ALS, may have the potential to delay the progression of the disease and the onset of motor neuron death.

Mitochondrial damage and oxidative stress. Mitochondria are the primary site of ATP production; they also have a major role in the maintenance of Ca^{2+} homeostasis, the production of free radicals and the regulation of intrinsic apoptotic pathways (74,75). Therefore, mitochondrial dysfunction may be involved in the initial degenerative processes of ALS (76).

Reactive oxygen species (ROS) are byproducts of aerobic metabolism. The cumulative production of ROS results in oxidative stress, which causes mitochondrial damage. ROS can induce mitochondrial DNA mutations, impair the mitochondrial respiratory chain, alter mitochondrial membrane permeability and ultimately cause cell death (77). Previous studies have suggested the time- and dose-dependent involvement of ROS, including superoxide ($^{\bullet}O_2^-$) and hydroxyl ($^{\bullet}OH$) radicals, and hydrogen peroxide (H_2O_2), in mitochondrial damage driving motor neuron degeneration (Fig. 1) (78,79). In sALS and fALS, post-mortem and biopsy samples from the SC and motor neurons revealed abnormalities in mitochondrial structure, number and localization, which were associated with defects in respiratory chain complexes (80). Furthermore, elevated ROS production and mitochondrial dysfunction have also been observed in SC samples isolated from a rat model of sALS (81).

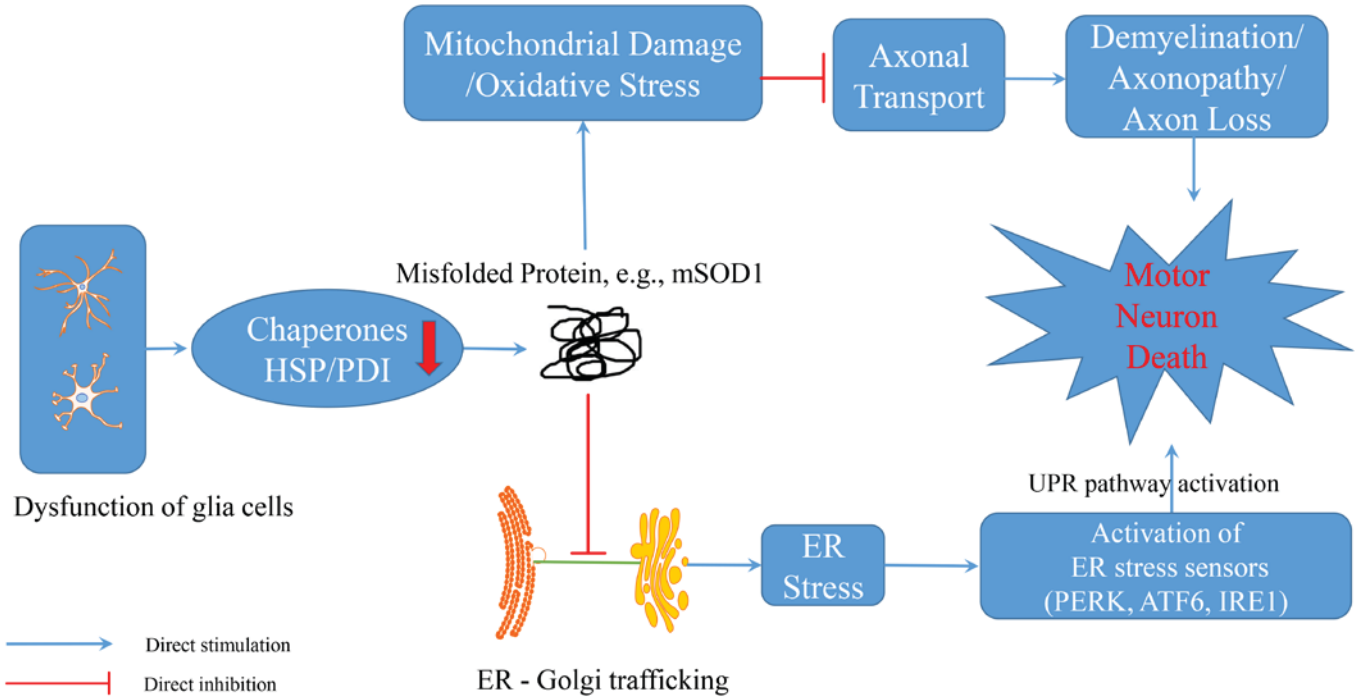


Figure 1. Schematic representation of the effects of mitochondrial damge and ER stress in ALS pathogenesis. Dysfunction of glial cells results in decreased levels of chaperone proteins, including HSPs and members of the PDI family. The impaired expression of chaperone proteins results in protein misfolding, which impairs ER-Golgi apparatus trafficking. The UPR signaling pathway is activated due to ER stress caused by impaired ER-Golgi trafficking, and initiates cell apoptosis. In addition, mutations in superoxide dismutase 1 cause mitochondrial damage and oxidative stress, ultimately leading to abnormalities in axonal transportation. ER, endoplasmic reticulum; ALS, amyotrophic lateral sclerosis; HSP, heat shock protein; PDI, protein disulphide isomerase; UPR, unfolded protein response; PERK, protein kinase R-like endoplasmic reticulum kinase; ATF, activating transcription factor; IRE, inositol-requiring enzyme.

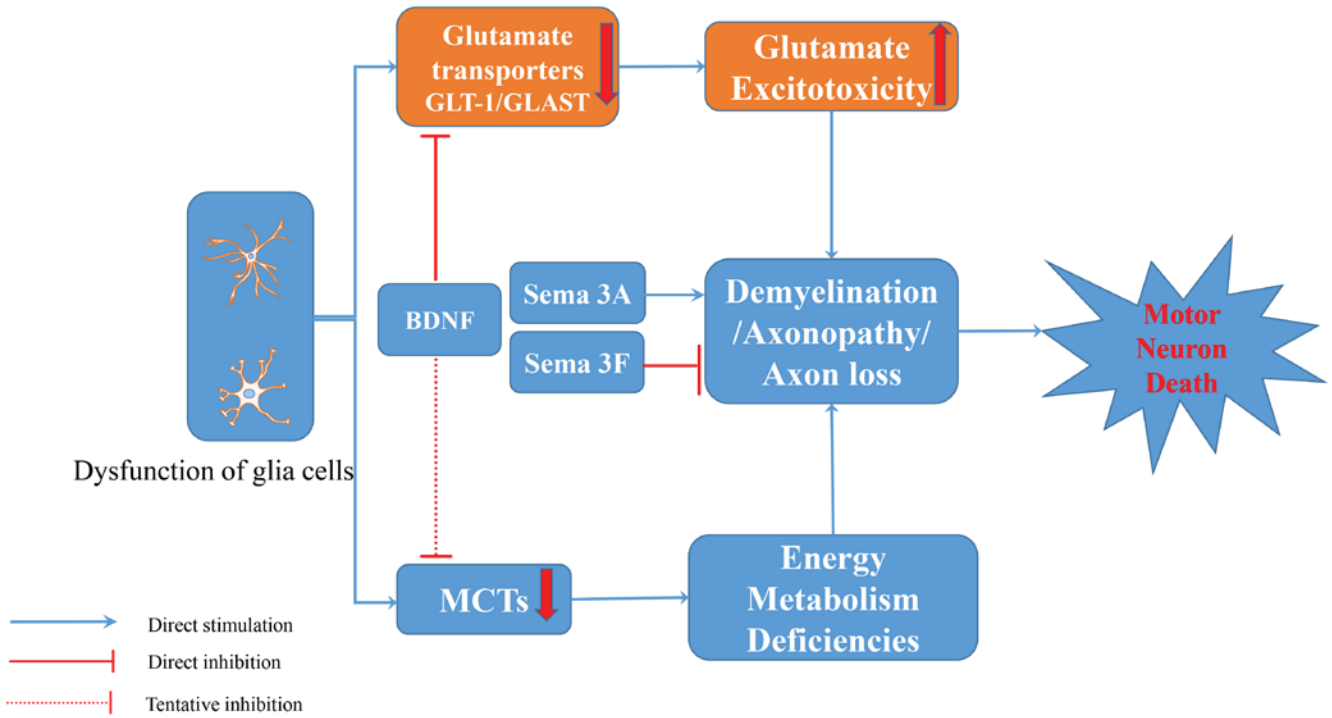


Figure 2. Schematic representation of the effects of glutamate excitotoxicity, energy metabolism deficiency and axonopathy in ALS pathogenesis. Dysfunction of glial cells results in the decreased expression of glutamate transporters, including GLT-1 and GLAST, leading to glutamate excitotoxicity. Although excitotoxicity can induce axonopathy and neuronal degeneration, interventions aimed at increasing BDNF production can attenuate excitotoxicity, enhance axonal repair and regrowth and eventually ameliorate the degeneration of motor neurons. Furthermore, glial cell dysfunction results in the downregulation of MCTs, thus impairing the axonal energy supply, which leads to axon loss and motor neuron degeneration. The BDNF signaling pathway is also implicated in MCT expression; however, further studies are required to investigate the molecular mechanisms that are involved. In addition, class 3 semaphorins are involved in oligodendroglial migration, and their dysregulation is implicated in remyelination impairments and axonopathy. ALS, amyotrophic lateral sclerosis; GLT, glutamate transporter; GLAST, glutamate aspartate transporter; BDNF, brain-derived neurotrophic factor; MCT, monocarboxylate transporter; Sema, semaphorin.

Cell type-specific mitochondrial damage has been demonstrated to contribute to the pathogenesis of ALS: Mitochondrial dysfunction in astrocytes has been associated with a neurotoxic phenotype that impairs motor neuron survival (82), with a mechanism that may involve mutant (m)SOD1 aggregation. mSOD1 aggregates cause mitochondrial damage due to a decrease in the antioxidant activity of the enzyme, thus resulting in ROS accumulation. In addition, mSOD1 may potentiate the formation of $^{\bullet}$OH, as suggested by the increased levels of oxidation products in mSOD1-transfected mice compared with controls (83). Furthermore, mSOD1 protein aggregates may be responsible for impairments in axonal transport, neurotrophic factor supply, endoplasmic reticulum (ER) stress and apoptosis in glial cells (84,85). mSOD1 is present in ~20% of patients with fALS and ~3% of patients with sALS (86); however, oxidative stress and mitochondrial damage are also present in non-SOD1-linked ALS cases (87).

ER stress. ER is an intracellular organelle that is responsible for protein quality control, as it ensures that proteins are correctly synthesized, folded, packaged and delivered in the appropriate locations. Under ER stress conditions, the unfolded protein response (UPR) signaling pathway is activated to restore cellular integrity or initiate apoptosis (88). Three ER stress sensors mediate the UPR, namely protein kinase R-like ER kinase (PERK), activating transcription factor 6 (ATF6) and inositol-requiring enzyme 1 (IRE1) (89). ER stress can be triggered by the accumulation of unfolded or misfolded proteins in the ER lumen, and by other mechanisms, including the inhibition of ER-to-Golgi apparatus transport. Notably, mSOD1 has been implicated in impaired ER-to-Golgi trafficking, which represents an early cellular disturbance before the induction of ER stress, Golgi fragmentation (90), mSOD1 aggregation and cell apoptosis (Fig. 1) (91).

Chaperone proteins, including heat shock proteins (HSP) and members of the protein disulphide isomerase (PDI) family, ensure proteins are folded correctly, and may have a cytoprotective role in ALS (92). Low levels of HSP in motor neurons increase their susceptibility to stress, thus increasing their vulnerability to cell death processes. Neuronal HSP levels depend upon the neuronal and glial production of HSP (93). Notably, periventricular WM damage induced by iron accumulation in oligodendrocytes may increase ER stress and mitochondrial disruption, ultimately resulting in glial cell death (94). Therefore, WM damage may be responsible for HSP deficits and increased ER stress, which eventually lead to motor neuron apoptosis.

The UPR signaling pathway has been implicated in WM tract myelination under normal physiological conditions. The ER stress sensors PERK, ATF6 and IRE1 are activated under physiological conditions, resulting in the upregulation of downstream molecules, including PDI, 78 kDa glucose-related protein and 94 kDa glucose-related protein. These molecules have been associated with oligodendrocyte damage, reduced axon numbers and demyelination, which are associated with ALS progression (95,96). Notably, increased PDI expression has been reported in WM microglia of the SC and in astrocytes of the SC ventral horn in an ALS mouse model, thus suggesting that the UPR in WM glia may occur early in the phase of motor neuron degeneration during ALS (97). Motor neurons in mice with fALS were revealed to be prone to ER stress and demonstrated upregulated ER stress marker expression accompanied by axonal degeneration (98). These studies suggested that the early mechanisms of WM damage in ALS may induce ER stress, which, in turn, may activate the UPR signaling pathway, ultimately resulting in motor neuron degeneration and death. Therefore, it may be hypothesized that therapeutic strategies aimed at attenuating or delaying WM damage may have potential in reducing motor neuron death and disease progression in patients with ALS, thus increasing their life expectancy.

Glutamate excitotoxicity. Accumulating evidence suggests that glutamate excitotoxicity may be implicated in the mechanisms of neuronal degeneration in ALS (99-101); imbalances between excitatory and inhibitory neurotransmission may contribute to the pathogenesis of the disease. Glutamate is the primary excitatory amino acid neurotransmitter in the CNS. Glutamate excitotoxicity has been associated with oligodendrocyte apoptosis and may induce WM degeneration following SC injury (26). An increase in excitatory neurotransmission, as indicated by increased levels of glutamine, has been reported in the motor cortex and WM of patients with ALS compared with healthy controls (101). Glutamine synthesis is catalyzed by the enzyme glutamine synthetase from glutamate and ammonia (102), and glutamine production is used as a marker of glutamate levels to detect glutamate-induced excitotoxicity.

Astrocyte-mediated cell-specific excitotoxicity has also been implicated in the pathogenesis of ALS. Astrocytes express two glutamate transporters (GLTs): GLT-1, also known as excitatory amino acid transporter (EAAT) 2, and glutamate aspartate transporter, also known as EAAT1, which participate in extracellular glutamate homeostasis and neuronal reuptake (Fig. 2) (103). Glutamate excitotoxicity, mediated by non-N-methyl-D-aspartate receptors, has been reported to cause axonopathy, including axonal swelling, cytoskeletal disruption and neurofilament accumulation, in the distal axonal segments of SC motor neurons (104). Studies suggested that glutamate excitotoxicity may be implicated in axonopathy, WM damage and long-term cognitive deficits in patients with ALS. Therefore, neuroprotective agents, including vasoactive intestinal peptide, may attenuate excitotoxic damage, and also increase BDNF production to promote secondary repair and axonal regrowth, thus limiting WM damage and ameliorating motor neuron degeneration (105,106).

The cell-specific effects of astrocytes have also been reported to participate in the activation of protein kinase C and mitogen-activated protein kinase (MAPK) pathways to induce neuroprotection (105,106). These results suggested that astrocyte activation may differentially facilitate or prevent motor neuron degeneration. Further studies are required to elucidate the differential functions of astrocytes in the pathology of degenerative diseases, including ALS (107) and MS (108).

Energy metabolism deficiencies. The human brain utilizes glucose and monocarboxylates, such as lactate, as primary energy sources. Lactate accounts for ~33% of the total energy substrates used by the brain, representing a more important fuel source for brain metabolism than glucose (109). Monocarboxylate transporters (MCTs) are responsible for

lactate and pyruvate transport. In the brain, three MCT isoforms have been identified, namely MCT1, MCT2 and MCT4, which are implicated in lactate flux in the CNS (109). MCT1 is expressed in astrocytes and oligodendrocytes, whereas MCT4 is expressed exclusively in astrocytes. WM astrocytes and oligodendrocytes are critical for the production and maintenance of myelin (110), and the delivery of essential energy (111), thus supporting the physiological function of the CNS. Oligodendrocytes exhibit higher MCT1 expression, and increased lactate oxidation and lipid synthesis compared with astrocytes (13). Therefore, oligodendrocyte dysfunction may contribute to motor neuron degeneration and death in ALS. Notably, oligodendrocyte pathology becomes apparent prior to disease onset and persists during disease progression (45,112). A previous study suggested that oligodendroglia may support axon survival and function through a myelin-independent mechanism, whereas deficiencies in energy metabolites may underlie neurodegeneration (113). In human studies and preclinical mouse ALS models, MCT1 expression was revealed to be decreased in affected brain regions, resulting in insufficient energy supply to the axons, thus leading to axon loss and motor neuron degeneration and death (13,111,114). These findings suggested that the molecular mechanisms involved in early-onset WM damage in ALS may also contribute to motor neuron death (Fig. 2). Therefore, therapeutic strategies aimed at attenuating early-onset WM damage may have potential for the effective treatment of patients with ALS.

Unlike MTC1 or MTC4, MTC2 is highly expressed in the dendrites and axons of CNS neurons (115). Notably, a marked downregulation in the axonal expression of glucose transporter 3 (GLUT3) and MCT2 has been reported in WM samples isolated from MS lesions, and has been suggested to impede the supply of essential nutrients (116). Furthermore, Robinet and Pellerin (117) suggested that BDNF signaling may be implicated in the upregulation of MCT2 expression in brain neurons following acute exercise; BDNF may increase neuronal MCT2 expression through the translational regulation of phosphatidylinositol-4,5-bisphosphate 3-kinase (PI3K)/Akt/mechanistic target of rapamycin/S6, p38 MAPK, and p44/p42 MAPK pathways (117).

Axonopathy. Motor neuron axonopathy has been proposed as an early initiating mechanism of ALS. Motor neuron pathology in ALS has been suggested to begin, at distal axon sites and proceeds in a retrograde manner, eventually leading to motor neuron degeneration, a hypothesis termed the 'dying back' mechanism (27). Axonopathy has also been demonstrated in animal models of ALS, including zebrafish (118), mice (119) and rats (120). In rats carrying the SOD1-G93A mutation, mitochondrial accumulation of mSOD1 was observed in motor neuron axons in discrete clusters located at regular intervals, instead of a homogeneous axonal distribution (120). Overexpression of mSOD1 (118), and excitotoxicity (104), have been suggested to trigger axonopathy. In addition, excitotoxic axonopathy has been associated with the aberrant colocalization of phosphorylated and dephosphorylated neurofilament proteins, which may subsequently induce axonal transport disruptions and swelling. In addition, axonopathy has been associated with abnormalities within the glial environment (121). Fast-fatigable motor neurons are highly susceptible to axonal degeneration, which is associated with deficiencies in protein and lipid supply to axons (27,122). As aforementioned, oligodendrocytes regulate axonal myelination to maintain axonal function, whereas astrocytes provide structural and trophic support for neurons. Abnormal glial-axonal interactions have been reported to be implicated in axonal swelling, neurofilament perturbations and microtubule transport defects during axonal degeneration (123).

Semaphorin proteins serve as axonal growth signaling cues and are responsible for axon guidance and neurofilament organization during nervous system development (124). Class 3 semaphorins are involved in oligodendroglial migration and remyelination. Semaphorin (Sema) 3A is a repulsive guidance cue for neuronal and glial cells, and induces the redistribution and depolymerization of actin filaments that results in growth cone collapse. In addition, Sema3A is expressed in MS lesions, where it impairs the recruitment and differentiation of oligodendrocyte precursor cells (OPCs) and inhibits remyelination (125,126). Conversely, Sema3F is an attractive guidance cue, which assists OPC recruitment and promotes axonal remyelination (126,127). The roles of Sema3A have also been investigated in ALS: In an ALS mouse model, Sema3A and its receptor neuropilin 1 were demonstrated to induce distal axonopathy (128). Furthermore, in humans, Sema3A levels in the motor cortex were significantly upregulated in patients with ALS compared with in controls. These results suggested that the increase in Sema3A expression may be implicated in axonal degeneration, and may be associated with the axonopathy and denervation that are observed in patients with ALS (129). Sema3A, and other class 3 semaphorins, are important regulators of axonal remyelination and of the immune responses that govern neuronal regeneration (Fig. 2) (130). Therefore, the inhibition of Sema3A may have potential as a novel therapeutic strategy for the treatment of patients with ALS. According to the 'dying back' hypothesis regarding motor neuron pathology (27), it may be necessary to focus on motor axons and nerve terminals in order to effectively delay or prevent motor neuron degradation (131).

Neuronal cell death. Several mechanisms, including oxidative stress, the aggregation of misfolded and mutant proteins, and excitotoxicity, may disrupt the homeostasis of motor neurons, ultimately causing cell death. MeCP2 is a nuclear protein with numerous biological functions, which serves a critical role in myelin damage in neurological conditions, including epilepsy (132) and MS (34). MeCP2E1 and MeCP2E2 are the two predominant isoforms of MeCP2 that exert diverse biological effects on neuronal survival. Previous studies have revealed that MeCP2E2 promotes neuronal death and apoptosis; however, these effects may be inhibited by Forkhead box protein G1 and Akt, which enhance neuronal survival (133,134).

MeCP2E1 has been reported to repress BDNF transcription, thus resulting in the failure of myelin repair mechanisms (34). BDNF serves a role in myelin repair and promotes the health of neurons, astrocytes and oligodendrocytes; therefore, BDNF deficiencies have been implicated in the pathological mechanisms of ALS (135,136). Notably, BDNF serum levels have been revealed to be significantly decreased in patients with ALS compared with in controls (137). Therefore, BDNF may have potential as a biomarker to reflect disease activity, and may

serve as a basis for the development of novel therapeutic strategies for ALS treatment (135). Neurotrophic factors, including BDNF, have been reported to exert beneficial effects in mouse models of ALS: Treatment of SOD1-G93A transgenic mice with neurotrophic factors has been reported to inhibit neuromuscular junction degeneration, enhance axon survival, delay the onset of ALS and prolong the average lifespan of the mice (138,139).

In ALS, apoptosis is the most common form of motor neuron death, and involves pro- and anti-apoptotic gene expression, caspase activation, cytochrome *c* release and apoptosis-inducing factor (AIF) nuclear translocation (140-142). Notably, in patients with ALS, apoptotic processes are not restricted to motor neurons, but also affect other neuronal and non-neuronal components of the CNS (143). A previous study reported increased neuronal apoptosis, accompanied by an increase in glial fibrillary acidic protein-positive astrocytes and increased microglia activation in the white and grey matter of several CNS regions (144). In addition, astrocytes, but not microglia, cortical neurons or myocytes, were suggested to have an integral role in the death of motor neurons in ALS (145).

At least three different molecular pathways have been reported to participate in programed cell death: the mitochondrial pathway, the death receptor pathway and the ER pathway (146). The present review explored only mitochondria-dependent apoptosis, as it is primarily responsible for neuronal and non-neuronal cell death in ALS. The mitochondrial apoptotic pathway is activated during the early stages of ALS, and proapoptotic signaling has been revealed to directly induce neuronal dysfunction (147). B-cell lymphoma (Bcl)-2 family members have also been reported to serve critical roles during apoptosis that lead to motor neuron death, via controlling mitochondrial permeability in ALS models. The expression and distribution of Bcl-2, Bcl-extra large, Bcl-2-associated death promoter (Bad) and Bcl-2-associated X protein (Bax) are altered in ALS mouse models, thus suggesting the presence of mitochondrial damage (143,148). In addition, inhibition of the PI3K/Akt signaling pathway can directly induce proapoptotic proteins, including Bad and Bax, and thus contribute to the degenerative and apoptotic pathways during ALS pathogenesis (149). Caspase activation and elevated cytosolic cytochrome *c* levels have also been observed in ALS cell lines, thus indicating that mitochondria-dependent apoptosis may contribute to cell death in ALS (150). However, the altered expression of Bcl-2 family proteins, the inhibition of PI3K/Akt signaling and the activation of caspases may not be the only pathways leading to motor neuron degeneration in ALS, as apoptosis is a complex process, and is known to be induced through numerous pathways (151).

AIF is a key regulator of caspase-independent apoptosis, and its increased expression has been associated with the progression of ALS. AIF has been revealed to co-translocate to motor neuron nuclei with cyclophilin A; following binding with cyclophilin A, AIF may induce mitochondrial membrane permeabilization and cell death in a model of ALS (152). Therefore, proapoptotic signaling may contribute to the neuronal and non-neuronal degeneration that causes WM damage and motor neuron death in ALS. Therefore, inhibition of the mitochondrial apoptotic pathway may have potential as another novel therapeutic approach to suppress myelin damage and/or preserve motor neuron viability and function in patients with fALS (147).

Microbiome. The gut microbiome can influence host biology and contribute to WM damage in CNS disorders. The microbiome-gut-brain axis is responsible for the association between the microbiome and neuroimmune and neuropsychiatric disorders (153), including MS (154,155), autism (156) and ALS (157). The microbiome-gut-brain axis refers to the interactions between the CNS, the gastrointestinal tract and the microorganisms in the gut. Several mechanisms have been suggested to explain the influence of the gut microbiome on brain health (158): Impaired intestinal barrier function has been suggested to promote the passage of toxins from the intestinal lumen into the blood circulation and the brain. A previous study demonstrated that *Clostridium perfringens* ε-toxin may be responsible for WM damage in the CNS of mice. ε-toxin secreted into the gut was revealed to bypass the blood-brain barrier and cause mature oligodendrocyte death, demyelination and WM injury; these effects were dependent on the expression of myelin and lymphocyte protein proteolipid (25). Notably, ε-toxin has been demonstrated to exert selective toxic effects on oligodendrocytes but not astrocytes, microglia or neurons in primary cultures (25). Furthermore, dysbiosis of the gut microbiota has been reported in patients with MS compared with in healthy controls (159,160), whereas gut-derived neurotoxins have been proposed as a cause of ALS (161,162). In an ALS mouse model (SOD1-G93A), impaired gut integrity and a shift in the profile of the gut microbiome have been observed at the early stages of the disease, and have been reported there to be associated with increased disease severity (163). These findings suggested a potential role for the microbiome in the progression of ALS. However, the precise alterations in the gut microbiome during ALS pathogenesis have yet to be elucidated. Numerous factors, including hygiene, antibiotic usage, microbiota composition, probiotics and diet, have been proposed to influence the link between the gut microbiome and the CNS (153). Understanding the relationship between the gut microbiome and neuroimmunology may aid the development of novel preventative and therapeutic strategies for the treatment of CNS disorders, including ALS.

4. Therapeutic strategies aimed to attenuate or delay WM damage and disease progression

Riluzole. Similar mechanisms have been proposed concerning the pathogenesis of WM damage and subsequent disease progression for ALS and MS; however, no cure exists for these chronic diseases. Currently available therapeutic interventions mainly focus on delaying the onset of the disease, slowing its progression and improving the survival rates.

Riluzole is the only drug approved by the US Food and Drug Administration for the treatment of patients with ALS, and it has been clinically available since 1995. However, treatment with riluzole can only marginally improve the neurological symptoms of the patients and prolong their survival by 3-4 months (164), whereas a previous epidemiological study reported that riluzole exerted a beneficial effect only during the first 6 months of therapy, with an apparent reversal of its beneficial effects after the 6-month time point (165).

The molecular mechanisms underlying the neuroprotective effects of riluzole in ALS have yet to be elucidated. It has been suggested that riluzole may exert its beneficial effects via preventing motor neuron excitotoxicity, through the blockade of voltage-dependent ion channels (166-168). However, riluzole has also been reported to act on astrocytes in the WM to induce neural growth factor production and improve the neuronal survival rate (168,169). In addition, it has been demonstrated to stimulate BDNF release (170,171). A previous study from our group suggested the importance of BDNF during myelin repair, as increased levels of BDNF were revealed to facilitate myelin repair and offer neuroprotection in the CNS (33). Therefore, the enhancing effects of riluzole on BDNF production may also contribute to its neuroprotective effects in patients with ALS.

Riluzole has been demonstrated to reduce inflammation, demyelination and axonal damage, and attenuate the clinical severity of the experimental autoimmune encephalomyelitis (EAE) model of MS, thus suggesting that riluzole may also be beneficial for the treatment of MS (172). A phase II clinical trial is currently in progress for the use of riluzole in patients with MS (173); however, a previous phase II trial in patients with early MS revealed that riluzole was not able to prevent the progression of brain atrophy (174). Furthermore, the acute and chronic treatment of ALS mice with riluzole exerted opposite effects on the production of trophic factors in the CNS, including glial cell-derived neurotrophic factor, BDNF, cardiotrophin-1 (CT-1) and nerve growth factor: Acute treatment with riluzole was revealed to induce trophic factor production in the SC, sciatic nerve and brain, whereas chronic treatment exerted inhibitory effects (169). In the study by Dennys *et al* (169), riluzole significantly increased CT-1 levels in the SC following 15 days of continuous treatment, which returned to baseline following 30 days of treatment. In addition, riluzole increased brain BDNF levels following 6 and 15 days of treatment, which were significantly decreased following 30 days of treatment.

The levels of released BDNF appear to be a critical factor in ALS pathology, since BDNF has been reported to serve an essential role in the development of pathologic pain (175). Increased BDNF levels have been suggested to induce the development of chronic pain, whereas BDNF deficits may result in the failure of myelin repair mechanisms (34,176). These findings suggested that a delicate equilibrium in the endogenous BDNF levels may be required for the maintenance of myelin repair without the induction of nociception. Therefore, therapeutic schemes that favor the acute effects of riluzole administration, and the close monitoring of BDNF levels may have the potential to improve the therapeutic outcomes of treatment with riluzole.

Other drugs on the market or in clinical trials. As the efficacy of riluzole is only marginal, and its administration can increase survival by only a few months, clinicians suggest that treatment with riluzole should be started at the early stages of the disease in order to maximize its benefits. Novel agents with higher efficacy are currently under investigation, and various administration routes are being evaluated in order to improve the efficacy and minimize the adverse effects of the treatments (177).

Novel experimental drugs are currently being evaluated in preclinical animal models and in human clinical trials (178). Pramipexole (PPX), is a D2/D3-preferring dopamine receptor agonist, which has been demonstrated to exert beneficial effects in the EAE model of MS (179): PPX blocked neuroinflammatory responses, demyelination and astroglial activation in the SC, and it inhibited the production of proinflammatory cytokines and ROS (179). In addition, dexpramipexole (RPPX), which is the R (+) enantiomer of PPX, has also demonstrated neuroprotective effects, via acting directly on mitochondria to stabilize mitochondrial ionic conductance and reduce free radical production, thus inhibiting cell death (180-182). Early phase clinical trials in patients with ALS suggested that RPPX has a promising safety and tolerability profile, and a phase III clinical trial is currently underway to investigate its efficacy in patients with ALS (183).

Pioglitazone is a peroxisome proliferator-activated receptor-γ agonist, which has been demonstrated to exert anti-inflammatory and neuroprotective actions. It has been suggested as a potential therapeutic agent for the treatment of MS, due to its ability to reduce TNF-α-induced myelin damage and mitochondrial dysfunction (184). In a phase I clinical trial in patients with relapsing remitting MS, treatment with pioglitazone was reported to reduce lesion development in WM, via inhibiting demyelination and axonal degeneration (185). However, pioglitazone did not exert beneficial effects on the survival of patients with ALS, as revealed by a phase II clinical trial evaluating it as an add-on therapy in combination with riluzole (186). However, riluzole was revealed to exert neurotoxic effects at concentrations between 3 and 30 μM, which may antagonize the neuroprotective effects of several compounds being evaluated in clinical trials, including resveratrol, memantine, minocycline and lithium (187). Therefore, further studies are required, using a group of patients without riluzole treatment to evaluate the neuroprotective potential of novel agents in ALS (187).

Flavonoids are bioactive compounds that are derived from fruit and vegetables. Epigallocatechin-3-gallate is a flavonoid that has been demonstrated to reduce neuroinflammation, and limit demyelination and axonal damage in the EAE model of MS (188) and the SOD1-G93A mouse model of ALS (189). The neuroprotective effects of flavonoids suggest that they may have potential as alternative therapeutic agents for the treatment of neurodegenerative diseases, including MS and ALS (190).

Stem cell transplantation has also been recognized as a potential therapeutic strategy for the treatment of patients with ALS and MS (191). A previous study demonstrated that a neural stem cell (NSC) population isolated from human induced pluripotent stem cells improved the neuromuscular function and increased the life span of ALS mice, following intrathecal or intravenous administration. The results revealed that the transplanted NSCs migrated and engrafted into the CNS, where they improved the production of neurotrophic factors and reduced micro- and macrogliosis (192). Furthermore, a human study demonstrated that transplantation of autologous stem cells into patients with ALS delayed disease progression and increased survival (193). In addition, neural precursor cell transplantation has been reported to

enhance remyelination in an EAE mouse MS model of extensive demyelination (194). Genetically engineered bone marrow stem cells have also been used to deliver BDNF in EAE mice, and resulted in the significant delay of EAE onset, which was accompanied by a reduction in demyelination and overall clinical severity (195).

ALS is a multi-syndrome disease, which is characterized by extensive genetic and phenotypic variability. Therefore, the discovery of a single agent that can be used for the treatment of all ALS patients is unlikely. Although MS and ALS differ in many aspects, they share a number of common pathogenic features, including inflammation, oxidative stress, mitochondrial dysfunction and WM damage (196). For this reason, early diagnosis, and early interventional therapies that target certain molecular and genetic pathways are urgently required for the treatment of patients with ALS and MS.

5. Conclusion

ALS is a complex multi-system and multi-syndrome disease that affects neuronal and non-neuronal populations, and is characterized by the progressive degeneration of motor neurons. Several pathological mechanisms are involved in WM damage in ALS, including mitochondrial dysfunction, oxidative stress, neuronal apoptosis, ER stress, glutamate excitotoxicity, energy metabolism defects and axonopathy, which bear a strong similarity to other WM disorders, such as MS (Figs. 1 and 2). Therefore, immunomodulatory agents that are currently available for the treatment of MS may have potential as early treatment options for patients with ALS characterized by early-onset WM damage.

The current review presented a comprehensive evaluation of ALS, discussing motor neuron death as the principal cause of the disease, and examining the impact of early-onset WM damage, which is a common pathology in ALS and MS, as confirmed by neuroimaging techniques (12,197-199). The immune system has been identified as a key regulator of pathological neuronal-glial interactions. However, the exact molecular mechanisms surrounding WM damage in ALS have yet to be elucidated. Although MS and ALS are distinct neurodegenerative CNS diseases, they share common pathogenic features. Therefore, understanding the molecular mechanisms that underlie WM damage in MS may aid the development of improved therapeutic strategies that address the early-onset WM damage occurring in ALS. The identification of potentially important molecular targets, including MeCP2E1, MeCP2E2, BDNF (34) and semaphorin (200,201) in MS may help advance our understanding of the molecular mechanisms underlying the pathogenesis of ALS. Current agents used for the treatment of ALS, including riluzole, and experimental drugs currently in clinical trials do not appear to affect the WM damage that is associated with the disease. Further studies are required to elucidate the roles of WM damage and neuroglial pathology in the development and progression of ALS.

Acknowledgements

The authors would like to acknowledge the support from the ALS Society of Canada (ALS Canada), the College of Pharmacy at the University of Manitoba, and the Joint Laboratory of Biological Psychiatry between Shantou University Medical College in Guangdong, China and the College of Medicine at the University of Manitoba.

References

1. Morris J: Amyotrophic lateral sclerosis (ALS) and related motor neuron diseases: An overview. Neurodiagn J 55: 180-194, 2015.
2. Therrien M, Dion PA and Rouleau GA: ALS: Recent developments from genetics studies. Curr Neurol Neurosci Rep 16: 59, 2016.
3. Li R, Strykowski R, Meyer M, Mulcrone P, Krakora D and Suzuki M: Male-specific differences in proliferation, neurogenesis, and sensitivity to oxidative stress in neural progenitor cells derived from a rat model of ALS. PLoS One 7: e48581, 2012.
4. McCombe PA and Henderson RD: Effects of gender in amyotrophic lateral sclerosis. Gend Med 7: 557-570, 2010.
5. Orsini M, Oliveira AB, Nascimento OJ, Reis CH, Leite MA,de Souza JA, Pupe C, de Souza OG, Bastos VH, de Freitas MR, *et al*: Amyotrophic lateral sclerosis: New perpectives and update. Neurol Int 7: 5885, 2015.
6. Bozzoni V, Pansarasa O, Diamanti L, Nosari G, Cereda C and Ceroni M: Amyotrophic lateral sclerosis and environmental factors. Funct Neurol 31: 7-19, 2016.
7. Talbot K: Motor neurone disease. Postgrad Med J 78: 513-519, 2002.
8. Riva N, Agosta F, Lunetta C, Filippi M and Quattrini A: Recent advances in amyotrophic lateral sclerosis. J Neurol 263: 1241-1254, 2016.
9. Mathis S, Couratier P, Julian A, Vallat JM, Corcia P and Le Masson G: Management and therapeutic perspectives in amyotrophic lateral sclerosis. Exp Rev Neurother 17: 263-276, 2017.
10. Martin LJ, Price AC, Kaiser A, Shaikh AY and Liu Z: Mechanisms for neuronal degeneration in amyotrophic lateral sclerosis and in models of motor neuron death (Review). Int J Mol Med 5: 3-13, 2000.
11. Rafałowska J and Dziewulska D: White matter injury in amyotrophic lateral sclerosis (ALS). Folia Neuropathol 34: 87-91, 1996.
12. Sach M, Winkler G, Glauche V, Liepert J, Heimbach B, Koch MA, Büchel C and Weiller C: Diffusion tensor MRI of early upper motor neuron involvement in amyotrophic lateral sclerosis. Brain 127: 340-350, 2004.
13. Li J, Zhang L, Chu Y, Namaka M, Deng B, Kong J and Bi X: Astrocytes in oligodendrocyte lineage development and white matter pathology. Front Cell Neurosci 10: 119, 2016.
14. Aggarwal S, Yurlova L and Simons M: Central nervous system myelin: Structure, synthesis and assembly. Trends Cell Biol 21: 585-593, 2011.
15. Morell P and Quarles RH: Characteristic Composition of Myelin. In: Basic Neurochemistry: Molecular, Cellular and Medical Aspects. Siegel GJ, Agranoff BW, Albers RW, *et al* (eds). 6th edition. Lippincott-Raven, Philadelphia, PA, 1999.
16. Mallucci G, Peruzzotti-Jametti L, Bernstock JD and Pluchino S: The role of immune cells, glia and neurons in white and gray matter pathology in multiple sclerosis. Prog Neurobiol 127-128: 1-22, 2015.
17. Stys PK: White matter injury mechanisms. Curr Mol Med 4: 113-130, 2004.
18. Sarro L, Agosta F, Canu E, Riva N, Prelle A, Copetti M, Riccitelli G, Comi G and Filippi M: Cognitive functions and white matter tract damage in amyotrophic lateral sclerosis: A diffusion tensor tractography study. AJNR Am J Neuroradiol 32: 1866-1872, 2011.
19. Duan JH, Wang HQ, Xu J, Lin X, Chen SQ, Kang Z and Yao ZB: White matter damage of patients with Alzheimer's disease correlated with the decreased cognitive function. Surg Radiol Anat 28: 150-156, 2006.
20. Della Nave R, Ginestroni A, Tessa C, Giannelli M, Piacentini S, Filippi M and Mascalchi M: Regional distribution and clinical correlates of white matter structural damage in Huntington disease: A tract-based spatial statistics study. AJNR Am J Neuroradiol 31: 1675-1681, 2010.
21. Agosta F, Galantucci S, Svetel M, Lukić MJ, Copetti M, Davidovic K, Tomić A, Spinelli EG, Kostić VS and Filippi M: Clinical, cognitive, and behavioural correlates of white matter damage in progressive supranuclear palsy. J Neurol 261: 913-924, 2014.

22. Bester M, Lazar M, Petracca M, Babb JS, Herbert J, Grossman RI and Inglese M: Tract-specific white matter correlates of fatigue and cognitive impairment in benign multiple sclerosis. J Neurol 330: 61-66, 2013.
23. Valdés Hernández Mdel C, Booth T, Murray C, Gow AJ, Penke L, Morris Z, Maniega SM, Royle NA, Aribisala BS, Bastin ME, *et al*: Brain white matter damage in aging and cognitive ability in youth and older age. Neurobiol Aging 34: 2740-2747, 2013.
24. Vontell R, Supramaniam V, Wyatt-Ashmead J, Gressens P, Rutherford M, Hagberg H and Thornton C: Cellular mechanisms of toll-like receptor-3 activation in the thalamus are associated with white matter injury in the developing brain. J Neuropathol Exp Neurol 74: 273-285, 2015.
25. Linden JR, Ma Y, Zhao B, Harris JM, Rumah KR, Schaeren-Wiemers N and Vartanian T: *Clostridium perfringens* epsilon toxin causes selective death of mature oligodendrocytes and central nervous system demyelination. MBio 6: e02513, 2015.
26. Park E, Velumian AA and Fehlings MG: The role of excitotoxicity in secondary mechanisms of spinal cord injury: A review with an emphasis on the implications for white matter degeneration. J Neurotrauma 21: 754-774, 2004.
27. Fischer LR, Culver DG, Tennant P, Davis AA, Wang M, Castellano-Sanchez A, Khan J, Polak MA and Glass JD: Amyotrophic lateral sclerosis is a distal axonopathy: Evidence in mice and man. Exp Neurol 185: 232-240, 2004.
28. Nonneman A, Robberecht W and Van Den Bosch L: The role of oligodendroglial dysfunction in amyotrophic lateral sclerosis. Neurodegener Dis Manag 4: 223-239, 2014.
29. Alonso-Lana S, Goikolea JM, Bonnin CM, Sarró S, Segura B, Amann BL, Monté GC, Moro N, Fernandez-Corcuera P, Maristany T, *et al*: Structural and functional brain correlates of cognitive impairment in euthymic patients with bipolar disorder. PLoS One 11: e0158867, 2016.
30. Bede P, Elamin M, Byrne S and Hardiman O: Sexual dimorphism in ALS: Exploring gender-specific neuroimaging signatures. Amyotroph Lateral Scler Frontotemporal Degener 15: 235-243, 2014.
31. Pryce G and Baker D: Endocannabinoids in multiple sclerosis and amyotrophic lateral sclerosis. Handb Exp Pharmacol 231: 213-231, 2015.
32. Compston A and Coles A: Multiple sclerosis. Lancet 359: 1221-1231, 2002.
33. Wijesekera LC and Leigh PN: Amyotrophic lateral sclerosis. Orphanet J Rare Dis 4: 3, 2009.
34. KhorshidAhmad T, Acosta C, Cortes C, Lakowski TM, Gangadaran S and Namaka M: Transcriptional Regulation of Brain-Derived Neurotrophic Factor (BDNF) by Methyl CpG Binding Protein 2 (MeCP2): A Novel Mechanism for Re-Myelination and/or Myelin Repair Involved in the Treatment of Multiple Sclerosis (MS). Mol Neurobiol 53: 1092-1107, 2016.
35. Zhu W, Frost EE, Begum F, Vora P, Au K, Gong Y, MacNeil B, Pillai P and Namaka M: The role of dorsal root ganglia activation and brain-derived neurotrophic factor in multiple sclerosis. J Cell Mol Med 16: 1856-1865, 2012.
36. Ebers GC: MS and autoimmune disorders. Neurogenetics 10: 1-3, 2009.
37. Etemadifar M, Abtahi SH, Akbari M and Maghzi AH: Multiple sclerosis and amyotrophic lateral sclerosis: Is there a link? Mult Scler 18: 902-904, 2012.
38. Saresella M, Piancone F, Tortorella P, Marventano I, Gatti A, Caputo D, Lunetta C, Corbo M, Rovaris M and Clerici M: T helper-17 activation dominates the immunologic milieu of both amyotrophic lateral sclerosis and progressive multiple sclerosis. Clin Immunol 148: 79-88, 2013.
39. Schirmer L, Antel JP, Brück W and Stadelmann C: Axonal loss and neurofilament phosphorylation changes accompany lesion development and clinical progression in multiple sclerosis. Brain Pathol 21: 428-440, 2011.
40. Wang Y, Liu G, Hong D, Chen F, Ji X and Cao G: White matter injury in ischemic stroke. Prog Neurobiol 141: 45-60, 2016.
41. Matute C and Ransom BR: Roles of white matter in central nervous system pathophysiologies. ASN Neuro 4: pii: e00079, 2012.
42. Purger D, Gibson EM and Monje M: Myelin plasticity in the central nervous system. Neuropharmacology 110: 563-573, 2016.
43. Hartline DK: What is myelin? Neuron Glia Biol 4: 153-163, 2008.
44. Debanne D, Campanac E, Bialowas A, Carlier E and Alcaraz G: Axon physiology. Physiol Rev 91: 555-602, 2011.
45. Edgar JM and Nave KA: The role of CNS glia in preserving axon function. Curr Opin Neurobiol 19: 498-504, 2009.
46. Franklin RJ and Ffrench-Constant C: Remyelination in the CNS: From biology to therapy. Nat Rev Neurosci 9: 839-855, 2008.
47. Stadelmann C: Multiple sclerosis as a neurodegenerative disease: Pathology, mechanisms and therapeutic implications. Curr Opin Neurol 24: 224-229, 2011.
48. Agosta F, Pievani M, Sala S, Geroldi C, Galluzzi S, Frisoni GB and Filippi M: White matter damage in Alzheimer disease and its relationship to gray matter atrophy. Radiology 258: 853-863, 2011.
49. Chew LJ, Fusar-Poli P and Schmitz T: Oligodendroglial alterations and the role of microglia in white matter injury: Relevance to schizophrenia. Dev Neurosci 35: 102-129, 2013.
50. Kumar A and Cook IA: White matter injury, neural connectivity and the pathophysiology of psychiatric disorders. Dev Neurosci 24: 255-261, 2002.
51. Menke RA, Gray E, Lu CH, Kuhle J, Talbot K, Malaspina A and Turner MR: CSF neurofilament light chain reflects corticospinal tract degeneration in ALS. Ann Clin Transl Neurol 2: 748-755, 2015.
52. Ferraiuolo L, Meyer K, Sherwood TW, Vick J, Likhite S, Frakes A, Miranda CJ, Braun L, Heath PR, Pineda R, *et al*: Oligodendrocytes contribute to motor neuron death in ALS via SOD1-dependent mechanism. Proc Natl Acad Sci USA 113: E6496-E6505, 2016.
53. Kang SH, Li Y, Fukaya M, Lorenzini I, Cleveland DW, Ostrow LW, Rothstein JD and Bergles DE: Degeneration and impaired regeneration of gray matter oligodendrocytes in amyotrophic lateral sclerosis. Nat Neurosci 16: 571-579, 2013.
54. Barateiro A, Brites D and Fernandes A: Oligodendrocyte development and myelination in neurodevelopment: Molecular mechanisms in health and disease. Curr Pharm Des 22: 656-679, 2016.
55. Zarei S, Carr K, Reiley L, Diaz K, Guerra O, Altamirano PF, Pagani W, Lodin D, Orozco G and Chinea A: A comprehensive review of amyotrophic lateral sclerosis. Sur Neurol Int 6: 171, 2015.
56. Renton AE, Majounie E, Waite A, Simón-Sánchez J, Rollinson S, Gibbs JR, Schymick JC, Laaksovirta H, van Swieten JC, Myllykangas L, *et al*: A hexanucleotide repeat expansion in C9ORF72 is the cause of chromosome 9p21-linked ALS-FTD. Neuron 72: 257-268, 2011.
57. Rosen DR, Siddique T, Patterson D, Figlewicz DA, Sapp P, Hentati A, Donaldson D, Goto J, O'Regan JP, Deng HX, *et al*: Mutations in Cu/Zn superoxide dismutase gene are associated with familial amyotrophic lateral sclerosis. Nature 362: 59-62, 1993.
58. Bannwarth S, Ait-El-Mkadem S, Chaussenot A, Genin EC, Lacas-Gervais S, Fragaki K, Berg-Alonso L, Kageyama Y, Serre V, Moore DG, *et al*: A mitochondrial origin for frontotemporal dementia and amyotrophic lateral sclerosis through CHCHD10 involvement. Brain 137: 2329-2345, 2014.
59. Johnson JO, Pioro EP, Boehringer A, Chia R, Feit H, Renton AE, Pliner HA, Abramzon Y, Marangi G, Winborn BJ, *et al*: Mutations in the Matrin 3 gene cause familial amyotrophic lateral sclerosis. Nat Neurosci 17: 664-666, 2014.
60. Cirulli ET, Lasseigne BN, Petrovski S, Sapp PC, Dion PA, Leblond CS, Couthouis J, Lu YF, Wang Q, Krueger BJ, *et al*: Exome sequencing in amyotrophic lateral sclerosis identifies risk genes and pathways. Science 347: 1436-1441, 2015.
61. Neumann M, Sampathu DM, Kwong LK, Truax AC, Micsenyi MC, Chou TT, Bruce J, Schuck T, Grossman M, Clark CM, *et al*: Ubiquitinated TDP-43 in frontotemporal lobar degeneration and amyotrophic lateral sclerosis. Science 314: 130-133, 2006.
62. Kwiatkowski TJ Jr, Bosco DA, Leclerc AL, Tamrazian E, Vanderburg CR, Russ C, Davis A, Gilchrist J, Kasarskis EJ, Munsat T, *et al*: Mutations in the FUS/TLS gene on chromosome 16 cause familial amyotrophic lateral sclerosis. Science 323: 1205-1208, 2009.
63. Maruyama H, Morino H, Ito H, Izumi Y, Kato H, Watanabe Y, Kinoshita Y, Kamada M, Nodera H, Suzuki H, *et al*: Mutations of optineurin in amyotrophic lateral sclerosis. Nature 465: 223-226, 2010.
64. Johnson JO, Mandrioli J, Benatar M, Abramzon Y, Van Deerlin VM, Trojanowski JQ, Gibbs JR, Brunetti M, Gronka S, Wuu J, *et al*: Exome sequencing reveals VCP mutations as a cause of familial ALS. Neuron 68: 857-864, 2010.

65. Deng HX, Chen W, Hong ST, Boycott KM, Gorrie GH, Siddique N, Yang Y, Fecto F, Shi Y, Zhai H, *et al*: Mutations in UBQLN2 cause dominant X-linked juvenile and adult-onset ALS and ALS/dementia. Nature 477: 211-215, 2011.
66. Fecto F, Yan J, Vemula SP, Liu E, Yang Y, Chen W, Zheng JG, Shi Y, Siddique N, Arrat H, *et al*: SQSTM1 mutations in familial and sporadic amyotrophic lateral sclerosis. Arch Neurol 68: 1440-1446, 2011.
67. Renton AE, Chiò A and Traynor BJ: State of play in amyotrophic lateral sclerosis genetics. Nat Neurosci 17: 17-23, 2014.
68. Wu CH, Fallini C, Ticozzi N, Keagle PJ, Sapp PC, Piotrowska K, Lowe P, Koppers M, McKenna-Yasek D, Baron DM, *et al*: Mutations in the profilin 1 gene cause familial amyotrophic lateral sclerosis. Nature 488: 499-503, 2012.
69. Kenna KP, van Doormaal PT, Dekker AM, Ticozzi N, Kenna BJ, Diekstra FP, van Rheenen W, van Eijk KR, Jones AR, Keagle P, *et al*: NEK1 variants confer susceptibility to amyotrophic lateral sclerosis. Nat Genet 48: 1037-1042, 2016.
70. Sica RE, Nicola AF, González Deniselle MC, Rodriguez G, Monachelli GM, Peralta LM and Bettini M: Sporadic amyotrophic lateral sclerosis: New hypothesis regarding its etiology and pathogenesis suggests that astrocytes might be the primary target hosting a still unknown external agent. Arq Neuropsiquiatr 69: 699-706, 2011.
71. Dib M: Amyotrophic lateral sclerosis: Progress and prospects for treatment. Drugs 63: 289-310, 2003.
72. Libro R, Bramanti P and Mazzon E: The role of the Wnt canonical signaling in neurodegenerative diseases. Life Sci 158: 78-88, 2016.
73. Abdelhak A, Junker A, Brettschneider J, Kassubek J, Ludolph AC, Otto M and Tumani H: Brain-specific cytoskeletal damage markers in cerebrospinal fluid: is there a common pattern between amyotrophic lateral sclerosis and primary progressive multiple sclerosis? Int J Mol Sci 16: 17565-17588, 2015.
74. Osellame LD, Blacker TS and Duchen MR: Cellular and molecular mechanisms of mitochondrial function. Best Pract Res Clin Endocrinol Metab 26: 711-723, 2012.
75. Duchen MR: Roles of mitochondria in health and disease. Diabetes 53 (Suppl 1): S96-S102, 2004.
76. Santa-Cruz LD, Guerrero-Castillo S, Uribe-Carvajal S and Tapia R: Mitochondrial dysfunction during the early stages of excitotoxic spinal motor neuron degeneration in vivo. ACS Chem Neurosci 7: 886-896, 2016.
77. Guo C, Sun L, Chen X and Zhang D: Oxidative stress, mitochondrial damage and neurodegenerative diseases. Neural Regen Res 8: 2003-2014, 2013.
78. Pardillo-Díaz R, Carrascal L, Muñoz MF, Ayala A and Nunez-Abades P: Time and dose dependent effects of oxidative stress induced by cumene hydroperoxide in neuronal excitability of rat motor cortex neurons. Neurotoxicology 53: 201-214, 2016.
79. Kaal EC, Veldman H, Sodaar P, Joosten EA and Dop Bär PR: Oxidant treatment causes a dose-dependent phenotype of apoptosis in cultured motoneurons. J Neurosci Res 54: 778-786, 1998.
80. Lin MT and Beal MF: Mitochondrial dysfunction and oxidative stress in neurodegenerative diseases. Nature 443: 787-795, 2006.
81. Sharma A, Varghese AM, Vijaylakshmi K, Sumitha R, Prasanna VK, Shruthi S, Chandrasekhar Sagar BK, Datta KK, Gowda H, Nalini A, *et al*: Cerebrospinal fluid from sporadic amyotrophic lateral sclerosis patients induces mitochondrial and lysosomal dysfunction. Neurochem Res 41: 965-984, 2016.
82. Miquel E, Cassina A, Martínez-Palma L, Bolatto C, Trías E, Gandelman M, Radi R, Barbeito L and Cassina P: Modulation of astrocytic mitochondrial function by dichloroacetate improves survival and motor performance in inherited amyotrophic lateral sclerosis. PLoS One 7: e34776, 2012.
83. Liu D, Wen J, Liu J and Li L: The roles of free radicals in amyotrophic lateral sclerosis: Reactive oxygen species and elevated oxidation of protein, DNA, and membrane phospholipids. FASEB J 13: 2318-2328, 1999.
84. Turner BJ and Talbot K: Transgenics, toxicity and therapeutics in rodent models of mutant SOD1-mediated familial ALS. Prog Neurobiol 85: 94-134, 2008.
85. Boillée S, Vande Velde C and Cleveland DW: ALS: A disease of motor neurons and their nonneuronal neighbors. Neuron 52: 39-59, 2006.
86. Hayashi Y, Homma K and Ichijo H: SOD1 in neurotoxicity and its controversial roles in SOD1 mutation-negative ALS. Adv Biol Regul 60: 95-104, 2016.
87. Carri MT, Valle C, Bozzo F and Cozzolino M: Oxidative stress and mitochondrial damage: Importance in non-SOD1 ALS. Front Cell Neurosci 9: 41, 2015.
88. Jaronen M, Goldsteins G and Koistinaho J: ER stress and unfolded protein response in amyotrophic lateral sclerosis-a controversial role of protein disulphide isomerase. Front Cell Neurosci 8: 402, 2014.
89. Karademir B, Corek C and Ozer NK: Endoplasmic reticulum stress and proteasomal system in amyotrophic lateral sclerosis. Free Radic Biol Med 88: 42-50, 2015.
90. Sundaramoorthy V, Sultana JM and Atkin JD: Golgi fragmentation in amyotrophic lateral sclerosis, an overview of possible triggers and consequences. Front Neurosci 9: 400, 2015.
91. Atkin JD, Farg MA, Soo KY, Walker AK, Halloran M, Turner BJ, Nagley P and Horne MK: Mutant SOD1 inhibits ER-Golgi transport in amyotrophic lateral sclerosis. J Neurochem 129: 190-204, 2014.
92. Parakh S and Atkin JD: Protein folding alterations in amyotrophic lateral sclerosis. Brain Res 1648: 633-649, 2016.
93. Kalmar B, Lu CH and Greensmith L: The role of heat shock proteins in Amyotrophic Lateral Sclerosis: The therapeutic potential of Arimoclomol. Pharmacol Ther 141: 40-54, 2014.
94. Rathnasamy G, Murugan M, Ling EA and Kaur C: Hypoxia-induced iron accumulation in oligodendrocytes mediates apoptosis by eliciting endoplasmic reticulum stress. Mol Neurobiol 53: 4713-4727, 2016.
95. Naughton MC, McMahon JM and FitzGerald U: Differential activation of ER stress pathways in myelinating cerebellar tracts. Int J Dev Neurosci 47: 347-360, 2015.
96. Underwood CK, Kurniawan ND, Butler TJ, Cowin GJ and Wallace RH: Non-invasive diffusion tensor imaging detects white matter degeneration in the spinal cord of a mouse model of amyotrophic lateral sclerosis. NeuroImage 55: 455-461, 2011.
97. Jaronen M, Vehviläinen P, Malm T, Keksa-Goldsteine V, Pollari E, Valonen P, Koistinaho J and Goldsteins G: Protein disulfide isomerase in ALS mouse glia links protein misfolding with NADPH oxidase-catalyzed superoxide production. Hum Mol Genet 22: 646-655, 2013.
98. Saxena S, Cabuy E and Caroni P: A role for motoneuron subtype-selective ER stress in disease manifestations of FALS mice. Nat Neurosci 12: 627-636, 2009.
99. King AE, Woodhouse A, Kirkcaldie MT and Vickers JC: Excitotoxicity in ALS: Overstimulation, or overreaction? Exp Neurol 275 Pt 1: 162-171, 2016.
100. Blizzard CA, Southam KA, Dawkins E, Lewis KE, King AE, Clark JA and Dickson TC: Identifying the primary site of pathogenesis in amyotrophic lateral sclerosis-vulnerability of lower motor neurons to proximal excitotoxicity. Dis Model Mech 8: 215-224, 2015.
101. Foerster BR, Pomper MG, Callaghan BC, Petrou M, Edden RA, Mohamed MA, Welsh RC, Carlos RC, Barker PB and Feldman EL: An imbalance between excitatory and inhibitory neurotransmitters in amyotrophic lateral sclerosis revealed by use of 3-T proton magnetic resonance spectroscopy. JAMA Neurol 70: 1009-1016, 2013.
102. Cooper AJ: The role of glutamine synthetase and glutamate dehydrogenase in cerebral ammonia homeostasis. Neurochem Res 37: 2439-2455, 2012.
103. Matyja E, Taraszewska A, Nagańska E, Rafałowska J and Gebarowska J: Astroglial alterations in amyotrophic lateral sclerosis (ALS) model of slow glutamate excitotoxicity in vitro. Folia Neuropathol 44: 183-190, 2006.
104. King AE, Dickson TC, Blizzard CA, Foster SS, Chung RS, West AK, Chuah MI and Vickers JC: Excitotoxicity mediated by non-NMDA receptors causes distal axonopathy in long-term cultured spinal motor neurons. Eur J Neurosci 26: 2151-2159, 2007.
105. Gressens P: VIP neuroprotection against excitotoxic lesions of the developing mouse brain. Ann N Y Acad Sci 897: 109-124, 1999.
106. Passemard S, Sokolowska P, Schwendimann L and Gressens P: VIP-induced neuroprotection of the developing brain. Curr Pharm Des 17: 1036-1039, 2011.
107. Lee J, Hyeon SJ, Im H, Ryu H, Kim Y and Ryu H: Astrocytes and microglia as non-cell autonomous players in the pathogenesis of ALS. Exp Neurobiol 25: 233-240, 2016.
108. Ludwin SK, Rao VTs, Moore CS and Antel JP: Astrocytes in multiple sclerosis. Mult Scler 22: 1114-1124, 2016.
109. Takimoto M and Hamada T: Acute exercise increases brain region-specific expression of MCT1, MCT2, MCT4, GLUT1, and COX IV proteins. J Appl Physiol (1985) 116: 1238-1250, 2014.

110. Lundgaard I, Osório MJ, Kress BT, Sanggaard S and Nedergaard M: White matter astrocytes in health and disease. Neuroscience 276: 161-173, 2014.
111. Morrison BM, Lee Y and Rothstein JD: Oligodendroglia: Metabolic supporters of axons. Trends Cell Biol 23: 644-651, 2013.
112. Philips T, Bento-Abreu A, Nonneman A, Haeck W, Staats K, Geelen V, Hersmus N, Küsters B, Van Den Bosch L, Van Damme P, *et al*: Oligodendrocyte dysfunction in the pathogenesis of amyotrophic lateral sclerosis. Brain 136: 471-482, 2013.
113. Fünfschilling U, Supplie LM, Mahad D, Boretius S, Saab AS, Edgar J, Brinkmann BG, Kassmann CM, Tzvetanova ID, Möbius W, *et al*: Glycolytic oligodendrocytes maintain myelin and long-term axonal integrity. Nature 485: 517-521, 2012.
114. Lee Y, Morrison BM, Li Y, Lengacher S, Farah MH, Hoffman PN, Liu Y, Tsingalia A, Jin L, Zhang PW, *et al*: Oligodendroglia metabolically support axons and contribute to neurodegeneration. Nature 487: 443-448, 2012.
115. Pierre K and Pellerin L: Monocarboxylate transporters in the central nervous system: Distribution, regulation and function. J Neurochem 94: 1-14, 2005.
116. Nijland PG, Michailidou I, Witte ME, Mizee MR, van der Pol SM, van Het Hof B, Reijerkerk A, Pellerin L, van der Valk P, de Vries HE and van Horssen J: Cellular distribution of glucose and monocarboxylate transporters in human brain white matter and multiple sclerosis lesions. Glia 62: 1125-1141, 2014.
117. Robinet C and Pellerin L: Brain-derived neurotrophic factor enhances the expression of the monocarboxylate transporter 2 through translational activation in mouse cultured cortical neurons. J Cereb Blood Flow Metab 30: 286-298, 2010.
118. Lemmens R, Van Hoecke A, Hersmus N, Geelen V, D'Hollander I, Thijs V, Van Den Bosch L, Carmeliet P and Robberecht W: Overexpression of mutant superoxide dismutase 1 causes a motor axonopathy in the zebrafish. Hum Mol Genet 16: 2359-2365, 2007.
119. Wong M and Martin LJ: Skeletal muscle-restricted expression of human SOD1 causes motor neuron degeneration in transgenic mice. Hum Mol Genet 19: 2284-2302, 2010.
120. Sotelo-Silveira JR, Lepanto P, Elizondo V, Horjales S, Palacios F, Martinez-Palma L, Marin M, Beckman JS and Barbeito L: Axonal mitochondrial clusters containing mutant SOD1 in transgenic models of ALS. Antioxid Redox Signal 11: 1535-1545, 2009.
121. King AE, Dickson TC, Blizzard CA, Woodhouse A, Foster SS, Chung RS and Vickers JC: Neuron-glia interactions underlie ALS-like axonal cytoskeletal pathology. Neurobiol Aging 32: 459-469, 2011.
122. Frey D, Schneider C, Xu L, Borg J, Spooren W and Caroni P: Early and selective loss of neuromuscular synapse subtypes with low sprouting competence in motoneuron diseases. J Neurosci 20: 2534-2542, 2000.
123. Nave KA and Trapp BD: Axon-glial signaling and the glial support of axon function. Annu Rev Neurosci 31: 535-561, 2008.
124. Anderson JE, Do MQ, Daneshvar N, Suzuki T, Dort J, Mizunoya W and Tatsumi R: The role of semaphorin3A in myogenic regeneration and the formation of functional neuromuscular junctions on new fibres. Biol Rev Camb Philos Soc: Jun 13, 2016 (Epub ahead of print).
125. Syed YA, Hand E, Möbius W, Zhao C, Hofer M, Nave KA and Kotter MR: Inhibition of CNS remyelination by the presence of semaphorin 3A. J Neurosci 31: 3719-3728, 2011.
126. Spassky N, de Castro F, Le Bras B, Heydon K, Quéraud-LeSaux F, Bloch-Gallego E, Chédotal A, Zalc B and Thomas JL: Directional guidance of oligodendroglial migration by class 3 semaphorins and netrin-1. J Neurosci 22: 5992-6004, 2002.
127. Piaton G, Aigrot MS, Williams A, Moyon S, Tepavcevic V, Moutkine I, Gras J, Matho KS, Schmitt A, Soellner H, *et al*: Class 3 semaphorins influence oligodendrocyte precursor recruitment and remyelination in adult central nervous system. Brain 134: 1156-1167, 2011.
128. Venkova K, Christov A, Kamaluddin Z, Kobalka P, Siddiqui S and Hensley K: Semaphorin 3A signaling through neuropilin-1 is an early trigger for distal axonopathy in the SOD1G93A mouse model of amyotrophic lateral sclerosis. J Neuropathol Exp Neurol 73: 702-713, 2014.
129. Korner S, Böselt S, Wichmann K, Thau-Habermann N, Zapf A, Knippenberg S, Dengler R and Petri S: The Axon Guidance Protein Semaphorin 3A Is increased in the motor cortex of patients with amyotrophic lateral sclerosis. J Neuropathol Exp Neurol: Feb 25, 2016 (Epub ahead of print).
130. Mecollari V, Nieuwenhuis B and Verhaagen J: A perspective on the role of class III semaphorin signaling in central nervous system trauma. Front Cell Neurosci 8: 328, 2014.
131. Dadon-Nachum M, Melamed E and Offen D: The 'dying-back' phenomenon of motor neurons in ALS. J Mol Neurosci 43: 470-477, 2011.
132. Tao S, Yang X, Chen Y, Wang X, Xiao Z, Wang H, Wu Q and Wang X: Up-regulated methyl CpG binding protein-2 in intractable temporal lobe epilepsy patients and a rat model. Neurochem Res 37: 1886-1897, 2012.
133. Dastidar SG, Bardai FH, Ma C, Price V, Rawat V, Verma P, Narayanan V and D'Mello SR: Isoform-specific toxicity of Mecp2 in postmitotic neurons: Suppression of neurotoxicity by FoxG1. J Neurosci 32: 2846-2855, 2012.
134. Dastidar SG, Landrieu PM and D'Mello SR: FoxG1 promotes the survival of postmitotic neurons. J Neurosci 31: 402-413, 2011.
135. Schulte-Herbrüggen O, Braun A, Rochlitzer S, Jockers-Scherübl MC and Hellweg R: Neurotrophic factors-a tool for therapeutic strategies in neurological, neuropsychiatric and neuroimmunological diseases? Curr Med Chem 14: 2318-2329, 2007.
136. Cellerino A, Carroll P, Thoenen H and Barde YA: Reduced size of retinal ganglion cell axons and hypomyelination in mice lacking brain-derived neurotrophic factor. Mol Cell Neurosci 9: 397-408, 1997.
137. Tremolizzo L, Pellegrini A, Conti E, Arosio A, Gerardi F, Lunetta C, Magni P, Appollonio I and Ferrarese C: BDNF serum levels with respect to multidimensional assessment in amyotrophic lateral sclerosis. Neurodegener Dis 16: 192-198, 2016.
138. Giménez y Ribotta M, Revah F, Pradier L, Loquet I, Mallet J and Privat A: Prevention of motoneuron death by adenovirus-mediated neurotrophic factors. J Neurosci Res 48: 281-285, 1997.
139. Dadon-Nachum M, Ben-Yaacov K, Ben-Zur T, Barhum Y, Yaffe D, Perlson E and Offen D: Transplanted modified muscle progenitor cells expressing a mixture of neurotrophic factors delay disease onset and enhance survival in the SOD1 mouse model of ALS. J Mol Neurosci 55: 788-797, 2015.
140. Xu R, Wu C, Zhang X, Zhang Q, Yang Y, Yi J, Yang R and Tao Y: Linking hypoxic and oxidative insults to cell death mechanisms in models of ALS. Brain Res 1372: 133-144, 2011.
141. Oh YK, Shin KS and Kang SJ: AIF translocates to the nucleus in the spinal motor neurons in a mouse model of ALS. Neurosci Lett 406: 205-210, 2006.
142. Pedrini S, Sau D, Guareschi S, Bogush M, Brown RH Jr, Naniche N, Kia A, Trotti D and Pasinelli P: ALS-linked mutant SOD1 damages mitochondria by promoting conformational changes in Bcl-2. Hum Mol Genet 19: 2974-2986, 2010.
143. Troost D, Aten J, Morsink F and de Jong JM: Apoptosis in amyotrophic lateral sclerosis is not restricted to motor neurons. Bcl-2 expression is increased in unaffected post-central gyrus. Neuropathol Appl Neurobiol 21: 498-504, 1995.
144. Petrik MS, Wilson JM, Grant SC, Blackband SJ, Tabata RC, Shan X, Krieger C and Shaw CA: Magnetic resonance microscopy and immunohistochemistry of the CNS of the mutant SOD murine model of ALS reveals widespread neural deficits. Neuromolecular Med 9: 216-229, 2007.
145. Nagai M, Re DB, Nagata T, Chalazonitis A, Jessell TM, Wichterle H and Przedborski S: Astrocytes expressing ALS-linked mutated SOD1 release factors selectively toxic to motor neurons. Nat Neurosci 10: 615-622, 2007.
146. Guégan C and Przedborski S: Programmed cell death in amyotrophic lateral sclerosis. J Clin Invest 111: 153-161, 2003.
147. Reyes NA, Fisher JK, Austgen K, VandenBerg S, Huang EJ and Oakes SA: Blocking the mitochondrial apoptotic pathway preserves motor neuron viability and function in a mouse model of amyotrophic lateral sclerosis. J Clin Invest 120: 3673-3679, 2010.
148. Vukosavic S, Dubois-Dauphin M, Romero N and Przedborski S: Bax and Bcl-2 interaction in a transgenic mouse model of familial amyotrophic lateral sclerosis. J Neurochem 73: 2460-2468, 1999.
149. Peviani M, Tortarolo M, Battaglia E, Piva R and Bendotti C: Specific induction of Akt3 in spinal cord motor neurons is neuroprotective in a mouse model of familial amyotrophic lateral sclerosis. Mol Neurobiol 49: 136-148, 2014.
150. Shrivastava M and Subbiah V: Elevated caspase 3 activity and cytosolic cytochrome c in NT2 cybrids containing amyotrophic lateral sclerosis subject mtDNA. Int J Neurosci 126: 839-849, 2016.
151. Sathasivam S and Shaw PJ: Apoptosis in amyotrophic lateral sclerosis-what is the evidence? Lancet Neurol 4: 500-509, 2005.

152. Tanaka H, Shimazaki H, Kimura M, Izuta H, Tsuruma K, Shimazawa M and Hara H: Apoptosis-inducing factor and cyclophilin A cotranslocate to the motor neuronal nuclei in amyotrophic lateral sclerosis model mice. CNS Neurosci Ther 17: 294-304, 2011.
153. Wang Y and Kasper LH: The role of microbiome in central nervous system disorders. Brain Behav Immun 38: 1-12, 2014.
154. Glenn JD and Mowry EM: Emerging Concepts on the Gut Microbiome and Multiple Sclerosis. J Interferon Cytokine Res 36: 347-357, 2016.
155. Bhargava P and Mowry EM: Gut microbiome and multiple sclerosis. Curr Neurol Neurosci Rep 14: 492, 2014.
156. Luna RA, Savidge TC and Williams KC: The Brain-Gut-Microbiome Axis: What Role Does It Play in Autism Spectrum Disorder? Curr Dev Disord Rep 3: 75-81, 2016.
157. Fang X: Potential role of gut microbiota and tissue barriers in Parkinson's disease and amyotrophic lateral sclerosis. Int J Neurosci 126: 771-776, 2016.
158. Galland L: The gut microbiome and the brain. J Med Food 17: 1261-1272, 2014.
159. Newland PK, Heitkemper M and Zhou Y: The Emerging Role of the Gut Microbiome in Adult Patients With Multiple Sclerosis. J Neurosci Nurs 48: 358-364, 2016.
160. Chen J, Chia N, Kalari KR, Yao JZ, Novotna M, Soldan MM, Luckey DH, Marietta EV, Jeraldo PR, Chen X, *et al*: Multiple sclerosis patients have a distinct gut microbiota compared to healthy controls. Sci Rep 6: 28484, 2016.
161. Kaneko K and Hachiya NS: Hypothesis: Gut as source of motor neuron toxin in the development of ALS. Med Hypotheses 66: 438-439, 2006.
162. Longstreth WT Jr, Meschke JS, Davidson SK, Smoot LM, Smoot JC and Koepsell TD: Hypothesis: A motor neuron toxin produced by a clostridial species residing in gut causes ALS. Med Hypotheses 64: 1153-1156, 2005.
163. Wu S, Yi J, Zhang YG, Zhou J and Sun J: Leaky intestine and impaired microbiome in an amyotrophic lateral sclerosis mouse model. Physiol Rep 3: pii: e12356, 2015.
164. Miller RG, Mitchell JD and Moore DH: Riluzole for amyotrophic lateral sclerosis (ALS)/motor neuron disease (MND). Cochrane Database Syst Rev: CD001447, 2012.
165. Cetin H, Rath J, Füzi J, Reichardt B, Fülöp G, Koppi S, Erdler M, Ransmayr G, Weber J, Neumann K, *et al*: Epidemiology of amyotrophic lateral sclerosis and effect of riluzole on disease course. Neuroepidemiology 44: 6-15, 2015.
166. Vucic S, Lin CS, Cheah BC, Murray J, Menon P, Krishnan AV and Kiernan MC: Riluzole exerts central and peripheral modulating effects in amyotrophic lateral sclerosis. Brain 136: 1361-1370, 2013.
167. Cheah BC, Vucic S, Krishnan AV and Kiernan MC: Riluzole, neuroprotection and amyotrophic lateral sclerosis. Curr Med Chem 17: 1942-1199, 2010.
168. Bellingham MC: A review of the neural mechanisms of action and clinical efficiency of riluzole in treating amyotrophic lateral sclerosis: What have we learned in the last decade? CNS Neurosci Ther 17: 4-31, 2011.
169. Dennys CN, Armstrong J, Levy M, Byun YJ, Ramdial KR, Bott M, Rossi FH, Fernández-Valle C, Franco MC and Estevez AG: Chronic inhibitory effect of riluzole on trophic factor production. Exp Neurol 271: 301-307, 2015.
170. Tsai SJ: Is riluzole a potential therapy for Rett syndrome? Med Hypotheses 85: 76-78, 2015.
171. Turck P and Frizzo ME: Riluzole stimulates BDNF release from human platelets. Biomed Res Int 2015: 189307, 2015.
172. Gilgun-Sherki Y, Panet H, Melamed E and Offen D: Riluzole suppresses experimental autoimmune encephalomyelitis: Implications for the treatment of multiple sclerosis. Brain Res 989: 196-204, 2003.
173. Shirani A, Okuda DT and Stüve O: Therapeutic advances and future prospects in progressive forms of multiple sclerosis. Neurotherapeutics 13: 58-69, 2016.
174. Waubant E, Maghzi AH, Revirajan N, Spain R, Julian L, Mowry EM, Marcus J, Liu S, Jin C, Green A, *et al*: A randomized controlled phase II trial of riluzole in early multiple sclerosis. Ann Clin Transl Neurol 1: 340-347, 2014.
175. Obata K and Noguchi K: BDNF in sensory neurons and chronic pain. Neurosci Res 55: 1-10, 2006.
176. Caumo W, Deitos A, Carvalho S, Leite J, Carvalho F, Dussán-Sarria JA, Lopes Tarragó Mda G, Souza A, Torres IL and Fregni F: Motor cortex excitability and BDNF levels in chronic musculoskeletal pain according to structural pathology. Front Hum Neurosci 10: 357, 2016.
177. Gutierrez J, Federici T, Peterson B, Bartus R, Betourne A and Boulis NM: 321 development of intrathecal riluzole: A new route of administration for the treatment of amyotrophic lateral sclerosis patients. Neurosurgery 63 (Suppl 1): S193, 2016.
178. Browne EC and Abbott BM: Recent progress towards an effective treatment of amyotrophic lateral sclerosis using the SOD1 mouse model in a preclinical setting. Eur J Med Chem 121: 918-925, 2016.
179. Lieberknecht V, Junqueira SC, Cunha MP, Barbosa TA, de Souza LF, Coelho IS, Santos AR, Rodrigues AL, Dafré AL and Dutra RC: Pramipexole, a Dopamine D2/D3 receptor-preferring agonist, prevents experimental autoimmune encephalomyelitis development in Mice. Mol Neurobiol 54: 1033-1045, 2017.
180. Ferrari-Toninelli G, Maccarinelli G, Uberti D, Buerger E and Memo M: Mitochondria-targeted antioxidant effects of S(-) and R(+) pramipexole. BMC Pharmacol 10: 2, 2010.
181. Abramova NA, Cassarino DS, Khan SM, Painter TW and Bennett JP Jr: Inhibition by R(+) or S(-) pramipexole of caspase activation and cell death induced by methylpyridinium ion or beta amyloid peptide in SH-SY5Y neuroblastoma. J Neurosci Res 67: 494-500, 2002.
182. Alavian KN, Dworetzky SI, Bonanni L, Zhang P, Sacchetti S, Mariggio MA, Onofrj M, Thomas A, Li H, Mangold JE, *et al*: Effects of dexpramipexole on brain mitochondrial conductances and cellular bioenergetic efficiency. Brain Res 1446: 1-11, 2012.
183. Corcia P and Gordon PH: Amyotrophic lateral sclerosis and the clinical potential of dexpramipexole. Ther Clin Risk Manag 8: 359-366, 2012.
184. De Nuccio C, Bernardo A, Cruciani C, De Simone R, Visentin S and Minghetti L: Peroxisome proliferator activated receptor-γ agonists protect oligodendrocyte progenitors against tumor necrosis factor-alpha-induced damage: Effects on mitochondrial functions and differentiation. Exp Neurol 271: 506-514, 2015.
185. Shukla DK, Kaiser CC, Stebbins GT and Feinstein DL: Effects of pioglitazone on diffusion tensor imaging indices in multiple sclerosis patients. Neurosci Lett 472: 153-156, 2010.
186. Dupuis L, Dengler R, Heneka MT, Meyer T, Zierz S, Kassubek J, Fischer W, Steiner F, Lindauer E, Otto M, *et al*: A randomized, double blind, placebo-controlled trial of pioglitazone in combination with riluzole in amyotrophic lateral sclerosis. PLoS One 7: e37885, 2012.
187. Yáñez M, Matías-Guiu J, Arranz-Tagarro JA, Galán L, Viña D, Gómez-Pinedo U, Vela A, Guerrero A, Martínez-Vila E and García AG: The neuroprotection exerted by memantine, minocycline and lithium, against neurotoxicity of CSF from patients with amyotrophic lateral sclerosis, is antagonized by riluzole. Neurodegener Dis 13: 171-179, 2014.
188. Herges K, Millward JM, Hentschel N, Infante-Duarte C, Aktas O and Zipp F: Neuroprotective effect of combination therapy of glatiramer acetate and epigallocatechin-3-gallate in neuroinflammation. PLoS One 6: e25456, 2011.
189. Koh SH, Lee SM, Kim HY, Lee KY, Lee YJ, Kim HT, Kim J, Kim MH, Hwang MS, Song C, *et al*: The effect of epigallocatechin gallate on suppressing disease progression of ALS model mice. Neurosci Lett 395: 103-107, 2006.
190. Solanki I, Parihar P, Mansuri ML and Parihar MS: Flavonoid-based therapies in the early management of neurodegenerative diseases. Adv Nutr 6: 64-72, 2015.
191. Feng Z and Gao F: Stem cell challenges in the treatment of neurodegenerative disease. CNS Neurosci Ther 18: 142-148, 2012.
192. Nizzardo M, Simone C, Rizzo F, Ruggieri M, Salani S, Riboldi G, Faravelli I, Zanetta C, Bresolin N, Comi GP and Corti S: Minimally invasive transplantation of iPSC-derived ALDHhiSSCloVLA4+ neural stem cells effectively improves the phenotype of an amyotrophic lateral sclerosis model. Hum Mol Genet 23: 342-354, 2014.
193. Martinez HR, Gonzalez-Garza MT, Moreno-Cuevas JE, Caro E, Gutierrez-Jimenez E and Segura JJ: Stem-cell transplantation into the frontal motor cortex in amyotrophic lateral sclerosis patients. Cytotherapy 11: 26-34, 2009.
194. Einstein O, Friedman-Levi Y, Grigoriadis N and Ben-Hur T: Transplanted neural precursors enhance host brain-derived myelin regeneration. J Neurosci 29: 15694-15702, 2009.
195. Makar TK, Bever CT, Singh IS, Royal W, Sahu SN, Sura TP, Sultana S, Sura KT, Patel N, Dhib-Jalbut S and Trisler D: Brain-derived neurotrophic factor gene delivery in an animal model of multiple sclerosis using bone marrow stem cells as a vehicle. J Neuroimmunol 210: 40-51, 2009.

196. Staines DR: Are multiple sclerosis and amyotrophic lateral sclerosis autoimmune disorders of endogenous vasoactive neuropeptides? Med Hypotheses 70: 413-418, 2008.
197. Spinelli EG, Agosta F, Ferraro PM, Riva N, Lunetta C, Falzone YM, Comi G, Falini A and Filippi M: Brain MR imaging in patients with lower motor neuron-predominant disease. Radiology 280: 545-556, 2016.
198. Prudlo J, Bissbort C, Glass A, Grossmann A, Hauenstein K, Benecke R and Teipel SJ: White matter pathology in ALS and lower motor neuron ALS variants: A diffusion tensor imaging study using tract-based spatial statistics. J Neurol 259: 1848-1859, 2012.
199. Beer A, Biberacher V, Schmidt P, Righart R, Buck D, Berthele A, Kirschke J, Zimmer C, Hemmer B and Mühlau M: Tissue damage within normal appearing white matter in early multiple sclerosis: Assessment by the ratio of T1- and T2-weighted MR image intensity. J Neurol 263: 1495-1502, 2016.
200. Gutiérrez-Franco A, Eixarch H, Costa C, Gil V, Castillo M, Calvo-Barreiro L, Montalban X, Del Río JA and Espejo C: Semaphorin 7A as a potential therapeutic target for multiple sclerosis. Mol Neurobiol: Oct 6, 2016 (Epub ahead of print).
201. Costa C, Martínez-Sáez E, Gutiérrez-Franco A, Eixarch H, Castro Z, Ortega-Aznar A, Ramón Y Cajal S, Montalban X and Espejo C: Expression of semaphorin 3A, semaphorin 7A and their receptors in multiple sclerosis lesions. Mult Scler 21: 1632-1643, 2015.

Subject: Spandidos Publications Esub no. : 182526
Date: Thursday, September 5, 2019 at 4:39:38 AM Central Daylight Time
From: mmr@osats.spandidos-publications.com
To:
CC: Mike.Namaka@umanitoba.ca, Ting Zhou

Dear Mr Ting Zhou,

Our reference: MMR-11352-182526

Title: Exploring the Molecular Mechanisms of White Matter Damage in Amyotrophic Lateral Sclerosis (ALS)

By: Ting Zhou

Thank you for your e-mail.

Please note, we give our permission for you to use parts of this review article in your thesis.

Yours sincerely,

Spandidos Publications

Biochemical and Biophysical Research Communications 516 (2019) 373–380

Contents lists available at ScienceDirect

Biochemical and Biophysical Research Communications

journal homepage: www.elsevier.com/locate/ybbrc

Therapeutic impact of orally administered cannabinoid oil extracts in an experimental autoimmune encephalomyelitis animal model of multiple sclerosis

Ting Zhou [a, b, f], Tina Khorshid Ahmad [a], Samaa Alrushaid [a, g], Marianna Pozdirca [a], Karen Ethans [d], Howard Intrater [e], Tyson Le [a], Frank Burczynski [a], Jiming Kong [b], Michael Namaka [a, b, c, d, e, *]

[a] College of Pharmacy, University of Manitoba, Winnipeg, MB, R3E 0T5, Canada
[b] Department of Human Anatomy and Cell Science, University of Manitoba, Winnipeg, MB, R3E 0W2, Canada
[c] College of Rehabilitation Medicine, Health Sciences Centre, Winnipeg, MB, R3A 1R9, Canada
[d] College of Medicine, University of Manitoba, Winnipeg, MB, R3E 3P5, Canada
[e] Department of Anesthesia and Perioperative Medicine, University of Manitoba, Winnipeg, MB, R3E 0Z3, Canada
[f] Chongqing General Hospital, Chongqing, 40000, China
[g] Department of Pharmaceutical Chemistry, Faculty of Pharmacy, Kuwait University, Safat, 13110, Kuwait

ARTICLE INFO

Article history:
Received 7 May 2019
Accepted 7 June 2019
Available online 15 June 2019

Keywords:
Multiple sclerosis
Neuropathic pain
Cannabinoid oil extracts
Neurological disability
TNF-α
BDNF

ABSTRACT

There is a growing surge of investigative research involving the beneficial use of cannabinoids as novel interventional alternatives for multiple sclerosis (MS) and associated neuropathic pain (NPP). Using an experimental autoimmune encephalomyelitis (EAE) animal model of MS, we demonstrate the therapeutic effectiveness of two cannabinoid oil extract formulations (10:10 & 1:20 – tetrahydrocannabinol/cannabidiol) treatment. Our research findings confirm that cannabinoid treatment produces significant improvements in neurological disability scoring and behavioral assessments of NPP that directly result from their ability to reduce tumor necrosis factor alpha (TNF-α) production and enhance brain derived neurotrophic factor (BDNF) production. Henceforth, this research represents a critical step in advancing the literature by scientifically validating the merit for medical cannabinoid use and sets the foundation for future clinical trials.

© 2019 Elsevier Inc. All rights reserved.

1. Introduction

Multiple sclerosis (MS) is a chronic, incurable disease characterized by inflammation and demyelination in the brain and spinal cord (SC) of the central nervous system (CNS). While the exact mechanism of the disease is unknown, it is widely considered as an autoimmune disease involving the infiltration of inflammatory cells through the blood-brain barrier into the CNS, resulting in the liberation of inflammatory mediators, such as tumor necrosis factor alpha (TNF-α), which are involved in neuropathic pain (NPP) and neuronal destruction [1,2]. MS-induced NPP remains a compelling clinical problem to patients and healthcare providers as it responds poorly to conventional treatments [3].

Anecdotal reports of the beneficial medicinal properties associated with the plant *Cannabis Sativa* have led to a recent surge in investigative research to explore the potential benefits of cannabinoids that are linked to their ability to modulate the immune system and promote analgesia in chronic pain syndromes such as MS-induced NPP [4–6]. The key cannabinoid components of interest are Δ9-tetrahydrocannabinol (THC) [7], cannabidiol (CBD) and cannabichromene (CBC) [8]. With recent advances in biotechnology, it is possible to consistently adjust the THC/CBD ratios within the plant to achieve the specific desired effect and therapeutic outcomes while minimizing adverse effects [9]. Henceforth, the use of genetically altered plants by certain licensed producers in Canada allows for a tighter control over the consistent reproducibility of the differential production of the three main active constituents: THC, CBD and CBC.

* Corresponding author. College of Pharmacy, University of Manitoba, Winnipeg, MB, R3E 0T5, Canada.
E-mail addresses: samaa.alrushaid@hsc.edu.kw (S. Alrushaid), mikemamakams@gmail.com (M. Namaka).

https://doi.org/10.1016/j.bbrc.2019.06.033
0006-291X/© 2019 Elsevier Inc. All rights reserved.

As such, the current research focused on confirming the potential therapeutic efficacy and specific molecular mechanisms by which interventional treatment with cannabinoids exerts their beneficial effects in MS associated NPP syndromes. Our results revealed that significant improvements in neurological assessments of MS induced neurological disability and behavioral assessments of NPP in EAE animals treated with the orally administered cannabinoids. In addition, we investigated the role of cannabinoids on the gene and protein expression of bio-markers, such as TNF-α and BDNF, in a rat EAE model. Moreover, we also determined the pharmacokinetic pattern of cannabinoid oil extracts. This research represents a critical step in scientifically validating the merit for cannabinoid use and sets the foundation for future pilot human clinical trials in patients suffering from MS.

2. Materials and methods

2.1. Experimental autoimmune encephalomyelitis (EAE) induction

Adolescent female Lewis rats 9–14 weeks of age (Charles River, Canada) were immunized subcutaneously with 500 μg myelin basic protein gp 69-88 in 1000 μl of Complete Freund's adjuvant at the lower back (0.2 ml/rat) at day 0 (Hooke Laboratories, Cat#. EK-3111, USA). Animals received two intraperitoneal injections of pertussis toxin at days 0 and 2. All animal experiments in this study were conducted according to protocols approved by the University of Manitoba Animal Protocol Management and Review Committee and in full compliance with the Canadian Council on Animal Care (Protocol Reference Number: 15-049/1/2 AC 11097).

2.2. Cannabinoid treatments

CanniMed Oil® Huile 10:10 (Lot# OL16007H) and 1:20 (Lot# OL16026J) were obtained from Prairie Plant Systems Inc (Saskatoon, Canada). A 215 mg/kg dose of the cannabinoid oil extracts is administered by oral gavage daily between day 6–18 post-disease based on the previous established in-house expertise with the EAE rat model of MS [10].

2.3. Neurological disability scoring (NDS)

NDS were conducted in accordance to our published criteria [11]. Animals were assessed daily for neurological disability until sacrificed. NDS were determined from mean clinical scores measured from a score of 0 (no disability) to 15 (maximal disability). The total score is the sum of the following individual scores obtained for each of the 6 specified clinical domains: *tail:* 0 = normal, 1 = weakness or partial paralysis, 2 = complete paralysis; *hind limbs and forelimbs:* 0 = normal, 1 = weakness, 2 = dragging or partial paralysis, 3 = complete paralysis; *bladder:* 0 = normal, 1 = incontinent. Only animals that progressed to the NDS of 4 or greater were included in the study.

2.4. Enzyme linked immunosorbent assay (ELISA)

Sandwich-style ELISA was performed using the Novex® rat TNF-α ELISA kit (Invitrogen, Cat#. KRC3011) and a BDNF Emax ImmunoAssay System (Promega, Cat#. G7611). TNF-α content was measured from standard curve runs for each plate (linear range of 0–200 ng/ml). BDNF protein concentration was interpolated from a standard curve with a range of 7.8–500 pg/ml.

2.5. Quantitative reverse transcriptase polymerase chain reaction (qRT- PCR)

The PCR reaction was performed using a SsoFast EvaGreen Supermix following manufacturers protocols (Bio-Rad, CA, USA) on a Real-Time PCR system (7500, Applied Biosystems, USA). TNF-α primers were forward: 5' -AGCCGATTTGCCATTTCATACCAG -3'; reverse: 5' -CACGCCAGTCGCTTCACAGAG -3′ at an annealing temperature of 60 °C. BDNF primers were forward: 5' -AGCTGAGCGTGTGTGACAGTATTAG -3'; reverse: 5' -GGGATTACACTTG GTCTCGTAGAAA -3′ at an annealing temperature of 57 °C. Expression levels were normalized to glyceraldehyde-3-phosphate dehydrogenase (GAPDH). GAPDH primers were forward: 5' -AAGAAGGTGGTGAAGCAGGCG -3'; reverse: 5' -AGACAACCTG GTCCTCAGTGTAGC -3'.

2.6. Dot Blot Analysis

The dot blot assay was performed as described previously [12]. Briefly, DNA samples were spotted on a nitrocellulose membrane at room temperature for 15 min. After incubation at 80 °C in an oven for 30 min, the membrane was blocked with 5% milk in phosphate-buffered saline with 0.1% Tween-20 for 1 h and incubated with primary antibodies (anti-5mc antibody, Millipore, USA; anti-5hmc antibody, Active Motif, USA) at 4 °C overnight. The membrane was incubated with horseradish peroxidase-conjugated secondary antibodies (Jackson ImmunoResearch Laboratories, USA) for 1 h on the second day. The membrane was developed captured on autoradiographic films. Densitometry of methylene blue staining was used as a loading control to evaluate the densitometries of 5mc and 5hmc.

2.7. Thermal sensory testing

Withdrawal latencies to a radiant heat stimulus were assessed for each rat using a Model 336G Plantar/Tail Stimulator Analgesia Meter (IITC Life Sciences, USA) [13]. Region specific withdrawal responses consisted of licking the paws and flicking the tail in response to the heat stimulus. Withdrawal latencies were recorded three times for each paw and tail in seconds with a maximum of 20 s cut-off point programmed into the timer to prevent tissue damage. These latencies were then normalized to baseline values and presented as percentages.

2.8. Pharmacokinetic (PK) analysis of collected blood samples

2.8.1. Liquid Chromatography–Mass spectrometry (LC-MS) system and conditions

The LC-MS system was comprised of a Shimadzu HPLC and a LCMS-2020 mass spectrophotometer (Kyoto, Japan). Separation was achieved at ambient temperature (22 ± 1 °C) with a flow rate of 0.4 ml/min using a C18 Waters (5 μm, 250 × 4.6 mm) with UV detection at 220 nm. The mobile phase was prepared by mixing acetonitrile:water (70:30 v/v).

2.8.2. Preparation of standard solutions and blood collection

Working solutions of CBD, THC, and CBC were freshly prepared by diluting analytical standards (Sigma) in methanol to obtain a final concentration of 0.25, 0.5, 1and 5 μg/ml in rat serum.

Blood was collected from the saphenous vein at 1 h pre- and post- oral gavage from day 6 onward. On day 18, the collection time points were at 1h pre-treatment, and 1h, 4h, 8h and 12h post-treatment. Serum was collected by centrifuging the blood at 4000 rpm for 10 min at 4 °C.

2.8.3. Treatment of serum samples for analysis

To a 50 μl aliqoute of rat serum sample, 0.5 ml of cold HPLC grade acetonitrile was added to precipitate plasma proteins, vortexed and centrifuged at 15,000 rpm for 10 min. The supernatant was transferred and evaporated to dryness using Savant SPD1010 SpeedVac Concentrator without heat (Thermo Fisher Scientific, USA). The residue reconstituted with 50 μl of acetonitrile was centrifuged at 15000 rpm for 5 min 10 μl of the supernatant was then injected into the LCMS system.

2.9. Statistical analysis

Statistics was performed using GraphPad Prism Software (San Diego, CA, USA). Statistical analysis was done using Two Way ANOVA, followed by Bonferroni post - hoc test.

3. Results

3.1. Neurological disability score (NDS)

At EAE day 7 neurological deficits began to be displayed in some animals in the form of tail weakness (Fig. 1A). By EAE day 8, all animals started to display clinical signs of neurological disability. Statistical analysis revealed significant decreases in severity of NDS on day 10–13 between EAE cannabinoid (10:10 formulation) treated and EAE untreated groups. In addition, results revealed a 2-day delay in an onset of peak NDS in cannabinoid treated (10:10) EAE animals. Significant decreases were also seen for EAE cannabinoid (1:20 formulation) compared with EAE untreated groups at 10 - 13 dpi. In addition, results revealed a 1-day delay in an onset peak NDS is seen in cannabinoid treated (1:20) EAE animals.

3.2. Behavioral analysis for neuropathic pain (NPP)

3.2.1. Tail results

With respect to the tail, there was statistically significant decrease in tail withdrawal latency at 11 dpi identified in the EAE treated with cannabinoid (10:10) relative to the EAE untreated animals (Fig. 1B). Although the withdrawal latencies in the EAE treated with cannabinoid (1:20) at day 11 to day 13 were markedly lower than that of EAE untreated animals, no significant reductions in withdrawal latency of the tail were noted at any time points between the EAE treated with cannabinoid (1:20) and EAE untreated or NC animals.

3.2.2. Right rear paw results

With respect to the rear right paw, the withdrawal latency for EAE treated with cannabinoid (10:10) was significantly lower at 12 dpi and marked lower at 13 dpi than that of the EAE untreated animals (Fig. 1C). Although there was a marked decrease in withdrawal latency in the EAE treated with cannabinoid (1:20) relative to EAE untreated animals at 13 dpi, overall there were no significant reductions in withdrawal latency of the right hind limb noted at any time points between the EAE treated with cannabinoid (1:20) and EAE untreated or NC animals.

3.2.3. Left rear paw results

With respect to the rear left paw, although the withdrawal latency in the EAE treated with cannabinoid (10:10) was markedly lower than that of EAE untreated animals between 11 and 13 dpi, these reductions in withdrawal latency never reached significance between the EAE treated with cannabinoid (10:10) and EAE untreated or NC animals. Interestingly, at 13 dpi, there was a significant reduction and marked reduction at 14 dpi in withdrawal latency in the EAE treated with cannabinoid (1:20) relative to that depicted in the EAE untreated animals (Fig. 1D).

3.3. TNF-α gene and protein analysis

3.3.1. Cannabinoid 10:10 formulation treatment results

Our results of qRT-PCR analysis of TNF-α mRNA expression in the SC show a significant reduction at 15 dpi between EAE treated with (10:10) cannabinoid formulation versus EAE untreated groups. Additionally, significant elevations in TNF-α mRNA expression were also seen at 15 dpi in EAE untreated animals relative to NC animal (Fig. 2A).

Our results also indicate significant elevations of TNF-α protein expression at 12 dpi between EAE untreated and NCs with corresponding significant reductions in TNF-α noted in EAE treated with (10:10) cannabinoid formulation versus EAE untreated (Fig. 2B). Significant reductions in TNF-α protein were also found at 18 dpi between EAE treated with (10:10) cannabinoid formulation as compared to TNF-α protein identified in the EAE untreated group.

3.3.2. Cannabinoid 1:20 formulation treatment results

Significant reductions in TNF-α mRNA expression were seen at 15 dpi in the EAE treated with (1:20) cannabinoid formulation versus EAE untreated groups (Fig. 2C). Significant reductions in TNF-α protein were also found at 12 and 18 dpi between EAE treated with (1:20) cannabinoid formulation as compared to TNF-α protein identified in the EAE untreated group (Fig. 2D).

3.4. BDNF gene and protein analysis

3.4.1. Cannabinoid 10:10 formulation treatment results

There was a significant increase in the BDNF mRNA expression at 18 dpi in the EAE animals treated with cannabinoid (10:10) relative to that of EAE untreated animals and NC control animals (Fig. 2E).

There was a significant increase in the BDNF protein expression in the EAE untreated and EAE treated with cannabinoid (10:10) as compared to the NC (Fig. 2F) at 12 dpi. This significant increase in BDNF protein expression was maintained at 15 dpi in the EAE treated with cannabinoid (10:10) relative to EAE untreated and relative to NC animals. Furthermore, this significant increase in BDNF protein expression was sustained in the EAE cannabinoid treated (10:10) animals over that of EAE untreated animals at 18 dpi.

3.4.2. Cannabinoid 1:20 formulation treatment results

qRT-PCR results revealed that EAE cannabinoid treated (1:20) had significant elevations of mRNA expression for BDNF at 18 dpi relative to EAE untreated animals and relative to NC animals (Fig. 2G). No significant differences were noted in BDNF protein expression at 12, 15 or 18 dpi between EAE untreated and EAE cannabinoid treated (1:20) (Fig. 2H).

3.5. Dot blot analysis

Dot blot analysis and methylene blue staining was conducted to find the relative levels of 5-methylcytosine (5mc) and 5-hydroxymethylcytosine (5hmc) in the NC, EAE, and EAE treated with cannabinoid (10:10) animals at 12 dpi and 15 dpi to determine if the changes in BDNF gene and protein could be correlated with the respective changes in 5mc and 5hmc. No significant differences were found in 5mc levels between EAE untreated and EAE treated with cannabinoid (10:10) at 12 or 15 dpi relative to each other or to NC's (Fig. 3A and B). However, at 12 and 15 dpi, significant reductions in 5hmc were found in EAE untreated relative to NC animals, while no significant differences in 5hmc levels were

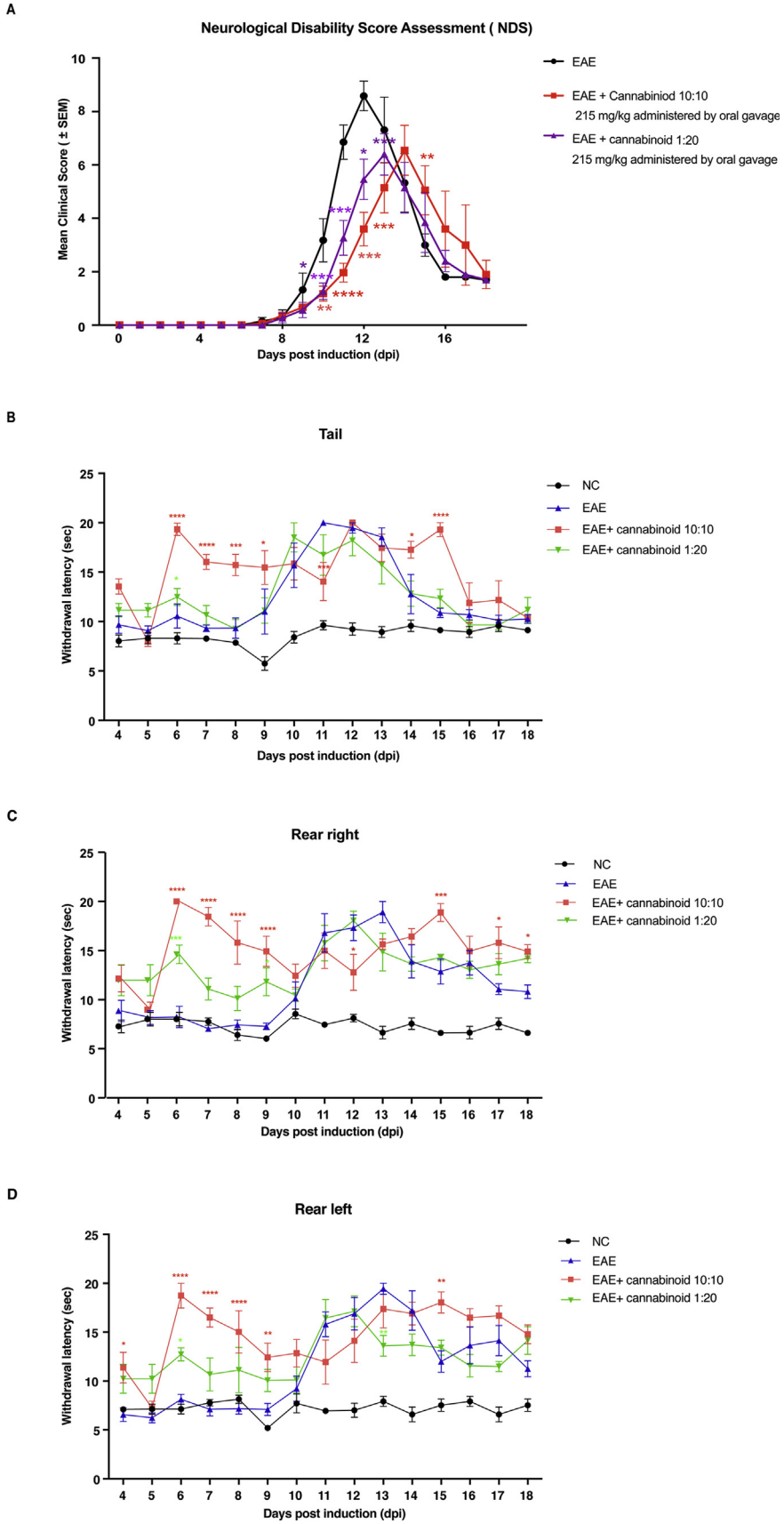


Fig. 1. Cannabinoid improved neurological disability score and showed benefits in behavioral analysis. (A) Neurological disability score assessment. (B-D) Behavioral analysis - thermal testing. Thermal sensitivity of three specific anatomical sites involving that of the tail (B), right (C) and left (D) hind paws were measured. (****$p < 0.0001$, ***$p < 0.001$, **$p < 0.01$, *$p < 0.05$ respectively).

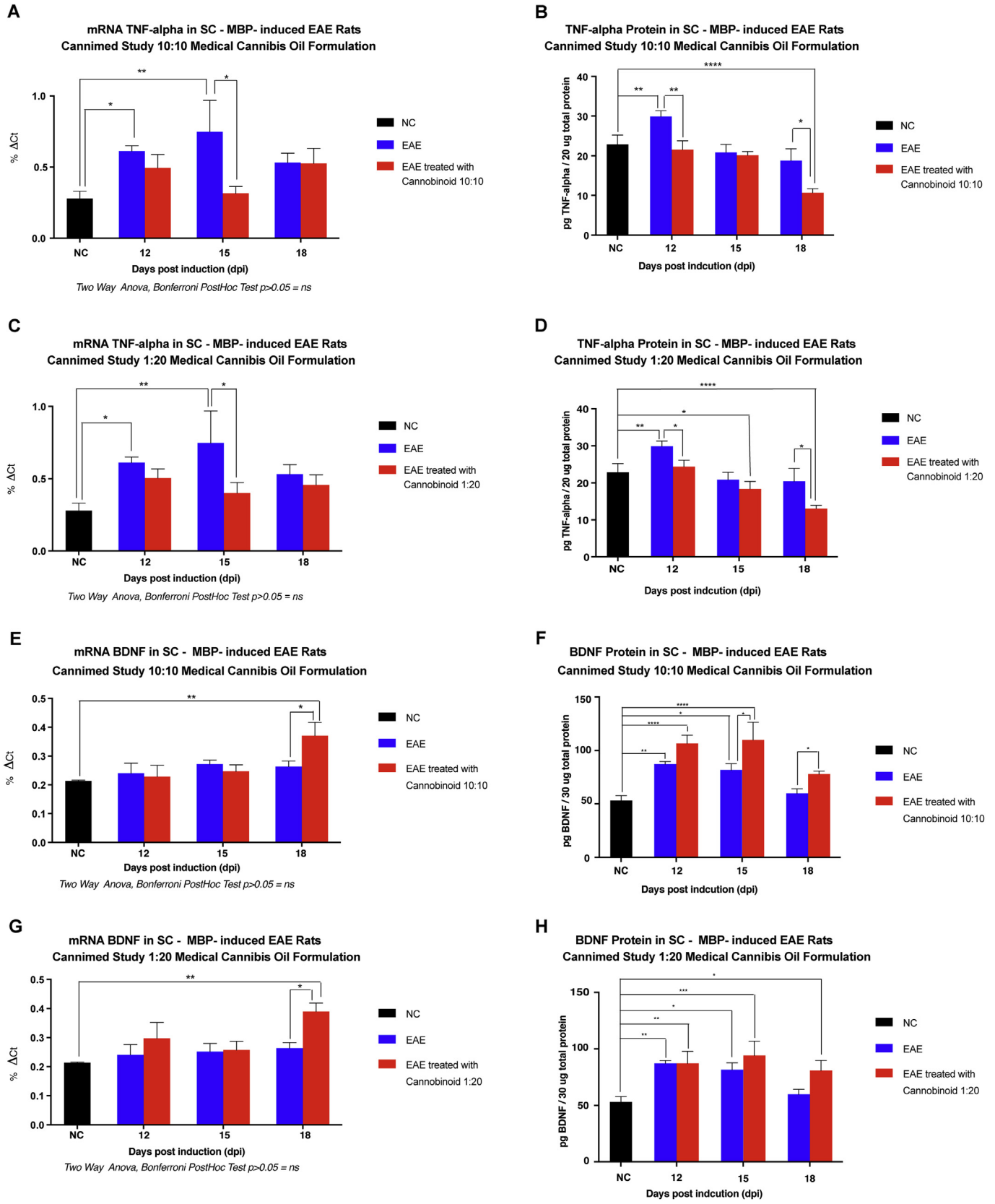


Fig. 2. TNF-α and BDNF gene and protein analysis. Comparative qRT-PCR analysis of TNF-α (A and C) and BDNF (E and G) mRNA expression was conducted between the NC, EAE untreated, and EAE treated with 2 cannabinoid formulations (10:10 and 1:20) at 12, 15, and 18 dpi. Data is presented as the fold difference in relative mRNA expression determined as the ratio of TNF-α (BDNF) mRNA/GAPDH mRNA (%ΔCt)
The protein expressions of TNF-α (B and D) and BDNF (F and H) in the rat SC were analyzed by ELISA at 12, 15, and 18 dpi. Data in B and D are presented in pg TNF-α/20 μg total protein. Data in F and H are presented in pg BDNF/30 μg total protein. (****p < 0.0001, ***p < 0.001, **p < 0.01, *p < 0.05 respectively).

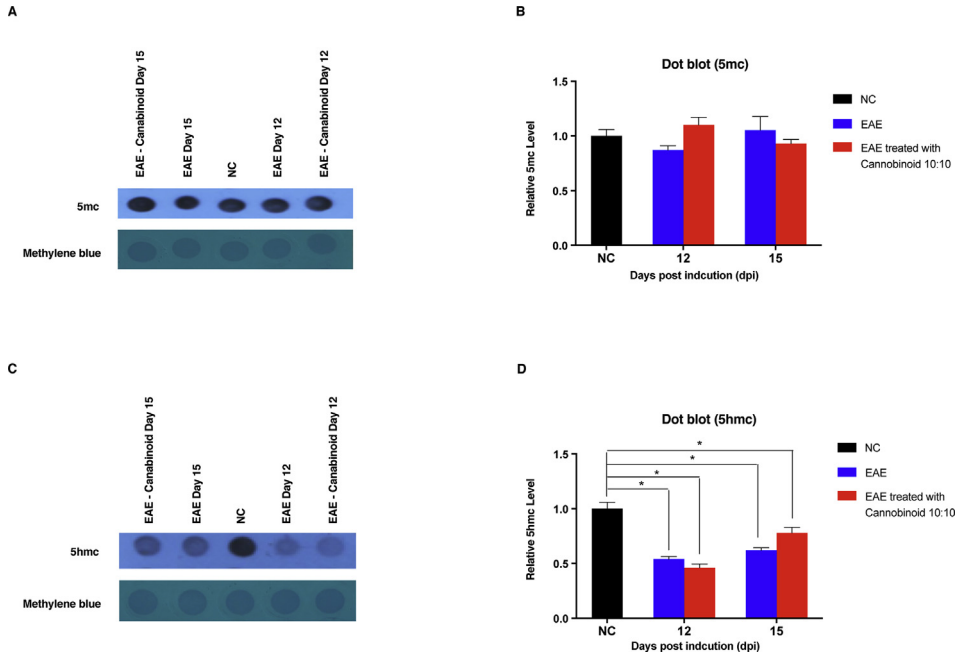


Fig. 3. Dot blot analysis. Dot blot staining and analysis indicate relative 5-mc (A, B) and 5-hmc (C, D) levels in rat SC.

identified between EAE untreated and EAE treated with cannabinoid (10:10) (Fig. 3C and D).

3.6. Serum drug levels

According to the product information for the 1:20 formulation, the amount of total CBD is 21.9 ± 0.6 mg/ml, while total THC is only 1.0 ± 0.1 mg/ml, which means the amount of CBD is 20 times higher than that of THC. Additionally, in the 10:10 formulation, the amount of total CBD was 10.2 ± 0.5 mg/ml, while total THC was 9.9 ± 0.5 mg/ml, which means the amount of CBD was approximately the same as that of THC.

3.6.1. Cannabinoid 10:10 formulation treatment results

Following the treatment administration with the 10:10 cannabinoid oil formulation, results revealed a significant increase in THC concentration in serum on days 7, 8, 9, 13 and 16. In addition, THC serum levels of 4 h post-drug administration following the last day of treatment (day 18) was statistically elevated (Fig. 4A). Marked increases of the CBD concentrations in serum were also seen after treatment (days 7, 8, 9, 13, 16), however, these increases did not reach statistical significance. CBC levels were undetectable at all days assessed in the EAE cannabinoid treated (10:10). In order to obtain a crude elimination rate constant for THC and CBD, we used regression analysis to approximate the elimination phase. Using the time points of 4 and 8 h the Kel for THC was calculated to be 0.776 ± 0.542 hrs^{-1} while the Kel for CBD was 0.181 ± 0.001 hrs^{-1} (n = 2). Half-life for THC was then calculated to be 0.9 h while CBD was 3.8 h.

3.6.2. Cannabinoid 1:20 formulation treatment results

In the 1:20 cannabinoid formulation, results showed significant increases in concentrations of CBD in serum only on days 6, 7, 13, 14, 16 and 18. Results demonstrated consistently higher CBD levels at all time points assessed relative to THC and CBC, level of which were undetectable in serum post-treatment (Fig. 4B). Interestingly, the peak temporal serum levels of CBD were similar in nature to the peak THC time points levels with the 10:10 cannabinoid formulation. Using the 4- and 8-h data points for CBD the calculated Kel was 0.235 ± 0.099 hrs^{-1} (n = 5) with a half-life of 2.9 h.

4. Discussion

Our pre-clinical research findings demonstrate significant improvements in NDS and behavioral assessments of MS induced NPP in EAE animals treated with the orally administered medical grade cannabinoids.

Based on the NDS data, both cannabinoid oral oil formulations (10:10 & 1:20) were able to partially reverse the disease progression after EAE induction as evident by their ability to delay the onset of peak neurological disability and reduce the peak severity. However, the 10:10 cannabinoid formulation appears to have a potential advantage to delay time to peak NDS by 2 days compared to the 1 day for the 1:20 cannabinoid formulation.

Our behavioral analysis assessment results showed that interventional treatment with cannabinoids could help improve (lessen) the withdrawal latency compared to that of EAE untreated animals. Additionally, the 10:10 cannabinoid formulation appears to have a potential advantage over the 1:20 formulation as evident by its ability to have a greater therapeutic impact on more domains of pain assessment. However, during the pre-EAE attack phase (6 - 10 dpi), both cannabinoids treated EAE groups (10:10 & 1:20) have higher withdrawal latency times than that of EAE untreated animals. These initial longer withdrawal latencies occurred due to the psychoactive side effects that are associated with the use of medical cannabinoids [14,15]. This effect particularly observed in the treatment with the 10:10 formulation during this same period was as expected due to its higher content of THC relative to the low THC levels observed in the 1:20 cannabinoid formulation (Fig. 4).

Our results of the TNF-α gene and protein analysis then suggested that cannabinoid interventional treatment reduces the overall liberation of TNF-α protein in SC during an immune system mediated attack that contributes to the delay in onset of peak NDS and to the reduced overall severity of NDS. Several studies have demonstrated the beneficial role of BDNF in re-myelination and myelin repair and its key role in MS induced NPP [10,16,17].

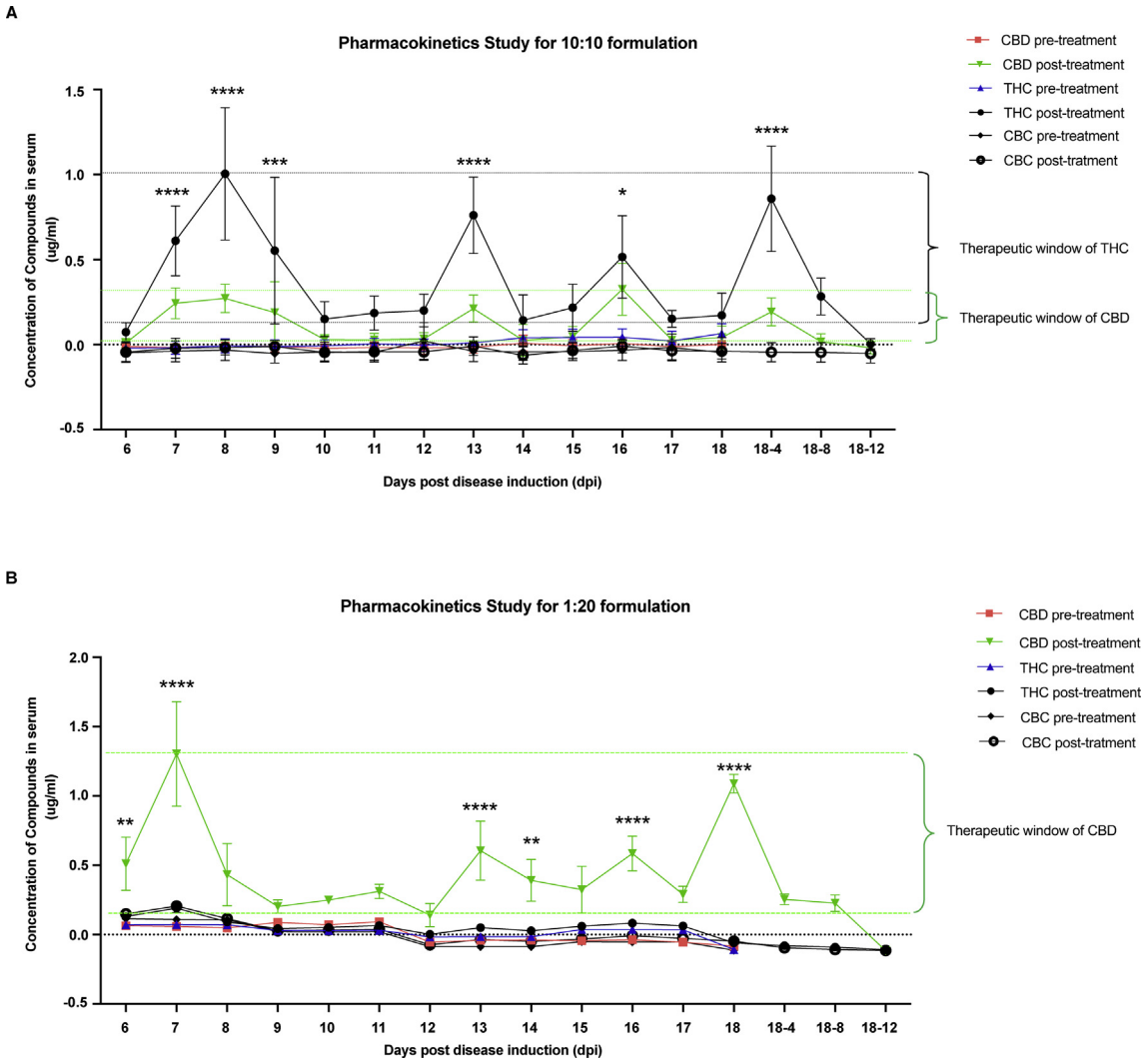


Fig. 4. Serum drug levels. Blood was collected from EAE animals that received interventional treatment with the 10:10 (A) or 1:20 (B) cannabinoid oral oil formulations at 1 h pre- and post-oral gavage from day 6 to day 18.

Henceforth, our current research also examined the temporal changes in BDNF expression at the gene and protein levels in EAE animals treated with cannabinoids. Our findings suggested that once the initial BDNF protein was released (12-15 dpi), the mRNA expression for BDNF was then subsequently activated at 18 dpi to replace the BDNF that was liberated at the time period of the peak EAE immune system mediated attack. As a result, we conclude that treatment of EAE animals with the cannabinoids contributed to the critical and timely release of BDNF protein and enhanced BDNF gene expression that in part facilitated the resultant onset delay and reduced overall severity of the NDS relative to EAE untreated animals.

A recent publication showed an increase in BDNF gene and protein expression that is directly associated with 5hmc abundance in BDNF promoter region [12]. As such, we conducted research to determine the effects of EAE induction and cannabinoid treatment (10:10 formulation) on regulating the 5hmc/5mc ratio. Our findings demonstrate that treatment of EAE animals with the cannabinoid did not alter the levels of 5mc and 5hmc relative to NC or EAE untreated animals (Fig. 3A and B). However, our research did confirm that EAE induction was responsible for the significant reduction of 5hmc at 12 and 15 dpi (Fig. 3C and D). Overall, the changes for 5mc and 5hmc do not account for the relative changes in BDNF gene and protein expression changes reported in the EAE treated with cannabinoid (10:10). As such, further research is warranted to confirm how cannabinoids may increase expression of BDNF to promote myelin repair during an EAE-induced immune system attack.

In our study, a validated HPLC-MS method was applied to investigate the THC, CBD, and CBC concentrations in serum to maximize the therapeutic effect and minimize drug side effect of each new formulation currently on the market for human consumption. Our study showed that 10:10 formulation treatment resulted in a higher concentration of THC in serum, while the concentration of CBD was significantly higher than the other two components (THC and CBC) in the 1:20 formulation treatment group. The results are consistent with the concentration of composing compounds. An interesting pattern for absorption was observed in the present study for the two cannabinoid formulations. Levels of component showed a circadian like pattern peaking at days 7–8, 13, 16 and 18. An explanation for this pattern is not readily apparent and needs to be verified using higher drug levels and longer sampling times.

THC and CBD have been shown to follow a two-compartment

open model with peak concentrations following oral administration ranging from 1 to 5 h in humans [18]. The elimination rates allowed us to calculate drug half-life, showing that THC is eliminated much faster, approximately four times that of CBD. It is recognized to obtain reliable pharmacokinetic parameters for THC, CBD, and CBC using these formulations, higher oral doses and longer sampling times are required. Nevertheless, the present preliminary elimination rates and half-life allow us to design proper kinetic animal studies for subsequent application to human clinical trials.

In summary, the successful application of this pre-clinical research can be extrapolated to human clinical trials in patients with MS and associated NPP thereby representing significant promise in improving patient's quality of life and reducing costs to the health care system.

Conflicts of interests

The authors declare no competing interests.

Acknowledgements

The authors gratefully acknowledge the research funding supplied by Prairie Plant Systems Inc. The authors also acknowledge support from Manitoba Multiple Sclerosis Research Network Organization (MMSRNO) for their indirect support provided to this pre-clinical research.

Transparency document

Transparency document related to this article can be found online at https://doi.org/10.1016/j.bbrc.2019.06.033.

References

[1] T. Zeis, U. Graumann, R. Reynolds, N. Schaeren-Wiemers, Normal-appearing white matter in multiple sclerosis is in a subtle balance between inflammation and neuroprotection, Brain : J. Neurol. 131 (2008) 288–303, https://doi.org/10.1093/brain/awm291.

[2] H. Lassmann, R.M. Ransohoff, The CD4-Th1 model for multiple sclerosis: a critical [correction of crucial] re-appraisal, Trends Immunol. 25 (2004) 132–137, https://doi.org/10.1016/j.it.2004.01.007.

[3] I. Gilron, J.M. Bailey, D. Tu, R.R. Holden, A.C. Jackson, R.L. Houlden, Nortriptyline and gabapentin, alone and in combination for neuropathic pain: a double-blind, randomised controlled crossover trial, Lancet 374 (2009) 1252–1261, https://doi.org/10.1016/S0140-6736(09)61081-3.

[4] A. Feliu, M. Moreno-Martet, M. Mecha, F.J. Carrillo-Salinas, E. de Lago, J. Fernandez-Ruiz, C. Guaza, A Sativex((R)) -like combination of phytocannabinoids as a disease-modifying therapy in a viral model of multiple sclerosis, Br. J. Pharmacol. 172 (2015) 3579–3595, https://doi.org/10.1111/bph.13159.

[5] S.M. Opal, V.A. DePalo, Anti-inflammatory cytokines, Chest 117 (2000) 1162–1172.

[6] X. Yang, V.L. Hegde, R. Rao, J. Zhang, P.S. Nagarkatti, M. Nagarkatti, Histone modifications are associated with Delta9-tetrahydrocannabinol-mediated alterations in antigen-specific T cell responses, J. Biol. Chem. 289 (2014) 18707–18718, https://doi.org/10.1074/jbc.M113.545210.

[7] G.A. Cabral, T.J. Rogers, A.H. Lichtman, Turning over a new leaf: cannabinoid and endocannabinoid modulation of immune function, J. Neuroimmune Pharmacol. : Off. J. Soc. Neuroimmune Pharmacol. 10 (2015) 193–203, https://doi.org/10.1007/s11481-015-9615-z.

[8] N. Shinjyo, V. Di Marzo, The effect of cannabichromene on adult neural stem/progenitor cells, Neurochem. Int. 63 (2013) 432–437, https://doi.org/10.1016/j.neuint.2013.08.002.

[9] S. Sirikantaramas, F. Taura, S. Morimoto, Y. Shoyama, Recent advances in Cannabis sativa research: biosynthetic studies and its potential in biotechnology, Curr. Pharmaceut. Biotechnol. 8 (2007) 237–243.

[10] W. Zhu, E.E. Frost, F. Begum, P. Vora, K. Au, Y. Gong, B. MacNeil, P. Pillai, M. Namaka, The role of dorsal root ganglia activation and brain-derived neurotrophic factor in multiple sclerosis, J. Cell Mol. Med. 16 (2012) 1856–1865, https://doi.org/10.1111/j.1582-4934.2011.01481.x.

[11] T. Khorshid Ahmad, T. Zhou, K. AlTaweel, C. Cortes, R. Lillico, T.M. Lakowski, K. Gozda, M.P. Namaka, Experimental autoimmune encephalomyelitis (EAE)-Induced elevated expression of the E1 isoform of methyl CpG binding protein 2 (MeCP2E1): implications in multiple sclerosis (MS)-Induced neurological disability and associated myelin damage, Int. J. Mol. Sci. 18 (2017), https://doi.org/10.3390/ijms18061254.

[12] Z. Miao, Y. He, N. Xin, M. Sun, L. Chen, L. Lin, J. Li, J. Kong, P. Jin, X. Xu, Altering 5-hydroxymethylcytosine modification impacts ischemic brain injury, Hum. Mol. Genet. 24 (2015) 5855–5866, https://doi.org/10.1093/hmg/ddv307.

[13] F. Begum, W. Zhu, C. Cortes, B. MacNeil, M. Namaka, Elevation of tumor necrosis factor alpha in dorsal root ganglia and spinal cord is associated with neuroimmune modulation of pain in an animal model of multiple sclerosis, J. Neuroimmune Pharmacol. 8 (2013) 677–690, https://doi.org/10.1007/s11481-013-9449-5.

[14] S. Narang, D. Gibson, A.D. Wasan, E.L. Ross, E. Michna, S.S. Nedeljkovic, R.N. Jamison, Efficacy of dronabinol as an adjuvant treatment for chronic pain patients on opioid therapy, J. Pain : Off. J. Am. Pain Soc. 9 (2008) 254–264, https://doi.org/10.1016/j.jpain.2007.10.018.

[15] E.A. Voth, R.H. Schwartz, Medicinal applications of delta-9-tetrahydrocannabinol and marijuana, Ann. Intern. Med. 126 (1997) 791–798.

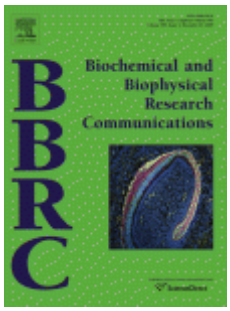
[16] T. KhorshidAhmad, C. Acosta, C. Cortes, T.M. Lakowski, S. Gangadaran, M. Namaka, Transcriptional regulation of brain-derived neurotrophic factor (BDNF) by methyl CpG binding protein 2 (MeCP2): a novel mechanism for Remyelination and/or myelin repair involved in the treatment of multiple sclerosis (MS), Mol. Neurobiol. 53 (2016) 1092–1107, https://doi.org/10.1007/s12035-014-9074-1.

[17] C.M. Acosta, C. Cortes, H. MacPhee, M.P. Namaka, Exploring the role of nerve growth factor in multiple sclerosis: implications in myelin repair, CNS Neurol. Disord. - Drug Targets 12 (2013) 1242–1256.

[18] M.A. Huestis, Human cannabinoid pharmacokinetics, Chem. Biodivers. 4 (2007) 1770–1804, https://doi.org/10.1002/cbdv.200790152.

Copyright Clearance Center RightsLink®

Home Account Info Help



Title: Therapeutic impact of orally administered cannabinoid oil extracts in an experimental autoimmune encephalomyelitis animal model of multiple sclerosis

Author: Ting Zhou,Tina Khorshid Ahmad,Samaa Alrushaid,Marianna Pozdirca,Karen Ethans,Howard Intrater,Tyson Le,Frank Burczynski,Jiming Kong,Michael Namaka

Publication: Biochemical and Biophysical Research Communications

Publisher: Elsevier

Date: 20 August 2019

© 2019 Elsevier Inc. All rights reserved.

Logged in as:
Ting Zhou
LOGOUT

Please note that, as the author of this Elsevier article, you retain the right to include it in a thesis or dissertation, provided it is not published commercially. Permission is not required, but please ensure that you reference the journal as the original source. For more information on this and on your other retained rights, please visit: https://www.elsevier.com/about/our-business/policies/copyright#Author-rights

BACK CLOSE WINDOW

Copyright © 2019 Copyright Clearance Center, Inc. All Rights Reserved. Privacy statement. Terms and Conditions.
Comments? We would like to hear from you. E-mail us at customercare@copyright.com

Journal of proteome research

Article

pubs.acs.org/jpr

Increased Post-Translational Lysine Acetylation of Myelin Basic Protein Is Associated with Peak Neurological Disability in a Mouse Experimental Autoimmune Encephalomyelitis Model of Multiple Sclerosis

Ryan Lillico,[†,#] Ting Zhou,[‡,§,#] Tina Khorshid Ahmad,[‡,#] Nicholas Stesco,[†] Kiana Gozda,[‡] Jessica Truong,[‡] Jiming Kong,[§] Ted M. Lakowski,[*,†] and Michael Namaka[*,‡,§,∥,⊥]

[†]The Rady Faculty of Health Sciences, College of Pharmacy, Pharmaceutical Analysis Laboratory, University of Manitoba, Winnipeg, Manitoba R3T 2N2, Canada

[‡]The Rady Faculty of Health Sciences, College of Pharmacy, University of Manitoba, Winnipeg, Manitoba R3T 2N2, Canada

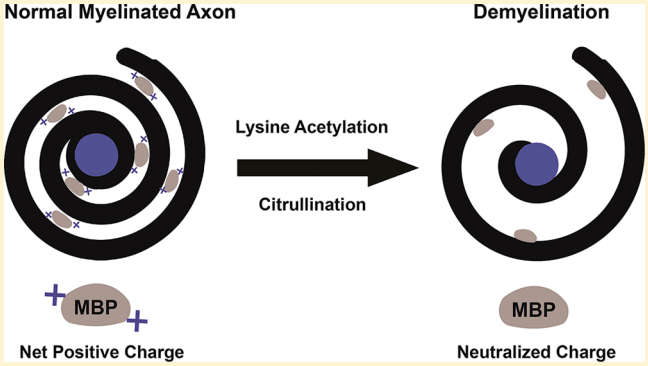
[§]Department of Human Anatomy and Cell Science, College of Medicine, University of Manitoba, Winnipeg, Manitoba R3T 2N2, Canada

[∥]Joint Laboratory of Biological Psychiatry Between Shantou University Medical College and College of Medicine, University of Manitoba, Winnipeg, Manitoba R3T 2N2, Canada

[⊥]Department of Rehabilitation Medicine, Health Sciences Centre (HSC), Winnipeg, Manitoba R3A 1R9, Canada

Supporting Information

ABSTRACT: Citrullination of arginine residues is a post-translational modification (PTM) found on myelin basic protein (MBP), which neutralizes MBPs positive charge, and is implicated in myelin damage and multiple sclerosis (MS). Here we identify lysine acetylation as another neutralizing PTM to MBP that may be involved in myelin damage. We quantify changes in lysine and arginine PTMs on MBP derived from mice induced with an experimental autoimmune encephalomyelitis (EAE) model of MS using liquid chromatography tandem mass spectrometry. The changes in PTMs are correlated to changes in neurological disability scoring (NDS), as a marker of myelin damage. We found that lysine acetylation increased by 2-fold on MBP during peak NDS post-EAE induction. We also found that mono- and dimethyl-lysine, as well as asymmetric dimethyl-arginine residues on MBP were elevated at peak EAE disability. These findings suggest that the acetylation and methylation of lysine on MBP are PTMs associated with the neurological disability produced by EAE. Since histone deacetylase (HDAC) inhibitors have been previously shown to improve neurological disability, we also show that treatment with trichostatin A (a HDAC inhibitor) improves the NDS of EAE mice but does not change MBP acetylation.



KEYWORDS: *myelin basic protein, experimental autoimmune encephalomyelitis, lysine acetylation, post-translational modifications, liquid chromatography−tandem mass spectrometry, multiple sclerosis*

INTRODUCTION

Multiple sclerosis (MS) is a chronic and progressive neurological disease characterized by immune-mediated destruction of central nervous system myelin and axonal degeneration.[1,2] In the early stages of MS, inflammation is prominent, and later there is neurodegeneration.[3] Immunogenic myelin damage disrupts the conduction of electrical impulses, and failure to repair these demyelinated lesions increases axonal loss, resulting in permanent MS symptoms.[4] At present, the molecular mechanisms underlying immune system-mediated myelin damage are not completely understood.[5−9]

Myelin basic protein (MBP) is a basic, positively charged protein that holds together the layers of myelin that surround nerve axons through an electrostatic interaction between the negatively charged myelin lipids and the positively charged amino acids (lysine and arginine) of MBP. Evidence suggests that myelin damage is, in part associated with post-translational modifications (PTMs) to these positively charged amino acids on MBP thereby reducing the net positive charge, leading to unwrapping of the myelin sheath and exposure of the axon.

Received: May 2, 2017
Published: November 7, 2017

Downloaded via UNIV OF MANITOBA on July 22, 2019 at 20:18:27 (UTC).
See https://pubs.acs.org/sharingguidelines for options on how to legitimately share published articles.

© 2017 American Chemical Society

DOI: 10.1021/acs.jproteome.7b00270
J. Proteome Res. 2018, 17, 55−62

Studies have identified arginine citrullination as the major contributing PTM of MBP that accounts for this neutralization.[10,11] Citrullination is now implicated in the molecular pathogenesis of MS-induced myelin damage[12,13] and the enzyme catalyzing this mark, peptidylarginine deiminase, has become a target for therapeutic intervention.[14,15] With citrullination, the normally charged guanidine group of arginine is converted into a neutral urea. This neutralization weakens the interaction between MBP and myelin lipids, leading to demyelination.

MBP is considered an intrinsically disordered protein because of its high net-positive charge, low mean hydrophobicity[16] and the large number or PTMs that result in eight distinct charge variants known as C1 through C8. The charge variant C1 is the major form in healthy humans having the lowest number of PTMs, and therefore the highest net charge of +19 at physiological pH.[17] The remaining charge variants arise from each successive PTM that neutralizes a +1 charge. The incremental reduction of net positive charge from C1 to C8 reduces the adhesiveness of MBP.[18] Studies have identified that neutralizing MBP by the citrullination of arginine residues leads to demyelination and neuropathic pain.[19−21] In addition, mono- and dimethyl-arginine residues have also been found on MBP in the brains of MS patients and in EAE mice models, suggesting that arginine methylation is also related to demyelination[22] and disruption of myelin compaction[23,24] even though it does not reduce the net charge of MBP.

Mouse MBP consists of at least 13 different isoforms ranging from 7−27 kDa in mass, with the full length (canonical) isoform having a negative grand average of hydropathy value (GRAVY) of −1.198 and a theoretical pI of 9.58[25] due to the large number of lysine and arginine residues resulting in a net positive charge at physiological pH. The canonical isoform of mouse MBP is composed of 23 arginine residues as well as 16 lysine residues that have the potential to be modified and we suspect that any neutralizing PTM to these residues may contribute to reducing the positive charge state of MBP. Here we hypothesize that the acetylation and methylation of lysine residues are also involved in demyelination and worsening of the neurological disability in MS. To determine this, we used a myelin oligodendrocyte glycoprotein (MOG)-induced EAE mouse model of MS and measured changes in lysine and arginine PTMs to MBP in spinal cord (SC) tissue using a previously validated liquid chromatography tandem mass spectrometry (LC−MS/MS) assay.[26] We correlated the changes in PTMs of MBP to clinical neurological disability scores (NDS) as a marker for the degree of myelin damage.

MATERIALS AND METHODS

Induction of EAE

We used the well-characterized MOG model of EAE.[2,27,28] Ten week old c57Bl/6 mice were randomly assigned to one of the following groups: Naïve control (NC), MOG-induced EAE (EAE), MOG-induced EAE treated with dimethyl sulfoxide (EAE+DMSO), or MOG-induced EAE treated with TSA (EAE +TSA). A total of $n = 4$ mice per group were used for each time point (every 3 days to day 45). As per our standard in house protocols,[7,9,29−31] EAE mice were immunized subcutaneously (SQ) with 200 μg MOGp35−55 in 200 μL of Complete Freund's adjuvant (CFA) in the lower/upper back at day 0 (induction kits from Hooke Laboratories (USA) Cat, EK-2110). Animals received two intraperitoneal (IP) injections of pertussis toxin (List Biological Laboratories; #179B) (0.2 μg in 100 μL of PBS at days 0 and 1) to open up the blood brain barrier and facilitate the entry of pathogenic T cells to the CNS. The CFA emulsion contains killed *Mycobacterium tuberculosis* (MT) H37Ra in Freund's adjuvant (FA) to enhance the immune system response to sensitization. The emulsion was administered SQ at two sites in the upper and lower back area. A 0.1 mL SQ dose of the emulsion was injected at each site (0.2 mL/mouse) at day 0. The mice treated with TSA received an IP injection of 7.5 mg/kg/dose/day TSA (EnzoLife Science, Cat. BML-GR309) (formulated as 10% DMSO in PBS)[32] once every other day starting at 4 days post-EAE disease induction (dpi). Female mice were specifically chosen because females are more predisposed to MS than males.[33]

Neurological Disability Scoring

Neurological disability scores (NDS) were conducted in accordance to our recently published criteria.[31] EAE groups were assessed daily for neurological disability until sacrificed. NDS were determined from mean clinical scores measured from a score of 0 (no disability) to 15 (maximal disability).[30] The total score is the sum of the following individual scores obtained for each of the 6 specified clinical domains: tail: 0 = normal, 1 = weakness or partial paralysis, 2 = limp or complete paralysis; right and left hind limbs: 0 = normal, 1 = weakness, 2 = dragging or partial paralysis, 3 = complete paralysis; right and left forelimbs: 0 = normal, 1 = weakness, 2 = unable to support weight or partial paralysis, 3 = complete paralysis; bladder: 0 = normal, 1 = incontinent. The disease course was divided into acute (9−18 dpi) and chronic (18−45 dpi) phases. In order to ensure consistency in regard to the degree of the MOG-induced EAE, only animals that progressed to the NDS of 4 or greater were included in the study. All other EAE-induced animals that did not meet the criteria were excluded from the data analysis.

Tissue Extraction

Mice were sacrificed at four different time points (15, 20, 30, and 42 days) post- EAE induction (dpi) and spinal cord (SC) tissue was collected. All animal experiments in this study were conducted according to protocols approved by the University of Manitoba Animal Protocol Management and Review Committee and in full compliance with the Canadian Council on Animal Care. (Protocol Reference Number: 11−067/1/2/3 (AC 10636).

Total Basic Protein Extraction

Fresh tissue was weighed and homogenized using a Dounce homogenizer. Proteins were extracted using the EpiQuik Total Histone Extraction Kit (EpiGentek, Cat. OP-0006) and precipitated with 4% perchloric acid. The kit was designed to isolate core histones (~15−11 kDa) that are small, positively charged and highly basic, much like MBP. Traditional techniques to isolate MBP from whole tissue use chloroform[34] or HCl extraction[35] and similarly, we found that using the histone extraction kit on mouse SC and brain tissue resulted bands between 10 and 25 kDa, which we identified as isoforms of mouse MBP by Western blot (see below).

Post-Translational Modifications (PTMs)

10 μg samples of protein extracts were digested by either exhaustive enzymatic proteolysis using 1:1 (w/w) Pronase (Sigma-Aldrich) or vapor phase acid hydrolysis to their constituent amino acids, according to previously validated techniques.[26] Briefly, the hydrolysates were dried, resuspended

DOI: 10.1021/acs.jproteome.7b00270
J. Proteome Res. 2018, 17, 55−62

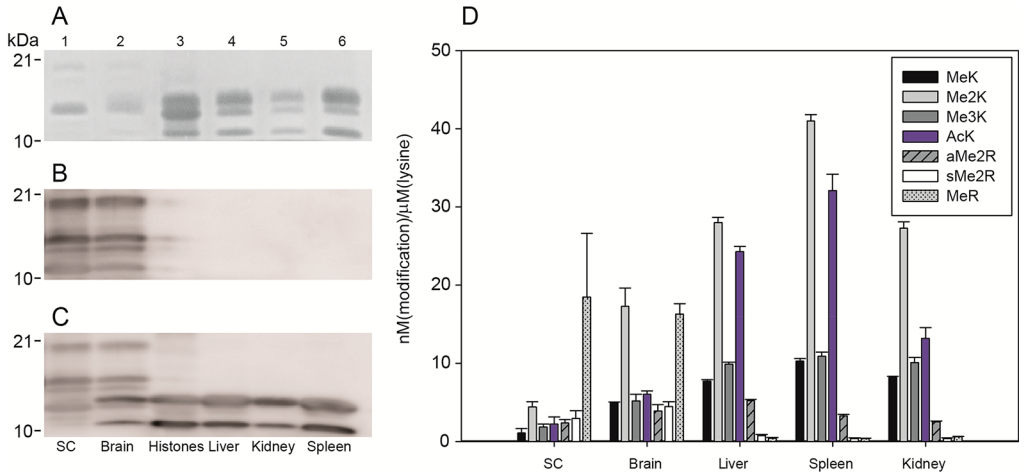


Figure 1. Validation and concentrations of PTMs of MBP and histones from mouse tissues. Tissues from mouse spinal cord (SC), brain, liver, kidney and spleen were extracted using the EpiQuik kit and analyzed for protein content by SDS-PAGE and compared to calf thymus histones (labeled Histones) (A) showing protein fractions from brain and SC were not histones. The same samples were analyzed for MBP by Western blot showing that those isolates from SC and brain were MBP and no immunoreactivity in the histone lanes[3−6] (B). These samples were analyzed for acetyl-lysine by Western blot, confirming the presence of acetyl-lysine on MBP as well as histones (C). The samples were analyzed for other lysine and arginine modifications using the LC−MS/MS assay (D). The unique profile of PTMs on MBP from SC and brain differs from those profiles from histone isolates showing a trend of increased monomethyl-arginine and symmetric dimethyl-arginine.

in mobile phase and injected into a Nexera Ultra High Performance Liquid Chromatograph (UHPLC). The amino acids were separated using a Primesep200 column and analyzed by tandem mass spectrometry using the Shimadzu 8040 mass spectrometer. PTMs from SC, brain, liver, spleen and kidney were quantified from the protein hydrolysates using analytical grade (>98% purity) synthetic standards of N^{ϵ}-monomethyl-L-lysine (MeK) and N^{ϵ}-dimethyl-L-lysine (Me2K) (Santa Cruz Biotechnology), N^{ϵ}-trimethyl-L-lysine (Me3K) (Chem-Impex International), N^{ϵ}-acetyl-L-lysine (AcK), N^{G}-monomethyl-L-arginine (MeR), N^{G},N^{G}(asymmetric)-dimethyl-L-arginine (aMe2R) and N^{G},N^{G}'(symmetric)-dimethyl-L-arginine (sMe2R) (Sigma-Aldrich). The concentrations of modifications (nM) were normalized to the concentration of lysine (μM) as an internal standard for total protein measured. The relative amounts of PTMs derived from the SC of EAE mice were compared to those isolated from the SC of NC mice with nonparametric Mann−Whitney test. Threshold significance was determined at a minimum of $p < 0.05$. Statistical Analyses were performed with Graph Pad software.

Western Blot Analysis

Western blot (WB) analysis was conducted for MBP on the proteins isolated from tissues using the EpiQuik kit. Protein concentrations were determined for each sample using Bicinchoninic Acid (BCA) protein assay kit (Novagen, CN: 71285−3). For each sample, 20 μg total protein was separated by 12% Tris-Glycine gradient SDS-PAGE (Thermoscientific, CN: 0025269) at 120 V for 1 h and electrophoretically blotted onto a PVDF membrane (Immobilon, CN: IPFL00010) for 1 h at 0.35A. The membranes were blocked with skim milk in TBS-T and then treated with primary antibodies including: Anti-MBP polyclonal antigoat IgG (Cat # sc-13914 Santa Cruz) 1/500, or Antiacetylated-lysine (Ac−K-100) Multi-Mab rabbit mAb mix (Cat # 9814 Cell Signaling) 1/1000. After incubation with primary antibodies, membranes were washed with TBS-T and incubated with secondary antibodies. The secondary antibodies used were mouse antigoat IgG-HRP (1:5000, Santa Cruz Biotechnology, sc-2354) against the anti-MBP antibody and mouse antirabbit IgG-HRP (1:5000, Santa Cruz, sc-2357) against the antiacetylated-lysine antibody. The antigen−antibody complexes were detected using ECL detection reagent (Pierce, CN: PI32209). Membranes were exposed to chemiluminescence. Western blot detection was performed using a ChemiDoc MP imaging system (Bio-Rad # 17001402).

RESULTS

Neurological Disability Scoring (NDS)

All animals in the EAE group underwent NDS. All animals in the NC experimental groups displayed a normal NDS of zero and did not show any sign of clinical disability. On the basis of our analysis, we observed acute clinical disabilities that became apparent between 9−18 dpi and were sustained up to 42 dpi. These observations of disease progression were consistent with other researchers that have used the same MOG model of EAE.[2] The onset of EAE occurred by 10 dpi and most mice began to show initial signs of clinical disability (tail weakness or paralysis).[36] By day 12 to 13 post-EAE induction, all animals experienced a full range of clinical neurological deficits such as tail and forelimb weakness, loss of bladder control, and hind-limb paralysis. These symptoms plateaued at day 15. As the disease characteristically progressed, the mice entered into a slight remission and regained motor function by day 18 postinduction. This was followed by a relapse of neurological disability at 28−30 dpi. Finally, we observed another remission phase from days 39−45 post-EAE induction (Supplemental Figure S1).

Validation of MBP Isolates Using the EpiQuik Kit

Tissues samples from control mice taken from the SC, brain, liver, spleen, and kidney were homogenized and extracted using the EpiQuik kit. The kit is designed to isolate histones, but we found that it will work for other small, basic proteins like MBP. The SC and brain contained undetectable amounts of histones compared to liver, spleen and kidney by Coomassie staining (Figure 1A). Moreover, there were no bands in common with

DOI: 10.1021/acs.jproteome.7b00270
J. Proteome Res. 2018, 17, 55−62

the control calf thymus histones (lane 3) but the liver, spleen and kidney all contained bands consistent with histones. It is important to note that histone are conserved throughout all vertebrates having the same amino acid sequence so bovine and murine histones would be expected to have the same molecular weight, while this in not the case for MBP. MBP was determined to be the major protein in the SC and brain by Western blot and no bands were detected in the lanes containing histones (Figure 1B). It is important to note that according to the manufactures product insert that when blotted with the anti-MBP antibody, mouse MBP appears as at least 3 distinct bands as we observed. It is not surprising that MBP is isolated from brain and SC due to its relative abundance in myelin and high isoelectric point. The theoretical pI of mouse MBP is ~9.6, which is similar to the calculated pI of rat MBP (10.8)[37] and histones (ranging from 9.4 to 10.8).[38] In an attempt to confirm that MBP contains the lysine acetylation PTM we performed a Western blot with a general antiacetyl-lysine antibody. As expected lysine acetylation was detected in all lanes containing histones (lanes 3 to 6). We also noted that the major bands for SC MBP all show lysine acetylation and that there are no bands in common between the lanes containing histones (lanes 3 to 6) and SC (lane 1) confirming that SC MBP is not significantly contaminated with histones.

To further validate the isolates from the EpiQuik kit, we analyzed the PTM profiles from proteins extracted from different tissues. We observed a distinct difference in PTM profile between histones isolated from liver, spleen, and kidney compared to MBP obtained from SC and brain. In particular, we found elevated levels of monomethyl-arginine and equal proportions of symmetric dimethyl-arginine and asymmetric dimethyl-arginine on MBP isolated from mouse brain and SC. This result is important because it is the first to identify aMe2R on mouse MBP.[39] We also found the presence of lysine PTMs in brain and SC including acetylation, which we confirmed by Western blot (Figure 1C). The PTM profile found from liver spleen and kidney tissues showed more acetyl- and dimethyl-lysine and less monomethyl- and symmetric dimethyl-arginine compared to MBP (Figure 1D). Furthermore, we compared the PTM profile between bovine MBP (Sigma-Aldrich) to bovine histones (Sigma-Aldrich) and found a similar trend of elevated monomethyl-arginine and symmetric dimethyl-arginine on MBP and elevated acetyl-lysine and dimethyl-lysine on histones (Supplemental Figure S2).

EAE-Induced Changes in PTMs of MBP

MBP was isolated from mouse SC at different stages of neurological disability: 15, 20, 30, 42 dpi of EAE. Changes in MBP lysine (Figure 2A) and arginine (Figure 2B) PTMs were measured with respect to the progression of EAE induced NDS. At peak disability (15 dpi of EAE), lysine acetylation and lysine mono- and dimethylation increased by 2-fold compared to control mice (NC) and asymmetric dimethyl-arginine increased by 30%. This was the maximum increase in lysine acetylation observed and was correlated to peak disability. As the mice progressed through each stage of NDS, all types of PTMs gradually returned to baseline. However, at the later stages of NDS when remission was apparent at 42 dpi, MBP lysine appears to be hypo-acetylated by 60% and symmetric dimethyl-arginine and monomethyl-arginine appear to decrease compared to control. Trimethyl-lysine was the only PTM measured that was consistently elevated (30−50%) throughout all time points.

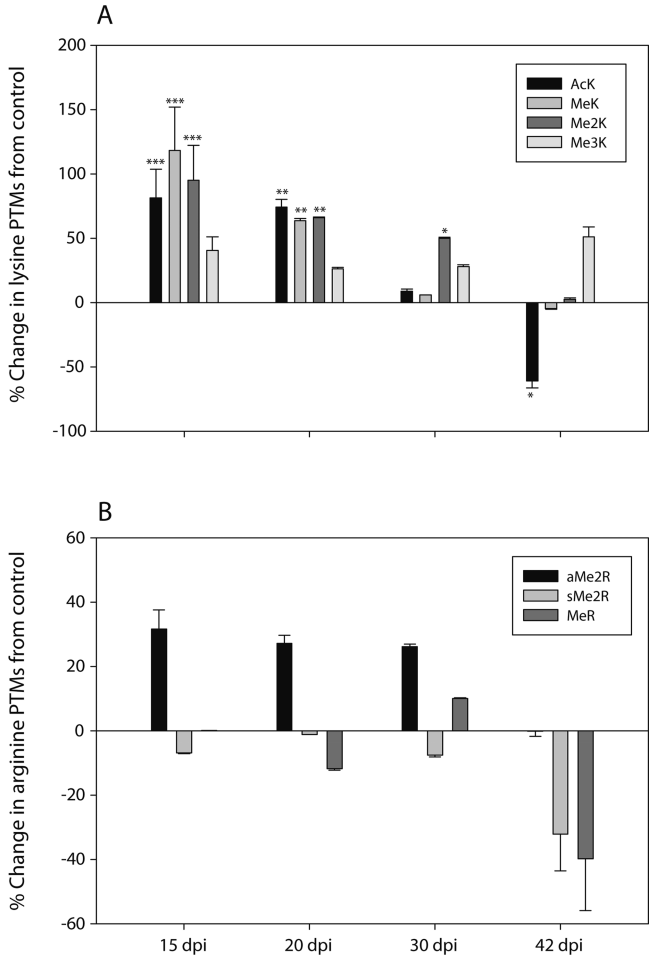


Figure 2. EAE-induced PTM changes of MBP relative to naïve control. The PTM changes in MBP lysines (A) and arginines (B) are significant (*$p < 0.05$, **$p < 0.01$, ***$p < 0.001$) and correspond to severity of NDS and progress of disability/remission. Peak increases of acetylated lysine, methylated lysine, and methylated arginine are observed at peak NDS at 15 dpi. Lysine PTMs gradually decrease to baseline until 42 dpi. Trimethyl-lysine and asymmetric dimethyl-arginine are consistently elevated between 15 and 30 dpi. At 42 dpi, a selective decrease is seen with acetyl-lysine (A) as well as with asymmetric dimethyl-arginine and monomethyl-arginine (B).

Effect of TSA Treatment on Neurological Disability Scoring and MBP Lysine Modifications

Results of mean NDS of EAE mice reflect a statistically significant reduction in clinical scores for mice treated with TSA (Figure 3). The mean NDS peak at 15 dpi was significantly reduced (***$p < 0.001$) in TSA treated mice compared to EAE mice. No significant differences were noted between EAE and EAE + DMSO treated animals at any time point (*$p > 0.05$) by Two Way ANOVA, following Bonferroni posthoc test.

Although treatments with TSA were able to reduce the effects of EAE induced NDS, it did not significantly reduce EAE induced changes in MBP lysine acetylation (Figure 4A). TSA did, however, significantly reduce EAE-induced increases in dimethyl-lysine at 30 and 42 dpi, finally resulting in hypo-methylation (Figure 4B). No other changes in MBP PTMs were measured to be significantly different from vehicle control at any time during TSA treatment.

DOI: 10.1021/acs.jproteome.7b00270
J. Proteome Res. 2018, 17, 55−62

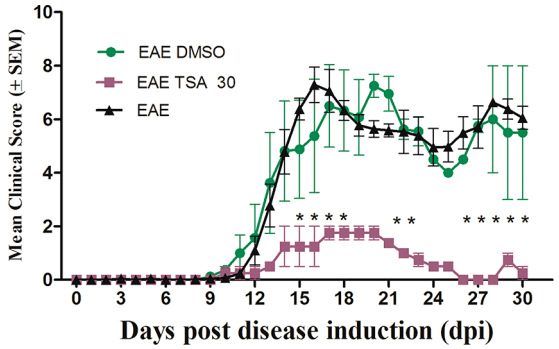


Figure 3. Effect of TSA interventional treatment on clinical course of neurological disability in MOG-induced EAE mice. In vivo treatment of mice with TSA (7.5 mg/kg/day i.p.) 4−30 dpi resulted in a significant improvement in EAE-induced NDS. Our results indicate that MOG-induced EAE mice exhibit clinical signs of the disease activity at ∼11 days after the initial immunization that peaked at ∼day 16 and at day 27. We also observed a slight remission at day 21. Mean clinical NDS at 16 dpi reflect statistically significant (***$p < 0.001$) reductions for the TSA treated EAE mice compared to EAE control groups not treated with TSA (EAE and EAE + DMSO).

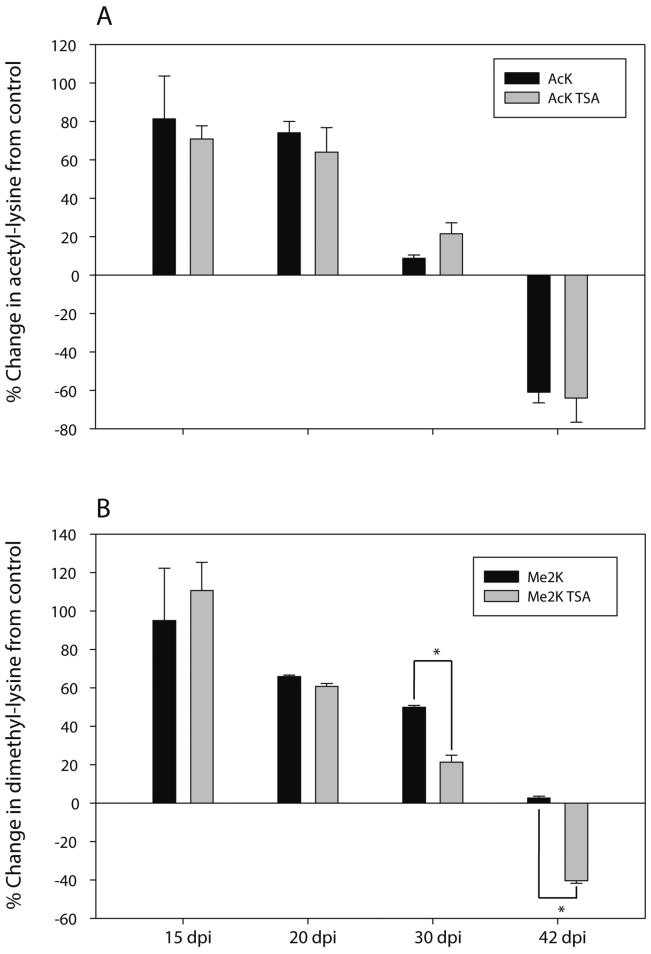


Figure 4. Effect of TSA treatment on MBP acetyl-lysine and dimethyl-lysine from SC of EAE induced mice. No significant differences in acetyl-lysine were observed in the TSA treated group with respect to the vehicle treated EAE mice (A). At 30 dpi and 42 dpi there was a significant reduction in dimethyl-lysine (*$p < 0.05$) in the TSA treated mice using nonparametric t test (B).

DISCUSSION

At present, the understanding of the exact pathophysiological molecular mechanism underlying MS-induced myelin damage is incomplete. Many researchers have identified that immune system-induced changes in PTMs of myelin proteins, specifically MBP, including arginine methylation, citrullination, and N-terminal acetylation of MBP are implicated in myelin damage[14,15,19] and in MS pathology.[19−21] For instance, Kim et al. showed increases in MBP mono- and dimethyl arginine in post-mortem MS brain tissue, as well as increases in arginine methylation and citrullination in an animal model correlated with the severity of demyelination.[16] Furthermore, Grant et al. used an iTRAQ labeled proteomics approach to identify several changes in PTMs of other proteins involved in MS pathology (excluding MBP) in the SC of EAE animals, finding increases in arginine methylation and citrullination as well as increases in lysine dimethylation.[40] To extend further insight, we quantified changes in PTMs to the lysine residues of MBP in the SC of a MOG-mouse model of EAE using a validated, analytical LC−MS/MS assay. This was used because it is a quantitative method for measuring total lysine methylation and acetylation, as well as arginine methylation. Other mass spectrometry methods that provide sequence information such as proteomic methods are not appropriate for this study because they usually do not provide complete sequence coverage, and as such cannot be completely quantitative.

The PTM Profile of MBP Differs from That Found on Histones

There are many types of PTMs found on histones that are important for controlling gene expression and they appear at different predictable concentrations.[41] Therefore, we compared PTMs found on histones isolated from various organs to MBP isolated from SC and brain as well as validated the EpiQuik extraction of MBP from brain and SC tissues (Figure 1A and 1B). To support our disease model for demyelination, we were most interested in lysine acetylation and found MBP to be acetylated when analyzed by Western blot using a general antiacetyl-lysine antibody (Figure 1C). We chose to supplement these results using an LC−MS/MS assay that can measure many types of lysine and arginine modifications, including acetyl-lysine. We found that PTMs on lysine residues of MBP are at lower concentrations than on histones when normalized for total protein. Nevertheless, many modifications were quantifiable on MBP isolated from the SC and brain of untreated (NC) mice. We found that asymmetric dimethyl-arginine in the SC and brain of NC mice to be slightly less than that found in histones, but unexpectedly, found up to 36-fold more monomethyl-arginine and 8-fold more symmetric dimethyl-arginine on MBP compared to histones (Figure 1D). We therefore show that the amounts of methyl arginines are characteristic to MBP and differ from that of histones. This may arise from differences in enzyme activity because the formation of some methyl arginines on MBP are catalyzed by MBP-specific protein methylase I,[42] whereas protein arginine methyltransferases modify histones and other proteins. Furthermore, we found mono-, di-, and trimethyl-lysine and acetyl-lysine PTMs on mouse MBP. These findings in particular are of greatest importance as lysine modifications of MBP have only recently began to be characterized.[43] This is the first identification of acetyl-lysine and asymmetric dimethyl-arginine on mouse MBP.

DOI: 10.1021/acs.jproteome.7b00270
J. Proteome Res. 2018, 17, 55−62

Lysine and Arginine Post-Translational Modifications to Myelin Basic Protein Increase with Disease Severity

We show that EAE-induction of the immune system causes increases in lysine acetylation as well as increases in lysine and arginine methylation on MBP. As previously indicated, NDS peaks at 15 dpi (Supplemental Figure S1), where a corresponding hyper-acetylation of lysine and hyper-methylation of lysine and arginine occur on MBP (Figure 2A and 2B). This result mirrors a corresponding phenomenon others have observed with arginine citrullination and methylation of MBP in MS.[10] Therefore, the changes in lysine PTMs of MBP that correlate with peak NDS can be associated with the myelin damage following MOG-induced EAE. Given the electrostatic model of myelin compaction (Figure 5A), lysine acetylation

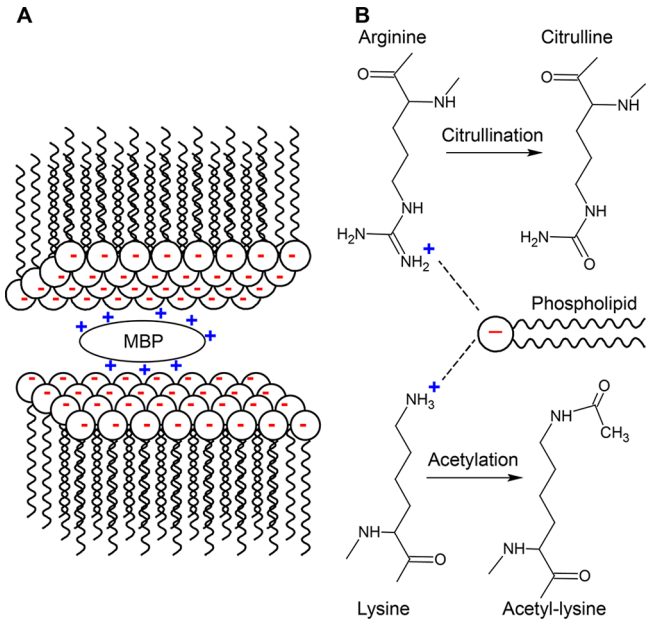


Figure 5. Charge neutralizing lysine acetylation and arginine citrullination of MBP. MBP acts to hold together the layers of myelin lipid through electrostatic interactions between its lysine and arginine basic residues and the anionic phosphates resulting in myelin compaction (A). Upon arginine citrullination and lysine acetylation the electrostatic interaction diminishes, thereby disrupting myelin compaction and resulting in axon exposure (B).

may share a similar role as arginine citrullination. Both modifications neutralize the positive charges on MBP suggesting that, like arginine citrullination, lysine acetylation may lead to myelin decompaction (Figure 5B). Importantly, increased amounts of MBP acetyl-lysine are correlated with increasing disability score. There is, however, a key difference with lysine acetylation in that it can be enzymatically removed by deacetylases, whereas citrullination cannot be reversed. This presents the possibility that MBP neutralization by lysine acetylation can be returned to its original charged state through the function of deacetylases. Citrulline is, however, an irreversible modification and requires protein recycling in order to reverse its neutralizing effect on MBP.

The dynamics of lysine acetylation and deacetylation on MBP may, in part, explain the relapsing and remitting nature of MS that is also observed in the mouse EAE model. For example, the partial remissions observed in NDS at 18 and 42 dpi may be partly caused by the increased activity of deacetylases on MBP decreasing lysine acetylation. This is supported by our finding of greater than 60% *reduction* in lysine acetylation (hypoacetylation) of MBP at 42 dpi (Figure 2A). Continuing with the example, the incomplete recovery at 42 dpi with respect to NDS could be partially explained by the irreversible nature of citrullination of MBP. Therefore, with this example, lysine acetylation may be reversed, but the remaining citrullination of MBP limits recovery. It should be noted that there are many theories as to the causes of the incomplete recovery, and the relapsing and remitting nature of MS and animal EAE models.[44] Therefore, lysine acetylation of MBP is likely a single component of a multifactorial pathological process or may even just be a marker for myelin damage.

We observed stable increases in asymmetric dimethyl-arginine on MBP until the second partial recovery observed at 42 dpi in the EAE model (Figure 2B), where the amount of asymmetric dimethyl-arginine returns to control levels. Importantly, methylation of arginine does not change the ionization state and will not alter the electrostatic interactions of MBP like citrullination. In fact, methylated arginine may protect MBP from citrullination since the enzyme that catalyzes this mark, peptidylarginine deiminase, cannot convert methylated arginine residues to citrulline.[45] On proteins, both methylation of arginine and its conversion to citrulline are irreversible; therefore the changes in the amounts of these modifications relative to control likely arise from turnover of MBP. This suggests an increase in the gene expression of MBP during recovery from EAE (42 dpi) is required for effective remyelination, as seen in other MOG models of EAE.[46]

Treatment with Histone Deacetylase (HDAC) Inhibitor TSA Reduces NDS without Affecting MBP Acetylation

We, and others[32] have shown that treatment with the HDAC inhibitor TSA improves the NDS of EAE animals, nearly abolishing all disability symptoms and continued treatment with TSA sustains these beneficial effects throughout each disease phase (Figure 3). Given that we have correlated MBP acetylation with deteriorating NDS, the choice of treatment with TSA (a lysine deacetlyase inhibitor) seems paradoxical because such a drug could potentially increase MBP acetylation and therefore should theoretically make the disease worse. However, previous literature has demonstrated the beneficial effects of TSA in various animal models of MS.[8,32] Interestingly, we identified no significant differences in MBP lysine acetylation in all of the TSA treatment groups, therefore, the beneficial effects of TSA occur by some other mechanism. Previous studies have shown that TSA inhibits HDAC 11, and this decreases the expression of MBP and other myelin proteins.[47] Initial studies with TSA in mouse models of MS show that TSA reduces production of pro-inflammatory mediators and this reduces demyelination.[32] The HDAC inhibitor vorinostat is known to reduce expression of TNF-α, IL-1-β, IL-12, IFN-γ.[48] These results suggest that TSA may work through an immunomodulatory mechanism without directly affecting MBP lysine acetylation.

Although TSA did not affect MBP lysine acetylation, we identified decreases in dimethyl-lysine following TSA treatment at 30 and 42 days post-EAE. These changes coincide with the nearly complete recovery with respect to NDS in TSA treated EAE mice (Figure 3 and 4). Our previous studies have shown that HDAC inhibitors can alter the expression of lysine demethylases, where depending of the type of HDAC inhibitor, they can either decrease or increase expression of certain lysine

DOI: 10.1021/acs.jproteome.7b00270
J. Proteome Res. 2018, 17, 55−62

demethylases.[26] Therefore, TSA may increase the expression of FAD-dependent lysine demethylases like LSD1, which selectively demethylates mono- and dimethyl-lysine,[41] resulting in the decreased in MBP dimethyl-lysine we observed (Figure 4B).

CONCLUSIONS

This is the first study to identify changes in the modifications of lysine residues of MBP in MOG-induced EAE mice. We associated the significant increases in MBP lysine acetylation as well as the increases in lysine and arginine methylation to the clinical neurological disability caused by demyelination. Our results suggest that, like citrullination, lysine acetylation reduces the positive charge state of MBP and therefore may be associated with myelin damage. Acetylation of lysine residues in bovine MBP has only recently been discovered,[43] and here we show in mice that increases of MBP lysine acetylation are correlated with the increased NDS caused by EAE. In addition, we also corroborate that TSA elicits beneficial effects by lowering NDS in our EAE mouse model, but that this effect is not related to the deacetylase activity of HDAC on MBP in the spinal cord, because we observed no effect on the lysine acetylation status of MBP.

ASSOCIATED CONTENT

Supporting Information

The Supporting Information is available free of charge on the ACS Publications website at DOI: 10.1021/acs.jproteome.7b00270.

Figures S1−S2 (PDF)

AUTHOR INFORMATION

Corresponding Authors

*E-mail: ted.lakowski@umanitoba.ca.
*E-mail: mike.namaka@umanitoba.ca.

ORCID

Michael Namaka: 0000-0002-4502-9558

Author Contributions

#R.L., T.Z., T.K.A. contributed equally to this work

Notes

The authors declare no competing financial interest.

ACKNOWLEDGMENTS

The authors acknowledge support from the Dr. Paul H.T. Thorlakson Foundation Fund, The Manitoba Medical Services Foundation [8-2014-03 2014], University of Manitoba Research Grants Program [UM Project # 43887, 2015], the Natural Sciences and Engineering Research Council (NSERC) Canada [RGPIN-2015-06543, 2015-2020] (to T.M.L.), and the Leslie F. Buggey Graduate Scholarship, 2014 (to R.L.). The authors would also like to acknowledge the funding from the following agencies: Canadian Paraplegic Association (CPA), University of Manitoba Research Grants Program (URGP) and Bayshore Health Care Systems.

ABBREVIATIONS

MBP, myelin basic protein; PTM, post-translational modification; MS, multiple sclerosis; EAE, experimental autoimmune encephalomyelitis; CNS, central nervous system; NDS, neurological disability score; HDAC, histone deacetylase; TSA, trichostatin A; MOG, myelin oligodendrocyte glycoprotein; LC−MS/MS, liquid chromatography−tandem mass spectrometry; WB, Western blot; AcK, acetyl-lysine; MeK, monomethyl-lysine; Me2K, dimethyl-lysine; Me3K, trimethyl-lysine; aMe2R, asymmetric dimethyl-arginine; sMe2R, symmetric dimethyl-arginine; MeR, monomethyl-arginine

REFERENCES

(1) Namaka, M. P.; Ethans, K.; Jensen, B.; Esfahani, F.; Frost, E. E. Multiple Sclerosis, In *Therapeutic Choices/e-Therapeutic*; Canadian Pharmacists Association Publishers, Inc: Ottawa, 2011; pp 309−319.

(2) Lacroix, S.; Hamilton, L. K.; Vaugeois, A.; Beaudoin, S.; Breault-Dugas, C.; Pineau, I.; Levesque, S. A.; Gregoire, C. A.; Fernandes, K. J. Central canal ependymal cells proliferate extensively in response to traumatic spinal cord injury but not demyelinating lesions. *PLoS One* **2014**, *9*, e85916.

(3) Gold, R.; Montalban, X. Multiple sclerosis: more pieces of the immunological puzzle. *Lancet Neurol.* **2012**, *11*, 9−10.

(4) Namaka, M.; Turcotte, D.; Leong, C.; Grossberndt, A.; Klassen, D. Multiple sclerosis: etiology and treatment strategies. *Consult Pharm.* **2008**, *23*, 886−896.

(5) Acosta, C. M. R.; Cortes, C.; MacPhee, H.; Namaka, M. P. Exploring the Role of Nerve Growth Factor in Multiple Sclerosis: Implications in Myelin Repair. *CNS Neurol. Disord.: Drug Targets* **2013**, *12*, 1242−1256.

(6) Acosta, C.; Cortes, C.; Altaweel, K.; MacPhee, H.; Hoogervorst, B.; Bhullar, H.; MacNeil, B.; Torabi, M.; F, F. B.; Namaka, M. P. Immune System Induction of Nerve Growth Factor in an Animal Model of Multiple Sclerosis: Implications in Re-Myelination and Myelin Repair. *CNS Neurol. Disord.: Drug Targets* **2015**, *14*, 1069.

(7) Begum, F.; Zhu, W.; Cortes, C.; Macneil, B.; Namaka, M. Elevation of Tumor Necrosis Factor Alpha in Dorsal Root Ganglia and Spinal Cord is Associated with Neuroimmune Modulation of Pain in an Animal Model of Multiple Sclerosis. *Journal of neuroimmune pharmacology: the official journal of the Society on NeuroImmune Pharmacology.* **2013**, *8*, 677−690.

(8) KhorshidAhmad, T.; Acosta, C.; Cortes, C.; Lakowski, T. M.; Gangadaran, S.; Namaka, M. Transcriptional Regulation of Brain-Derived Neurotrophic Factor (BDNF) by Methyl CpG Binding Protein 2 (MeCP2): a Novel Mechanism for Re-Myelination and/or Myelin Repair Involved in the Treatment of Multiple Sclerosis (MS). *Mol. Neurobiol.* **2016**, *53*, 1092.

(9) Wenjun Zhu, C. A.; MacNeil, B. J.; Klonisch, T.; Cortes, C.; Doupe, M.; Gong, Y.; Namaka, M. Spinal cord brain derived neurotrophic factor (BDNF) responsive cells in an experimental autoimmune encephalomyelitis (EAE) model of multiple sclerosis (MS): Implications in myelin repair. *Res. Immunol.: Int. J.* **2014**, 1.

(10) Moscarello, M. A.; Mastronardi, F. G.; Wood, D. D. The Role of Citrullinated Proteins Suggests a Novel Mechanism in the Pathogenesis of Multiple Sclerosis. *Neurochem. Res.* **2007**, *32*, 251−256.

(11) Harauz, G.; Musse, A. A. A tale of two citrullines–structural and functional aspects of myelin basic protein deimination in health and disease. *Neurochem. Res.* **2007**, *32*, 137−158.

(12) Moscarello, M. A.; Lei, H.; Mastronardi, F. G.; Winer, S.; Tsui, H.; Li, Z.; Ackerley, C.; Zhang, L.; Raijmakers, R.; Wood, D. D. Inhibition of peptidyl-arginine deiminases reverses protein-hypercitrullination and disease in mouse models of multiple sclerosis. *Dis. Models & Mech.* **2013**, *6*, 467−478.

(13) Yang, L.; Tan, D.; Piao, H. Myelin Basic Protein Citrullination in Multiple Sclerosis: A Potential Therapeutic Target for the Pathology. *Neurochem. Res.* **2016**, *41*, 1845−1856.

(14) Small, D. H.; Carnegie, P. R.; Anderson, R. M. Cycloleucine-induced vacuolation of myelin is associated with inhibition of protein methylation. *Neurosci. Lett.* **1981**, *21*, 287−292.

(15) Lee, C. C.; Surtees, R.; Duchen, L. W. Distal motor axonopathy and central nervous system myelin vacuolation caused by cycloleucine, an inhibitor of methionine adenosyltransferase. *Brain* **1992**, *115* (Pt 3), 935−955.

DOI: 10.1021/acs.jproteome.7b00270
J. Proteome Res. 2018, 17, 55−62

(16) Kim, J. K.; Mastronardi, F. G.; Wood, D. D.; Lubman, D. M.; Zand, R.; Moscarello, M. A. Multiple sclerosis: an important role for post-translational modifications of myelin basic protein in pathogenesis. *Mol. Cell. Proteomics* **2003**, *2*, 453−462.
(17) Moscarello, M. A.; Wood, D. D.; Ackerley, C.; Boulias, C. Myelin in multiple sclerosis is developmentally immature. *J. Clin. Invest.* **1994**, *94*, 146−154.
(18) Brady, G. W.; Fein, D. B.; Wood, D. D.; Moscarello, M. A. The role of charge microheterogeneity of human myelin basic protein in the formation of phosphatidylglycerol multilayers. *Biochem. Biophys. Res. Commun.* **1985**, *126*, 1161−1165.
(19) Musse, A. A.; Harauz, G. Molecular "negativity" may underlie multiple sclerosis: role of the myelin basic protein family in the pathogenesis of MS. *Int. Rev. Neurobiol.* **2007**, *79*, 149−172.
(20) Whitaker, J. N.; Heinemann, M. A. The degradation of human myelin basic protein peptide 43−88 by human renal neutral proteinase. *Neurology* **1983**, *33*, 744−749.
(21) Whitaker, J. N.; Layton, B. A.; Herman, P. K.; Kachelhofer, R. D.; Burgard, S.; Bartolucci, A. A. Correlation of myelin basic protein-like material in cerebrospinal fluid of multiple sclerosis patients with their response to glucocorticoid treatment. *Ann. Neurol.* **1993**, *33*, 10−17.
(22) Chernoff, G. F. Shiverer: an autosomal recessive mutant mouse with myelin deficiency. *J. Hered.* **1981**, *72*, 128.
(23) Amur, S. G.; Shanker, G.; Pieringer, R. A. Regulation of myelin basic protein (arginine) methyltransferase by thyroid hormone in myelinogenic cultures of cells dissociated from embryonic mouse brain. *J. Neurochem.* **1984**, *43*, 494−498.
(24) Young, P. R.; Vacante, D. A.; Waickus, C. M. Mechanism of the interaction between myelin basic protein and the myelin membrane; the role of arginine methylation. *Biochem. Biophys. Res. Commun.* **1987**, *145*, 1112−1118.
(25) Gasteiger, E.; Hoogland, C.; Gattiker, A.; Ducaud, S.; Wilkens, M. R.; Appel, R. D.; Bairoch, A. Protein Identification and Analysis Tools on the ExPASy Server, In *The Proteomics Protocols Handbook*; Walker, J. M., Ed.; Humana Press, 2005; pp 571−607.
(26) Lillico, R.; Sobral, M. G.; Stesco, N.; Lakowski, T. M. HDAC inhibitors induce global changes in histone lysine and arginine methylation and alter expression of lysine demethylases. *J. Proteomics* **2016**, *133*, 125−133.
(27) Mendel, I.; Kerlero de Rosbo, N.; Ben-Nun, A. A myelin oligodendrocyte glycoprotein peptide induces typical chronic experimental autoimmune encephalomyelitis in H-2b mice: fine specificity and T cell receptor V beta expression of encephalitogenic T cells. *Eur. J. Immunol.* **1995**, *25*, 1951−1959.
(28) Marcondes, M. C.; Furtado, G. C.; Wensky, A.; Curotto de Lafaille, M. A.; Fox, H. S.; Lafaille, J. J. Immune regulatory mechanisms influence early pathology in spinal cord injury and in spontaneous autoimmune encephalomyelitis. *Am. J. Pathol.* **2005**, *166*, 1749−1760.
(29) Zhu, W.; Acosta, C.; MacNeil, B.; Cortes, C.; Intrater, H.; Gong, Y.; Namaka, M. Elevated expression of fractalkine (CX3CL1) and fractalkine receptor (CX3CR1) in the dorsal root ganglia and spinal cord in experimental autoimmune encephalomyelitis: implications in multiple sclerosis-induced neuropathic pain. *BioMed Res. Int.* **2013**, *2013*, 480702.
(30) Melanson, M.; Miao, P.; Eisenstat, D.; Gong, Y.; Gu, X.; Au, K.; Zhu, W.; Begum, F.; Frost, E. E.; Namaka, M. Experimental autoimmune encephalomyelitis-induced upregulation of tumor necrosis factor-alpha in the dorsal root ganglia. *Multiple sclerosis.* **2009**, *15*, 1135−1145.
(31) Khorshid Ahmad, T.; Zhou, T.; AlTaweel, K.; Cortes, C.; Lillico, R.; Lakowski, T. M.; Gozda, K.; Namaka, M. P. Experimental Autoimmune Encephalomyelitis (EAE)-Induced Elevated Expression of the E1 Isoform of Methyl CpG Binding Protein 2 (MeCP2E1): Implications in Multiple Sclerosis (MS)-Induced Neurological Disability and Associated Myelin Damage. *Int. J. Mol. Sci.* **2017**, *18*, 1254.
(32) Camelo, S.; Iglesias, A. H.; Hwang, D.; Due, B.; Ryu, H.; Smith, K.; Gray, S. G.; Imitola, J.; Duran, G.; Assaf, B.; Langley, B.; Khoury, S. J.; Stephanopoulos, G.; De Girolami, U.; Ratan, R. R.; Ferrante, R. J.; Dangond, F. Transcriptional therapy with the histone deacetylase inhibitor trichostatin A ameliorates experimental autoimmune encephalomyelitis. *J. Neuroimmunol.* **2005**, *164*, 10−21.
(33) Orton, S. M.; Herrera, B. M.; Yee, I. M.; Valdar, W.; Ramagopalan, S. V.; Sadovnick, A. D.; Ebers, G. C. Sex ratio of multiple sclerosis in Canada: a longitudinal study. *Lancet Neurol.* **2006**, *5*, 932−936.
(34) Maatta, J.; Hinkkanen, A. Extraction of myelin basic protein US 5849886 A, December 15, 1998.
(35) Martenson, R. E.; Deibler, G. E.; Kies, M. W. Extraction of Rat Myelin Basic Protein Free of Other Basic Proteins of Wholse Central Nervous System Tissue: An Analysis of its Electrophoretic Heterogeneity. *J. Biol. Chem.* **1969**, *244*, 4268−4272.
(36) Costa, O.; Divoux, D.; Ischenko, A.; Tron, F.; Fontaine, M. Optimization of an animal model of experimental autoimmune encephalomyelitis achieved with a multiple MOG(35−55)peptide in C57BL6/J strain of mice. *J. Autoimmun.* **2003**, *20*, 51−61.
(37) Gil-Dones, F.; Alonso-Orgaz, S.; Avila, G.; Martin-Rojas, T.; Moral-Darde, V.; Barroso, G.; Vivanco, F.; Scott-Taylor, J.; Barderas, M. G. An Optimal Protocol to Analyze the Rat Spinal Cord Proteome. *Biomarker Insights* **2009**, *4*, 135−164.
(38) Wu, G.; McArthur, A. G.; Fiser, A.; Šali, A.; Sogin, M. L.; M, M. Core Histones of the Amitochondriate Protist, Giardia lamblia. *Mol. Biol. Evol.* **2000**, *17*, 1156−1163.
(39) Small, D. H.; Carnegie, P. R. In vivo methylation of an arginine in chicken myelin basic protein. *J. Neurochem.* **1982**, *38*, 184−190.
(40) Grant, J. E.; Hu, J.; Liu, T.; Jain, M. R.; Elkabes, S.; Li, H. Post-translational modifications in the rat lumbar spinal cord in experimental autoimmune encephalomyelitis. *Journal of proteome research.* **2007**, *6*, 2786−2791.
(41) Lillico, R.; Stesco, N.; Khorshid Amhad, T.; Cortes, C.; Namaka, M. P.; Lakowski, T. M. Inhibitors of enzymes catalyzing modifications to histone lysine residues: structure, function and activity. *Future Med. Chem.* **2016**, *8*, 879−897.
(42) Ghosh, S. K.; Rawal, N.; Syed, S. K.; Paik, W. K.; Kim, S. D. Enzymic methylation of myelin basic protein in myelin. *Biochem. J.* **1991**, *275*, 381−387.
(43) Zhang, C.; Walker, A. K.; Zand, R.; Moscarello, M. A.; Yan, J. M.; Andrews, P. C. Myelin basic protein undergoes a broader range of modifications in mammals than in lower vertebrates. *Journal of proteome research.* **2012**, *11*, 4791−4802.
(44) Kipp, M.; Nyamoya, S.; Hochstrasser, T.; Amor, S. Multiple sclerosis animal models: a clinical and histopathological perspective. *Brain Pathol.* **2017**, *27*, 123−137.
(45) Raijmakers, R.; Zendman, A. J.; Egberts, W. V.; Vossenaar, E. R.; Raats, J.; Soede-Huijbregts, C.; Rutjes, F. P.; van Veelen, P. A.; Drijfhout, J. W.; Pruijn, G. J. Methylation of arginine residues interferes with citrullination by peptidylarginine deiminases in vitro. *J. Mol. Biol.* **2007**, *367*, 1118−1129.
(46) Matthieu, J. M.; Comte, V.; Tosic, M.; Honegger, P. Myelin gene expression during demyelination and remyelination in aggregating brain cell cultures. *J. Neuroimmunol.* **1992**, *40*, 231−234.
(47) Liu, H.; Hu, Q.; D'Ercole A, J.; Ye, P. Histone deacetylase 11 regulates oligodendrocyte-specific gene expression and cell development in OL-1 oligodendroglia cells. *Glia.* **2009**, *57*, 1−12.
(48) Leoni, F.; Zaliani, A.; Bertolini, G.; Porro, G.; Pagani, P.; Pozzi, P.; Dona, G.; Fossati, G.; Sozzani, S.; Azam, T.; Bufler, P.; Fantuzzi, G.; Goncharov, I.; Kim, S. H.; Pomerantz, B. J.; Reznikov, L. L.; Siegmund, B.; Dinarello, C. A.; Mascagni, P. The antitumor histone deacetylase inhibitor suberoylanilide hydroxamic acid exhibits antiinflammatory properties via suppression of cytokines. *Proc. Natl. Acad. Sci. U. S. A.* **2002**, *99*, 2995−3000.

DOI: 10.1021/acs.jproteome.7b00270
J. Proteome Res. 2018, 17, 55−62

Subject: Re: Inquiry for letter of copyright permission
Date: Tuesday, October 15, 2019 at 6:56:08 PM Central Daylight Time
From: Joshua Labaer
To: Ting Zhou

Ting Zhou,

It is fine if you wish to include the paper "Increased Post-Translational Lysine Acetylation of Myelin Basic Protein is Associated with Peak Neurological Disability in a Mouse Experimental Autoimmune Encephalomyelitis Model of Multiple Sclerosis" in your PhD thesis. Permission granted! Does this email suffice?

Sincerely,
Joshua LaBaer
Associated Editor
Journal of Proteome Research

From: Ting Zhou <zhout346@myumanitoba.ca>
Sent: Wednesday, October 9, 2019 12:56 PM
To: Joshua Labaer <jlabaer@jpr.acs.org>
Subject: Inquiry for letter of copyright permission

Dear Joshua,

Hope this email finds you well!

This is Ting Zhou. I am the co-first author of a published paper in your journal named" Increased Post-Translational Lysine Acetylation of Myelin Basic Protein is Associated with Peak Neurological Disability in a Mouse Experimental Autoimmune Encephalomyelitis Model of Multiple Sclerosis" (Manuscript ID: pr-2017-002702.R2)

This email is to inquire whether you could offer me letter of permission to include this published paper in my Ph.D. thesis as an appendix.

Would you please indicate if there is any process I should go? And is there any copyright issue I need to pay attention?

Thank you for your time and help! Have a nice day!

Ting Zhou

Ph.D Student
Faculty of Pharmacy & Department of Human Anatomy and Cell Science
University of Manitoba
750 McDermot Avenue
Winnipeg, MB, Canada R3E 0T5
zhout346@myumanitoba.ca

Copyright Clearance Center RightsLink®

Home Create Account Help

ACS Publications Most Trusted. Most Cited. Most Read.

Title: Increased Post-Translational Lysine Acetylation of Myelin Basic Protein Is Associated with Peak Neurological Disability in a Mouse Experimental Autoimmune Encephalomyelitis Model of Multiple Sclerosis

Author: Ryan Lillico, Ting Zhou, Tina Khorshid Ahmad, et al

Publication: Journal of Proteome Research

Publisher: American Chemical Society

Date: Jan 1, 2018

Copyright © 2018, American Chemical Society

LOGIN

If you're a copyright.com user, you can login to RightsLink using your copyright.com credentials.

Already **a RightsLink user** or want to learn more?

PERMISSION/LICENSE IS GRANTED FOR YOUR ORDER AT NO CHARGE

This type of permission/license, instead of the standard Terms & Conditions, is sent to you because no fee is being charged for your order. Please note the following:

- Permission is granted for your request in both print and electronic formats, and translations.
- If figures and/or tables were requested, they may be adapted or used in part.
- Please print this page for your records and send a copy of it to your publisher/graduate school.
- Appropriate credit for the requested material should be given as follows: "Reprinted (adapted) with permission from (COMPLETE REFERENCE CITATION). Copyright (YEAR) American Chemical Society." Insert appropriate information in place of the capitalized words.
- One-time permission is granted only for the use specified in your request. No additional uses are granted (such as derivative works or other editions). For any other uses, please submit a new request.

BACK CLOSE WINDOW

Copyright © 2019 Copyright Clearance Center, Inc. All Rights Reserved. Privacy statement. Terms and Conditions.
Comments? We would like to hear from you. E-mail us at customercare@copyright.com

International Journal of
Molecular Sciences

MDPI

Article

Experimental Autoimmune Encephalomyelitis (EAE)-Induced Elevated Expression of the E1 Isoform of Methyl CpG Binding Protein 2 (MeCP2E1): Implications in Multiple Sclerosis (MS)-Induced Neurological Disability and Associated Myelin Damage

Tina Khorshid Ahmad [1], Ting Zhou [1], Khaled AlTaweel [1], Claudia Cortes [1], Ryan Lillico [1], Ted Martin Lakowski [1], Kiana Gozda [1] and Michael Peter Namaka [1,2,3,4,*]

1 College of Pharmacy, Faculty of Health Sciences, University of Manitoba, Manitoba, Winnipeg, MB R3E 0T5, Canada; khorshit@myumanitoba.ca (T.K.A.); zhout346@myumanitoba.ca (T.Z.); khaledta72@gmail.com (K.A.); claudiacortesp@gmail.com (C.C.); umlillic@myumanitoba.ca (R.L.); Ted.Lakowski@umanitoba.ca (T.M.L.); gozdak@myumanitoba.ca (K.G.)
2 College of Pharmacy, Third Military Medical University, Chongqing 400038, China
3 Department of Medical Rehabilitation, College of Medicine, Faculty of Health Sciences, Winnipeg, MB R3E 0T6, Canada
4 Department of Internal Medicine, College of Medicine, Faculty of Health Sciences, University of Manitoba, Winnipeg, MB R3A 1R9, Canada
* Correspondence: Mike.Namaka@umanitoba.ca; Tel.: +1-204-474-8380; Fax: +1-204-789-3744

Academic Editor: Guiting Lin
Received: 21 February 2017; Accepted: 13 May 2017; Published: 12 June 2017

Abstract: Multiple sclerosis (MS) is a chronic neurological disease characterized by the destruction of central nervous system (CNS) myelin. At present, there is no cure for MS due to the inability to repair damaged myelin. Although the neurotrophin brain derived neurotrophic factor (BDNF) has a beneficial role in myelin repair, these effects may be hampered by the over-expression of a transcriptional repressor isoform of methyl CpG binding protein 2 (MeCP2) called MeCP2E1. We hypothesize that following experimental autoimmune encephalomyelitis (EAE)-induced myelin damage, the immune system induction of the pathogenic MeCP2E1 isoform hampers the myelin repair process by repressing BDNF expression. Using an EAE model of MS, we identify the temporal gene and protein expression changes of MeCP2E1, MeCP2E2 and BDNF. The expression changes of these key biological targets were then correlated with the temporal changes in neurological disability scores (NDS) over the entire disease course. Our results indicate that MeCP2E1 mRNA levels are elevated in EAE animals relative to naïve control (NC) and active control (AC) animals during all time points of disease progression. Our results suggest that the EAE-induced elevations in MeCP2E1 expression contribute to the repressed BDNF production in the spinal cord (SC). The sub-optimal levels of BDNF result in sustained NDS and associated myelin damage throughout the entire disease course. Conversely, we observed no significant differences in the expression patterns displayed for the MeCP2E2 isoform amongst our experimental groups. However, our results demonstrate that baseline protein expression ratios between the MeCP2E1 versus MeCP2E2 isoforms in the SC are higher than those identified within the dorsal root ganglia (DRG). Thus, the DRG represents a more conducive environment than that of the SC for BDNF production and transport to the CNS to assist in myelin repair. Henceforth, the sub-optimal BDNF levels we report in the SC may arise from the elevated MeCP2E1 vs. MeCP2E2 ratio in the SC that creates a more hostile environment thereby preventing local BDNF production. At the level of transcript, we demonstrate that EAE-induces the pathological enhanced expression of MeCP2E1 that contributes to enhanced NDS during the

entire disease course. Thus, the pathological induction of the MeCP2E1 isoform contributes to the disruption of the normal homeostatic signaling equilibrium network that exists between cytokines, neurotrophins and chemokines that regulate the myelin repair process by repressing BDNF. Our research suggests that the elevated ratio of MeCP2E1 relative to MeCP2E2 may be a useful diagnostic marker that clinicians can utilize to determine the degree of neurological disability with associated myelin damage. The elevated MeCP2E1 vs. MeCP2E2 ratios (E1/E2) in the SC prevent BDNF from reaching optimal levels required for myelin repair. Thus, the lower E1/E2 ratios in the DRG, allow the DRG to serve as a weak secondary compensatory mechanism for enhanced production and delivery of BDNF to the SC to try to assist in myelin repair.

Keywords: multiple sclerosis (MS); experimental autoimmune encephalomyelitis (EAE); methyl CpG binding protein 2 (MeCP2); brain-derived neurotrophic factor (BDNF); neurological disability scoring (NDS); myelin repair

1. Introduction

Multiple sclerosis (MS) is a chronic progressive neurological disease of central nervous system (CNS) characterized by destruction of myelin [1,2]. It is considered a biphasic autoimmune disease with an acute inflammatory phase followed by a chronic degenerative, demyelinating phase [3]. Myelin is the insulating coating that surrounds nerve axons. It is essential for propagation of nerve impulses to effector target cells. Hence, patients diagnosed with MS have regionalized areas along axons where electrical impulse transmission is compromised due to damaged segments of myelin. Thus, MS patients suffer a variety of neurological disabilities that negatively impact their quality of life [1,4].

Using an animal model of MS, we have published several publications that identify the importance of the anatomical connection between the dorsal root ganglia (DRG) and spinal cord (SC) [5–7] in regard to myelin repair. In addition, several of our publications have identified a common interactive signaling network among cytokines, chemokines and neurotrophins that regulate the myelin repair process [6–9]. We have identified several key biological targets in this pathway [5,7–11], However, we have now expanded this list of biological targets to include the upstream transcriptional repressor of BDNF known as methyl CpG binding protein 2 (MeCP2) [11–13].

BDNF has a well-established role in myelin repair [12,14–16]. It has been shown to be involved in proliferation, differentiation and migration of oligodendrocyte progenitor cells (OPCs) [17,18]. Furthermore, BDNF also has a direct effect on myelination via its effect on oligodendrocytes (OGs) [19–21]. In addition, BDNF has been shown to regulate the distribution pattern of myelin proteins that govern in the structural integrity of myelin [22–24]. Other researchers in this area have also confirmed the beneficial effects of BDNF in re-myelination and/or myelin repair. For example, several studies have shown that fingolimod [25], the first approved oral drug for MS, glatiramer acetate [26–28] and laquinimod [29,30] exert their beneficial effect in treating relapsing remitting MS (RRMS) by increasing BDNF levels. In addition to these findings, we have also published evidence to support the role of BDNF via tropomyosin-related kinase receptors (TrkB) in SC myelin repair [11].

Since its identification in 1998 [31], MeCP2 has received a wide range of attention as a genome-wide epigenetic factor [32]. In fact, MeCP2 was the first member of methyl binding protein that was able to bind a single methyl CpG pair [33] by its methyl binding domain (MBD) [34]. BDNF is one of several prominent targets of MeCP2 [35,36]. MeCP2 was first identified to be a transcriptional repressor of BDNF [35,37] exerting its effect by directly forming a repressor complex with its transcriptional repressor domain (TRD) and histone deacetylase (HDAC) Sin3A complex [38,39] (Figure 1A). MeCP2 can also indirectly regulate BDNF gene expression by affecting the expression of other BDNF transcriptional repressors like RE1 silencing transcription factor (REST) and CoREST [40].

Interestingly, studies conducted in MeCP2 null mice [36,41,42] and human tissues [43] show decreased gene and protein expression of BDNF. Thus, these reported findings in MeCP2 null mice suggest that other factors must be involved in the regulation of BDNF expression besides MeCP2. Irrespective, MeCP2's ability to directly and/or indirectly effect BDNF expression warrants its investigation as a primary biological target by which targeted interventional strategies could be developed to promote myelin repair.

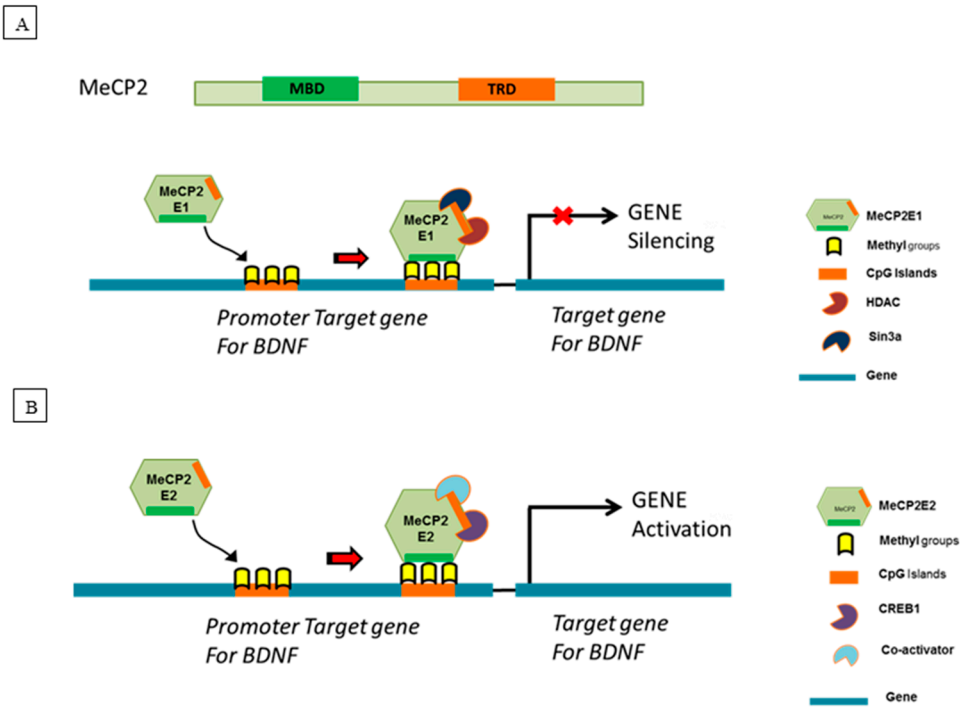


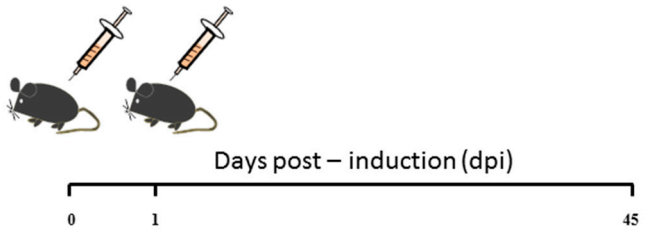
Figure 1. Proposed molecular mechanism of action of MeCP2E1 and MeCP2E2. *BDNF* gene is very complex. Aid et al. described 10 exons in human and rodent *BDNF* gene [44]. MeCP2 has been shown to bind to promoter region of exon III in rats [35] and exon IV in mice and humans. (**A**) Proposed MeCP2E1 mechanism of gene repression: MeCP2E1 binds to methylated CpG dinucleotide in CpG islands of promoter region for *BDNF* gene with its methyl binding domain (MBD) and recruits a transcriptional co-repressor complex containing mSin3A and histone deacetylase 1 (HDAC1) and 2 (HDAC2) with its transcriptional repressor domain (TRD) to repress the expression of BDNF during an MS attack leading to MS induced myelin damage; (**B**) Proposed MeCP2E2 mechanism of gene activation: MeCP2E2 binds to methylated CpG dinucleotide in CpG islands of promoter region for *BDNF* gene and recruits a transcriptional activator complex containing cAMP response element-binding protein (CREB) and co-activators [45]. This leads to activation of *BDNF* gene during an MS attack in order to help in re-myelination and/or myelin repair.

MeCP2 exists in two different biologically active isoforms, MeCP2E1 and MeCP2E2 [46,47]. Both isoforms have been shown to have differential biological effects on neuronal survival [48] and embryonic development [49]. Based on our current investigative research in this area [50], we believe these two isoforms may have distinctly different biological roles in regard to the re-myelination and/or the myelin repair process that may be linked to their ability to differentially regulate the expression of BDNF [13,35,37,51–53]. Thus, the MeCP2E1 isoform may be pathogenically activated by an immune system mediated insult such as in MS. The resultant disease-induced elevation of MeCP2E1 represses BDNF production that alters the homeostatic molecular signaling between cytokines, chemokines and neurotrophins resulting in myelin damage [50]. For example, studies have confirmed repression of BDNF by MeCP2E1 in an inflammatory stimulus induced pain model [54,55]. Specifically, this study showed increased expression of the MeCP2E1 isoform in an inflammatory pain model that utilized

complete Freund's adjuvant (CFA) injection as the nociceptive inflammatory pain stimulus [54]. This increase was also correlated with increase HDAC1 and HDAC2 levels both of which are part of MeCP2 repressor complex [54]. Recent research suggests that the MS induced pathological production of MeCP2 may be the result of epigenetic effects. For example, recent epigenetic studies involving changes in DNA methylation and histone acetylation have also linked MeCP2 to MS [56,57]. Conversely, the MeCP2E2 isoform may be involved in myelin repair by promoting BDNF production by activating the BDNF gene (Figure 1B). However, detailed research in this newly evolving area is lacking, thus additional studies are required before we can draw any definitive conclusions in this regard.

Interestingly, MeCP2 has also been shown to be involved in regulation of myelin gene expression thereby governing the structural integrity of myelin [51,58]. A recent study in MeCP2 knock down cultured oligodendrocytes identified its effects on the transcriptional induction of myelin proteins [58]. These studies suggest that MeCP2 may be critical component that regulates the structural integrity of myelin by altering the ratios of the myelin structural proteins that comprise myelin.

To the best of our knowledge, there are no other studies that have evaluated the differential expression of the two biologically active but different isoforms of MeCP2 in experimental autoimmune encephalomyelitis (EAE) animal model of MS (Figure 2). Given the wealth of literature linked MeCP2 to myelin damage in neurological conditions such as Rett Syndrome [53,59,60], it became apparent the importance of conducting similar research studies in other white matter disorders such as MS. Thus, this is the first study to demonstrate the pathological effects of the MeCP2E1 in regard to its ability to suppress the expression of BDNF resulting in severe neurological disability scoring (NDS) and associated myelin damage. Specifically, our current research study examines the temporal gene expression of MeCP2E1, MeCP2E2 and BDNF in SC tissue obtained from a myelin oligodendrocyte glycoprotein (MOG)-induced model of EAE. In addition, we correlated these temporal changes in gene expression with the temporal changes in NDS during the acute and chronic phases of disease progression.



Animal Group	Treatment [via]	Days	Clinical Score
EAE	MOG_{35-55} + CFA [SQ]	0 dpi	NDS
	PTX [IP]	0 & 1 dpi	
AC	CFA [SQ]	0 dpi	None NDS
	PTX [IP]	0 & 1 dpi	
NC	No treatment	----	None NDS

Figure 2. Experimental autoimmune encephalomyelitis (EAE) induction by myelin oligodendrocyte glycoprotein (MOG). Our EAE animals were immunized with 200 µg $MOG_{35–55}$ in 200 µL of complete Freund's adjuvant (CFA) subcutaneously (SQ) on Day 0. Active control (AC) animals only received the CFA adjuvant. Both EAE and AC animals received intraperitoneal (IP) injections of pertussis toxin (PTX) on Days 0 and 1. Naïve control (NC) did not receive any treatment. EAE = experimental autoimmune encephalomyelitis, AC = active control, NC = naïve control, MOG = myelin oligodendrocyte glycoprotein, CFA = complete Freund's adjuvant, PTX = pertussis toxin, NDS = neurological disability scoring, dpi = days post induction, SQ = subcutaneous, IP = intraperitoneal.

Our current study identifies the importance of the pathological induction of MeCP2E1 in an EAE animal model of MS. Our results suggests that EAE-induced expression of MeCP2E1 (transcriptional repressor of BDNF) contributes to the sub-optimal levels of BDNF resulting in sustained elevated NDS with associated myelin damage. Our research also suggests the pathogenic involvement of immune system mediated induction of MeCP2E1 repression of BDNF. Based on our previously published findings in this area, we believe that this EAE-induced MeCP2E1 expression contributes in part to the disruption of the homeostatic signaling balance between cytokines, chemokines and neurotrophins resulting in enhanced neurological disability with associated myelin damage.

2. Results

2.1. Neurological Disability Scoring (NDS)

All animals in the EAE groups underwent NDS. All animals in the NC and AC experimental groups displayed a normal NDS of zero. Based on our NDS analysis, we observed an acute disease phase that became apparent during Days 9–18 post-induction. We also observed a chronic disease phase that started between Days 18 and 45 post-induction. Our identified phases of disease progression are consistent with other researchers that have used the same MOG model of EAE [2]. Specifically, we identified that during the acute phase animals begin to develop mild clinical symptoms by Day 10 post-induction (tail weakness or paralysis) [61] (Figure 3). By Days 12–13 post-induction, all animals experience a full range of clinical neurological deficits such as tail and forelimb weakness, loss of bladder control and hind-limb paralysis. As the disease characteristically progresses, the mice enter into a slight remission and regain motor function by Day 18 post-induction. The chronic disease phase is followed by a second peak of neurological disability (associated with de-myelination) at 28–30 days post-induction with another slight remission phase identified from Days 39–45 post-induction. The control groups (NC and AC) did not show any clinical signs of disability (data not shown).

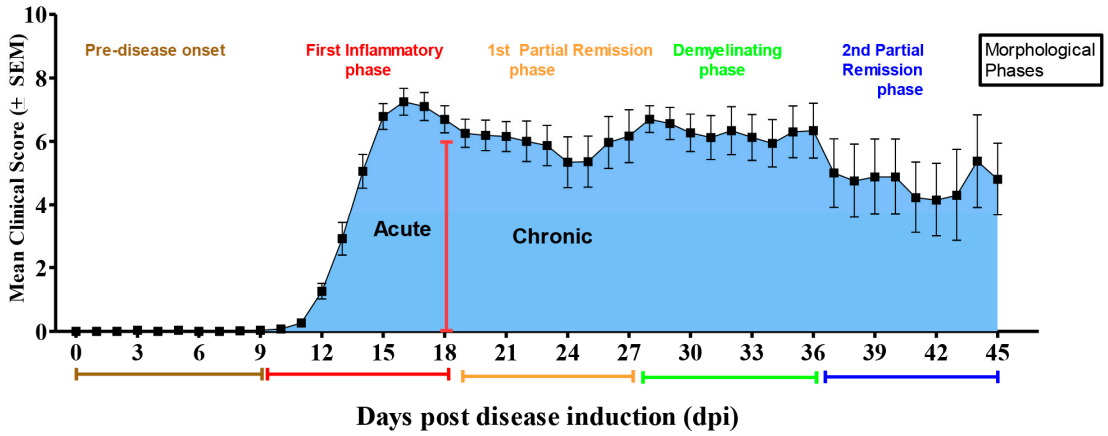


Figure 3. Clinical course of EAE-induced neurological disability in MOG-induced EAE mice. Preliminary results of mean neurological disability scores recorded in MOG-induced EAE mice at different time points of disease progression. For example, Days 3, 6, and 9 (pre-disease onset), Days 12, 15, and 18 (first inflammatory phase prior to de-myelination), Days 21, 24 and 27 (during first partial incomplete remission), Days 30, 33, and 36 (demyelinating phase), and Days 39, 42 and 45 (during the second period of partial incomplete remission: re-myelination phase). Mean global neurological disability scores were obtained following assessment of all six specific clinical domains. Neurological disability scores (NDS) range from a score of 0 (no disability) to 15 (maximal disability). Our preliminary results indicate that MOG-induced EAE mice exhibit clinical signs of the disease activity at ~11 days after the initial immunization (disease onset phase) that peaked at approximately Days 17 (pre-demyelinating disease phase) and 27 (de-myelinating disease phase). We also observed the remission (re-myelinating phase) at Day 21.

2.2. mRNA Expression of MeCP2E1 and MeCP2E2 Isoforms in the SC

In order to determine which MeCP2 isoform contributes to the regulation of BDNF during EAE disease course, we quantified the changes in MeCP2E1 and MeCP2E2 gene expression in the SC. Quantitative real time polymerase chain reaction (qRT-PCR) analysis was conducted on SC tissue isolated from the three experimental groups (EAE, NC and ACs), at the pre-determined experimental time points (Figure 4A). The MeCP2E1 mRNA expression was assessed in parallel with that of the housekeeping gene (GAPDH). Following ΔC_t analysis, EAE animals (red bar) show a significant increase of MeCP2E1 expression in SC over NC (black bar) and AC (blue bars) animal groups at 12, 15 (acute disease phase) and 21 dpi (chronic disease phase). However, NC and AC do not show significant difference at all different time points. We used the same method to evaluate gene expression for MeCP2E2 in SC on our three experimental groups (EAE, NC and ACs), at the pre-determined experimental time points (Figure 4B). However, we observed no significant differences in expression among our groups.

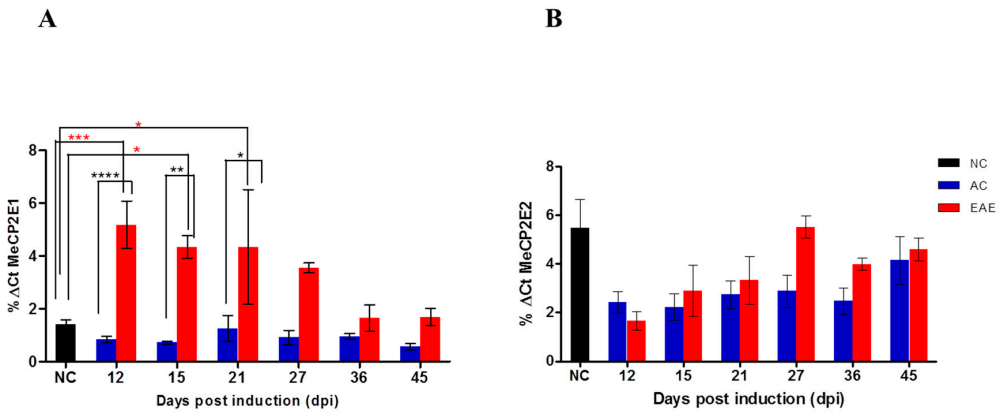


Figure 4. RNA expression of MeCP2 isoforms in the Spinal Cord (SC). (**A**) Quantitative real time polymerase chain reaction (RT-PCR) shows MeCP2E1 mRNA gene expression in SC at different times in the disease progression. $\%\Delta C_t$ analysis of real time RT-PCR of MeCP2E1-EAE animals show a significant increase of MeCP2E1 expression in SC over NC animal groups at 12, 15 and 21 dpi. EAE animals show a significant increase of MeCP2E1 expression in SC over AC at 12, 15 and 21 dpi. In comparison, NC and AC do not show significant difference at all different time points; (**B**) Quantitative RT-PCR shows MeCP2E2 mRNA gene expression in SC at different times in the disease progression. $\%\Delta C_t$ analysis of real time RT-PCR of MeCP2E2 expression in SC do not shows significant difference in mRNA expression between the NC control animal and EAE group. (**** $p < 0.0001$; *** $p < 0.001$; ** $p < 0.01$; * $p < 0.05$). (Two-way ANOVA followed by Bonferroni's post *hoc* test). Values are mean ± SEM.

2.3. BDNF Gene and Protein Expression in SC

BDNF is involved in re-myelination and is regulated by MeCP2 [35,36]. Therefore, we conducted gene and protein quantification of BDNF in SC tissue obtained from NC, AC and EAE animals to determine if regulation of BDNF expression is isoform specific (Figure 5). ELISA was employed to quantify differential protein expression for BDNF. For each sample, results are given as pg BDNF per 30 μg total protein. We identify significant differences between NC, and EAE (** $p < 0.01$) at Day 27 post-induction that corresponds to the second relapse phase of the disease and also at Day 45 (* $p < 0.05$) that corresponds to second partial remission phase of the disease (Figure 3). In addition, there are significant differences between EAE and AC (*** $p < 0.001$) at Day 45 post-induction (Figure 5A). For comparison we measured BDNF gene expression in SC, via qRT-PCR. Significant differences exist between the NC animals (black bars) and EAE (red bars) at Days 12 (**** $p < 0.0001$), 15 (**** $p < 0.0001$), 21 (** $p < 0.01$) and 27 (*** $p < 0.001$) post-induction. There are also significant differences between EAE and AC (blue bars) at Day 36 and 45 post-induction (** $p < 0.01$). Finally, NC and AC showed significant differences (**** $p < 0.0001$) at all-time points (Figure 5B).

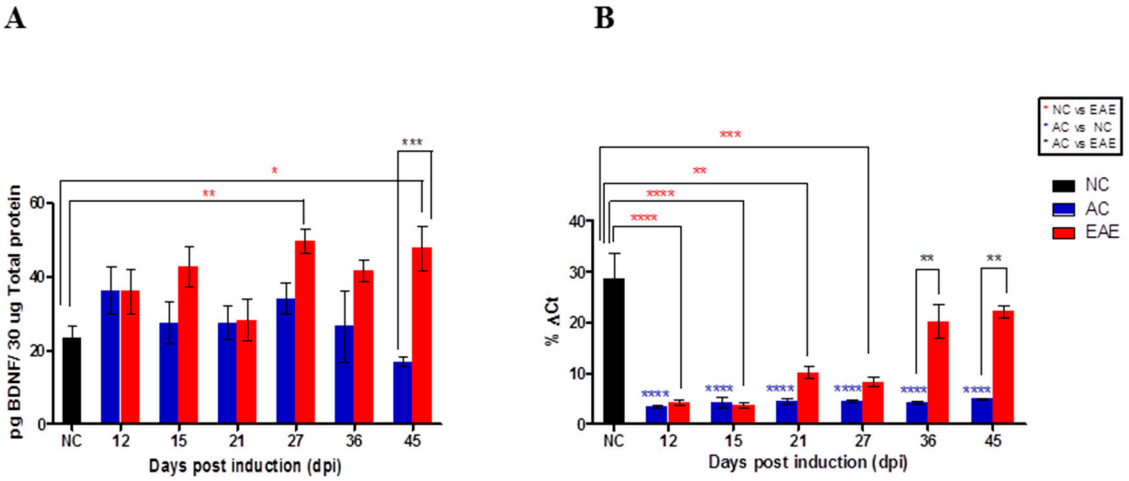


Figure 5. Transcript and protein expression of BDNF in the spinal cord (SC). (**A**) ELISA quantification of BDNF expression in the SC. BDNF expression in the SC was quantified using ELISA. There is significant differences between NC and EAE at Day 27 (** $p < 0.01$) and 45 (* $p < 0.05$) and between AC and EAE (*** $p < 0.001$) at Day 45. (Two-way ANOVA followed by Bonferroni's post hoc test). Values are mean ± SEM; (**B**) RT-PCR quantification of BDNF mRNA expression in the SC. %ΔCt analysis of real time RT-PCR of BDNF expression in SC shows significant differences in mRNA expression between the NC animals (black bars) and EAE (red bars) at 12, 15, 21 and 27 dpi. EAE group show significant increase compared to AC animal (blue bars) at 36 and 45 dpi. There are significant differences between NC and AC at all-time points. (**** $p < 0.0001$; *** $p < 0.001$; ** $p < 0.01$; * $p < 0.05$). (Two-way ANOVA followed by Bonferroni's post hoc test). Values are mean ± SEM.

2.4. MeCP2E1 and MeCP2E2 Protein Expression in SC during Acute and Chronic Disease Phase of EAE

To compare MeCP2E1 and MeCP2E2 protein expression during the acute and chronic phase in SC, we conducted Western blot. Quantification of MeCP2E1 protein expression shows a significant increase for EAE over NC+ AC animal groups at 15 (* $p < 0.05$) and 21 dpi (*** $p < 0.001$) (Figure 6A). Furthermore, EAE animals show a significant increase of MeCP2E2 expression in SC over NC + AC animal groups at 12 (**** $p < 0.0001$), 15 (** $p < 0.01$) and 36 dpi (**** $p < 0.0001$) (Figure 7B).

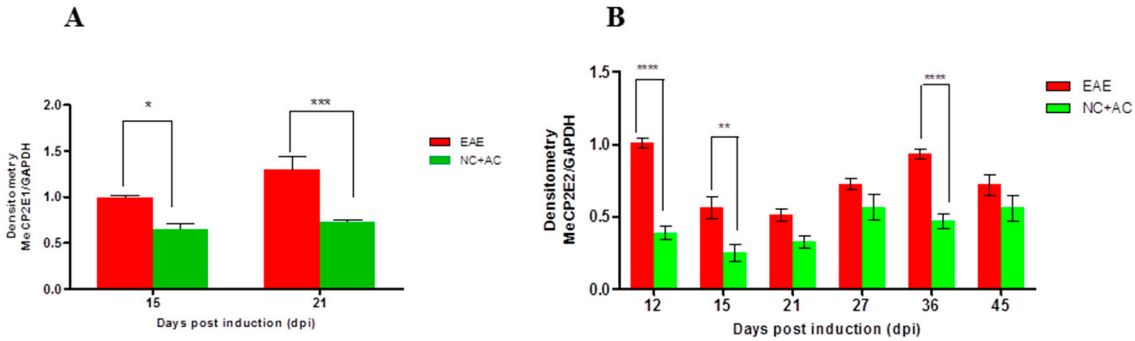


Figure 6. MeCP2E1 and MeCP2E2 protein expression in SC during acute and chronic disease phase of EAE. (**A**) Western blot quantification of MeCP2E1 expression in SC. Results are shown as the ratio of MeCP2E1/GAPDH. EAE animals show a significant increase of MeCP2-E1 expression in SC over NC+ AC animal groups at 15 and 21 dpi. (*** $p < 0.001$; * $p < 0.05$). (Two-way ANOVA followed by Bonferroni's post hoc test). Values are mean + SEM; (**B**) Western blot quantification of MeCP2E2 expression in SC. Results are shown as the ratio of MeCP2E2/GAPDH EAE animals show a significant increase of MeCP2-E2 expression in SC over NC+ AC animal groups at 12, 15 and 36 dpi. (**** $p < 0.0001$; ** $p < 0.01$). (Two-way ANOVA followed by Bonferroni's post hoc test). Values are mean ± SEM.

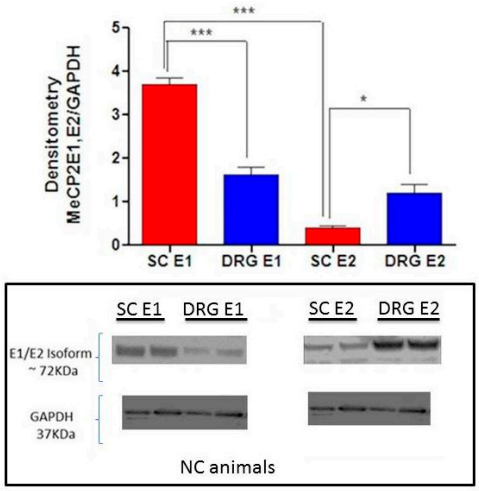


Figure 7. Baseline MeCP2E1 and MeCP2E2 expression in DRG and SC of NC animals. Results are shown as the ratio of MeCP2E1/GAPDH and MeCP2E2/GAPDH. There are significant differences between MeCP2E1 (*** $p < 0.001$) and MeCP2E2 (* $p < 0.05$) expression level in DRG and SC. Relative expression of MeCP2E1/ MeCP2E2 is 9.25 in SC, whereas it is 1.36 in DRG. SC E1 = protein expression of MeCP2E1 in spinal cord, DRG E1 = protein expression of MeCP2E1 in dorsal root ganglia, SC E2 = protein expression of MeCP2E2 in spinal cord, DRG E2 = protein expression of MeCP2E2 in DRG.

2.5. Baseline Protein Expression of MeCP2E1 and MeCP2E2 Isoforms in Spinal Cord (SC) and Dorsal Root Ganglia (DRG) in Naïve Control (NC) Animals

In order to compare protein expression of MeCP2E1 and MECP2E2 isoforms in the DRG and SC, we conducted WB analysis. Quantification of MeCP2E1 and MeCP2E2 protein by WB densitometry in the SC and DRG indicates significant differences between MeCP2E1 (*** $p < 0.001$) and MeCP2E2 (* $p < 0.05$) expression level (Figure 7). Relative expression ratio of MeCP2E1/MeCP2E2 is 9.25 in SC, versus a ratio of 1.36 in DRG.

3. Discussion

At present, the exact pathophysiological molecular mechanisms underlying MS-induced neurological deficits due to associated myelin damage is still unknown. However, BDNF has been suggested as one of the lead biological target molecules due to its well established beneficial role in myelin repair [19–21,62]. For example, BDNF has been shown to regulate OPCs via molecular signaling through TrkB receptors to induce their proliferation, migration and differentiation [18]. Recent MS research has turned to other white matter neurological disorders such as Rett Syndrome, to provide insight into the additional factors that may regulate the transcriptional expression of BDNF. Based on the research conducted in Rett Syndrome, researchers have only recently identified MeCP2 as an upstream transcriptional repressor of BDNF [35,37,52,53].

In our current study we hypothesized that transcriptional repression of BDNF by the EAE-induced upregulation of MeCP2E1 disrupts homeostatic signaling network equilibrium between inflammatory cytokines, chemokines and neurotrophins resulting in elevated NDS due to associated myelin damage. To address this issue we used a MOG-mouse model of EAE. EAE animals characteristically exhibited two distinct disease phases, acute and chronic. The acute phase includes inflammation, displaying early signs of myelin damage that leads to peak NDS at Day 18 followed by a chronic demyelinating disease phase that encompasses Days 18–45 (Figure 3). The disease pattern displayed in our animal model is consistent with the relapsing remitting models previously described in other studies [63].

Based on our current study, we are the first researchers to show the differential expression of the biologically active MeCP2E1 and MeCP2E2 isoforms at the mRNA level in a MOG-induced EAE model of MS. In addition, we are also the first to demonstrate that MeCP2E1 and MeCP2E2 isoforms regulate

the temporal changes in BDNF gene and protein expression. Our results demonstrated significant elevations in the mRNA expression levels of the MeCP2E1 isoform (relative to NCs and ACs) during the first inflammatory acute phase of disease prior to de-myelination (EAE 12–18) (Figure 4A). These results correlated with our observed significant decrease in BDNF mRNA expression (Figure 5B) relative to NC's that were also associated with elevated NDS during this same time period (Figure 3). Thus, our results suggest that the EAE-induced MeCP2E1 expression, contributed to the repressed BDNF expression resulting in sustained elevated NDS known to occur during an EAE-induced attack on CNS myelin. According to our reported data, the progressive decreasing levels of MeCP2E1 isoform from EAE 21–27 (first slight remission phase) appeared to promote the marked increase in BDNF mRNA expression at these later time points. However, since the mRNA levels for BDNF did not rise to significant levels above that of NC's, we believe that these sub-optimal levels failed to facilitate re-myelin repair resulting in sustained elevations in NDS even in the later stages of disease. (Figures 3, 4A and 5B). Although, our results show that MeCP2E1 isoform mRNA expression continually decreased during the chronic phase of disease progression (EAE 30–36), the lower levels of MeCP2E1 were still higher than those of NC and AC animals. Thus, we believe that the persistent elevated MeCP2E1 levels that even extend out to the later time points of the chronic disease phase (EAE 39–45) are responsible in part for the continued repression of BDNF (Figure 5) that results in the sustained elevations in NDS with associated myelin damage. Hence, the EAE animals never achieve full neurological recovery, as evident by the persistent elevations in NDS that never returns to baseline (Figures 3, 4A and 5A,B). Overall, our findings suggest that the persistent elevated levels of MeCP2E1 in the SC, creates a hostile environment that prevents the localized production of BDNF protein from ever reaching the required optimal physiological levels that are beneficial for myelin repair. Based on the very limited availability of antibodies the protein analysis for the MeCP2E1 and MeCP2E2 isoforms were not conducted. However, recent research involving the use of a C-terminal anti-MeCP2 antibody raised to the C-terminus may prove to be of significant importance to other researchers conducting this type of analysis [47].

During the acute disease phase (EAE 12 and EAE 15), the MeCP2E2 protein expression levels are elevated relative to NC + AC in an attempt to increase BDNF production and facilitate re-myelination and/or myelin repair during the initial EAE insult (Figure 6B). Similarly, during the chronic disease phase, MeCP2E2 protein levels remain elevated with a second significant peak at ~EAE 36, which corresponds to a significant surge of BDNF protein production in an attempt to increase BDNF production and facilitate re-myelination and/or myelin repair. Overall, the elevated protein levels of MeCP2E2 during the entire course of EAE attempt to counteract the damaging BDNF repressive effects of MeCP2E1. However, due to high MeCP2 E1/E2 ratio of 1.6 and 2.6, during the acute and chronic phase (EAE 15 and 21) (Figure 6A), MeCP2E2 protein levels never fully reach the desired levels to accomplish complete BDNF induced re-myelination and/or myelin repair with associated full neurological recovery. Thus, EAE animals are left with residual neurological deficits and at best only achieve partial remissions during the course of the disease.

While the differential expression of two isoforms of MeCP2 in the SC compared to the DRG is of interest (Figure 7), this observation could also be due to differential representation of neuronal vs. non-neuronal nuclei. However, detailed studies focused on identifying the exact cellular sources of the isoforms including manipulation of the expression of the different isoforms in relevant cell types represent an essential research direction for future studies that include SC and DRG tissues. These studies will be instrumental in confirming the importance of the DRG-SC anatomical connection in the myelin repair process. Although our current study did not evaluate the anterograde transport of BDNF from DRG to SC, our previous publication demonstrated BDNF transport from DRG to SC by kinesin protein that support this concept [8]. Thus, the ratio of MeCP2E1 versus MeCPE2E2 in the DRG and SC may be of critical importance as a useful clinical diagnostic test as a measure of the degree of neurological disability and associated myelin damage.

Studies have suggested that MeCP2 induced transcriptional regulation of BDNF is dependent on several factors including extracellular calcium [35], DNA methylation [37] status and phosphorylation of MeCP2 at serine 421 during neuronal depolarization, all leading to MeCP2 release from the promoter and subsequent transcription of BDNF [35,52]. Martinowich et al. showed this is associated with reduced methylation at promoter site [37]. Thus, their research showed that MeCP2 regulation of BDNF gene is context dependent. Furthermore, recent studies confirm the complexity by which the BDNF gene is regulated. For example, researchers have suggested that the regulation of the BDNF gene depends on the specific cell types, brain structure and promoter region [53]. Hence, although our research demonstrates an association between MeCP2E1 in regards to BDNF repression, it is clearly not the only factor involved in the regulation of the BDNF gene. Adding further complexity to this issue, other researchers have shown the transcriptional activation of BDNF by MeCP2 through cAMP response element-binding protein (CREB) activator complex (Figure 1B) [45,64]. However, these types of studies did not differentiate between the two biological isoforms of MeCP2. Our results show that the MeCP2E2 isoform may have a beneficial role that involves the activation of the BDNF gene. Hence, resultant severe neurological disability caused by associated myelin damage occurs from the EAE-induced increase in the MeCP2E1 isoform relative to MeCP2E2. For instance, the increased expression ratio of MeCP2E1 versus MeCP2E2 has also been reported in the brain tissue obtained from a mouse model of Rett syndrome [65]. However, detailed research in the area of differential biological activity between the two isoforms is just starting to evolve. We must also realize that the BDNF gene is very complex, generating multiple transcripts by splicing of 8 exons, each under a different transcriptional promoter [44]. Hence, additional research is required in specific regard to the mRNA levels of all BDNF splice variants. In addition, further research is also required in regard to the transcriptional regulation by MeCP2E1 and MeCP2E2 at the different BDNF promoter regions. These additional types of studies are required to unveil the exact mechanisms by which the BDNF gene is regulated by MeCP2 and other molecules.

Our research at the transcript level, also aimed to evaluate the role of MeCP2E2 isoform in regulation of BDNF. We observed that during the first inflammatory acute disease phase prior to de-myelination (EAE 12–18), the MeCP2E2 isoform mRNA expression levels are markedly low relative to NCs (Figure 4B). Interestingly, the marked reduced expression levels of MeCP2E2 correspond to the reduced BDNF levels during the acute disease phase (EAE 12–18) (Figure 5). However, as the EAE disease progressions, our results identify that the MeCP2E2 mRNA levels continue to increase during EAE 21–27 (chronic disease phase) peaking at EAE 27 (Figure 4B). We speculate that the gradual increase in the MeCP2E2 isoform during this time period represents a failed attempt to activate the BDNF gene by the MeCP2E2 isoform. We also speculate that the failure of MeCP2E2 to reach significant levels to counteract the pathological MeCP2E1 expression result in the sustained elevated NDS throughout the acute and chronic phases of disease. Our results also identify that the reduced MeCP2E2 expression during the chronic disease phase (EAE 30–36) (Figure 4B) corresponds in part with the reduction in BDNF expression (Figure 5A). However, this is a weak correlation and further research in regard to the effects of MeCP2E2 activation of BDNF are required to conclusively determine this link as cause or effect. Interestingly, our data presented for MeCP2E2 expression in the chronic disease phase (EAE 39–45) (Figure 4B) identify a marked increase in MeCP2E2 mRNA, that correspond more closely as we would have expected with the reported increases in BDNF protein during the same time period (Figure 5A). Irrespective, additional research in this area is required before definitive conclusions can be drawn in regard to MeCP2E2 effects on BDNF expression.

Although MeCP2E1 and MeCP2E2 isoforms have over 95% similar sequence homology, other studies support our current research findings which suggest the isoforms may have differential biological activity [49]. For example, it has recently been reported that mutations in exon 1 [66,67] have been suggested to implicate MeCP2E1 in causing the white matter damage that is known to occur in Rett syndrome. Furthermore, other studies have also confirmed the differential effects on different target gene expression profiles that are regulated by the MeCP2E1 and MeCP2E2 isoforms [68].

For instance, Milacic et al. evaluated different gene expression patterns for MeCP2 isoforms in neuronal cells over-expressing predominantly MeCP2E1 or MeCP2E2 [68]. They found that many genes involved in axon genesis, neuronal differentiation and tyrosine kinase receptor signaling are regulated by MeCP2E1 [68]. In addition, they also found that genes involved in tyrosine kinase signaling and immune response were down regulated by MeCP2E1 [68]. However, the MeCP2E2 isoform mostly regulates those genes involved in chromatin organization and transcriptional regulation [68]. These functional biological differences may be related to differences in N-terminal sequence of two isoforms that causes shorter half-life for MeCP2E2 [69] and different DNA binding specificity. As a result, the functional differences reported for each MeCP2 isoform may also account for the suggested differential role of each isoform in regard to myelin repair. Hence, targeted attenuation of the pathological MeCP2E1 isoform warrants further investigation to determine the merit in designing epigenetic interventional strategies aimed at restoring a normalized balance between MeCP2E1 and MeCP2E2. However, despite our intriguing results, we also realize that the EAE-induced changes identified for MeCP2 and BDNF may be a cause rather than a consequence of the associated myelin damage following an immune system attack on CNS myelin. In addition, we also realize the importance of identifying the specific cellular source of MeCP2 will be instrumental in designing targeted treatment strategies to promote myelin repair. Thus, future studies are required in these areas in order to help us establish a stronger connection for MeCP2 that is causative rather than consequential.

Research suggests that both mutations and duplication in MeCP2 could lead to neurodevelopmental abnormalities [70,71]. Thus, it is imperative to keep MeCP2 in a narrow range for normal neurological functioning. Our study also provides supportive evidence in regard to the potential importance of the MeCP2E1/MeCP2E2 ratio in EAE model of MS. The present study suggests that the pathological over-expression of MeCP2E1 represses BDNF resulting in a disruption of the homeostatic signaling equilibrium between cytokines, chemokines and neurotrophins resulting in incomplete re-myelination and/or myelin repair with corresponding neurological disability.

Although the tissue heterogeneity could be an alternative explanation for our results, there are a number of feasible explanations for the changes in expression that are observed that should be considered. For example, the mRNA analysis in the study is performed on whole tissue that is undergoing dramatic inflammation and rearrangement during this experiment. It is very possible that the changes in MeCP2 isoform expression or BDNF expression that are observed arise from changes in cellular composition that occur due to the inflammation. For example, the MeCP2E1 isoform is specifically enriched in neurons, so if the tissue assessed by protein analysis is infiltrated with a large amount of immune cells, the relative contribution of MeCP2E1 relative to loading controls would be expected to go down. The cellular source of MeCP2 in the SC has been evaluated in other studies which have identified astroglia and neurons as the key sources of MeCP2 [72]. However, the focus of this manuscript was to present the molecular changes in the biological targets that our result shows were involved in causing neurological disability through the molecular mechanisms that facilitate myelin damage. Thus, we did not conduct detailed immunohistochemistry and/or in situ hybridization to identify the specific cellular sources of the molecular changes at the gene and protein level. However, identifying the specific cellular source(s) of these molecular changes represents the next phase of research that is required to be conducted now that we have identified and confirmed the changes in the biological targets we believed were responsible for promoting myelin damage. Furthermore, although we have provided data that suggest MeCP2E1 is involved in the transcriptional repression of BDNF, further studies involving MeCP2E1 knockouts must be conducted to confirm its regulation of BDNF in an animal model of MS.

4. Materials and Methods

4.1. Induction of EAE

The MOG mouse model of EAE is the preferred model of MS [2,73,74]. Ten-week-old C57 BL/6 mice were randomly assigned to either: naïve control (NC), active control (AC) and MOG-induced EAE. A total of n = 4 mice were used per time point per group. As per our standard in house protocols [6,7,9,11], EAE mice were immunized subcutaneously (SQ) with 200 µg MOGp35–55 in 200 µL of Complete Freund's adjuvant (CFA) at the lower/upper back at Day 0 (induction kits from Hooke Laboratories (Lawrence, MA 01843, USA) (Cat, EK-2110)). Animals received two intraperitoneal (IP) injections of pertussis toxin (PTX: List Biological Laboratories; #179B) (0.2 µg in 100 µL of PBS at Days 0 and 1) to open up the blood brain barrier and facilitate the entry of pathogenic T cells to the CNS. AC mice received all the same treatment as the EAE mice with the exception of the omission of the MOG antigen. NC animals did not receive any treatment (Figure 2). The CFA emulsion contains killed mycobacterium tuberculosis (MT) H37Ra in incomplete Freund's adjuvant (FA) to enhance the immune system response to sensitization. The emulsion was administered SQ at two sites in the upper and lower back area. A 0.1 mL SQ dose of the emulsion was injected at each site (0.2 mL/mouse) at Day 0. The DRG and SC tissue were collected during the acute phase at Days 12 and 15 (first inflammatory phase prior to de-myelination). In addition, DRG and SC tissue were collected during the chronic phase of the disease: Days 21 and 27 (during first remission), Day 36 (de-myelinating phase), and Day 45 (during the second period of remission: re-myelination phase). The DRG and SC tissue were removed to conduct molecular gene and protein analysis. Female mice were specifically chosen because females are more predisposed to be affected by MS than males [75]. The AC and EAE groups were assessed daily for neurological disability until sacrificed. NDS were determined from mean clinical scores measured from a score of 0 (no disability) to 15 (maximal disability) [7]. The total score is the sum of the following individual scores obtained for each of the 6 specified clinical domains, according to the following specifications: tail: 0 = normal, 1 = weakness or partial paralysis, 2 = limp or complete paralysis; right and left hind limbs: 0 = normal, 1 = weakness, 2 = dragging or partial paralysis, 3 = complete paralysis; right and left forelimbs: 0 = normal, 1 = weakness, 2 = unable to support weight or partial paralysis, 3 = complete paralysis; bladder: 0 = normal, 1 = incontinent. The experimental groups were sacrificed at 12, 15, 21, 27, 36 and 45 days post induction (dpi). The disease course could be divided into acute (9–18 dpi) and chronic (18–45 dpi) phase. In order to ensure consistency in regard to the degree of the MOG-induced EAE, only animals that progressed to the NDS of 4 ± 1 for the acute disease phase and 6 ± 2 for the chronic phase were included in our study. All other EAE-induced animals that did not meet the criteria were excluded from the data analysis.

All animal experiments and procedures in this study were conducted according to protocols approved by the University of Manitoba Animal Protocol Management and Review Committee, are in full compliance with the Canadian Council on Animal Care, and are in accordance with standards set forth in the 8th Edition of Guide for the Care and Use of Laboratory Animals (Protocol Reference Number: 11-067/1/2/3 (AC 10636)).

4.2. Gene/Protein Assay

SC and DRG tissue were harvested at pre-determined time points for gene and protein expression analysis of MeCP2E1, MeCP2E2 and BDNF. Freshly harvested DRG and SC tissue were placed in RNA later stabilization solution (Ambion Cat#AM7020, Burlington, ON, Canada) until being processed. Whole DNA/RNA and protein was purified using commercially available kits (AllPrep DNA/RNA/protein, Qiagen, Toronto, ON, Canada) as described in our previous publications [6,8,51].

4.3. Quantitative Real Time Reverse Transcription Polymerase Chain Reaction (qRT-PCR)

RNA purified from SC tissue, converted into cDNA using the iScript™ cDNA Synthesis Kit #170-8891, Bio-Rad and Bio Rad S1000 Thermal cycler instrument (Hercules, CA, USA). Final

concentration of cDNA used in qRT-PCR was 5 ng/μL. The PCR reaction was performed by the CFX96 real-time PCR detection system using SsoFast™ EvaGreen® Supermix (#172-5202) following manufacturers protocols (Bio-Rad, Hercules, CA, USA). MeCP2E1 primers were forward: 5′-GGAGAGAGGGCTGTGGTAAA-3′; reverse: 5′-CTGGAGATCCTGGTCTTCTGA-3′ at annealing temperature of 56 °C. MeCP2E2 primers were forward: 5′-GGAGGAGAGACTGCTCCATAAA-3′; reverse: 5′-GGAGATCCTGGTCTTCTGACTT-3′ at annealing temperature of 59 °C. BDNF primers were forward: 5′-AGCTGAGCGTGTGTGACAGTATTAG-3′; reverse: 5′-GGGATTACACTTGGTCT CGTAGAAA-3′ at annealing temperature of 56 °C. The Δ*C*t method was applied to determine differences in gene expression levels after normalization to the arithmetic mean of glyceraldehyde 3-phosphate dehydrogenase (GAPDH) as an internal standard.

4.4. Western Blot (WB) Analysis

For our NC group, we conducted WB analysis for MeCP2E1 and MeCP2E2 isoforms. DRG and SC tissues were homogenized and total supernatant protein concentration was determined for each sample using Bicinchoninic Acid (BCA) protein assay kit (Novagen, CN: 71285-3, Etobicoke, ON, Canada). For each sample, 60 μg total protein was separated by 10% Tris-Glycine gradient SDS-PAGE (Thermoscientific, CN: 0025269, Burlington, ON, Canada) at 120 V for 1 h and electrophoretically blotted onto a PVDF membrane (Immobilon, CN: IPFL00010, Etobicoke, ON, Canada) for 1 h at 0.35 A. The membranes were blocked in skim milk in TBS-T and then treated with primary antibody including: Anti-MeCP2 Isoform B polyclonal anti rabbit IgG (Cat No. ABE 333 Millipore, Etobicoke, ON, Canada) 1/500, Anti-MeCP2 E2 chicken poly clonal antibody custom-made by Dr. Rastegar (1/100), or rabbit polyclonal IgG against GAPDH (1:1000, Santa Cruz, CN: sc-25778, Mississauga, ON, Canada) overnight at 4 °C. GAPDH was utilized as a loading control to ensure equivalent amounts of protein were loaded. The primary anti-MeCP2E1 and MeCP2E2 antibodies were intended to detect the 75 kDa isoform, while the primary anti-GAPDH antibody was intended to detect 37 kDa GAPDH. After incubation with primary antibodies, membranes were washed with TBS-T and incubated with secondary antibodies. The secondary antibodies used were peroxidase-conjugated donkey anti-rabbit IgG (1:10,000, Millipore, CN: AP182P) against the anti-MeCP2E1 and GAPDH antibody and peroxidase-conjugated donkey anti-mouse IgY (1:2000, Thermoscientific, SA1-72004, Burlington, ON, Canada) against the anti-MeCP2 E2 antibody. The antigen-antibody complexes were detected using ECL detection reagent (Pierce, CN: PI32209, Burlington, ON, Canada). Membranes were exposed to chemiluminescence. However, for MeCP2E1 and E2 different exposure time were applied because of difference of efficiency between these two antibodies. Densitometry was performed using a FluorChem 8900 scanner (Alpha Innotech, Santa Clara, CA, USA) with Alpha Ease FC software. Densitometry analysis was conducted with ImageJ (verison 1.48). The individual MeCP2E1, MeCP2E2 and GAPDH band densities for each sample were normalized to an internal standard. The sample and loading control density ratios obtained relative to the internal standard were subsequently used to calculate the relative density ratio of MeCP2E1 and MeCP2E2 respectively relative to GAPDH.

4.5. Quantitative Enzyme-Linked Immunosorbent Assay (ELISA) Analysis

Total protein was extracted and protein concentration was determined as described above by BCA assay [10]. Protein concentration was adjusted to 30 μg in 100 μL total sample volume. Sandwich-format ELISA was performed using a BDNF Emax ImmunoAssay System (Promega, Madison, WI, USA, cat# G7611) according to manufacturer's instructions. BDNF protein concentration was interpolated from a standard curve with a range of 7.8–500 pg/mL.

4.6. Statistical Analysis

Statistics was performed using GraphPad Prism version 5.04 for Windows, GraphPad Software, San Diego, CA, USA. Data from all samples analyzed from each animal group are reported as mean ± standard error of the mean (SEM). Statistical analysis for ELISA, WB and Real Time-PCR

(RT-PCR) was performed using two-way analysis of variance (ANOVA) followed by a Bonferroni post hoc test.

5. Conclusions

The focus of this manuscript was to present the molecular changes in the biological targets that were involved in causing neurological disability through the molecular mechanisms that facilitate myelin damage. However, we also realize that the EAE-induced changes identified for MeCP2 and BDNF may be a cause rather than a consequence of the associated myelin damage following an immune system attack on CNS myelin. Although we have provided data that suggest MeCP2E1 is involved in the transcriptional repression of BDNF, further studies involving MeCP2E1 knockouts must be conducted to confirm its regulation of BDNF in an animal model of MS. Furthermore, our results suggest the potential importance of tracking the expression ratios between MeCP2E1 and MeCP2E2 isoforms. Henceforth, a potential therapeutic implication of this research would be to design a screening test in those patients pre-disposed to the known risk factors for MS and subject them to biological testing of the MeCPE1/MeCP2E2 ratio. For example, patients presenting with a high ratio may be at greater risk for going on to develop MS and therefore, could serve as a useful diagnostic screening test that could be added to the battery of diagnostic tests currently used to diagnose MS patients [76,77]. Thus, MeCP2 represents a key biological target molecule where epigenetic interventional strategies aimed at both DNA methylation and histone modifications could be optimized to generate a novel therapeutic drug to halt myelin damage associated with MS [78]. Therefore, studying the link between MeCP2 and BDNF and other downstream biological targets such as NGF [5,10], TNFα [6], and CX3CL1 [9] in MS may lead to new epigenetic therapeutic approaches to promote re-myelination and myelin repair in MS.

Acknowledgments: Special thanks to the Manitoba Multiple Sclerosis Research Network Organization (MMSRNO) for their continued support of advanced research in MS. The authors would also like to acknowledge the support from The Manitoba Medical Service Foundation Grant (MMSF) Canadian Paraplegic Association (CPA); University of Manitoba Research Grants Program (URGP), Bayshore Health Care Systems, College of Pharmacy at the University of Manitoba; and endMS for their continued support of research, training and education to advance our knowledge in the specialized field of MS. The authors would also like to thank Crystal Acosta, Yuewen Gong, Qingjun Huang, Jue He, Xingshun Xu, Xiaohui Li, Jiming Kong and Lan Xiao for their kind assistance with the technical aspects related to this manuscript.

Author Contributions: Tina Khorshid Ahmad was the lead researcher performing and analyzing experiments. Ting Zhou performed and analyzed protein data for MeCP2. Khaled AlTaweel performed and analyzed mRNA analysis. Claudia Cortes performed animal studies and contributed to mRNA and protein analysis. Ryan Lillico performed statistical analysis for mRNA and protein. Ted Martin Lakowski designed experiments and assisted in writing the paper. Kiana Gozda helped in writing the paper and protein extraction. Michael Peter Namaka designed the study and assisted in writing the paper. All authors reviewed the results and approved the final version of the manuscript.

Conflicts of Interest: The authors declare that they have no conflict of interest. This project was supported by the funding from the following agencies: Canadian Paraplegic Association (CPA), University of Manitoba Research Grants Program (URGP) and Bayshore Health Care Systems.

References

1. Namaka, M.P.; Ethans, K.; Jensen, B.; Esfahani, F.; Frost, E.E. Multiple sclerosis. In *Therapeutic Choices/e-Therapeutic*; Canadian Pharmacists Association Publishers, Inc.: Ottawa, ON, Canada, 2011; pp. 309–319.
2. Lacroix, S.; Hamilton, L.K.; Vaugeois, A.; Beaudoin, S.; Breault-Dugas, C.; Pineau, I.; Levesque, S.A.; Gregoire, C.A.; Fernandes, K.J. Central canal ependymal cells proliferate extensively in response to traumatic spinal cord injury but not demyelinating lesions. *PLoS ONE* **2014**, *9*, e85916. [CrossRef] [PubMed]
3. Gold, R.; Montalban, X. Multiple sclerosis: More pieces of the immunological puzzle. *Lancet Neurol.* **2012**, *11*, 9–10. [CrossRef]
4. Namaka, M.; Turcotte, D.; Leong, C.; Grossberndt, A.; Klassen, D. Multiple sclerosis: Etiology and treatment strategies. *Consult. Pharm.* **2008**, *23*, 886–896. [CrossRef] [PubMed]

5. Acosta, C.M.R.; Cortes, C.; MacPhee, H.; Namaka, M.P. Exploring the role of nerve growth factor in multiple sclerosis: Implications in myelin repair. *CNS Neurol. Disord. Drug Targets* **2013**, *12*, 1242–1256. [CrossRef] [PubMed]
6. Begum, F.; Zhu, W.; Cortes, C.; Macneil, B.; Namaka, M. Elevation of tumor necrosis factor α in dorsal root ganglia and spinal cord is associated with neuroimmune modulation of pain in an animal model of multiple sclerosis. *J. Neuroimm. Pharmacol.* **2013**, *8*, 677–690. [CrossRef] [PubMed]
7. Melanson, M.; Miao, P.; Eisenstat, D.; Gong, Y.; Gu, X.; Au, K.; Zhu, W.; Begum, F.; Frost, E.E.; Namaka, M. Experimental autoimmune encephalomyelitis-induced upregulation of tumor necrosis factor-α in the dorsal root ganglia. *Mult. Scler.* **2009**, *15*, 1135–1145. [CrossRef] [PubMed]
8. Zhu, W.; Frost, E.E.; Begum, F.; Vora, P.; Au, K.; Gong, Y.; Macneil, B.; Pillai, P.; Namaka, M. The role of dorsal root ganglia activation and brain-derived neurotrophic factor in multiple sclerosis. *J. Cell Mol. Med.* **2012**, *16*, 1856–1865. [CrossRef] [PubMed]
9. Zhu, W.; Acosta, C.; MacNeil, B.; Cortes, C.; Intrater, H.; Gong, Y.; Namaka, M. Elevated expression of fractalkine (cx3cl1) and fractalkine receptor (cx3cr1) in the dorsal root ganglia and spinal cord in experimental autoimmune encephalomyelitis: Implications in multiple sclerosis-induced neuropathic pain. *BioMed Res. Int.* **2013**, *2013*, 480702. [CrossRef] [PubMed]
10. Acosta, C.; Cortes, C.; Altaweel, K.; MacPhee, H.; Hoogervorst, B.; Bhullar, H.; MacNeil, B.; Torabi, M.; Burczynski, F.; Namaka, M.P. Immune system induction of nerve growth factor in an animal model of multiple sclerosis: Implications in re-myelination and myelin repair. *CNS Neurol. Disord. Drug Targets* **2015**, *14*, 1069–1078. [CrossRef] [PubMed]
11. Zhu, W.; Brian, C.A.; MacNeil, J.; Klonisch, T.; Cortes, C.; Doupe, M.; Gong, Y.; Namaka, M. Spinal cord brain derived neurotrophic factor (BDNF) responsive cells in an experimental autoimmune encephalomyelitis (EAE) model of multiple sclerosis (MS): Implications in myelin repair. *Res. Immunol.* **2014**, in press. [CrossRef]
12. VonDran, M.W.; Singh, H.; Honeywell, J.Z.; Dreyfus, C.F. Levels of BDNF impact oligodendrocyte lineage cells following a cuprizone lesion. *J. Neurosci.* **2011**, *31*, 14182–14190. [CrossRef] [PubMed]
13. Faraco, G.; Cavone, L.; Chiarugi, A. The therapeutic potential of hdac inhibitors in the treatment of multiple sclerosis. *Mol. Med.* **2011**, *17*, 442–447. [CrossRef] [PubMed]
14. Vondran, M.W.; Clinton-Luke, P.; Honeywell, J.Z.; Dreyfus, C.F. $BDNF^{+/-}$ mice exhibit deficits in oligodendrocyte lineage cells of the basal forebrain. *Glia* **2010**, *58*, 848–856. [CrossRef] [PubMed]
15. Linker, R.A.; Lee, D.H.; Demir, S.; Wiese, S.; Kruse, N.; Siglienti, I.; Gerhardt, E.; Neumann, H.; Sendtner, M.; Luhder, F.; et al. Functional role of brain-derived neurotrophic factor in neuroprotective autoimmunity: Therapeutic implications in a model of multiple sclerosis. *Brain* **2010**, *133*, 2248–2263. [CrossRef] [PubMed]
16. Linker, R.; Gold, R.; Luhder, F. Function of neurotrophic factors beyond the nervous system: Inflammation and autoimmune demyelination. *Crit. Rev. Immunol.* **2009**, *29*, 43–68. [CrossRef] [PubMed]
17. McTigue, D.M.; Horner, P.J.; Stokes, B.T.; Gage, F.H. Neurotrophin-3 and brain-derived neurotrophic factor induce oligodendrocyte proliferation and myelination of regenerating axons in the contused adult rat spinal cord. *J. Neurosci.* **1998**, *18*, 5354–5365. [PubMed]
18. Van't Veer, A.; Du, Y.; Fischer, T.Z.; Boetig, D.R.; Wood, M.R.; Dreyfus, C.F. Brain-derived neurotrophic factor effects on oligodendrocyte progenitors of the basal forebrain are mediated through TRKB and the MAP kinase pathway. *J. Neurosci. Res.* **2009**, *87*, 69–78. [CrossRef] [PubMed]
19. Xiao, J.; Ferner, A.H.; Wong, A.W.; Denham, M.; Kilpatrick, T.J.; Murray, S.S. Extracellular signal-regulated kinase 1/2 signaling promotes oligodendrocyte myelination in vitro. *J. Neurochem.* **2012**, *122*, 1167–1180. [CrossRef] [PubMed]
20. Wong, A.W.; Xiao, J.; Kemper, D.; Kilpatrick, T.J.; Murray, S.S. Oligodendroglial expression of TRKB independently regulates myelination and progenitor cell proliferation. *J. Neurosci.* **2013**, *33*, 4947–4957. [CrossRef] [PubMed]
21. Xiao, J.; Wong, A.W.; Willingham, M.M.; van den Buuse, M.; Kilpatrick, T.J.; Murray, S.S. Brain-derived neurotrophic factor promotes central nervous system myelination via a direct effect upon oligodendrocytes. *Neuro-Signals* **2010**, *18*, 186–202. [CrossRef] [PubMed]
22. Cellerino, A.; Carroll, P.; Thoenen, H.; Barde, Y.-A. Reduced size of retinal ganglion cell axons and hypomyelination in mice lacking brain-derived neurotrophic factor. *Mol. Cell. Neurosci.* **1997**, *9*, 397–408. [CrossRef] [PubMed]

23. Djalali, S.; Holtje, M.; Grosse, G.; Rothe, T.; Stroh, T.; Grosse, J.; Deng, D.R.; Hellweg, R.; Grantyn, R.; Hortnagl, H.; et al. Effects of brain-derived neurotrophic factor (BDNF) on glial cells and serotonergic neurones during development. *J. Neurochem.* **2005**, *92*, 616–627. [CrossRef] [PubMed]
24. Du, Y.; Lercher, L.D.; Zhou, R.; Dreyfus, C.F. Mitogen-activated protein kinase pathway mediates effects of brain-derived neurotrophic factor on differentiation of basal forebrain oligodendrocytes. *J. Neurosci. Res.* **2006**, *84*, 1692–1702. [CrossRef] [PubMed]
25. Di Nuzzo, L.; Orlando, R.; Nasca, C.; Nicoletti, F. Molecular pharmacodynamics of new oral drugs used in the treatment of multiple sclerosis. *Drug Design Dev. Ther.* **2014**, *8*, 555–568.
26. Arnon, R.; Aharoni, R. Neuroprotection and neurogeneration in MS and its animal model EAE effected by glatiramer acetate. *J. Neural. Transm.* **2009**, *116*, 1443–1449. [CrossRef] [PubMed]
27. La Mantia, L.; Munari, L.M.; Lovati, R. Glatiramer acetate for multiple sclerosis. *Cochrane Database Syst. Rev.* **2010**, *5*, CD004678.
28. Kala, M.; Miravalle, A.; Vollmer, T. Recent insights into the mechanism of action of glatiramer acetate. *J. Neuroimmunol.* **2011**, *235*, 9–17. [CrossRef] [PubMed]
29. Comi, G.; Pulizzi, A.; Rovaris, M.; Abramsky, O.; Arbizu, T.; Boiko, A.; Gold, R.; Havrdova, E.; Komoly, S.; Selmaj, K.; et al. Effect of laquinimod on MRI-monitored disease activity in patients with relapsing-remitting multiple sclerosis: A multicentre, randomised, double-blind, placebo-controlled phase IIB study. *Lancet* **2008**, *371*, 2085–2092. [CrossRef]
30. Thone, J.; Ellrichmann, G.; Seubert, S.; Peruga, I.; Lee, D.H.; Conrad, R.; Hayardeny, L.; Comi, G.; Wiese, S.; Linker, R.A.; et al. Modulation of autoimmune demyelination by laquinimod via induction of brain-derived neurotrophic factor. *Am. J. Pathol.* **2012**, *180*, 267–274. [CrossRef] [PubMed]
31. Meehan, R.R.; Lewis, J.D.; McKay, S.; Kleiner, E.L.; Bird, A.P. Identification of a mammalian protein that binds specifically to DNA containing methylated CPGs. *Cell* **1989**, *58*, 499–507. [CrossRef]
32. Zachariah, R.M.; Olson, C.O.; Ezeonwuka, C.; Rastegar, M. Novel MECP2 isoform-specific antibody reveals the endogenous MECP2e1 expression in murine brain, primary neurons and astrocytes. *PLoS ONE* **2012**, *7*, e49763. [CrossRef] [PubMed]
33. Lewis, J.D.; Meehan, R.R.; Henzel, W.J.; Maurer-Fogy, I.; Jeppesen, P.; Klein, F.; Bird, A. Purification, sequence, and cellular localization of a novel chromosomal protein that binds to methylated DNA. *Cell* **1992**, *69*, 905–914. [CrossRef]
34. Nan, X.; Campoy, F.J.; Bird, A. MECP2 is a transcriptional repressor with abundant binding sites in genomic chromatin. *Cell* **1997**, *88*, 471–481. [CrossRef]
35. Chen, W.G.; Chang, Q.; Lin, Y.; Meissner, A.; West, A.E.; Griffith, E.C.; Jaenisch, R.; Greenberg, M.E. Derepression of bdnf transcription involves calcium-dependent phosphorylation of MECP2. *Science* **2003**, *302*, 885–889. [CrossRef] [PubMed]
36. Chang, Q.; Khare, G.; Dani, V.; Nelson, S.; Jaenisch, R. The disease progression of MECP2 mutant mice is affected by the level of bdnf expression. *Neuron* **2006**, *49*, 341–348. [CrossRef] [PubMed]
37. Martinowich, K.; Hattori, D.; Wu, H.; Fouse, S.; He, F.; Hu, Y.; Fan, G.; Sun, Y.E. DNA methylation-related chromatin remodeling in activity-dependent *BDNF* gene regulation. *Science* **2003**, *302*, 890–893. [CrossRef] [PubMed]
38. Wade, P.A.; Jones, P.L.; Vermaak, D.; Veenstra, G.J.; Imhof, A.; Sera, T.; Tse, C.; Ge, H.; Shi, Y.B.; Hansen, J.C.; et al. Histone deacetylase directs the dominant silencing of transcription in chromatin: Association with MECP2 and the MI-2 chromodomain SWI/SNF ATPase. *Cold Spring Harb. Symp. Quant. Biol.* **1998**, *63*, 435–445. [CrossRef] [PubMed]
39. Jones, P.L.; Veenstra, G.J.; Wade, P.A.; Vermaak, D.; Kass, S.U.; Landsberger, N.; Strouboulis, J.; Wolffe, A.P. Methylated DNA and MECP2 recruit histone deacetylase to repress transcription. *Nat. Genet.* **1998**, *19*, 187–191. [CrossRef] [PubMed]
40. Abuhatzira, L.; Makedonski, K.; Kaufman, Y.; Razin, A.; Shemer, R. MECP2 deficiency in the brain decreases bdnf levels by rest/corest-mediated repression and increases TRKB production. *Epigenetics* **2007**, *2*, 214–222. [CrossRef] [PubMed]
41. Wang, H.; Chan, S.-A.; Ogier, M.; Hellard, D.; Wang, Q.; Smith, C.; Katz, D.M. Dysregulation of brain-derived neurotrophic factor expression and neurosecretory function in MECP2 null mice. *J. Neurosci.* **2006**, *26*, 10911–10915. [CrossRef] [PubMed]

42. Ogier, M.; Wang, H.; Hong, E.; Wang, Q.; Greenberg, M.E.; Katz, D.M. Brain-derived neurotrophic factor expression and respiratory function improve after ampakine treatment in a mouse model of rett syndrome. *J. Neurosci.* **2007**, *27*, 10912–10917. [CrossRef] [PubMed]
43. Deng, V.; Matagne, V.; Banine, F.; Frerking, M.; Ohliger, P.; Budden, S.; Pevsner, J.; Dissen, G.A.; Sherman, L.S.; Ojeda, S.R. FXYD1 is an MECP2 target gene overexpressed in the brains of rett syndrome patients and MECP2-null mice. *Hum. Mol. Genet.* **2007**, *16*, 640–650. [CrossRef] [PubMed]
44. Aid, T.; Kazantseva, A.; Piirsoo, M.; Palm, K.; Timmusk, T. Mouse and rat *BDNF* gene structure and expression revisited. *J. Neurosci. Res.* **2007**, *85*, 525–535. [CrossRef] [PubMed]
45. Chahrour, M.; Jung, S.Y.; Shaw, C.; Zhou, X.; Wong, S.T.; Qin, J.; Zoghbi, H.Y. MECP2, a key contributor to neurological disease, activates and represses transcription. *Science* **2008**, *320*, 1224–1229. [CrossRef] [PubMed]
46. Mnatzakanian, G.N.; Lohi, H.; Munteanu, I.; Alfred, S.E.; Yamada, T.; MacLeod, P.J.; Jones, J.R.; Scherer, S.W.; Schanen, N.C.; Friez, M.J.; et al. A previously unidentified MECP2 open reading frame defines a new protein isoform relevant to rett syndrome. *Nat. Genet.* **2004**, *36*, 339–341. [CrossRef] [PubMed]
47. Kriaucionis, S.; Bird, A. The major form of MECP2 has a novel N-terminus generated by alternative splicing. *Nucleic Acids Res.* **2004**, *32*, 1818–1823. [CrossRef] [PubMed]
48. Dastidar, S.G.; Bardai, F.H.; Ma, C.; Price, V.; Rawat, V.; Verma, P.; Narayanan, V.; D'Mello, S.R. Isoform-specific toxicity of MECP2 in postmitotic neurons: Suppression of neurotoxicity by FOXG1. *J. Neurosci.* **2012**, *32*, 2846–2855. [CrossRef] [PubMed]
49. Liyanage, V.R.; Zachariah, R.M.; Rastegar, M. Decitabine alters the expression of MECP2 isoforms via dynamic DNA methylation at the MECP2 regulatory elements in neural stem cells. *Mol. Autism* **2013**, *4*, 46. [CrossRef] [PubMed]
50. KhorshidAhmad, T.; Acosta, C.; Cortes, C.; Lakowski, T.M.; Gangadaran, S.; Namaka, M. Transcriptional regulation of brain-derived neurotrophic factor (BDNF) by methyl CPG binding protein 2 (MECP2): A novel mechanism for re-myelination and/or myelin repair involved in the treatment of multiple sclerosis (MS). *Mol. Neurobiol.* **2015**. [CrossRef] [PubMed]
51. Vora, P.; Mina, R.; Namaka, M.; Frost, E.E. A novel transcriptional regulator of myelin gene expression: Implications for neurodevelopmental disorders. *Neuroreport* **2010**, *21*, 917–921. [CrossRef] [PubMed]
52. Zhou, Z.; Hong, E.J.; Cohen, S.; Zhao, W.N.; Ho, H.Y.; Schmidt, L.; Chen, W.G.; Lin, Y.; Savner, E.; Griffith, E.C.; et al. Brain-specific phosphorylation of MECP2 regulates activity-dependent BDNF transcription, dendritic growth, and spine maturation. *Neuron* **2006**, *52*, 255–269. [CrossRef] [PubMed]
53. Rousseaud, A.; Delepine, C.; Nectoux, J.; Billuart, P.; Bienvenu, T. Differential expression and regulation of brain-derived neurotrophic factor (BDNF) mrna isoforms in brain cells from MECP2 mouse model. *J. Mol. Neurosci.* **2015**, *56*, 758–767. [CrossRef] [PubMed]
54. Tochiki, K.K.; Cunningham, J.; Hunt, S.P.; Geranton, S.M. The expression of spinal methyl-CPG-binding protein 2, DNA methyltransferases and histone deacetylases is modulated in persistent pain states. *Mol. Pain* **2012**, *8*, 14. [CrossRef] [PubMed]
55. Zhang, R.; Huang, M.; Cao, Z.; Qi, J.; Qiu, Z.; Chiang, L.Y. MECP2 plays an analgesic role in pain transmission through regulating creb/miR-132 pathway. *Mol. Pain* **2015**, *11*, 19. [CrossRef] [PubMed]
56. Pedre, X.; Mastronardi, F.; Bruck, W.; Lopez-Rodas, G.; Kuhlmann, T.; Casaccia, P. Changed histone acetylation patterns in normal-appearing white matter and early multiple sclerosis lesions. *J. Neurosci.* **2011**, *31*, 3435–3445. [CrossRef] [PubMed]
57. Yang, H.; Lee, S.M.; Gao, B.; Zhang, J.; Fang, D. Histone deacetylase sirtuin 1 deacetylates IRF1 protein and programs dendritic cells to control TH17 protein differentiation during autoimmune inflammation. *J. Biol. Chem.* **2013**, *288*, 37256–37266. [CrossRef] [PubMed]
58. Sharma, K.; Singh, J.; Pillai, P.P.; Frost, E.E. Involvement of MECP2 in regulation of myelin-related gene expression in cultured rat oligodendrocytes. *J. Mol. Neurosci.* **2015**, *57*, 176–184. [CrossRef] [PubMed]
59. De Felice, C.; Della Ragione, F.; Signorini, C.; Leoncini, S.; Pecorelli, A.; Ciccoli, L.; Scalabri, F.; Marracino, F.; Madonna, M.; Belmonte, G.; et al. Oxidative brain damage in MECP2-mutant murine models of rett syndrome. *Neurobiol. Dis.* **2014**, *68*, 66–77. [CrossRef] [PubMed]
60. Ben-Zeev, B.; Aharoni, R.; Nissenkorn, A.; Arnon, R. Glatiramer acetate (GA, copolymer-1) an hypothetical treatment option for rett syndrome. *Med. Hypotheses* **2011**, *76*, 190–193. [CrossRef] [PubMed]

61. Costa, O.; Divoux, D.; Ischenko, A.; Tron, F.; Fontaine, M. Optimization of an animal model of experimental autoimmune encephalomyelitis achieved with a multiple MOG(35–55)peptide in c57bl6/j strain of mice. *J. Autoimmun.* **2003**, *20*, 51–61. [CrossRef]
62. Namaka, M.; Kapoor, S.; Simms, L.; Leong, C.; Grossberndt, A.; Prout, M.; Frost, E.; Esfahani, F.; Gomori, A.; Mulvey, M.R. Molecular mimicry and multiple sclerosis. *Neural Regen Res.* **2011**, *6*, 1322–1333.
63. Berard, J.L.; Wolak, K.; Fournier, S.; David, S. Characterization of relapsing-remitting and chronic forms of experimental autoimmune encephalomyelitis in c57bl/6 mice. *Glia* **2010**, *58*, 434–445. [CrossRef] [PubMed]
64. Ben-Shachar, S.; Chahrour, M.; Thaller, C.; Shaw, C.A.; Zoghbi, Y.H. Mouse models of MECP2 disorders share gene expression changes in the cerebellum and hypothalamus. *Hum. Mol. Genet.* **2009**, *18*, 2431–2442. [CrossRef] [PubMed]
65. Dragich, J.M.; Kim, Y.H.; Arnold, A.P.; Schanen, N.C. Differential distribution of the MECP2 splice variants in the postnatal mouse brain. *J. Comparative Neurol.* **2007**, *501*, 526–542. [CrossRef] [PubMed]
66. Saunders, C.J.; Minassian, B.E.; Chow, E.W.; Zhao, W.; Vincent, J.B. Novel exon 1 mutations in MECP2 implicate isoform MECP2_e1 in classical rett syndrome. *Am. J. Med. Genet. Part A* **2009**, *149A*, 1019–1023. [CrossRef] [PubMed]
67. Fichou, Y.; Nectoux, J.; Bahi-Buisson, N.; Rosas-Vargas, H.; Girard, B.; Chelly, J.; Bienvenu, T. The first missense mutation causing rett syndrome specifically affecting the MECP2_e1 isoform. *Neurogenetics* **2009**, *10*, 127–133. [CrossRef] [PubMed]
68. Orlic-Milacic, M.; Kaufman, L.; Mikhailov, A.; Cheung, A.Y.; Mahmood, H.; Ellis, J.; Gianakopoulos, P.J.; Minassian, B.A.; Vincent, J.B. Over-expression of either MECP2_e1 or MECP2_e2 in neuronally differentiated cells results in different patterns of gene expression. *PLoS ONE* **2014**, *9*, e91742. [CrossRef] [PubMed]
69. Meinnel, T.; Peynot, P.; Giglione, C. Processed N-termini of mature proteins in higher eukaryotes and their major contribution to dynamic proteomics. *Biochimie* **2005**, *87*, 701–712. [CrossRef] [PubMed]
70. Del Gaudio, D.; Fang, P.; Scaglia, F.; Ward, P.A.; Craigen, W.J.; Glaze, D.G.; Neul, J.L.; Patel, A.; Lee, J.A.; Irons, M.; et al. Increased *MECP2* gene copy number as the result of genomic duplication in neurodevelopmentally delayed males. *Genet. Med.* **2006**, *8*, 784–792. [CrossRef] [PubMed]
71. Van Esch, H.; Bauters, M.; Ignatius, J.; Jansen, M.; Raynaud, M.; Hollanders, K.; Lugtenberg, D.; Bienvenu, T.; Jensen, L.R.; Gecz, J.; et al. Duplication of the MECP2 region is a frequent cause of severe mental retardation and progressive neurological symptoms in males. *Am. J. Human Genet.* **2005**, *77*, 442–453. [CrossRef] [PubMed]
72. Chatrchyan, S.; Khachatryan, V.; Sirunyan, A.M.; Tumasyan, A.; Adam, W.; Bergauer, T.; Dragicevic, M.; Ero, J.; Fabjan, C.; Friedl, M.; et al. Evidence of *b*-Jet quenching in PbPb collisions at radical(s[NN]) = 2.76 TeV. *Phys. Rev. Lett.* **2014**, *113*, 132301. [CrossRef] [PubMed]
73. Mendel, I.; Kerlero de Rosbo, N.; Ben-Nun, A. A myelin oligodendrocyte glycoprotein peptide induces typical chronic experimental autoimmune encephalomyelitis in H-2B mice: Fine specificity and T cell receptor V β expression of encephalitogenic T cells. *Eur. J. Immunol.* **1995**, *25*, 1951–1959. [CrossRef] [PubMed]
74. Marcondes, M.C.; Furtado, G.C.; Wensky, A.; Curotto de Lafaille, M.A.; Fox, H.S.; Lafaille, J.J. Immune regulatory mechanisms influence early pathology in spinal cord injury and in spontaneous autoimmune encephalomyelitis. *Am. J. Pathol.* **2005**, *166*, 1749–1760. [CrossRef]
75. Orton, S.M.; Herrera, B.M.; Yee, I.M.; Valdar, W.; Ramagopalan, S.V.; Sadovnick, A.D.; Ebers, G.C. Canadian Collaborative Study Group. Sex ratio of multiple sclerosis in canada: A longitudinal study. *Lancet Neurol.* **2006**, *5*, 932–936. [CrossRef]
76. Rounds, W.H.; Salinas, E.A.; Wilks, T.B., 2nd; Levin, M.K.; Ligocki, A.J.; Ionete, C.; Pardo-Villamizar, C.; Vernino, S.; Greenberg, B.M.; Bigwood, D.W.; et al. Msprecise: A molecular diagnostic test for multiple sclerosis using next generation sequencing. *Gene* **2015**, *572*, 191–197. [CrossRef] [PubMed]
77. Sinha, S.; Crawford, M.P.; Ortega, S.B.; Karandikar, N.J. Multiparameter flow cytometric assays to quantify effector and regulatory T-cell function in multiple sclerosis. *J. Mult. Scler.* **2015**, *2*. [CrossRef]
78. Zachariah, R.M.; Rastegar, M. Linking epigenetics to human disease and rett syndrome: The emerging novel and challenging concepts in MECP2 research. *Neural Plast.* **2012**, *2012*, 415825. [CrossRef] [PubMed]



© 2017 by the authors. Licensee MDPI, Basel, Switzerland. This article is an open access article distributed under the terms and conditions of the Creative Commons Attribution (CC BY) license (http://creativecommons.org/licenses/by/4.0/).

Subject: Re: Inquiry for letter of copyright permission
Date: Friday, October 11, 2019 at 9:46:51 PM Central Daylight Time
From: IJMS
To: Ting Zhou

Dear Dr. Zhou,

Thank you for your email. As all our papers are fully open access and distributed under the terms and conditions of the Creative Commons Attribution License (CC BY), i.e., authors retain the copyright of their own paper. You can re-use the materials under the conditions stated here: https://creativecommons.org/licenses/by/4.0/. Therefore, you don't need our permission to re-use this article, as long as you cite this paper where you will reference.

Let us know if you have any other questions.

Kind regards,

Qi Yan
Managing Editor

IJMS (International Journal of Molecular Sciences)
Impact Factor 4.183 (2018 Journal Citation Reports)
Homepage: http://www.mdpi.com/journal/ijms
LinkedIn: http://www.linkedin.com/in/ijmsjournal
IJMS channel on Twitter (@IJMS_MDPI)

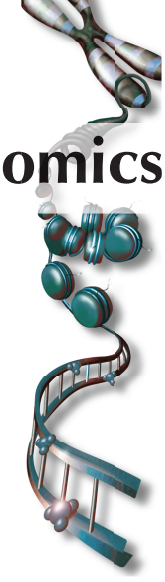
On 2019/10/10 4:12, Ting Zhou wrote:
> Dear editors of International Journal of Molecular Sciences,
>
> Hope this email finds you well!
>
> This is Ting Zhou. I am the second author of a published paper in
> your journal in 2017 named ”Experimental Autoimmune Encephalomyelitis
> (EAE)-Induced Elevated Expression of the E1 Isoform of Methyl CpG
> Binding Protein 2 (MeCP2E1): Implications in Multiple Sclerosis
> (MS)-Induced Neurological Disability and Associated Myelin Damage ”.
>
> This email is to inquire whether you could offer me letter of
> permission to include this published paper in my Ph.D. thesis as an
> appendix?
>
> Would you please indicate if there is any process I should go? And is
> there any copyright issue I need to pay attention?
>
> Thank you for your time and help! Have a nice day!
>
> Ting Zhou
>
> Ph.D Student
>

> Faculty of Pharmacy & Department of Human Anatomy and Cell Science
>
> University of Manitoba
>
> 750 McDermot Avenue
>
> Winnipeg, MB, Canada R3E 0T5
>
> zhout346@myumanitoba.ca <mailto:zhout346@myumanitoba.ca>
>

Research Article

For reprint orders, please contact: reprints@futuremedicine.com

Epigenomics



DNA hydroxymethylation changes in response to spinal cord damage in a multiple sclerosis mouse model

Yan Tang[‡,1,2,3], Man Luo[‡,1], Kailing Pan[3], Tina Ahmad[2], Ting Zhou[2], Zhigang Miao[3], Hang Zhou[3], Hao Sun[4], Xingshun Xu[**,1,3], Michael Namaka[***,2] & Yongxiang Wang[*,4,5]

[1]Department of Neurology, The Second Affiliated Hospital of Soochow University, Suzhou City, PR China
[2]Faculty of Health Sciences, College of Pharmacy, University of Manitoba, Manitoba, Winnipeg R3E 3P4, Canada
[3]Institute of Neuroscience, Soochow University, Suzhou City, PR China
[4]Department of Orthopedics, Clinical Medical College, Yangzhou University, Yangzhou City, PR China
[5]Department of Orthopedics, Northern Jiangsu People's Hospital, Yangzhou City, PR China
*Author for correspondence: Tel.: +86 514 873 73012; wyx918spine@163.com
**Author for correspondence: Tel.: +86 512 658 83252; Xingshunxu@suda.edu.cn
***Author for correspondence: Tel.: +1 204 474 8380; mikemamakams@gmail.com
‡Authors contributed equally

Aim: Roles of DNA 5-hydroxymethylcytosine (5hmC) in myelin repair were investigated in an experimental autoimmune encephalomyelitis (EAE) mouse model via its regulation on brain-derived neurotrophic factor (*BDNF*). **Methods:** DNA 5hmC level and its limiting enzymes were detected in EAE mice. **Results:** Global 5hmC modification, Tet1 and Tet2 significantly decreased in the spinal cord tissues of EAE mice. BDNF protein and mRNA decreased and were highly associated with *BDNF* 5hmC. Vitamin C, a Tet co-factor, increased global DNA 5hmC and reduced the neurological deficits at least by increasing *BDNF* 5hmC modification and protein levels. **Conclusion:** Tet protein-mediated 5hmC modifications represent a critical target involved in EAE-induced myelin damage. Targeting epigenetic modification may be a therapeutic strategy for multiple sclerosis.

First draft submitted: 30 September 2018; Accepted for publication: 29 October 2018; Published online: 14 November 2018

Keywords: *5-hydroxymethylcytosine* • *BDNF* • experimental autoimmune encephalomyelitis • multiple sclerosis • spinal cord • Ten-eleven translocation enzymes

Chronic, progressive demyelinating neurological diseases such as multiple sclerosis (MS) are characterized by abnormal responses of the immune system directed against the body's own CNS myelin. Based on the pathology of this autoimmune disease, the progressive damage and loss of the myelin sheath that surrounds nerve fibers in the brain and spinal cord (SC) results in a variety of diseases induced neurologic deficits such as muscle weakness, cognitive disability, limb pain, memory loss, ataxia, and blurred vision [1,2]. Although the exact molecular mechanisms of MS are unknown, several different factors have been considered in its pathogenesis that include abnormal immunological responses, genetic factors, environmental stress and a variety of infections [1,3]. Among these factors, environmental induced contributions in regard to MS pathology have gained considerably more attention from researchers [4–7]. Increasing scientific evidence strongly suggest that environmental factors like smoke and Epstein–Barr virus infections influence the molecular pathology that drives the underlying pathogenesis of MS [5,6,8,9]. Recent studies have shown that environmental factors change epigenetic processes such as histone acetylation and DNA methylation and regulate disease progression [10–13]. As such, this suggests the possibility of using epigenetic-based therapeutic interventional strategy for the treatment of MS [13]. 5-hydroxymethylcytosine (5hmC) represents a key DNA modification that results from the oxidization of 5-methylcytosine (5mC) by Ten-eleven translocation enzymes (Tets). This DNA modification is widespread in mammalian DNA and serves as an intermediate in the demethylation of active DNA. Several studies have showed that 5hmC was involved in many normal functions such as neuronal differentiation of human brain, development in mice brain and self-renewal in embryonic stem cells. A recent report showed that *5hmC*, was found to decrease in the peripheral mononuclear cells

Future Medicine

of MS patients [14]. However, it is still unclear whether DNA *5hmC* modification is involved the disease progression or the functional recovery of MS.

Based on our previously published studies and the research conducted by other researchers in this area, *brain-derived neurotrophic factor (BDNF)* has been confirmed to have a critical role in myelin repair and neurological recovery in MS [15–18], whose expression is directly regulated by *5hmC*. Results from our previous research confirmed that DNA 5hmC modification regulates the expression of *BDNF* in ischemia-induced brain injury [19]. However, in the current study, we are examining the role of 5hmC in regulating *BDNF* expression in an experimental autoimmune encephalomyelitis (EAE)-induced model.

Materials & methods

Animals

Female C57BL/6 mice (6–8 weeks old) in this study were acquired from the SLAC Company (PR China). All animal procedures conducted in the study were approved by the University Committee on Animal Care of Soochow University and performed according to the guidelines of the Animal Use and Care of the NIH and the ARRIVE (Animal Research: Reporting *In Vivo* Experiments).

Experimental autoimmune encephalomyelitis mouse model

After the anesthetization with intraperitoneal injection of 4% chloral hydrate (350 mg/kg), mice were subcutaneous injected with 200 ug myelin oligodendrocyte glycoprotein peptide (MOG) 35–55 (MEVGWYRSPFSRVVH-LYRNGK, Shanghai, PR China) dissolved in 50 ul of complete Freund's adjuvant containing 4 mg/ml heat-killed mycobacterium tuberculosis H37Ra (Difco Laboratories, MI, USA) at two sites, followed by two intraperitoneal injections of 200 ng pertussis toxin at 0 and 48 h after MOG injection. Neurological deficits were scored according to previously established in house methodology and recorded every day. Finally, mice were sacrificed with overdose injection of 4% chloral hydrate.

Animal experimental groups & Vitamin C administration

Mice were divided into four groups: naive control (NC) mice did not receive any treatment; active control (AC) mice were given all the same treatment as the EAE mice except the MOG antigen; EAE mice were injected with MOG and pertussis toxin; Vitamin C (VC)-treated EAE mice (EAE+VC) received an intraperitoneal injections with VC (Sigma-Aldrich Company, MO, USA; 0.5 g/kg body weight daily) starting immediately once they reach a neurological disability score (NDS) of 0.5.

NDS after EAE induction

The NDS of EAE-induced mice were scored according to neurological symptoms in accordance to the following previously established in house expertise for EAE scoring system: 0, no clinical symptom; 0.5, weak tail tip; 1, limp tail; 1.5, one weak hind limb; 2, two weak hind limbs; 2.5, paralysis of one hind limb; 3, complete hind limb paralysis; 3.5, complete hind limb paralysis and one weak forelimb; 4, complete hind limb paralysis and weak forelimbs; 5, moribund, death. The mean EAE score was calculated every day based on all available animals per group.

SC tissue collection

Mice were sacrificed at day 28 after EAE. After removing the ribs on both sides of the vertebra, the vertebrae were clipped by small tweezers. After the exposure of SC, about 5-mm length of thoracic SC was collected for further analysis.

Dot blot analysis

About at day 28 after EAE induction, SC tissues were collected and stored at -80°C. The genomic DNA was extracted for dot blot analysis by a DNA extraction protocol. The dot blot assay was performed as described previously [19]. Briefly, DNA samples were pretreated with 2N NaOH and then spotted on a nitrocellulose membrane at room temperature for 15 min. After incubation at 80°C in an oven for 30 min, the membrane was blocked with 5% milk in phosphate-buffered saline with 0.1% Tween 20 (PBST) for 1 h. After washing, the membrane was incubated with the primary antibodies (anti-5mC mouse antibody, MO, USA; anti-5hmC rabbit antibody, Active Motif Inc., CA, USA) at 4°C overnight. On the second day, the membrane was incubated with horseradish peroxidase-conjugated

Table 1. The primers for PCR.

Primers	Sequences
For DNA samples	
Tet1 forward	CACGCGTTTGAGACGTACCC
Tet1 reverse	CCAGGATCCCAGAACCAGTC
Tet2 forward	GGCTGGTTCGGGAAGAACAG
Tet2 reverse	ATGGAGTCTGGAGGACTGCC
BDNF forward	ACAGAGCCAGCGGATTTGTC
BDNF reverse	CGAGCTCAATGAGGGGACCA
For RNA samples	
Tet1 forward	TCTCCGACATTTGCCCAGAC
Tet1 reverse	GGAGGTGGTGACACTCATGG
Tet2 forward	CACTCCAGAGGCACCTTCAG
Tet2 reverse	AGGAGTAGGCTGTCTCGTGT
Tet3 forward	GAG CAC GCC AGA GAA GAT CAA
Tet3 reverse	CAG GCT TTG CTG GGA CAA TC
BDNF forward	GCCTCCTCTACTCTTTCTGC
BDNF reverse	ATGGGATTACACTTGGTCTC

BDNF: Brain-derived neurotrophic factor.

secondary antibodies (Jackson ImmunoResearch Laboratories, PA, USA) for 1h. The membrane was developed with the ECL chemiluminescence system (Thermo Thermo Fisher Scientific, MA, USA). The immunoreactive dots were captured on autoradiographic films. The densitometry of the dots was analyzed with Alpha Ease Image Analysis Software (V3.1.2, Alpha Innotech Corp., CA, USA).

Methylene blue staining

The dot blot membrane was incubated 0.02% methylene blue (Sigma-Aldrich) dissolved in 0.3 M sodium acetate (pH 5.2) for 10 min. After washing, photos were taken and the densitometry of methylene blue staining was analyzed with Alpha Ease Image Analysis Software and was used a loading control to evaluate the densitometries of *5mC* and *5hmC*.

Western blot analysis

At day 28 after EAE induction, SC tissues were collected and sonicated in lysis buffer on ice. After centrifuging, supernatants were collected and protein concentrations were determined by a bicinchoninic acid method. Same amount of total proteins (about 20–30 μg) was separated by SDS-PAGE and then transferred to nitrocellulose membranes. After blocking with 5% milk in PBST, blots were incubated with antirabbit *Tet2* antibody (Abcam, ab124297, NY, USA) or antimouse *β-tubulin* antibody (Sigma-Aldrich, T8328) at 4°C overnight. After washing with PBST, blots were incubated with horseradish peroxidase-conjugated secondary antibodies for 1 h at room temperature. Blots were developed with the ECL chemiluminescence system. The densitometry of immunoreactive bands obtained on autoradiographic films was analyzed with Alpha Ease Image Analysis Software.

Quantitative PCR (qPCR)

SC tissues obtained at day 28 after EAE induction were incubated with RNAiso plus on ice for 10 min. After centrifuging, supernatants were collected to new tubes. After adding the same volume of chloroform, the mixtures were centrifuged and the supernatants were collected. After adding the same volume of isopropyl alcohol, the samples were centrifuged and the pellets were collected. After air dry, RNA samples were dissolved in double distilled water. Reverse transcription was performed by using the Transcriptor First Strand cDNA Synthesis Kit (Roche Applied Science, Penzberg, Germany). Q-PCR was conducted with SYBR Green (Roche Applied Science) on a Real-Time PCR system (7500, Applied Biosystems, MA, USA). *GAPDH* was used as an endogenous control. The primer sequences for PCR were shown in Table 1. qPCR analysis was performed by using the $2^{-\Delta\Delta CT}$ method [20].

DNA *5hmC* detection by hydroxymethylated DNA immunoprecipitation

5hmC level was detected by using the EpiQuik™ hMeDIP Kit (P1038, Epigentek, Farmingdale, NY, USA). Briefly, 100 µl buffer AB was added to each well of plates along with following antibodies to incubate at room temperature for 60 min: 1 µl of nonimmune IgG to the negative control well, 1 µl of *5hmC* antibody to the sample wells and 1 µl of *5hmC* antibody to the positive control wells. After removing buffer AB from the wells, the wells were washed twice with 200 µl diluted WB buffer. After washing, the mixture (50 µl HS solution and 50 µl sample DNA diluted to 10 ng/µl) was added to wells and incubated at room temperature for 90 min with slight shaking. After the solution was pipetted out from each well, the wells were washed for five-times with 200 µl diluted WB. Further, 1 µl Proteinase K and 39 µl DRB solution were added to each well. Finally, wells were placed into a thermal cycler and incubated at 60°C for 15 min, followed by incubation at 95°C for 3 min. The captured DNA in wells was used for qPCR analysis. The primer sequences of qPCR for *BDNF* and *Tet2* genes were listed in Table 1.

Statistical analysis

All data are expressed as means ± standard error of the mean. GraphPad Prism 5 (Graph-Pad Software, Inc., USA) was used for statistical analysis. Student's *t*-test (factor: mouse group) was used to determine the differences between two groups; two-way analysis of variance followed by Bonferroni *post hoc* tests (the EAE clinical score curves, factors: mouse group and time; the *5hmC*, mRNA and protein levels after VC treatment, factors: mouse group and treatment) was used to compare the differences among groups if there were significant differences. Correlation analysis by Spearman's rank test was performed between *BDNF* mRNA levels and *5hmC* levels. $p < 0.05$ was considered statistically significant.

Results

Global DNA *5hmC* decreased in SC tissues in an EAE mouse model of MS

After female C57BL/6 mice were administered with MOG35-55 peptide to induce EAE, neurological behaviors were recorded. At 19–20 days after the induction, neurological deficits on gait, righting reflex model deficiency and loss of tail/limb tonicity were observed. Neurological impairments reached the peak at days 27–29 and then had a slight functional recovery (Figure 1A). At this time point (day 28), the body weight also decreased in mice with EAE induction (Figure 1B). Our results were consistent with previous reports [21], confirming the successful establishing of EAE mouse model. Therefore, we chose day 28 for the following experiments.

Previous studies have shown that histone acetylation and DNA methylation have been recently identified as a potential contributing factor in the demyelination process in MS [14]. Interestingly, a recent study has showed that DNA *5hmC* in peripheral blood cells decreased in patients with MS [14]. However, the changes of DNA *5hmC* in SC tissues are currently unknown. The EAE animal model is a useful and widely used model to study the molecular mechanisms associated with the underlying pathology of MS. Therefore, we examined *5hmC* levels in SC tissues by using MOG-induced EAE mouse model. As mentioned above, at day 28 after EAE induction, in which EAE mice had severe neurological impairments, DNA *5hmC* levels were determined and found that DNA *5hmC* in SC tissues significantly decreased (Figure 1C); This was confirmed by quantitative analysis ($p < 0.05$; Figure 1D). These results clearly demonstrated the alteration of DNA *5hmC* in SC tissues after EAE-induced nontraumatic SC damage.

Tet1 & *Tet2* expression reduced in EAE–SC tissues

Because DNA *5hmC* modification is oxidized from DNA *5mC* with the catalization of Tet proteins including *Tet1*, *Tet2* and *Tet3*, we examined the mRNA levels of *Tet1*, *Tet2* and *Tet3* by qPCR at day 28 after EAE induction. We found that *Tet1* and *Tet2* mRNA levels were significantly decreased after EAE-induced nontraumatic SC damage ($p < 0.05$; Figures 2A & B); however, *Tet3* mRNA level was not significantly changed ($p > 0.05$; Figure 2C). Our data were consistent with previous results in peripheral blood cells of MS patients [14]. We further confirmed the change of Tet1 and Tet2 protein expression by Western Blot analysis. We found that *Tet1* and *Tet2* protein significantly decreased at day 28 after EAE induction (Figures 2D & F). Quantitative analysis confirmed the reduction of Tet1 and Tet2 protein ($p < 0.05$; Figures 2E & G). Therefore, the reduced expression of Tet1 and Tet2 protein represents an important cause of MS-induced myelin damage that leads to the decrease of DNA *5hmC* in EAE-induced nontraumatic SC damage.

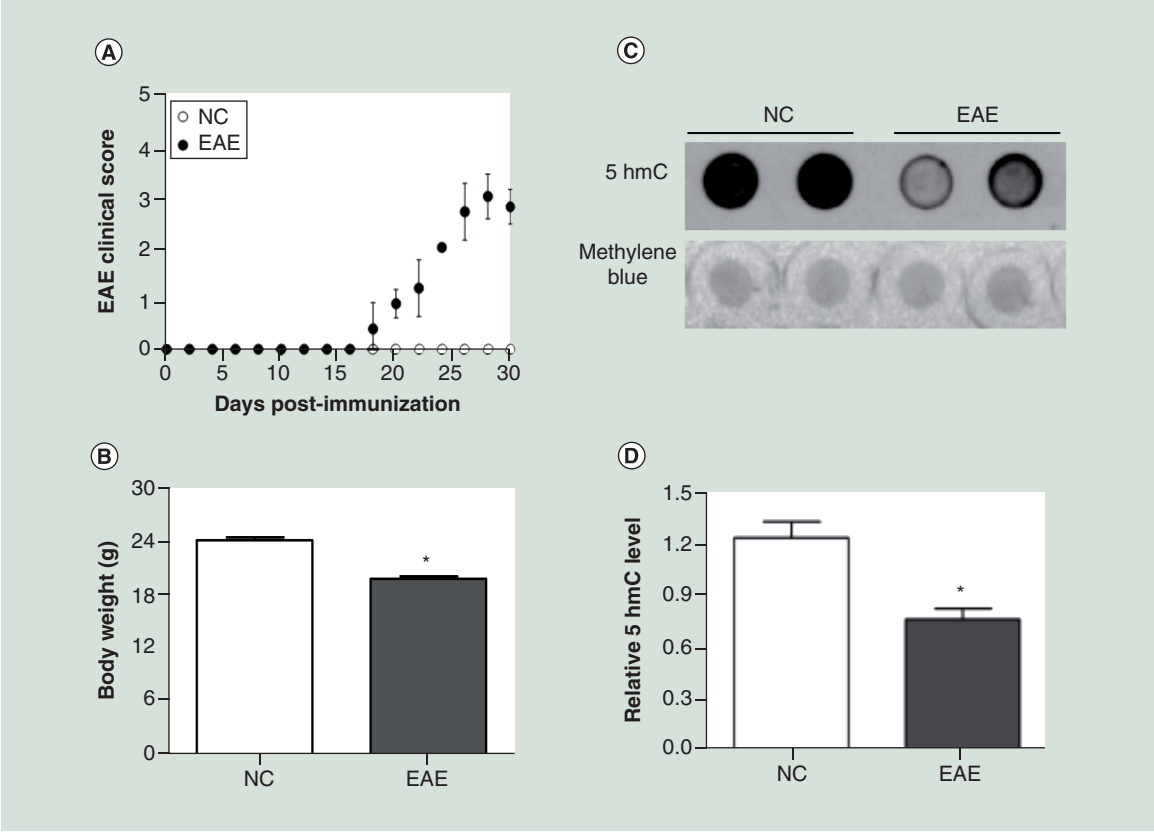


Figure 1. Global DNA *5-hydroxymethylcytosine* modification decreased in spinal cord tissues in the mouse experimental autoimmune encephalomyelitis model. Female C57BL/6 mice (6–8 weeks old) were subcutaneous injected with 200 ug MOG peptide and intraperitoneal injected with 200 ng pertussis toxin to induce the EAE mouse model. Neurological scores were recorded every other day for 1 month. Two-way ANOVA was performed **(A)**. The body weight was measured at 28 days after EAE induction and was analyzed by *t*-test. *$p < 0.05$ versus control group. N = 9–10 mice **(B)**. At day 28 after EAE induction, SC tissues were collected and total DNA was further extracted. Global *5hmC* modification was determined by dot blot analysis **(C)** and quantified **(D)**. Methylene blue staining was performed in DNA samples to use as loading controls. *T*-test was used for analysis. *$p < 0.05$ versus control group. N = 6 mouse samples.
5hmc: 5-hydroxymethylcytosine; EAE: Experimental autoimmune encephalomyelitis; MOG: Myelin oligodendrocyte glycoprotein; SC: Spinal cord.

Tet protein activator Vitamin C increased DNA *5hmC* modification & improved neurological deficits in the EAE mouse model

To determine whether the alteration of DNA *5hmC* modification in SC tissues affect EAE-induced nontraumatic SC damage, we used a previously reported *Tet* activator/co-factor, VC which was administered via intraperitoneal injection with a dose at 0.5 g/kg daily starting immediately once they reach a NDS of 0.5 [22]. Four experimental groups were used for comparative assessment to determine the effects of VC administration. Our results indicated that VC reversed the decrease of DNA *5hmC* in the EAE-induced mouse model (Figure 3A). Quantitative analysis demonstrated that VC significantly increased DNA *5hmC* in SC tissues after EAE induction ($p < 0.05$; Figure 3B). At the same time, VC significantly decreased the NDS from the day 20 after EAE induction ($p < 0.05$; Figure 3C).

Surprisingly, VC interventional treatment increased *Tet1* and *Tet2* mRNA levels in SC tissues and reversed the decrease of *Tet1* and *Tet2* mRNA induced by EAE ($p < 0.05$; Figures 4A & B). Western Blot analysis indicated the increase of *Tet2* at the protein level after VC treatment (Figure 4C). Quantitative analysis further showed the significant increase of Tet2 protein after VC treatment ($p < 0.05$; Figure 4D), indicating that *Tet2* may be regulated by its DNA *5hmC* modification.

10.2217/epi-2018-0162

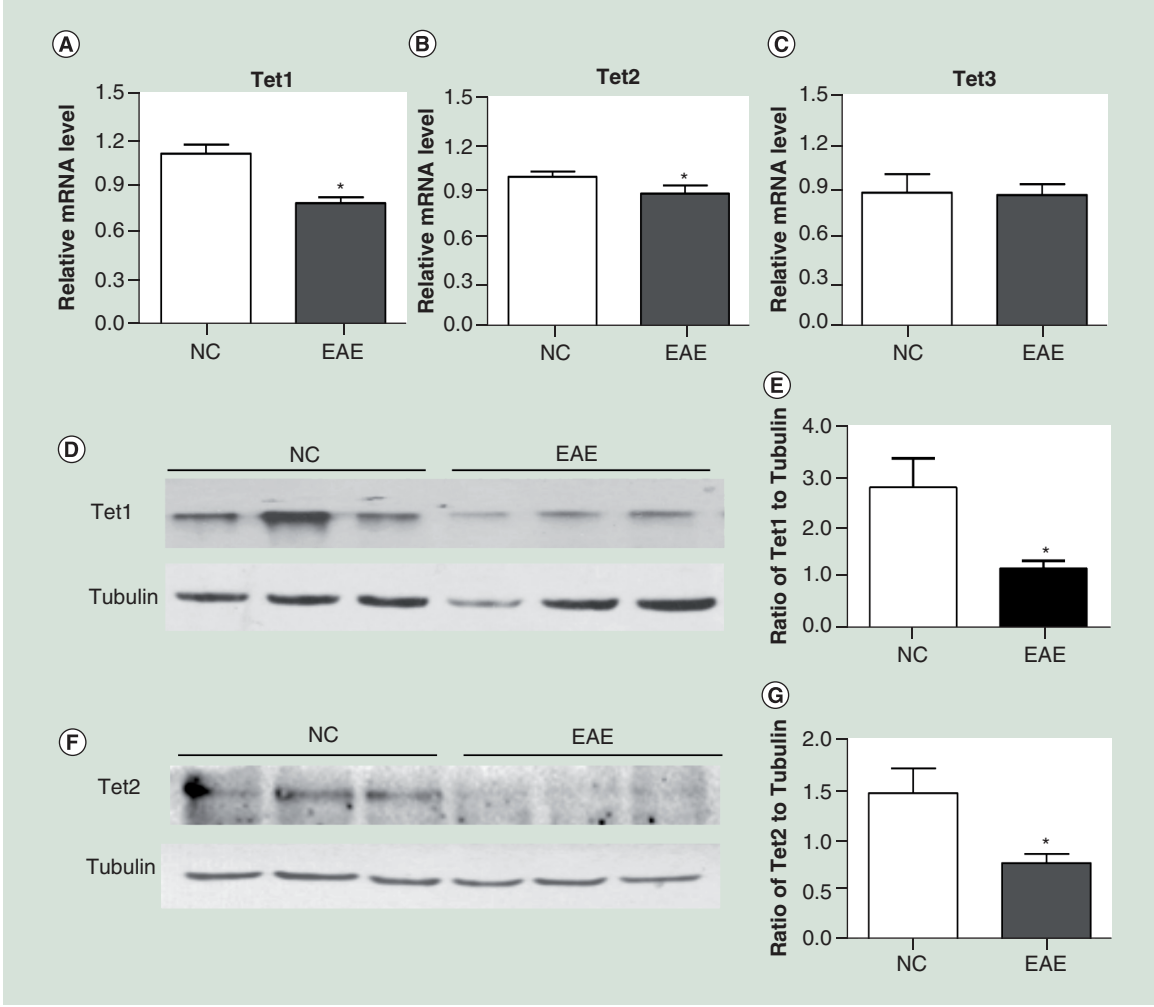


Figure 2. *Tet1* and *Tet2* expression decreased in spinal cord tissues after experimental autoimmune encephalomyelitis induction. At day 28 after EAE induction, SC tissues were collected and total RNA was extracted. Total mRNA levels of *Tet1*, *Tet2* and *Tet3* were determined by qPCR **(A–C)**. *Tet1* **(D)** and *Tet2* **(F)** protein levels were examined by Western Blot. *β-tubulin* was used as a loading control. The quantitative analysis of *Tet1* **(E)** and *Tet2* **(G)** protein levels was performed. *T*-test was used for the analysis; *$p < 0.05$ versus control group. N = 6–7 mouse samples. qPCR: Quantitative PCR; SC: Spinal cord.

BDNF level decreased in SC tissues after EAE induction & was reversed by VC interventional treatment

Previously studies and our data showed that *BDNF* is a critical neurotrophic factor for remyelination and/or myelin repair that facilitates the recovery of neurological deficits associated with MS [16]. In this study, we confirmed the decrease of *BDNF* protein at day 28 after EAE induction ($p < 0.05$, Figures 5A & B). Consistent with our neurological disability behavioral scoring results, *BDNF* mRNA level decreased at day 28 after EAE induction; however, VC treatment not only improved the neurological behavioral deficits but also increased *BDNF* mRNA ($p < 0.05$, Figure 5C). Therefore, VC interventional treatment was responsible for the increase of *BDNF* mRNA that also subsequently correlated with the improvement of neurological deficits.

VC increased DNA *5hmC* modification in the promoter regions of *BDNF* & *Tet1/2* genes in SC tissues after EAE induction

To examine the relationship between the *5hmC* modification and *BDNF* expression, we detected the DNA *5hmC* level in the *BDNF* gene promoter in SC tissues at the day 28 after EAE induction. Our data showed that *5hmC* level in *BDNF* gene significantly decreased after EAE induction and reversed with VC interventional treatment (p

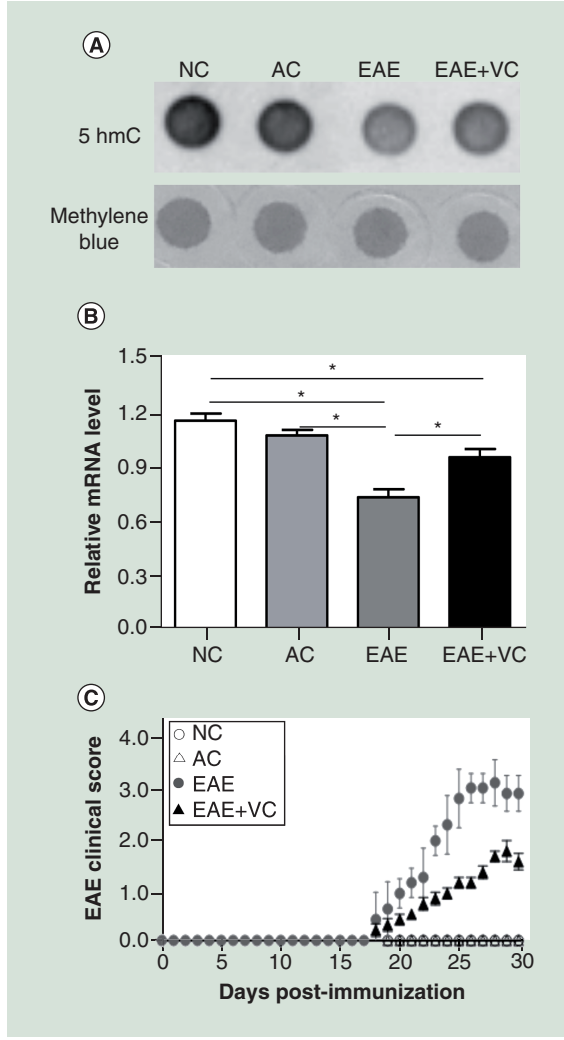


Figure 3. Vitamin C increased DNA *5hmC* modifications and improved neurological deficits in experimental autoimmune encephalomyelitis mice. The EAE model was induced in female mice. Mice were randomly divided into four groups: NC group, AC group, EAE group and VC-treated EAE group (EAE + VC). Mice were treated with VC (0.5 g/kg, ip.) daily or same volume of vehicle. The DNA *5hmC* modifications were detected by dot blot analysis at 28 days after treatment **(A)** and the quantitative analysis was performed **(B)**. *$p < 0.05$. N = 3–4 samples. Neurological scores were recorded every day for 1 month **(E)**. Two-way ANOVA was used; *$p < 0.05$. N = 9–10 mice.
AC: Active control; EAE: Experimental autoimmune encephalomyelitis; NC: Naive control; VC: Vitamin C.

< 0.05, Figure 6A). In addition, we further examined *5hmC* modification levels in *Tet1* and *Tet2* genes. We found that *5hmC* significantly decreased at day 28 after EAE induction and increased with VC treatment ($p < 0.05$, Figures 6B & C). Finally, we performed a correlation analysis between *BDNF* mRNA levels and *5 hmC* levels; the Spearman r value was 0.3638 ($p < 0.05$, Figure 6D).

Discussion

BDNF has been considered as a critical mediator in myelin repair and functional neurological recovery in MS [16]. In this study, our data demonstrated for the first time that *Tet1* and *Tet2* regulate the level of *BDNF* expression by increasing *BDNF* gene *5hmC* modification in an EAE mouse model. Our results showed that DNA *5hmC* decreased at day 28 after EAE induction (Figure 1). Western blot WB and qPCR results indicated that *Tet1* and *Tet2* were mainly responsible for the decrease of DNA *5hmC* upon the EAE-induced injury to CNS myelin (Figure 2). Interestingly, VC, a co-factor of *Tet* enzymes, increased the level of DNA *5hmC* modification and mRNA levels of *Tet1* and *Tet2* and reversed the neurological behavioral deficits in the EAE mouse model (Figures 3 & 4). Furthermore, our result showed that *BDNF* expression markedly decreased after EAE induction (Figure 5). Finally, our data suggests that the reduction of *BDNF* expression may very well be related to the decrease of *5hmC* level in the promoter regions of *BDNF* (Figure 6).

After *Tet* enzymes were found to catalyze the conversion reaction from *5mC* to *5hmC* [23,24], *5hmC* has attracted significant attention in the epigenetic field. The role of *5hmC* has been previously examined in many diseases and is regarded as a key biological target that is involved in the pathogenesis of a variety of diseases such as tumors [25], Huntington's disease [26], Alzheimer's disease [27], kidney ischemia [28] and stroke [29]. However, the role of *5hmC*

10.2217/epi-2018-0162

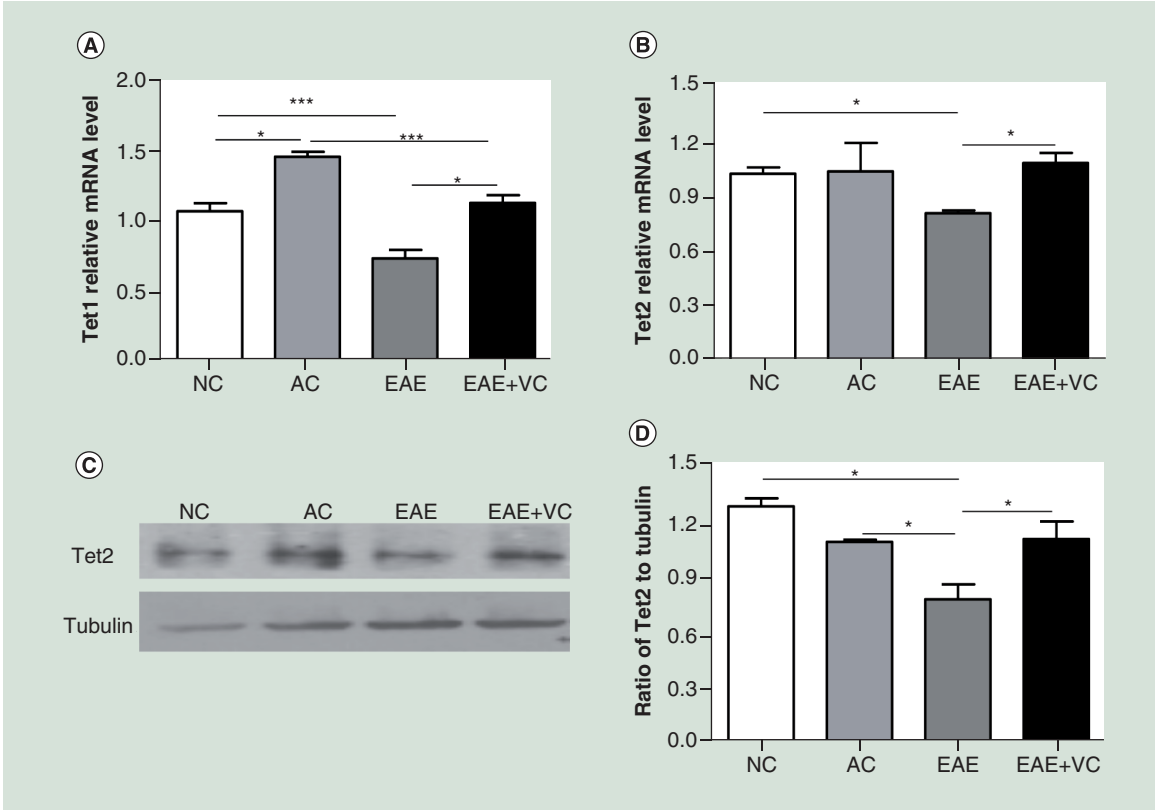


Figure 4. Vitamin C increased *Tet1* and *Tet2* expression in spinal cord tissues in experimental autoimmune encephalomyelitis mice. The EAE model was induced in female mice. Mice were randomly divided into four groups: NC group, AC group, EAE group and VC-treated EAE group (EAE + VC). Mice were treated with VC (0.5 g/kg, ip.) daily immediately once they reach a NDS of 0.5. SC tissues were collected at 28 days after treatment and total RNA was extracted. Total mRNA levels of *Tet1* and *Tet2* were determined by qPCR **(A & B)**. The proteins were extracted and Tet2 protein level was examined by Western Blot in four experimental groups. *β-tubulin* was used as a loading control **(C)**. The quantitative analysis of *Tet2* protein was performed **(D)**. Two-way ANOVA was used; *$p < 0.05$. N = 5–6 mouse samples.
AC: Active control; EAE: Experimental autoimmune encephalomyelitis; NC: Naive control; NDS: Neurological disability score; qPCR: Quantitative PCR; SC: Spinal cord; VC: Vitamin C.

modification in SC damage remains unknown. Previous studies have reported that DNA methylation plays an important role in SC damage. For example, Wang *et al.* showed that increased global DNA methylation and MeCP2 expression after SC damage may play an important role in neuropathic pain and the inhibition of DNA methyltransferases may be a new therapeutic approach for neuropathic pain [30]. Thus, we speculated that 5hmC as a demethylation mechanism may also play an important role in regulating gene expression after SC damage. In this study, our results showed that *5hmC* decreased after EAE induction (Figure 1); this is consistent with the study of kidney injury [31], but contrary to the cerebral ischemia [19]. This discrepancy may be due to tissue differences when exposed to different injury stimuli.

Previous studies have reported that VC can improve functional recovery after SC damage [32]. Furthermore, additional evidence also suggests that VC acts as an activator or co-factor of *Tet* protein to enhance its protective effects except for its antioxidant activity [33,34]. In this study, VC reversed the decrease of 5hmC and neurological deficits after EAE induction (Figure 3). To demonstrate whether *BDNF* partially mediate the protection of VC, we examined *BDNF* expression and *5hmC* modification in the promoter of *BDNF* after VC treatment. We showed that VC treatment increased *BDNF*, *Tet1* and *Tet2* expression, *5hmC* modification of *BDNF* gene (Figures 5, 6), and functional improvement after nontraumatic SC damage induced by EAE. In addition, some studies report that VC has no effect or exacerbates the disease development in Scorbutic guinea pig and mouse models of MS [35,36]. This seems inconsistent with our study and other studies that showed the benefit effects of VC in animal models of MS [37,38]. This inconsistency may be explained by different model species and different doses of VC. In this study,

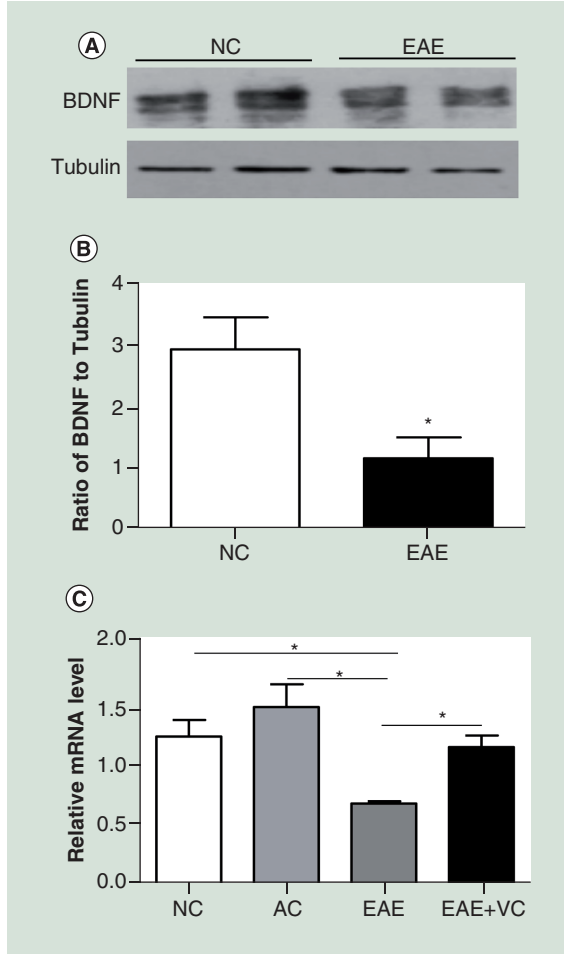


Figure 5. Vitamin C increased *brain-derived neurotrophic factor* expression in spinal cord tissues in experimental autoimmune encephalomyelitis mice. At 28 days after EAE induction, SC tissues were collected and *BDNF* protein was examined by Western Blot **(A)**. The quantitative analysis of *BDNF* protein was performed by the *t*-test **(B)**. After the treatment with VC for 28 days, the SC tissues from four groups were collected and the mRNA of *BDNF* was examined by qPCR. Two-way ANOVA was used **(C)**. $^{*}p < 0.05$. N = 5–6 mouse samples.
BDNF: Brain-derived neurotrophic factor; EAE: Experimental autoimmune encephalomyelitis; qPCR: Quantitative PCR; VC: Vitamin C.

we used a small dose of VC (0.5 g/kg body weight) as a co-factor of Tet enzymes. This suggests that EAE mice in this study may benefit from VC as a co-factor of *Tet* enzymes but not as an antioxidant. However, the possible roles and mechanisms of VC in MS still need more investigations [39].

Importantly, previous study showed the decease of *Tet2* in the peripheral blood of patients with MS [14]. Our results obtained from this study confirmed the decrease of *5hmC* and *Tet2* protein/mRNA in the SC after EAE induction. Therefore, DNA *5hmC* and Tet proteins may also mediate the pathophysiology in regard to myelin damage in MS patients. Promotion of *5hmC* modifications and *Tet2* level represents a novel therapeutic strategy for MS or other white matter diseases. In addition, our data also demonstrated *5hmC* modifications levels in *Tet1* and *Tet2* promoters also significant decreased that subsequently resulted in the reduction of Tet proteins and 5hmC modification. Therefore, VC as a co-factor to increase Tet protein activity represents a novel and economical treatment approach that requires further investigation for chronic neurological conditions such as MS.

In this study, there are some limitations. Cell-type specific epigenetic 5hmC changes in response to the immunostimulant MOG35-55 peptides are not explored. In addition, although VC is proved a *Tet* co-factor and activator [33,40], its protective roles on neurological deficits in EAE mice by increasing *BDNF* 5hmC should be further validated by functionally abolishing *Tet1*, *Tet2* and *BDNF* in the future studies.

Conclusion

In summary, our study demonstrates that genome-wide hydroxymethylation occurs during EAE induction and Tet proteins act as important regulators in this process. Tet1 and Tet2-mediated *5hmC* modifications in genes are crucial for EAE injury and VC can be used as an adjunctive treatment approach for patients with MS and other white matter disorders.

10.2217/epi-2018-0162

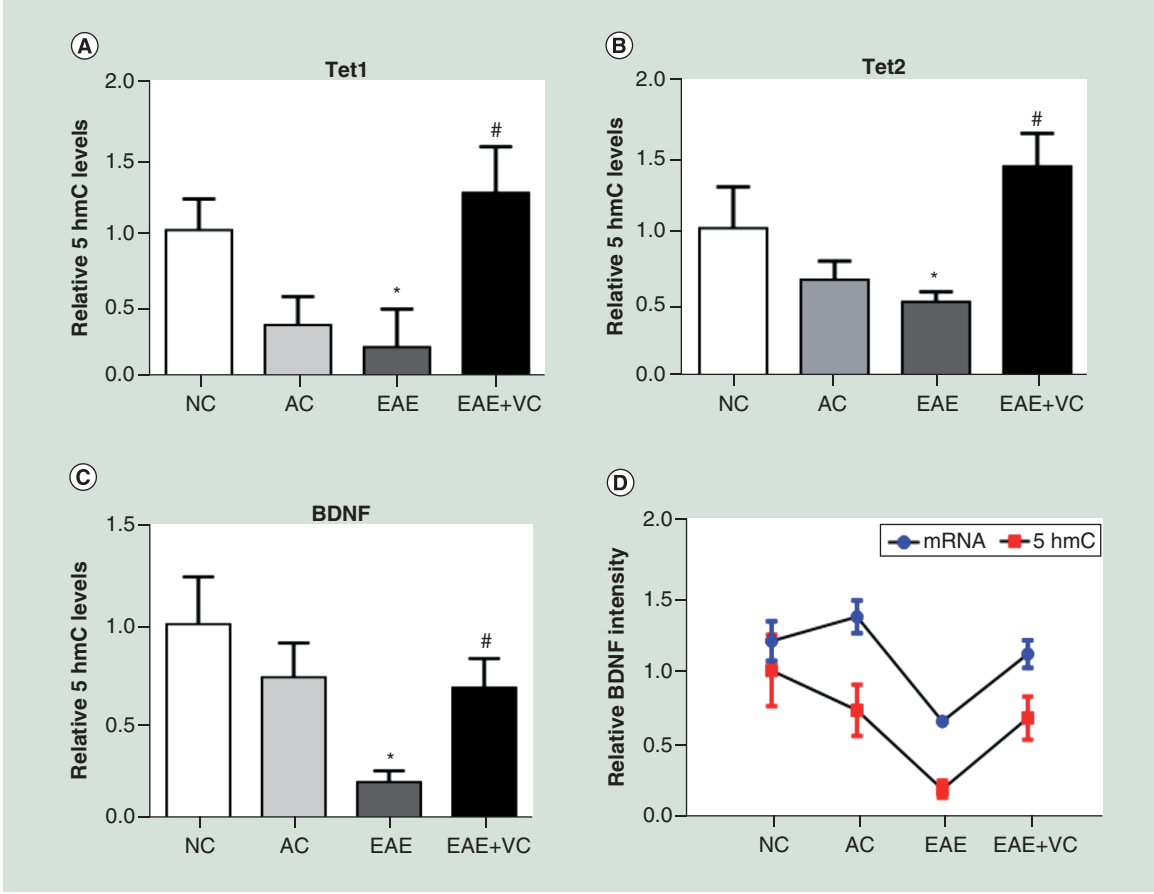


Figure 6. Vitamin C increased *5-hydroxymethylcytosine* modifications in the promoters of *brain-derived neurotrophic factor* and *Tet2*. The EAE model was induced in female mice. Mice were randomly divided into four groups: NC group, AC group, EAE group and VC-treated EAE group (EAE + VC). Mice were treated with VC (0.5 g/kg, ip.) daily immediately once they reach a NDS of 0.5. SC tissues were collected at 28 days after treatment. *5hmC* modification in the promoters of *BDNF*, *Tet1*, and *Tet2* were detected by hMeIP and qPCR **(A–C)**. Two-way ANOVA was used; *$p < 0.05$ versus saline-treated control group; $^{\#}p < 0.05$ versus EAE group. N = 6 mouse samples. Correlation analysis between *BDNF* mRNA levels and *5hmC* levels was performed by Spearman's rank test **(D)**. $p < 0.05$; N = 23 mice.
5hmc: 5-hydroxymethylcytosine; AC: Active control; BDNF: Brain-derived neurotrophic factor; EAE: Experimental autoimmune encephalomyelitis; NC: Naive control; NDS: Neurological disability score; qPCR: Quantitative PCR; SC: Spinal cord; VC: Vitamin C.

Future perspective

Because many immunological diseases like MS are affected by environmental factors, targeting environment-induced epigenetic modification will be an important factor warranting future consideration for disease treatments. DNA methylation as one important epigenetic mechanism involved in the pathogenesis of MS; however, the role of Tet proteins in regard to how they interact with other transcriptional factors to coordinately regulate MS-related gene expression like *BDNF* will be an important direction that may provide potential therapeutic targets for MS.

Author contributions

Y Tang and M Luo performed the research experiments. X Xu, M Namaka and Y Wang designed the research study. Z Miao, Y Tang, Z Miao, K Pan, T Ahmad, T Zhou and H Zhou analyzed the data. Y Tang, X Xu, M Namaka and Y Wang wrote the paper.

Acknowledgments

The authors would also like to acknowledge the in-kind support from the Manitoba Multiple Sclerosis Research Network Organization (MMSRNO).

Financial & competing interests disclosure

This study was supported by the grants from National Key R&D Program of China (2017YFE0103700); the National Natural Science Foundation of China (81601154); Natural Science Foundation of Jiangsu Province (BK20141281); Special Foundation Project on the Prospective Study of Social Development in Jiangsu Province (BE2013911); Jiangsu Six Categories of Talent Summit Fund (WSW-133); Social Development of Science and Technology Research Project in Yangzhou (YZ2011082); and Jiangsu Province 333 talent Project (BRA2016159). The authors have no other relevant affiliations or financial involvement with any organization or entity with a financial interest in or financial conflict with the subject matter or materials discussed in the manuscript apart from those disclosed.

No writing assistance was utilized in the production of this manuscript.

Ethical disclosure

The authors state that they have obtained appropriate institutional review board approval or have followed the principles outlined in the Declaration of Helsinki for animal experimental investigations.

Summary points

- Although the molecular mechanisms of multiple sclerosis (MS) still remain unknown, environmental stress-induced epigenetic regulation is considered to be an important aspect in its underlying pathogenesis.
- We examined the role of 5-hydroxymethylcytosine (5hmC) in myelin repair in an experimental autoimmune encephalomyelitis (EAE) mouse model via its regulation on *brain-derived neurotrophic factor* (*BDNF*) expression.
- Our findings showed that global 5hmC modification and its limiting enzymes *Tet1* and *Tet2* significantly decreased in the spinal cord of EAE-induced mouse model of MS.
- *BDNF* protein level, an important neurotrophic factor in myelin repair and recovery from neurological disability in MS, was highly associated with *BDNF* 5hmC level.
- Vitamin C, a co-factor of *Tet* enzymes, reduces the neurological deficits and increases 5hmC modification level and protein level in *BDNF*.
- Tet protein-mediated 5hmC modifications in *BDNF* gene or other genes are crucial for EAE injury.
- Targeting epigenetic modification may be a therapeutic strategy for MS.

References

Papers of special note have been highlighted as: • of interest

1. Ghasemi N, Razavi S, Nikzad E. Multiple sclerosis: pathogenesis, symptoms, diagnoses and cell-based therapy. *Cell J.* 19(1), 1–10 (2017).
2. Vidal-Jordana A, Montalban X. Multiple sclerosis: epidemiologic, clinical, and therapeutic aspects. *Neuroimaging Clin. N. Am.* 27(2), 195–204 (2017).
3. Choi BY, Jung JW, Suh SW. The emerging role of zinc in the pathogenesis of multiple sclerosis. *Int. J. Mol. Sci.* 18(10), 2070 (2017).
4. Correale J, Farez MF, Gaitan MI. Environmental factors influencing multiple sclerosis in Latin America. *Mult. Scler. J. Exp. Transl. Clin.* 3(2), 2055217317715049 (2017).
5. Ascherio A. Environmental factors in multiple sclerosis. *Expert Rev. Neurother.* 13(12 Suppl.), 3–9 (2013).
6. Hedstrom AK, Olsson T, Alfredsson L. The role of environment and lifestyle in determining the risk of multiple sclerosis. *Curr. Top. Behav. Neurosci.* 26, 87–104 (2015).
7. Correale J, Gaitan MI. Multiple sclerosis and environmental factors: the role of vitamin D, parasites, and Epstein-Barr virus infection. *Acta Neurol. Scand.* 132(199), 46–55 (2015).
8. Ramanujam R, Hedstrom AK, Manouchehrinia A *et al.* Effect of smoking cessation on multiple sclerosis prognosis. *JAMA Neurol.* 72(10), 1117–1123 (2015).
9. Farrell RA, Antony D, Wall GR *et al.* Humoral immune response to EBV in multiple sclerosis is associated with disease activity on MRI. *Neurology* 73(1), 32–38 (2009).
10. Huynh JL, Casaccia P. Epigenetic mechanisms in multiple sclerosis: implications for pathogenesis and treatment. *Lancet Neurol.* 12(2), 195–206 (2013).

• **This article summarized roles of environmental stimuli-induced different epigenetic changes including methylation and demethylation in the pathogenesis of multiple sclerosis.**

11. Pedre X, Mastronardi F, Bruck W, Lopez-Rodas G, Kuhlmann T, Casaccia P. Changed histone acetylation patterns in normal-appearing white matter and early multiple sclerosis lesions. *J. Neurosci.* 31(9), 3435–3445 (2011).
12. Chomyk AM, Volsko C, Tripathi A *et al.* DNA methylation in demyelinated multiple sclerosis hippocampus. *Sci. Rep.* 7(1), 8696 (2017).

13. Zheleznyakova GY, Piket E, Marabita F *et al.* Epigenetic research in multiple sclerosis: progress, challenges, and opportunities. *Physiol. Genomics* 49(9), 447–461 (2017).

14 . Calabrese R, Valentini E, Ciccarone F *et al. TET2* gene expression and 5-hydroxymethylcytosine level in multiple sclerosis peripheral blood cells. *Biochim. Biophys. Acta* 1842(7), 1130–1136 (2014).

- **Global *5hmC* level and *Tet2* gene expression are found to decrease in the blood cells of patient with multiple sclerosis, which is consistent with the change in our study.**

15. Khorshidahmad T, Acosta C, Cortes C, Lakowski TM, Gangadaran S, Namaka M. Transcriptional regulation of brain-derived neurotrophic factor (BDNF) by methyl CpG binding protein 2 (MeCP2): a novel mechanism for re-myelination and/or myelin repair involved in the treatment of multiple sclerosis (MS). *Mol. Neurobiol.* 53(2), 1092–1107 (2016).

16. Khorshid Ahmad T, Zhou T, Altaweel K *et al.* Experimental autoimmune encephalomyelitis (EAE)-induced elevated expression of the E1 isoform of methyl CpG binding protein 2 (MeCP2E1): implications in multiple sclerosis (MS)-induced neurological disability and associated myelin damage. *Int. J. Mol. Sci.* 18(6), pii:E1254 (2017).

17. Mehrpour M, Akhoundi FH, Delgosha M *et al.* Increased serum brain-derived neurotrophic factor in multiple sclerosis patients on interferon-beta and its impact on functional abilities. *Neurologist* 20(4), 57–60 (2015).

18. Makar TK, Nimmagadda VK, Singh IS *et al.* TrkB agonist, 7,8-dihydroxyflavone, reduces the clinical and pathological severity of a murine model of multiple sclerosis. *J. Neuroimmunol.* 292, 9–20 (2016).

19. Miao Z, He Y, Xin N *et al.* Altering 5-hydroxymethylcytosine modification impacts ischemic brain injury. *Hum. Mol. Genet.* 24(20), 5855–5866 (2015).

20. Livak KJ, Schmittgen TD. Analysis of relative gene expression data using real-time quantitative PCR and the 2(T)(-Delta Delta C) method. *Methods* 25(4), 402–408 (2001).

21. Nimmagadda VK, Bever CT, Vattikunta NR *et al.* Overexpression of SIRT1 protein in neurons protects against experimental autoimmune encephalomyelitis through activation of multiple SIRT1 targets. *J. Immunol.* 190(9), 4595–4607 (2013).

22. Giacoppo S, Pollastro F, Grassi G, Bramanti P, Mazzon E. Target regulation of PI3K/Akt/mTOR pathway by cannabidiol in treatment of experimental multiple sclerosis. *Fitoterapia* 116, 77–84 (2017).

23 . Tahiliani M, Koh KP, Shen Y *et al.* Conversion of 5-methylcytosine to 5-hydroxymethylcytosine in mammalian DNA by MLL partner TET1. *Science* 324(5929), 930–935 (2009).

- **Domstrates that Tet proteins are important limiting enzymes in the epigenetic regulation through the conversion from 5mC to 5hmC.**

24. Ito S, D'alessio AC, Taranova OV, Hong K, Sowers LC, Zhang Y. Role of Tet proteins in 5mC to 5hmC conversion, ES-cell self-renewal and inner cell mass specification. *Nature* 466(7310), 1129–1133 (2010).

25. Strand SH, Hoyer S, Lynnerup AS *et al.* High levels of 5-hydroxymethylcytosine (5hmC) is an adverse predictor of biochemical recurrence after prostatectomy in ERG-negative prostate cancer. *Clin. Epigenetics* 7, 111 (2015).

26. Ng CW, Yildirim F, Yap YS *et al.* Extensive changes in DNA methylation are associated with expression of mutant huntingtin. *Proc. Natl Acad. Sci. USA* 110(6), 2354–2359 (2013).

27. Irier HA, Jin P. Dynamics of DNA methylation in aging and Alzheimer's disease. *DNA Cell. Biol.* 31, S42–S48 (2012).

28. Huang N, Tan L, Xue ZG, Cang J, Wang H. Reduction of DNA hydroxymethylation in the mouse kidney insulted by ischemia reperfusion. *Biochem. Biophys. Res. Commun.* 422(4), 697–702 (2012).

29. Miao ZG, He YQ, Xin N *et al.* Altering 5-hydroxymethylcytosine modification impacts ischemic brain injury. *Hum. Mol. Genet.* 24(20), 5855–5866 (2015).

30. Wang Y, Liu C, Guo QL *et al.* Intrathecal 5-azacytidine inhibits global DNA methylation and methyl- CpG-binding protein 2 expression and alleviates neuropathic pain in rats following chronic constriction injury. *Brain Res.* 1418, 64–69 (2011).

31. Huang N, Tan L, Xue Z, Cang J, Wang H. Reduction of DNA hydroxymethylation in the mouse kidney insulted by ischemia reperfusion. *Biochem. Biophys. Res. Commun.* 422(4), 697–702 (2012).

32. Lee JY, Choi HY, Yune TY. Fluoxetine and vitamin C synergistically inhibits blood-spinal cord barrier disruption and improves functional recovery after spinal cord injury. *Neuropharmacology* 109, 78–87 (2016).

33. Blaschke K, Ebata KT, Karimi MM *et al.* Vitamin C induces Tet-dependent DNA demethylation and a blastocyst-like state in ES cells. *Nature* 500(7461), 222–226 (2013).

34. Chen J, Guo L, Zhang L *et al.* Vitamin C modulates TET1 function during somatic cell reprogramming. *Nat. Genet.* 45(12), 1504–1509 (2013).

35 . Mueller PS, Kies MW, Alvord EC Jr, Shaw CM. Prevention of experimental allergic encephalomyelitis (EAE) by vitamin C deprivation. *J. Exp. Med.* 115, 329–338 (1962).

36. Spitsin SV, Scott GS, Mikheeva T *et al.* Comparison of uric acid and ascorbic acid in protection against EAE. *Free Radic. Biol. Med.* 33(10), 1363–1371 (2002).

37. Mangas A, Covenas R, Bodet D, De Leon M, Duleu S, Geffard M. Evaluation of the effects of a new drug candidate (GEMSP) in a chronic EAE model. *Int. J. Biol. Sci.* 4(3), 150–160 (2008).

38. Babri S, Mehrvash F, Mohaddes G, Hatami H, Mirzaie F. Effect of intrahippocampal administration of vitamin C and progesterone on learning in a model of multiple sclerosis in rats. *Adv. Pharm. Bull.* 5(1), 83–87 (2015).

39. Kocot J, Luchowska-Kocot D, Kielczykowska M, Musik I, Kurzepa J. Does Vitamin C influence neurodegenerative diseases and psychiatric disorders? *Nutrients* 9(7), 659 (2017).

40. Yin R, Mao SQ, Zhao B *et al.* Ascorbic acid enhances Tet-mediated 5-methylcytosine oxidation and promotes DNA demethylation in mammals. *J. Am. Chem. Soc.* 135(28), 10396–10403 (2013).

10.2217/epi-2018-0162

Copyright Clearance Center Marketplace™

Future Medicine Ltd. - License Terms and Conditions

Order Date	01-Nov-2019
Order license ID	1001779-1
ISSN	1750-1911
Type of Use	Republish in a thesis/dissertation
Publisher	Future Medicine, Ltd.
Portion	Chapter/article

LICENSED CONTENT

Publication Title	Epigenomics	**Country**	United Kingdom of Great Britain and Northern Ireland
Date	12/31/2008	**Rightsholder**	Future Medicine Ltd.
Language	English	**Publication Type**	Journal

REQUEST DETAILS

Portion Type	Chapter/article	**Rights Requested**	Main product
Page range(s)	1-13	**Distribution**	Worldwide
Total number of pages	13	**Translation**	Original language of publication
Format (select all that apply)	Electronic	**Copies for the disabled?**	No
Who will republish the content?	Academic institution	**Minor editing privileges?**	No
Duration of Use	Life of current edition	**Incidental promotional use?**	No
Lifetime Unit Quantity	Up to 499	**Currency**	CAD

NEW WORK DETAILS

Title	Selective Knockdown of Misfolded SOD1 as a Therapy for Amyotrophic Lateral Sclerosis	**Institution name**	University of Manitoba
		Expected presentation date	2019-11-25
Instructor name	Ting Zhou		

ADDITIONAL DETAILS

Order reference number	N/A	**The requesting person / organization to appear on the license**	Ting Zhou/University of Manitoba

REUSE CONTENT DETAILS

Title, description or numeric reference of the portion(s)	Appendix	**Title of the article/chapter the portion is from**	N/A

Editor of portion(s)	N/A	**Author of portion(s)**	N/A
Volume of serial or monograph	N/A	**Issue, if republishing an article from a serial**	N/A
Page or page range of portion	208-221	**Publication date of portion**	2019-11-25

CCC Republication Terms and Conditions

1. Description of Service; Defined Terms. This Republication License enables the User to obtain licenses for republication of one or more copyrighted works as described in detail on the relevant Order Confirmation (the "Work(s)"). Copyright Clearance Center, Inc. ("CCC") grants licenses through the Service on behalf of the rightsholder identified on the Order Confirmation (the "Rightsholder"). "Republication", as used herein, generally means the inclusion of a Work, in whole or in part, in a new work or works, also as described on the Order Confirmation. "User", as used herein, means the person or entity making such republication.

2. The terms set forth in the relevant Order Confirmation, and any terms set by the Rightsholder with respect to a particular Work, govern the terms of use of Works in connection with the Service. By using the Service, the person transacting for a republication license on behalf of the User represents and warrants that he/she/it (a) has been duly authorized by the User to accept, and hereby does accept, all such terms and conditions on behalf of User, and (b) shall inform User of all such terms and conditions. In the event such person is a "freelancer" or other third party independent of User and CCC, such party shall be deemed jointly a "User" for purposes of these terms and conditions. In any event, User shall be deemed to have accepted and agreed to all such terms and conditions if User republishes the Work in any fashion.

3. Scope of License; Limitations and Obligations.

    3.1. All Works and all rights therein, including copyright rights, remain the sole and exclusive property of the Rightsholder. The license created by the exchange of an Order Confirmation (and/or any invoice) and payment by User of the full amount set forth on that document includes only those rights expressly set forth in the Order Confirmation and in these terms and conditions, and conveys no other rights in the Work(s) to User. All rights not expressly granted are hereby reserved.

    3.2. General Payment Terms: You may pay by credit card or through an account with us payable at the end of the month. If you and we agree that you may establish a standing account with CCC, then the following terms apply: Remit Payment to: Copyright Clearance Center, 29118 Network Place, Chicago, IL 60673-1291. Payments Due: Invoices are payable upon their delivery to you (or upon our notice to you that they are available to you for downloading). After 30 days, outstanding amounts will be subject to a service charge of 1-1/2% per month or, if less, the maximum rate allowed by applicable law. Unless otherwise specifically set forth in the Order Confirmation or in a separate written agreement signed by CCC, invoices are due and payable on "net 30" terms. While User may exercise the rights licensed immediately upon issuance of the Order Confirmation, the license is automatically revoked and is null and void, as if it had never been issued, if complete payment for the license is not received on a timely basis either from User directly or through a payment agent, such as a credit card company.

    3.3. Unless otherwise provided in the Order Confirmation, any grant of rights to User (i) is "one-time" (including the editions and product family specified in the license), (ii) is non-exclusive and non-transferable and (iii) is subject to any and all limitations and restrictions (such as, but not limited to, limitations on duration of use or circulation) included in the Order Confirmation or invoice and/or in these terms and conditions. Upon completion of the licensed use, User shall either secure a new permission for further use of the Work(s) or immediately cease any new use of the Work(s) and shall render inaccessible (such as by deleting or by removing or severing links or other locators) any further copies of the Work (except for copies printed on paper in accordance with this license and still in User's stock at the end of such period).

    3.4. In the event that the material for which a republication license is sought includes third party materials (such as photographs, illustrations, graphs, inserts and similar materials) which are identified in such

material as having been used by permission, User is responsible for identifying, and seeking separate licenses (under this Service or otherwise) for, any of such third party materials; without a separate license, such third party materials may not be used.

3.5. Use of proper copyright notice for a Work is required as a condition of any license granted under the Service. Unless otherwise provided in the Order Confirmation, a proper copyright notice will read substantially as follows: "Republished with permission of [Rightsholder's name], from [Work's title, author, volume, edition number and year of copyright]; permission conveyed through Copyright Clearance Center, Inc. " Such notice must be provided in a reasonably legible font size and must be placed either immediately adjacent to the Work as used (for example, as part of a by-line or footnote but not as a separate electronic link) or in the place where substantially all other credits or notices for the new work containing the republished Work are located. Failure to include the required notice results in loss to the Rightsholder and CCC, and the User shall be liable to pay liquidated damages for each such failure equal to twice the use fee specified in the Order Confirmation, in addition to the use fee itself and any other fees and charges specified.

3.6. User may only make alterations to the Work if and as expressly set forth in the Order Confirmation. No Work may be used in any way that is defamatory, violates the rights of third parties (including such third parties' rights of copyright, privacy, publicity, or other tangible or intangible property), or is otherwise illegal, sexually explicit or obscene. In addition, User may not conjoin a Work with any other material that may result in damage to the reputation of the Rightsholder. User agrees to inform CCC if it becomes aware of any infringement of any rights in a Work and to cooperate with any reasonable request of CCC or the Rightsholder in connection therewith.

4. Indemnity. User hereby indemnifies and agrees to defend the Rightsholder and CCC, and their respective employees and directors, against all claims, liability, damages, costs and expenses, including legal fees and expenses, arising out of any use of a Work beyond the scope of the rights granted herein, or any use of a Work which has been altered in any unauthorized way by User, including claims of defamation or infringement of rights of copyright, publicity, privacy or other tangible or intangible property.

5. Limitation of Liability. UNDER NO CIRCUMSTANCES WILL CCC OR THE RIGHTSHOLDER BE LIABLE FOR ANY DIRECT, INDIRECT, CONSEQUENTIAL OR INCIDENTAL DAMAGES (INCLUDING WITHOUT LIMITATION DAMAGES FOR LOSS OF BUSINESS PROFITS OR INFORMATION, OR FOR BUSINESS INTERRUPTION) ARISING OUT OF THE USE OR INABILITY TO USE A WORK, EVEN IF ONE OF THEM HAS BEEN ADVISED OF THE POSSIBILITY OF SUCH DAMAGES. In any event, the total liability of the Rightsholder and CCC (including their respective employees and directors) shall not exceed the total amount actually paid by User for this license. User assumes full liability for the actions and omissions of its principals, employees, agents, affiliates, successors and assigns.

6. Limited Warranties. THE WORK(S) AND RIGHT(S) ARE PROVIDED "AS IS". CCC HAS THE RIGHT TO GRANT TO USER THE RIGHTS GRANTED IN THE ORDER CONFIRMATION DOCUMENT. CCC AND THE RIGHTSHOLDER DISCLAIM ALL OTHER WARRANTIES RELATING TO THE WORK(S) AND RIGHT(S), EITHER EXPRESS OR IMPLIED, INCLUDING WITHOUT LIMITATION IMPLIED WARRANTIES OF MERCHANTABILITY OR FITNESS FOR A PARTICULAR PURPOSE. ADDITIONAL RIGHTS MAY BE REQUIRED TO USE ILLUSTRATIONS, GRAPHS, PHOTOGRAPHS, ABSTRACTS, INSERTS OR OTHER PORTIONS OF THE WORK (AS OPPOSED TO THE ENTIRE WORK) IN A MANNER CONTEMPLATED BY USER; USER UNDERSTANDS AND AGREES THAT NEITHER CCC NOR THE RIGHTSHOLDER MAY HAVE SUCH ADDITIONAL RIGHTS TO GRANT.

7. Effect of Breach. Any failure by User to pay any amount when due, or any use by User of a Work beyond the scope of the license set forth in the Order Confirmation and/or these terms and conditions, shall be a material breach of the license created by the Order Confirmation and these terms and conditions. Any breach not cured within 30 days of written notice thereof shall result in immediate termination of such license without further notice. Any unauthorized (but licensable) use of a Work that is terminated immediately upon notice thereof may be liquidated by payment of the Rightsholder's ordinary license price therefor; any unauthorized (and unlicensable) use that is not terminated immediately for any reason (including, for example, because materials containing the Work cannot reasonably be recalled) will be subject to all remedies available at law or in equity, but in no event to a payment of

less than three times the Rightsholder's ordinary license price for the most closely analogous licensable use plus Rightsholder's and/or CCC's costs and expenses incurred in collecting such payment.

8. Miscellaneous.

8.1. User acknowledges that CCC may, from time to time, make changes or additions to the Service or to these terms and conditions, and CCC reserves the right to send notice to the User by electronic mail or otherwise for the purposes of notifying User of such changes or additions; provided that any such changes or additions shall not apply to permissions already secured and paid for.

8.2. Use of User-related information collected through the Service is governed by CCC's privacy policy, available online here: https://marketplace.copyright.com/rs-ui-web/mp/privacy-policy

8.3. The licensing transaction described in the Order Confirmation is personal to User. Therefore, User may not assign or transfer to any other person (whether a natural person or an organization of any kind) the license created by the Order Confirmation and these terms and conditions or any rights granted hereunder; provided, however, that User may assign such license in its entirety on written notice to CCC in the event of a transfer of all or substantially all of User's rights in the new material which includes the Work(s) licensed under this Service.

8.4. No amendment or waiver of any terms is binding unless set forth in writing and signed by the parties. The Rightsholder and CCC hereby object to any terms contained in any writing prepared by the User or its principals, employees, agents or affiliates and purporting to govern or otherwise relate to the licensing transaction described in the Order Confirmation, which terms are in any way inconsistent with any terms set forth in the Order Confirmation and/or in these terms and conditions or CCC's standard operating procedures, whether such writing is prepared prior to, simultaneously with or subsequent to the Order Confirmation, and whether such writing appears on a copy of the Order Confirmation or in a separate instrument.

8.5. The licensing transaction described in the Order Confirmation document shall be governed by and construed under the law of the State of New York, USA, without regard to the principles thereof of conflicts of law. Any case, controversy, suit, action, or proceeding arising out of, in connection with, or related to such licensing transaction shall be brought, at CCC's sole discretion, in any federal or state court located in the County of New York, State of New York, USA, or in any federal or state court whose geographical jurisdiction covers the location of the Rightsholder set forth in the Order Confirmation. The parties expressly submit to the personal jurisdiction and venue of each such federal or state court.If you have any comments or questions about the Service or Copyright Clearance Center, please contact us at 978-750-8400 or send an e-mail to info@copyright.com.

v 1.1